Final Report

Metabolic Responses of *Aspergillus niger* ES4 to Ethanol Stress and Effects on Ethanol Tolerance

By Nawaporn Vinayavekhin

April 2020

Contract No. MRG6180002

Final Report

Metabolic Responses of *Aspergillus niger* ES4 to Ethanol Stress and Effects on Ethanol Tolerance

Asst. Prof. Dr. Nawaporn Vinayavekhin — Department of Chemistry

Asst. Prof. Dr. Jittra Piapukiew — Department of Botany

Asst. Prof. Dr. Warinthorn Chavasiri — Department of Chemistry

Faculty of Science, Chulalongkorn University

Project Granted by the Thailand Research Fund

Abstract

Project Code: MRG6180002

Project Title: Metabolic responses of *Aspergillus niger* ES4 to ethanol stress and effects on ethanol tolerance

Investigator:

Asst. Prof. Dr. Nawaporn Vinayavekhin Department of Chemistry, Faculty of Science, CU

Asst. Prof. Dr. Jittra Piapukiew Department of Botany, Faculty of Science, CU

Asst. Prof. Dr. Warinthorn Chavasiri Department of Chemistry, Faculty of Science, CU

E-mail Address: nawaporn.v@chula.ac.th

Project Period: May 2, 2018 – May 1, 2020

Abstract:

The knowledge of how *Aspergillus niger* responds to ethanol can lead to the design of strains with enhanced ethanol tolerance to be utilized in numerous industrial bioprocesses. However, the current understanding about the response mechanisms of *A. niger* toward ethanol stress remains quite limited. Here, we first applied a cell growth assay to test the ethanol tolerance of *A. niger* strain ES4, which was isolated from the wall near a chimney of an ethanol tank of a petroleum company, and found that it was capable of growing in 5% (*v*/*v*) ethanol to 30% of the ethanol-free control level. Subsequently, the metabolic responses of this strain toward ethanol were investigated using untargeted metabolomics, which revealed the elevated levels of triacylglycerol (TAG) in the extracellular components, and of diacylglycerol, TAG and hydroxy-TAG in the intracellular components. Lastly, stable isotope labelling mass spectrometry with ethanol-d_6 showed altered isotopic patterns of molecular ions of lipids in the ethanol-d_6 samples, compared to the non-labelled ethanol controls, suggesting the ability of *A. niger* ES4 to utilize ethanol as a carbon source. Together, the studies revealed the upregulation of glycerolipid metabolism and ethanol utilization pathway as novel response mechanisms of *A. niger* ES4 toward ethanol stress, thereby underlining the utility of untargeted metabolomics and the overall approaches as tools for elucidating new biological insights.

(Most contents presented in this report were adapted from the published article; the final publication is available at Wiley Online Library via https://doi.org/10.1002/mbo3.948.)

Keywords: *Aspergillus niger*, ethanol response, ethanol utilization pathway, glycerolipid metabolism, metabolomics

บทคัดย่อ

รหัสโครงการ: MRG6180002

ชื่อโครงการ: การตอบสนองทางเมแทบอลิซึมของ *Aspergillus niger* ES4 ต่อความเครียดจากเอทานอลและผลต่อความทนทานต่อเอทานอล

ชื่อนักวิจัย และสถาบัน:

ผศ. ดร.นวพร วินยเวคิน ภาควิชาเคมี คณะวิทยาศาสตร์ จุฬาลงกรณ์มหาวิทยาลัย

ผศ. ดร.จิตรตรา เพียภูเขียว ภาควิชาพฤกษศาสตร์ คณะวิทยาศาสตร์ จุฬาลงกรณ์มหาวิทยาลัย

ผศ. ดร.วรินทร ชวศิริ ภาควิชาเคมี คณะวิทยาศาสตร์ จุฬาลงกรณ์มหาวิทยาลัย

อีเมล์: nawaporn.v@chula.ac.th

ระยะเวลาโครงการ: 2 พฤษภาคม 2561 – 1 พฤษภาคม 2563

บทคัดย่อ:

ความรู้เกี่ยวกับกลไกที่ *Aspergillus niger* ตอบสนองต่อเอทานอลสามารถนำไปสู่การออกแบบสายพันธุ์ที่มีความทนทานต่อเอทานอลสูงขึ้น เพื่อใช้ในชีวกระบวนการในภาคอุตสาหกรรมหลากหลาย อย่างไรก็ตาม ความเข้าใจในปัจจุบันเกี่ยวกับกลไกการตอบสนองของ *A. niger* ต่อความเครียดจากเอทานอลยังมีอยู่ค่อนข้างจำกัด ในที่นี้ คณะวิจัยเริ่มด้วยการประยุกต์ใช้การทดสอบการเจริญเติบโตของเซลล์เพื่อทดสอบความทนทานต่อเอทานอลของ *A. niger* สายพันธุ์ ES4 ซึ่งแยกมาจากผนังใกล้ปล่องปล่อยไอของถังเอทานอลของบริษัทปิโตรเลียมบริษัทหนึ่ง และพบว่า *A. niger* ES4 สามารถเจริญเติบโตได้ในเอทานอลความเข้มข้น 5% (*v*/*v*) ได้ถึง 30% ของระดับของชุดควบคุมที่ไม่มีเอทานอล จากนั้น สืบสวนการตอบสนองทางเมตาบอลิซึมของสายพันธุ์นี้ต่อเอทานอลโดยใช้วิธีการเมตาบอโลมิกส์แบบไม่มีเป้าหมาย ซึ่งแสดงให้เห็นการเพิ่มขึ้นของระดับของไตรเอซิลกลีเซอรอล (TAG) ในส่วนประกอบนอกเซลล์ และของไดเอซิลกลีเซอรอล TAG และ ไฮดรอกซี-TAG ในส่วนประกอบในเซลล์ สุดท้าย การทดลองแมสสเปกโตรเมทรีโดยการติดฉลากไอโซโทปเสถียรแสดงให้เห็นรูปแบบไอโซโทปที่เปลี่ยนไปของไอออนโมเลกุลของไขมันในตัวอย่างที่ใส่ ethanol-d_6 เปรียบเทียบกับชุดควบคุมที่ใส่เอทานอลที่ไม่ติดฉลาก ซึ่งบ่งชี้ถึงความสามารถของ *A. niger* ES4 ในการใช้เอทานอลเป็นแหล่งคาร์บอน เมื่อรวมกัน ผลการศึกษาเปิดเผยถึงการเพิ่มขึ้นของการควบคุมวิถีเมตาบอลิซึมของกลีเซอโรลิพิดและวิถีของการใช้เอทานอล ซึ่งเป็นกลไกการตอบสนองของ *A. niger* ES4 ต่อความเครียดจากเอทานอลในรูปแบบใหม่ แสดงถึงการเน้นความสำคัญของการใช้ประโยชน์ของเมตาบอโลมิกส์แบบไม่มีเป้าหมายและวิธีการทั้งหมดสำหรับใช้เป็นเครื่องมือทำความเข้าใจทางชีววิทยาอย่างลึกซึ้ง

คำหลัก: *Aspergillus niger*, การตอบสนองต่อเอทานอล, วิถีการใช้เอทานอล, วิถีเมแทบอลิซึมของกลีเซอโรลิพิด, เมตาบอโลมิกส์

Executive Summary

Introduction

Organic solvent-tolerant microbes play key roles in many industrial bioprocesses, such as biofuel production, biocatalysis and bioremediation[1]. To obtain strains with tolerance to these solvents, an approach involves genetically engineering selected strains based on the knowledge of organic solvent-induced stresses and responses[2,3], which include repression or activation of sporulation[4], induction of stress proteins[5], biodegradation or secretion of toxic organic solvents[6,7], alteration in cell morphology[8], and adaptation of the cell surface and cell membrane[9,10]. Because these responses might be triggered to counteract chemical toxins, the elevation in their levels might lead to the development of tolerance traits in these microorganisms[11-14].

Aspergillus niger is a filamentous ascomycete fungus, which can be found in almost every environment. It is known as the black mold on rotting fruits and vegetables. Yet, despite these common views of *A. niger* as an undesirable contaminant, it rarely causes disease in humans[15]. In fact, it has the GRAS (generally regarded as safe) status for many of its processes[16] and is one of the most economically useful fungi in the biotechnological industry[17]. It has been applied in the fermentation process for the production of organic acids, such as gluconic[18] and citric acids, with production of the latter exceeding one million metric tons annually[19], and of various extracellular enzymes, including α-amylase or β-glucosidase[20]. Apart from these industrial usages, *A. niger* has also been utilized in bioremediation processes[21,22], as heterologous hosts for proteins and secondary metabolites production[23] and as a co-fermentation partner with *Saccharomyces cerevisiae* for the simultaneous saccharification and fermentation in bioethanol production[24]. The further studies and usages of *A. niger* have also been facilitated by the availability of the genome sequence of three different *A. niger* strains (NRRL3, ATCC1015 and CBS513.88)[17,19].

Recently, one of the black spots found on the roof and outside upper wall of an ethanol tank of a petroleum company was investigated and identified as a living organism, *A. niger* strain ES4 (Figure 1). The black spots could be found most densely near the valved chimney of the tank where ethanol was allowed to evaporate, which indicated the preference of this strain of *A. niger* for ethanol. This finding was rather surprising, as most non-ethanol-producing species are not capable of tolerating a high concentration of ethanol.

Relating to ethanol tolerance, *A. niger* isolated from spoiled pastry products was shown previously to be able to grow on potato dextrose agar containing ethanol up to about 3% (*w*/*w*) with almost no growth defect and up to 4% (*w*/*w*) with about 50% reduction in its growth[25]. Another unrelated study also exhibited the capabilities of *A. niger* to grow weakly on a plate containing 1% ethanol as a sole carbon source[26]. However, while *A. niger* was demonstrated to be capable of tolerating some concentrations of ethanol in many cases, and while a transcriptomic analysis of its closely related fungus *Aspergillus nidulans* revealed a 10-fold and two-fold upregulation of alcohol dehydrogenase *alcA* and *aldA* genes in minimal medium containing ethanol compared to glucose, respectively[27], there have so far been no reports on the metabolic responses of *A. niger* toward

ethanol. The knowledge of which would allow for the engineering of the strain to have either higher tolerance toward ethanol for utilization in biotechnological industry or for designing novel methods for eradication of the strain in unwanted situations, such as in food spoilage or on a wall of an ethanol tank. We therefore decided to study the metabolic responses of *A. niger* ES4 toward ethanol further.

Figure 1 | *Aspergillus niger* strain ES4 growing on the roof and outside upper wall of an ethanol tank of a petroleum company.

In this study, ethanol tolerance of *A. niger* ES4 was first examined. Then, to understand its metabolic responses toward ethanol, untargeted metabolomics analysis was conducted to assay extracellular and intracellular hydrophobic compound changes in *A. niger* ES4 when put under ethanol stress. Lastly, since it was possible that this strain of *A. niger* might intake ethanol for nutrients or substrates for production of some metabolites, the incorporation of ethanol into its metabolites was interrogated by stable isotope labelling mass spectrometry (MS) experiments using ethanol-d_6.

Literature Review

Metabolites

Metabolites are small molecules produced by every living organism to serve critical roles in biology. They are one of the key components of life and are crucial for survival of organisms in various environments. In microbes, metabolites are typically divided into two types based on their functions: primary and secondary metabolites[28]. Primary metabolites are involved in central

metabolism and energy storage[29], which include, for example, amino acids, lipids, and carbohydrates. Secondary metabolites, on the other hand, are found in diverse pathways and are synthesized largely to respond to the immediate environments the microbes are in[29]. Their functions include signal transduction, antibiotic activity against other organisms, virulence factors, metal acquisition, and reduction of oxidative stress[30-33].

Through natural products discovery programs of many laboratories worldwide, we are fortunate to have learnt about diverse structures of primary and secondary metabolites. However, the biological roles leading to their production are still largely unknown. In addition, as many metabolites are not produced by microbes under standard laboratory conditions, a handful number of them are still awaiting further discovery. For example, *Aspergillus niger* itself was reported to express fewer than 30% of its 31 distinct polyketide synthase (PKS), 15 non-ribosomal peptide synthase (NRPS), and 9 hybrid PKS-NRPS biosynthetic gene clusters under common *in vitro* conditions[34,35]. As one of the known small-molecule elicitors[35], ethanol might potentially induce transcription of commonly silent PKS or NRPS genes in *A. niger* and lead to discovery of novel metabolites and metabolic pathways. Further, the global metabolite profiling of both known and unknown metabolites of *A. niger* under ethanol stress might help assign novel functions to the altering metabolites as for alleviating stress from or moderating tolerance in ethanol of the microbe.

Known metabolic responses of microbes to ethanol

Ethanol is one of the most important biofuels in the past decades, is the key ingredient in alcoholic beverages, and is one of the most common disinfection agent. With many usages, many laboratories have therefore spent tremendous efforts on understanding response mechanisms of microorganisms to ethanol in hope of modulating its ethanol tolerance.

With regards to metabolic responses to ethanol, the main focus has been on measuring changes in the composition of fatty acids, which are known to affect fluidity of cell surfaces and cell membranes[1]. Ethanol was reported to cause an increase in the ratio of unsaturated to saturated fatty acids in the membrane of *E. coli*[36] and *S. cerevisiae*[37], and a decrease in *B. subtilis*[38] and *C. acetobutylicum*[39,40]. Apart from fatty acids, the levels of sterol glucosides were also reported to accumulate within 4 hours after induction of ethanol stress in *S. cerevisiae*, whereas those of cerebrosides slightly decreased[41].

As an elicitor of metabolites, ethanol can also induce production of otherwise suppressed secondary metabolites[35]. A chlorinated benzophenone antibiotic, pestalone, for example, was biosynthesized by the marine fungus *Pestalotia* sp. strain CNL-365 only upon addition of 1% ethanol to the culture medium. Other examples of ethanol elicitation included enhanced production of tetracenomycin C in *Streptomyces glaucescens*[42], of the antibiotic jadomycin B in *Streptomyces venezuelae* ISP5230[43], and of carotenoid production in *Phaffia rhodozyma*[44]. Nonetheless, the roles of these metabolites on ethanol tolerance are still elusive.

For *A. niger*, while *A. niger* with its amylolytic activity has been applied to ferment potato starch to ethanol in cocultures with *S. cerevisiae*[45], there has never been any reports on how it

metabolically responds to ethanol either intracellularly and extracellularly. The ability to measure and identify wider range of ethanol-induced or suppressed metabolites simultaneously in untargeted metabolomics experiments of *A. niger* should allow for discovery of novel response mechanisms of microorganisms to ethanol, which might include the use of special metabolic or biotransformation pathways; suggest alternative strategies to increase or reduce ethanol tolerance of *A. niger*; or at least provide a system-level view on the question.

The relevance of stress responses to tolerance

Since cellular responses of microbes to chemical stresses might confer the benefits of counteracting these toxins, thereby protecting organisms from them, one might expect these responses to lead to development of tolerance traits in these microorganisms. While the issues remain largely unresolved, a few studies have demonstrated the possible correlation between stress responses and tolerance[1].

In particular, in 2007, Kang and coworkers[12] studied protein profiles of the psychrophile *Bacillus psychrosaccharolyticus* in isopropanol (IPA) and found upregulated levels of a heat-shock protein Hsp33 upon stress. They then proceeded to test the correlation between the stress response and tolerance by overexpressing the *HSP33* genes of *B. psychrosaccharolyticus* in *Escherichia coli*, which resulted in the improved tolerance of the strain in organic solvents compared to the wildtype.

In another more metabolic-related example, Kajiwara *et al.*[11] evaluated the correlation between fatty acid composition and ethanol tolerance in *Saccharomyces cerevisiae*. As mentioned earlier, it was known that the ratio of unsaturated to saturated fatty acids in *S. cerevisiae* increases, as the cells are grown in the presence of ethanol. In this work, the authors successfully increased this ratio by overexpressing the *FAD2* gene from *Arabidopsis thaliana* in *S. cerevisiae*. The subsequent examination of the growth of this strain in 15% ethanol confirmed greater resistance toward ethanol of this overexpressing strain compared to the control cells, thereby suggesting the relevance between stress responses and tolerance.

Yet, while the above two examples supported the correlation, when Luo *et al.*[46] attempted to perform similar experiments to the latter example by modulating fatty acid composition in *E. coli*, the results turned out to be opposite to those predicted. As is the case for *S. cerevisiae*, the presence of ethanol led to the increased ratio of unsaturated to saturated fatty acids in *E. coli*. The overexpression of *des* gene encoding fatty acid desaturase from *Bacillus subtilis*, which increased the desired ratio of fatty acids in *E. coli*, should therefore elevate resistance of the strain toward ethanol. However, in this case, the tolerance appeared to be reduced.

It might seem unfortunate that not every engineered expression conferred tolerance as expected. Nevertheless, what was most valuable about the stress response knowledge was that it did suggest potential gene or metabolite targets to begin strain engineering or modulating levels. In fact, in the last example, when the authors overexpressed another gene in the pathway, *fabA*, which yielded contrasting fatty acid composition in *E. coli*, they could obtain the *E. coli* strain with increased resistance toward ethanol.

Metabolomics

Metabolomics is a global profiling approach used for comparing levels of large numbers of metabolites simultaneously under conditions of interest (*e.g.*, stress-induced *vs.* normal states)[28]. The changes in levels of these metabolites or their metabolic pathways suggested their association with the conditions, thereby generating hypothesis for subsequent downstream studies. One mode for performing metabolomics analysis is untargeted mode[47]. Utilizing liquid chromatography (LC)–mass spectrometry (MS) as a quantitative tool, untargeted metabolomics analysis quantified metabolites based on their absolute mass ion intensities without prior specification of target metabolites. The analysis therefore allows for quantitative comparison of both known and novel metabolites alike.

The previous work in our laboratory, which was supported by the Thailand Research Fund (TRG5780194), developed and applied untargeted metabolomics platforms for studying intracellular components of *Bacillus subtilis* strain 168 subjected to 1-butanol stress[48]. The studies found the levels of phosphatidylethanolamine (PE), diglucosyldiacylglycerol (DGDAG), and phosphatidylserine (PS) to be increased upon 6 h treatment of 1-butanol, whereas diacylglycerol (DAG) and lysylphosphatidylglycerol (lysylPG) were decreased (Figure 2). Because these lipids are in the membrane lipid biosynthetic pathways, the findings from untargeted metabolomics analysis led to the examination of the levels of all gene transcripts in the pathways by real-time reverse transcriptase PCR, which exhibited elevated levels of *ywiE* transcripts and reduction in levels of *cdsA*, *pgsA*, *mprF*, *clsA*, and *yfnI* transcripts. The untargeted metabolomics analysis therefore provides novel knowledge of how *B. subtilis* responds to 1-butanol stress and the potential gene targets for strain engineering *B. subtilis* to have higher resistance toward 1-butanol. In fact, our laboratory has recently explored this possibility and obtained a strain with mutation in the *mprF* gene in the membrane lipid biosynthetic pathways that exhibited 29% increased tolerance in 1-butanol after 12-h exposure compared to the original strain[14].

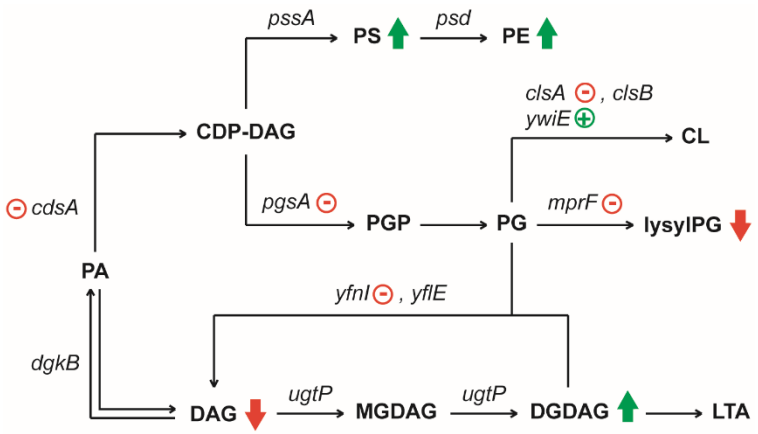

Figure 2 | Membrane lipid biosynthetic pathways in *B. subtilis* showing key lipids and enzyme-encoding genes. The block arrows represent lipids with elevated (green upward arrows) or decreased (red downward arrows) levels under 1-butanol stress. The arithmetic symbols indicate genes with up- (pluses) or down- (minuses) regulated expression levels. (Adapted from ref. 48).

The above studies focused on analyzing the intracellular metabolomes, which mostly contained primary metabolites. For extracellular secondary metabolites in microbes, the following example illustrated the efforts of utilizing untargeted metabolomics analysis. Specifically, when Vinayavekhin *et al.*[49] examined the pyochelin (*pch*) gene cluster in *Pseudomonas aeruginosa* for its potential abilities to biosynthesize or regulate other metabolites, they compared the extracellular metabolomes of pyochelin (*pch*) gene cluster mutants to those of wild-type *P. aeruginosa* (strain PA14). The untargeted metabolomics analysis then allowed for the identification of 198 ions regulated by the *pch* genes (Figure 3). Subsequent downstream analysis using a combination of mass spectrometry, chemical synthesis, and stable isotope labeling with cysteine-3,3-d_2 then led to the characterization of known biosynthetic intermediates, as well as a pair of novel metabolites as 2-alkyl-4,5-dihydrothiazole-4-carboxylates (ATCs). ATCs appeared to be able to bind iron and depend on *pchE* gene in the *pch* gene cluster for their biosynthesis.

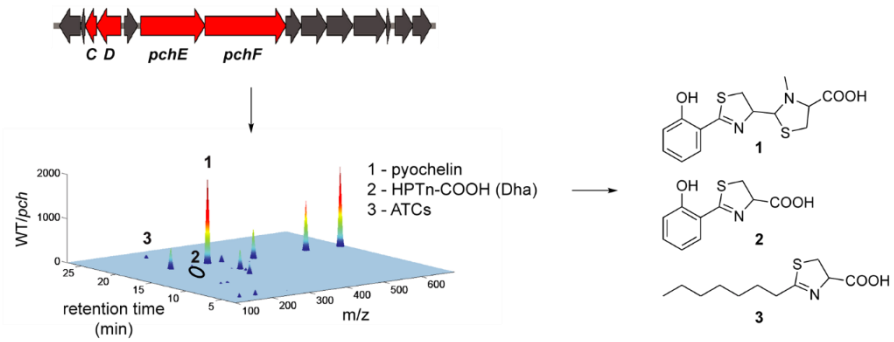

Figure 3 | Untargeted metabolomics of the pyochelin (*pch*) gene cluster in *P. aeruginosa* allowed discovery of known and novel metabolites, 2-alkyl-4,5-dihydrothiazole-4-carboxylates (ATCs), regulated by the *pch* genes.

Likewise, a comprehensive untargeted metabolomics analysis of *A. niger* in the presence and absence of ethanol will provide opportunities for discovery of novel metabolites and metabolic pathways, assignment of new functions to known metabolites, as well as increasing our knowledge about mechanisms of ethanol response and tolerance in *A. niger*.

Objectives

I. **Untargeted metabolomics analysis of extracellular hydrophobic metabolomes of *A. niger* strain ES4 in the presence or absence of ethanol.** The first step for probing metabolic responses of *A. niger* to ethanol is to identify metabolites whose levels are altered upon ethanol exposure. This aim is therefore to apply untargeted metabolomics platforms to globally measure levels of extracellular hydrophobic metabolites in *A. niger* cultures incubated with or without ethanol, in order to uncover metabolites potentially impacting resistance of *A. niger* toward ethanol.

II. **Untargeted metabolomics analysis of intracellular hydrophobic metabolomes of *A. niger* strain ES4 in the presence or absence of ethanol.** Apart from extracellular hydrophobic metabolomes in aim 1, we will also explore changes in levels of intracellular hydrophobic metabolites in *A. niger* culture in the presence and absence of ethanol as well, so as to obtain a full picture of how *A. niger* responds to ethanol metabolically.

III. **Characterization of metabolites as metabolic responses to ethanol stress.** Knowledge about metabolite structures will allow us to link these metabolites to metabolic or biosynthetic pathways, as well as to predict their molecular functions. In this aim, we propose to employ bioinformatics, chemical, analytical, and chromatographic techniques to characterize differential metabolites found in aims 1 and 2.

IV. **Identification of ethanol-incorporated metabolites.** As *A. niger* strain ES4 was isolated from the outside wall of an ethanol tank, the strain might possess special metabolic or biotransformation pathways for making use of ethanol. To test this hypothesis, we propose to trace the possible incorporation of ethanol into metabolites with increased levels in ethanol-treated samples found in aim 1 by using stable-isotope labelling mass spectrometry experiments with ethanol-d_6.

Research Methodology

Fungal strain and growth conditions

Aspergillus niger strain ES4 was isolated from a black spot on the outside upper wall of an ethanol tank of a petroleum company by the serial dilution method[50]. It was identified based on morphological characteristics and then confirmed using molecular technique. The nucleotide sequence data was submitted into the DDBJ/EMBL/GenBank nucleotide sequence databases with accession number MK621333.

The fungus was grown on potato dextrose agar for 7 d, before three agar plugs were inoculated in 20 mL of potato dextrose broth and shaken at 180 rpm, room temperature for 3 d. The culture was then diluted 20-fold into 20 mL of minimal medium (MM; per liter: 6 g $NaNO_3$, 0.52 g KCl, 0.52 g $MgSO_4{\cdot}7H_2O$, 1.52 g KH_2PO_4, 10 g glucose, 2 mL Hutner's trace elements, pH 6.8)[51] with ethanol (Merck, absolute, $\geq$ 99.9%), water (as control), or ethanol-d_6 (Merck, deuteration degree $\geq$ 99%; for stable isotope labelling MS) at the indicated concentrations and shaken further until the predetermined time.

Determination of the dry weight (DW)

Mycelia from three 20-mL cultures were combined and collected on a dry, pre-weighed Whatman paper no. 1 by vacuum filtration. They were then washed with distilled water (4 x 5 mL, then 2 x 20 mL) and dried on the filter paper at 70 °C until at a constant weight (DW).

Metabolites extraction and analysis

Mycelia and supernatant from the 3-d-old 20-mL *A. niger* culture were separated by gravity filtration through a cotton ball. A mixture of 10 mL of chloroform and 5 mL of methanol was added to the supernatant, while mycelia were washed once with 10 mL of distilled water and soaked overnight in a mixture of 3 mL of chloroform and 1.5 mL of methanol, before 1.5 mL of MM without glucose was added to them. Subsequently, all mixtures were shaken vigorously, and centrifuged at 1500*g*, room temperature for 3 min to separate the organic layer (bottom) from the aqueous layer (top). The organic layer was transferred to another glass vial, evaporated to dryness under a steam of nitrogen, and placed at –20 °C for storage. The extracts were reconstituted in 200 μL of chloroform prior to analysis by liquid chromatography (LC)–MS.

For LC–MS and LC–MS/MS analyses, 40 μL of each sample was quantitated on an Ultimate DGP-3600SD LC coupled to a Bruker MicrOTOF Q-II MS instrument, both in the positive and negative ion modes, as described previously[52].

LC–MS untargeted data analysis

The total ion chromatograms from each sample group (*i.e.*, control *vs.* ethanol treatment) were obtained in triplicate. The total of six chromatograms for mycelia samples and six chromatograms for supernatant samples were then subjected to comparative data analyses separately as previously described[53], except that (i) the data were normalized by the average DW of the cultures instead of the optical density at 600 nm and (ii) the minimum integrated mass ion intensity (MSII) was set at 5,000 instead of 30,000.

Stable isotope labelling MS with ethanol-d_6

Intracellular metabolites from *A. niger* cultures treated with ethanol-d_6 were extracted and analyzed by LC–MS exactly as described above in the section “Metabolites extraction and analysis”. The resulting chromatograms were then inspected manually to obtain the mass spectra of the indicated ions.

Results

Ethanol tolerance of *A. niger* ES4

Since *A. niger* ES4 was isolated from the outside upper wall of an ethanol tank, we first assessed its ethanol tolerance. It, however, was not possible to monitor the growth of *A. niger* on the solid agar medium containing ethanol, which best mimicked its growth on the wall of the tank, because its spore interfered with the radial growth (data not shown). We therefore determined its ethanol tolerance using a cell growth assay in a defined liquid medium instead[13]. In this assay, *A. niger* ES4 mycelia (60 mL) were cultured in MM adapted slightly from that used by Barratt *et al.*[51] for

culturing *Aspergillus nidulans*, and with ethanol added at concentrations up to 5% (*v*/*v*). Then, their growth was monitored daily over a 5-d period by measuring the DW of mycelia.

The *A. niger* strain ES4 was able to grow in ethanol at all tested concentrations (2–5% (*v*/*v*)), although at slower growth rates than the no-ethanol control (Figure 4). Increasing ethanol concentrations decreased the DW at each measured time point in a dose-dependent manner and became lowest at 5% (*v*/*v*) ethanol. The DW amounted to 78%, 65%, 49%, and 30% of that of the ethanol-free control at 2%, 3%, 4%, and 5% (*v*/*v*) ethanol, respectively, at day 4 when the cells were solidly in the stationary phase. Overall, the data revealed some degree of tolerance toward ethanol by the *A. niger* ES4 strain.

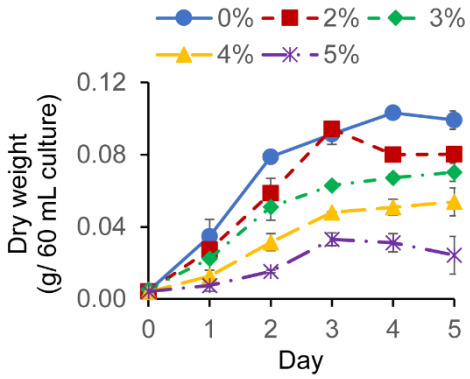

Figure 4 | Growth curves of A. niger ES4 in MM with concentrations of ethanol from 0–5% (v/v). Data are shown as the average DW of mycelia from a 60-mL culture ± standard error of the mean for triplicate experiments per concentration.

Metabolomics of *A. niger* under ethanol stress

To further characterize the microbe and understand the responses of *A. niger* toward ethanol, metabolomics analysis was performed on both the extracellular and intracellular components of *A. niger* ES4 cultures in the presence and absence of 4% (*v*/*v*) ethanol at day 3, which was the condition that induced moderate stress levels to the fungi (*i.e.*, 52% growth of that without ethanol) and at the day the cells entered early stationary phase (Figure 4). The mycelia or culture supernatant were then extracted for analysis of the hydrophobic metabolites using a 2:1 (*v*/*v*) ratio of chloroform: methanol, and the extracts were concentrated and analyzed by LC–MS using a previously-developed untargeted metabolomics platform[53].

To identify differential metabolites related to ethanol stress responses, the XCMS program[54] was used to obtain an MSII value for each detectable metabolite ion in each LC–MS chromatogram, and the MSII values were normalized by the DW to account for the differences in fungal growth. Ions were then regarded as potential responses to ethanol stress only if they were up- or down-regulated by four-fold or more with statistical significance (Student's *t* test with $p < 0.05$) in the ethanol-treated samples compared to the controls, and only if they also met these criteria in another set of independent experimental repeat. Using these criteria, the unbiased comparative analyses revealed 68 and 7 upregulated ions and 1 and 1 downregulated ions in the supernatant, and 322 and 29

upregulated ions and 14 and 24 downregulated ions in the mycelia under ethanol stress in the positive and negative ion modes, respectively, (Figure 5).

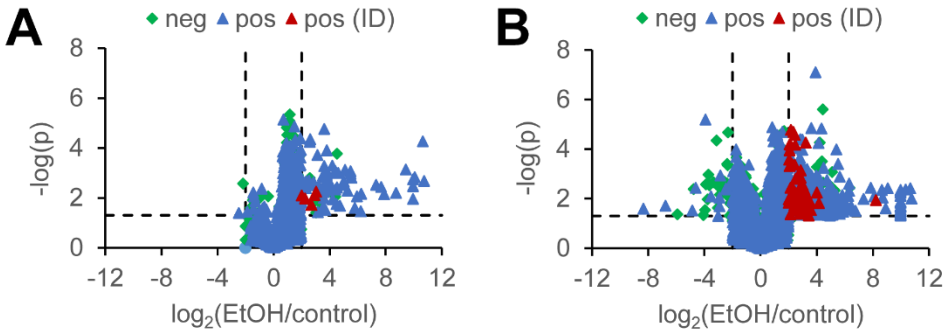

Figure 5 | Volcano plots of metabolite changes in *A. niger* ES4 at day 3 caused by 4% (*v*/*v*) ethanol. Each **(A)** extracellular and **(B)** intracellular metabolite ion in the hydrophobic components with an average MSII above 5,000 counts is plotted as its statistical significance (*p*-value) against the fold change of ethanol (EtOH) over the control. The ions that locate above the horizontal dash line and outside the two vertical dash lines have a *p*-value of less than 0.05 and a fold change of greater than 4, respectively. Each plot contains data from both negative (neg) and positive (pos) ion modes. However, only some positive-mode MS ions with $p < 0.05$ could be identified (pos (ID)) in this study.

Next, the structural characterization of these ions with altered levels following ethanol treatment was undertaken manually using the combined clues from the accurate mass, previously-reported retention time (RT)[52,53], and tandem mass spectra (Tables 1–2, and Appendix 1 Figure A1). Structures could be assigned to 5 extracellular and 63 intracellular upregulated positive-mode ions. All of these ions were in the family of triacylglycerol (TAG) for the extracellular components, and the families of diacylglycerol (DAG), TAG and hydroxy-(h)TAG for the intracellular components (Tables 1–3 with the *sn*-1, *sn*-2 and *sn*-3 side chains written in random order and exact positions of the hydroxyl groups on hTAG unspecified). The most commonly found acyl chains in these altered lipids were 16:0, 18:0, 18:1 and 18:2. The remaining uncharacterized changed ions could not be grouped into the same families as other changed ions, were detected at relatively lower MSII, or were potentially classified as ion fragments or adducts of other smaller or larger molecules. As references, we also performed targeted analyses of other lipids in the biosynthetic pathways of DAG and TAG, such as phospholipids (see Figure 7 for details), and found their levels under ethanol stress more or less undifferentiated from those of the controls (Tables 3–4, and Appendix 1 Figure A1). Together, the untargeted metabolomics analysis suggested the involvement of glycerolipids in response to ethanol stress in *A. niger* ES4.

Table 1: Identified positive-mode ions with statistically significantly elevated levels in ethanol-treated extracellular *A. niger* samples compared to the untreated control showing the mass-to-charge ratio (m/z), retention time (RT) and (**a**) potential identification and MS/MS spectrum, (**b**) integrated mass ion intensity (MSII) and (**c**) adjusted mass ion intensity (aMSII). The MSII and aMSII data are shown for three *A. niger* samples without (Con-1–3) or with ethanol treatment (EtOH-1–3) and their respective averages (Con-avg and EtOH-avg, respectively).

(a) Identified significantly elevated positive-mode ions in ethanol-treated extracellular *A. niger* samples (potential identification and MS/MS spectrum)

#	m/z	RT (min)	Ion	Potential identification	MS/MS spectrum
1	874.7830	48.3	$[M + NH_4]^+$	TAG (16:0/18:1/18:2)	A3
2	898.7839	48.1	$[M + NH_4]^+$	TAG (18:1/18:2/18:2)	A4
3	900.7989	48.6	$[M + NH_4]^+$	TAG (18:1/18:1/18:2)	A5
4	902.8136	48.7	$[M + NH_4]^+$	TAG (18:1/18:1/18:1)	A6
5	904.8272	48.9	$[M + NH_4]^+$	TAG (18:0/18:1/18:1)	A7

(b) Identified significantly elevated positive-mode ions in ethanol-treated extracellular *A. niger* samples (MSII)

#	m/z	RT (min)	Integrated mass ion intensity (MSII)							
			EtOH-1	EtOH-2	EtOH-3	EtOH-avg	Con-1	Con-2	Con-3	Con-avg
1	874.7830	48.3	3.27E+06	2.51E+06	2.47E+06	2.75E+06	1.30E+06	1.02E+06	9.02E+05	1.07E+06
2	898.7839	48.1	1.01E+07	7.88E+06	6.70E+06	8.24E+06	2.79E+06	2.21E+06	2.08E+06	2.36E+06
3	900.7989	48.6	1.17E+07	8.98E+06	8.84E+06	9.85E+06	8.84E+06	2.66E+06	2.16E+06	4.55E+06
4	902.8136	48.7	7.59E+06	5.94E+06	5.82E+06	6.45E+06	2.02E+06	1.55E+06	1.18E+06	1.58E+06
5	904.8272	48.9	4.85E+06	3.76E+06	4.10E+06	4.23E+06	1.17E+06	9.80E+05	7.42E+05	9.64E+05

(c) Identified significantly elevated positive-mode ions in ethanol-treated extracellular *A. niger* samples (aMSII)

#	m/z	RT (min)	Adjusted integrated mass ion intensity (aMSII)							
			EtOH-1	EtOH-2	EtOH-3	EtOH-avg	Con-1	Con-2	Con-3	Con-avg
1	874.7830	48.3	4.71E+06	3.62E+06	3.55E+06	3.96E+06	9.95E+05	7.83E+05	6.91E+05	8.23E+05
2	898.7839	48.1	1.46E+07	1.13E+07	9.65E+06	1.19E+07	2.14E+06	1.69E+06	1.59E+06	1.81E+06
3	900.7989	48.6	1.69E+07	1.29E+07	1.27E+07	1.42E+07	6.77E+06	2.04E+06	1.65E+06	3.49E+06
4	902.8136	48.7	1.09E+07	8.56E+06	8.38E+06	9.29E+06	1.55E+06	1.19E+06	9.04E+05	1.21E+06
5	904.8272	48.9	6.98E+06	5.41E+06	5.90E+06	6.10E+06	8.95E+05	7.51E+05	5.68E+05	7.38E+05

Table 2: Identified positive-mode ions with statistically significantly elevated levels in ethanol-treated intracellular *A. niger* samples compared to the untreated control showing the mass-to-charge ratio (m/z), retention time (RT) and (**a**) potential identification and MS/MS spectrum, (**b**) integrated mass ion intensity (MSII) and (**c**) adjusted mass ion intensity (aMSII). The MSII and aMSII data are shown for three *A. niger* samples without (Con-1–3) or with ethanol treatments (EtOH-1–3) and their respective averages (Con-avg and EtOH-avg, respectively).

(a) Identified significantly elevated positive-mode ions in ethanol-treated intracellular *A. niger* samples (potential identification and MS/MS spectrum)

#	m/z	RT (min)	Ion	Potential identification	MS/MS spectrum
1	243.2090	43.8	-	Fragment of DAG (18:2/18:2)	-
2	261.2182	43.8	-	Fragment of DAG (18:2/18:2)	-
3	263.2362	44.0	-	Fragment of DAG (16:0/18:2)	-
4	299.2571	44.2	-	Fragment of DAG (16:0/18:2)	-
5	331.2789	44.0	-	Fragment of DAG (16:0/18:2)	-
6	337.2740	44.0	-	Fragment of DAG (16:0/18:2)	-
7	339.2896	44.6	-	Fragment of DAG (18:2/20:2)	-
8	357.2972	44.4	-	Fragment of DAG (18:1/18:2)	-
9	505.3885	43.8	-	Fragment of DAG (18:2/18:2) (?)	-
10	577.5185	44.6	$[M - H_2O + H]^+$	DAG (16:0/18:1)	-
11	593.5154	44.1	$[M + H]^+$	DAG (16:0/18:2)	-
12	595.5281	44.6	$[M + H]^+$	DAG (16:0/18:1)	-
13	599.5026	43.8	$[M - H_2O + H]^+$	DAG (18:2/18:2)	-
14	601.5186	44.4	$[M - H_2O + H]^+$	DAG (18:1/18:2)	-
15	603.5334	44.9	$[M - H_2O + H]^+$	DAG (18:1/18:1)	-
16	605.5484	44.0	$[M - H_2O + C_2H_6 + H]^+$	DAG (16:0/18:2)	-
17	617.5133	43.7	$[M + H]^+$	DAG (18:2/18:2)	-
18	617.5101	44.7	$[M - H_2 + H]^+$	DAG (18:1/18:2)	-
19	619.5266	44.4	$[M + H]^+$	DAG (18:1/18:2)	-
20	621.5416	44.9	$[M + H]^+$	DAG (18:1/18:1)	-
21	631.5539	44.2	$[M - H_2O + C_2H_6 + H_2 + H]^+$	DAG (18:2/18:2)	-
22	633.5441	44.6	$[M + CH_2 + H]^+$	DAG (18:1/18:2)	-
23	634.5394	43.8	$[M + NH_4]^+$	DAG (18:2/18:2)	A8
24	636.5550	44.4	$[M + NH_4]^+$	DAG (18:1/18:2)	A9
25	638.5700	44.9	$[M + NH_4]^+$	DAG (18:1/18:1)	A10
26	639.4951	43.8	$[M + Na]^+$	DAG (18:2/18:2)	-
27	640.5815	45.3	$[M + NH_4]^+$	DAG (18:0/18:1)	A11

#	m/z	RT (min)	Ion	Potential identification	MS/MS spectrum
28	641.5108	44.3	$[M + Na]^+$	DAG (18:1/18:2)	-
29	643.5256	44.9	$[M + Na]^+$	DAG (18:1/18:1)	-
30	645.5386	45.4	$[M + Na]^+$	DAG (18:0/18:1)	-
31	655.4700	43.7	$[M + K]^+$	DAG (18:2/18:2)	-
32	657.4889	44.3	$[M + K]^+$	DAG (18:1/18:2)	-
33	659.5346	44.9	$[M + K]^+$	DAG (18:1/18:1)	-
34	662.5667	44.6	$[M + NH_4]^+$	DAG (18:2/20:2)	A12
35	664.6204	45.1	$[M + NH_4]^+$	DAG (18:2/20:1) and some DAG (18:1/20:2)	A13
36	667.5271	44.6	$[M + Na]^+$	DAG (18:2/20:2)	-
37	816.7036	47.6	$[M + NH_4]^+$	TAG (12:0/18:2/18:2) and isomers	A14
38	844.7360	47.8	$[M + NH_4]^+$	TAG (14:0/18:2/18:2) and isomers	A15
39	860.7302	46.6	$[M + NH_4]^+$	hTAG (16:1/16:1(OH)/18:2) (?)	-
40	862.7455	46.9	$[M + NH_4]^+$	hTAG (16:0/16:1(OH)/18:2)	A16
41	864.7565	47.2	$[M + NH_4]^+$	hTAG (16:0/16:0/18:2(OH))	A17
42	879.7409	46.5	$[M + H]^+$	TAG (18:2/18:2/18:2)	-
43	886.7387	46.8	$[M + NH_4]^+$	hTAG (16:0/18:2(OH)/18:3) (?)	-
44	888.7606	47.1	$[M + NH_4]^+$	hTAG (16:0/18:2/18:2(OH))	A18
45	890.7736	47.3	$[M + NH_4]^+$	hTAG (16:0/18:1/18:2(OH))	A19
46	904.8319	49.0	$[M + NH_4]^+$	TAG (18:0/18:1/18:1)	A20
47	906.8451	49.1	$[M + NH_4]^+$	TAG (18:0/18:0/18:1)	A21
48	912.7626	46.9	$[M + NH_4]^+$	hTAG (18:1/18:2(OH)/18:3) and isomers	A22
49	914.7771	47.2	$[M + NH_4]^+$	hTAG (18:1/18:2/18:2(OH))	A23
50	916.7929	47.5	$[M + NH_4]^+$	hTAG (18:1/18:1/18:2(OH))	A24
51	918.8068	47.7	$[M + NH_4]^+$	hTAG (18:0/18:1/18:2(OH))	A25
52	934.8749	49.5	$[M + NH_4]^+$	TAG (18:0/18:1/20:0) and other isomers	A26
53	990.9377	50.2	$[M + NH_4]^+$	TAG (18:0/18:1/24:0)	A27
54	1002.9375	50.2	$[M + NH_4]^+$	TAG (18:1/18:1/25:0)	A28
55	1004.9508	50.4	$[M + NH_4]^+$	TAG (18:0/18:1/25:0) (?)	-
56	1018.9654	50.5	$[M + NH_4]^+$	TAG (18:0/18:1/26:0)	A29
57	1231.9962	43.8	$[2M - H_2 + H]^+$	DAG (18:2/18:2)	-
58	1234.0106	44.1	$[2M + H]^+$	DAG (18:2/18:2) (?)	-
59	1236.0261	44.3	$[2M - H_2 + H]^+$	DAG (18:1/18:2)	-
60	1238.0424	44.8	$[M + H]^+$	DAG (18:1/18:1) + DAG (18:2/18:2)	-
61	1255.9951	43.7	$[2M + Na]^+$	DAG (18:2/18:2)	-
62	1260.0226	44.3	$[2M + Na]^+$	DAG (18:1/18:2)	-
63	1264.0575	45.0	$[2M + Na]^+$	DAG (18:1/18:1)	-

(b) Identified significantly elevated positive-mode ions in ethanol-treated intracellular *A. niger* samples (MSII)

#	m/z	RT (min)	Integrated mass ion intensity (MSII)							
			EtOH-1	EtOH-2	EtOH-3	EtOH-avg	Con-1	Con-2	Con-3	Con-avg
1	243.2090	43.8	6.14E+04	4.25E+04	4.54E+04	4.98E+04	1.68E+04	1.42E+04	1.86E+04	1.65E+04
2	261.2182	43.8	3.14E+05	2.07E+05	2.35E+05	2.52E+05	8.54E+04	6.46E+04	1.16E+05	8.86E+04
3	263.2362	44.0	9.81E+05	7.13E+05	8.18E+05	8.37E+05	3.26E+05	2.60E+05	4.16E+05	3.34E+05
4	299.2571	44.2	1.72E+04	2.82E+04	2.56E+04	2.37E+04	7.81E+03	8.39E+03	8.35E+03	8.18E+03
5	331.2789	44.0	1.87E+05	1.27E+05	1.54E+05	1.56E+05	7.13E+04	5.52E+04	9.16E+04	7.27E+04
6	337.2740	44.0	1.18E+07	8.40E+06	9.33E+06	9.86E+06	2.82E+06	2.33E+06	3.69E+06	2.95E+06
7	339.2896	44.6	1.09E+07	9.04E+06	9.03E+06	9.67E+06	2.18E+06	1.64E+06	2.92E+06	2.25E+06
8	357.2972	44.4	8.13E+04	6.16E+04	6.28E+04	6.86E+04	1.91E+04	1.51E+04	2.27E+04	1.89E+04
9	505.3885	43.8	6.89E+04	3.99E+04	4.40E+04	5.10E+04	1.32E+04	1.17E+04	1.58E+04	1.35E+04
10	577.5185	44.6	2.10E+06	1.80E+06	2.14E+06	2.02E+06	8.52E+05	6.66E+05	1.19E+06	9.04E+05
11	593.5154	44.1	3.19E+05	2.27E+05	2.70E+05	2.72E+05	1.25E+05	1.01E+05	1.56E+05	1.28E+05
12	595.5281	44.6	1.90E+05	1.73E+05	1.70E+05	1.78E+05	7.65E+04	6.12E+04	1.03E+05	8.01E+04
13	599.5026	43.8	2.80E+06	1.70E+06	1.90E+06	2.13E+06	5.39E+05	4.38E+05	5.83E+05	5.20E+05
14	601.5186	44.4	4.16E+06	3.46E+06	3.26E+06	3.63E+06	9.62E+05	7.49E+05	1.16E+06	9.58E+05
15	603.5334	44.9	3.49E+06	3.09E+06	2.97E+06	3.18E+06	8.51E+05	6.37E+05	9.90E+05	8.26E+05
16	605.5484	44.0	8.82E+05	9.92E+05	1.22E+06	1.03E+06	0.00E+00	3.30E+05	3.98E+05	2.42E+05
17	617.5133	43.7	6.33E+06	3.80E+06	4.06E+06	4.73E+06	1.14E+06	9.60E+05	1.34E+06	1.15E+06
18	617.5101	44.7	5.45E+04	7.25E+04	1.01E+05	7.59E+04	4.26E+04	2.30E+04	3.19E+04	3.25E+04
19	619.5266	44.4	2.09E+06	1.66E+06	1.57E+06	1.77E+06	4.97E+05	3.95E+05	6.40E+05	5.11E+05
20	621.5416	44.9	5.78E+05	5.25E+05	4.47E+05	5.17E+05	1.34E+05	1.05E+05	1.84E+05	1.41E+05
21	631.5539	44.2	5.90E+04	6.91E+04	8.55E+04	7.12E+04	0.00E+00	0.00E+00	1.34E+03	4.47E+02
22	633.5441	44.6	1.14E+04	2.51E+04	2.37E+04	2.01E+04	0.00E+00	4.73E+03	5.80E+03	3.51E+03
23	634.5394	43.8	3.66E+06	2.28E+06	2.11E+06	2.68E+06	7.41E+05	5.42E+05	7.47E+05	6.77E+05
24	636.5550	44.4	2.82E+06	2.21E+06	1.89E+06	2.30E+06	6.98E+05	4.98E+05	7.58E+05	6.51E+05
25	638.5700	44.9	2.01E+06	1.78E+06	1.49E+06	1.76E+06	5.18E+05	3.72E+05	5.97E+05	4.96E+05
26	639.4951	43.8	1.03E+06	7.02E+05	8.05E+05	8.45E+05	1.82E+05	1.16E+05	2.06E+05	1.68E+05
27	640.5815	45.3	6.84E+05	6.19E+05	4.95E+05	5.99E+05	1.32E+05	1.02E+05	1.54E+05	1.29E+05
28	641.5108	44.3	7.54E+05	7.40E+05	8.55E+05	7.83E+05	2.20E+05	1.42E+05	2.41E+05	2.01E+05
29	643.5256	44.9	5.60E+05	6.48E+05	6.90E+05	6.33E+05	2.65E+05	1.51E+05	2.12E+05	2.09E+05
30	645.5386	45.4	2.36E+05	3.23E+05	3.02E+05	2.87E+05	9.56E+04	6.22E+04	6.83E+04	7.53E+04
31	655.4700	43.7	3.34E+04	2.28E+04	2.56E+04	2.73E+04	7.36E+03	6.12E+03	7.46E+03	6.98E+03
32	657.4889	44.3	2.75E+04	2.54E+04	2.73E+04	2.67E+04	1.10E+04	7.86E+03	1.09E+04	9.90E+03
33	659.5346	44.9	5.13E+04	3.76E+04	4.59E+04	4.49E+04	1.48E+04	6.56E+03	9.97E+03	1.05E+04

#	m/z	RT (min)	Integrated mass ion intensity (MSII)							
			EtOH-1	EtOH-2	EtOH-3	EtOH-avg	Con-1	Con-2	Con-3	Con-avg
34	662.5667	44.6	9.14E+04	7.21E+04	5.92E+04	7.42E+04	1.87E+04	1.33E+04	2.06E+04	1.75E+04
35	664.6204	45.1	7.79E+04	6.74E+04	5.29E+04	6.61E+04	1.70E+04	1.54E+04	2.07E+04	1.77E+04
36	667.5271	44.6	2.50E+04	2.23E+04	2.28E+04	2.34E+04	7.71E+03	2.65E+03	3.69E+03	4.68E+03
37	816.7036	47.6	1.89E+05	1.63E+05	1.50E+05	1.68E+05	4.36E+04	3.54E+04	3.32E+04	3.74E+04
38	844.7360	47.8	1.24E+06	1.11E+06	1.04E+06	1.13E+06	5.17E+05	4.83E+05	4.51E+05	4.84E+05
39	860.7302	46.6	4.87E+04	3.27E+04	3.70E+04	3.94E+04	2.95E+03	3.49E+03	5.87E+03	4.10E+03
40	862.7455	46.9	1.11E+05	8.84E+04	1.09E+05	1.03E+05	3.89E+04	3.38E+04	5.26E+04	4.18E+04
41	864.7565	47.2	1.13E+05	1.06E+05	1.06E+05	1.08E+05	4.50E+04	4.77E+04	5.22E+04	4.83E+04
42	879.7409	46.5	3.85E+05	2.77E+05	3.44E+05	3.35E+05	0.00E+00	6.04E+04	5.62E+04	3.89E+04
43	886.7387	46.8	4.56E+05	3.16E+05	4.05E+05	3.92E+05	1.89E+05	9.46E+04	1.17E+05	1.34E+05
44	888.7606	47.1	6.34E+05	4.53E+05	5.12E+05	5.33E+05	1.27E+05	9.66E+04	1.45E+05	1.23E+05
45	890.7736	47.3	5.16E+05	4.09E+05	4.70E+05	4.65E+05	1.84E+05	1.46E+05	1.58E+05	1.63E+05
46	904.8319	49.0	1.20E+07	1.17E+07	1.12E+07	1.16E+07	5.20E+06	5.14E+06	4.32E+06	4.89E+06
47	906.8451	49.1	6.89E+06	6.87E+06	6.62E+06	6.79E+06	2.54E+06	2.70E+06	1.83E+06	2.36E+06
48	912.7626	46.9	6.04E+05	3.94E+05	4.14E+05	4.71E+05	8.59E+04	7.87E+04	7.21E+04	7.89E+04
49	914.7771	47.2	7.27E+05	5.06E+05	5.55E+05	5.96E+05	9.83E+04	9.24E+04	9.40E+04	9.49E+04
50	916.7929	47.5	5.63E+05	4.16E+05	4.71E+05	4.84E+05	7.59E+04	6.54E+04	1.68E+05	1.03E+05
51	918.8068	47.7	2.68E+05	2.07E+05	2.53E+05	2.43E+05	4.88E+04	4.53E+04	4.49E+04	4.63E+04
52	934.8749	49.5	9.33E+05	1.02E+06	9.33E+05	9.62E+05	4.54E+05	4.52E+05	3.34E+05	4.13E+05
53	990.9377	50.2	4.77E+06	4.56E+06	4.16E+06	4.50E+06	2.04E+06	2.45E+06	1.71E+06	2.07E+06
54	1002.9375	50.2	8.96E+05	8.10E+05	7.02E+05	8.02E+05	3.15E+05	3.43E+05	2.54E+05	3.04E+05
55	1004.9508	50.4	7.08E+05	6.30E+05	5.66E+05	6.34E+05	1.78E+05	1.91E+05	1.33E+05	1.67E+05
56	1018.9654	50.5	7.98E+05	7.61E+05	6.96E+05	7.52E+05	2.94E+05	3.54E+05	2.54E+05	3.01E+05
57	1231.9962	43.8	2.92E+04	2.23E+04	2.21E+04	2.45E+04	9.12E+03	5.33E+03	9.03E+03	7.83E+03
58	1234.0106	44.1	4.12E+04	3.93E+04	3.15E+04	3.73E+04	1.59E+04	9.40E+03	1.51E+04	1.35E+04
59	1236.0261	44.3	4.62E+04	4.30E+04	3.95E+04	4.29E+04	1.65E+04	1.09E+04	1.74E+04	1.49E+04
60	1238.0424	44.8	5.91E+04	6.23E+04	5.54E+04	5.89E+04	2.47E+04	1.28E+04	2.30E+04	2.02E+04
61	1255.9951	43.7	4.14E+04	3.05E+04	2.37E+04	3.19E+04	6.23E+03	3.47E+03	5.24E+03	4.98E+03
62	1260.0226	44.3	4.14E+04	4.31E+04	3.21E+04	3.89E+04	1.00E+04	6.42E+03	9.24E+03	8.56E+03
63	1264.0575	45.0	8.14E+04	9.04E+04	6.78E+04	7.99E+04	2.49E+04	1.43E+04	2.03E+04	1.98E+04

(c) Identified significantly elevated positive-mode ions in ethanol-treated intracellular *A. niger* samples (aMSII)

#	m/z	RT (min)	Adjusted integrated mass ion intensity (aMSII)							
			EtOH-1	EtOH-2	EtOH-3	EtOH-avg	Con-1	Con-2	Con-3	Con-avg
1	243.2090	43.8	8.85E+04	6.12E+04	6.54E+04	7.17E+04	1.29E+04	1.09E+04	1.42E+04	1.27E+04
2	261.2182	43.8	4.52E+05	2.99E+05	3.39E+05	3.63E+05	6.54E+04	4.95E+04	8.86E+04	6.78E+04
3	263.2362	44.0	1.41E+06	1.03E+06	1.18E+06	1.21E+06	2.50E+05	1.99E+05	3.18E+05	2.56E+05
4	299.2571	44.2	2.47E+04	4.07E+04	3.68E+04	3.41E+04	5.98E+03	6.42E+03	6.39E+03	6.27E+03
5	331.2789	44.0	2.70E+05	1.83E+05	2.22E+05	2.25E+05	5.46E+04	4.23E+04	7.02E+04	5.57E+04
6	337.2740	44.0	1.71E+07	1.21E+07	1.34E+07	1.42E+07	2.16E+06	1.78E+06	2.83E+06	2.26E+06
7	339.2896	44.6	1.58E+07	1.30E+07	1.30E+07	1.39E+07	1.67E+06	1.25E+06	2.23E+06	1.72E+06
8	357.2972	44.4	1.17E+05	8.87E+04	9.04E+04	9.87E+04	1.46E+04	1.15E+04	1.74E+04	1.45E+04
9	505.3885	43.8	9.92E+04	5.75E+04	6.34E+04	7.34E+04	1.01E+04	8.93E+03	1.21E+04	1.04E+04
10	577.5185	44.6	3.03E+06	2.60E+06	3.08E+06	2.90E+06	6.53E+05	5.10E+05	9.14E+05	6.92E+05
11	593.5154	44.1	4.59E+05	3.27E+05	3.89E+05	3.92E+05	9.60E+04	7.73E+04	1.20E+05	9.77E+04
12	595.5281	44.6	2.73E+05	2.49E+05	2.45E+05	2.56E+05	5.86E+04	4.69E+04	7.86E+04	6.14E+04
13	599.5026	43.8	4.04E+06	2.45E+06	2.74E+06	3.07E+06	4.13E+05	3.35E+05	4.46E+05	3.98E+05
14	601.5186	44.4	5.99E+06	4.98E+06	4.70E+06	5.22E+06	7.37E+05	5.74E+05	8.92E+05	7.34E+05
15	603.5334	44.9	5.03E+06	4.45E+06	4.28E+06	4.59E+06	6.52E+05	4.88E+05	7.58E+05	6.33E+05
16	605.5484	44.0	1.27E+06	1.43E+06	1.76E+06	1.49E+06	0.00E+00	2.52E+05	3.05E+05	1.86E+05
17	617.5133	43.7	9.12E+06	5.47E+06	5.85E+06	6.81E+06	8.77E+05	7.35E+05	1.03E+06	8.79E+05
18	617.5101	44.7	7.85E+04	1.04E+05	1.45E+05	1.09E+05	3.26E+04	1.76E+04	2.44E+04	2.49E+04
19	619.5266	44.4	3.00E+06	2.39E+06	2.26E+06	2.55E+06	3.81E+05	3.03E+05	4.90E+05	3.91E+05
20	621.5416	44.9	8.32E+05	7.56E+05	6.44E+05	7.44E+05	1.03E+05	8.02E+04	1.41E+05	1.08E+05
21	631.5539	44.2	8.49E+04	9.96E+04	1.23E+05	1.03E+05	0.00E+00	0.00E+00	1.03E+03	3.43E+02
22	633.5441	44.6	1.64E+04	3.62E+04	3.42E+04	2.89E+04	0.00E+00	3.62E+03	4.44E+03	2.69E+03
23	634.5394	43.8	5.27E+06	3.28E+06	3.04E+06	3.86E+06	5.67E+05	4.15E+05	5.72E+05	5.18E+05
24	636.5550	44.4	4.06E+06	3.18E+06	2.73E+06	3.32E+06	5.34E+05	3.82E+05	5.81E+05	4.99E+05
25	638.5700	44.9	2.89E+06	2.56E+06	2.15E+06	2.53E+06	3.97E+05	2.85E+05	4.58E+05	3.80E+05
26	639.4951	43.8	1.48E+06	1.01E+06	1.16E+06	1.22E+06	1.40E+05	8.91E+04	1.57E+05	1.29E+05
27	640.5815	45.3	9.84E+05	8.91E+05	7.12E+05	8.62E+05	1.01E+05	7.84E+04	1.18E+05	9.92E+04
28	641.5108	44.3	1.09E+06	1.07E+06	1.23E+06	1.13E+06	1.69E+05	1.09E+05	1.85E+05	1.54E+05
29	643.5256	44.9	8.07E+05	9.34E+05	9.94E+05	9.11E+05	2.03E+05	1.16E+05	1.63E+05	1.60E+05
30	645.5386	45.4	3.39E+05	4.65E+05	4.35E+05	4.13E+05	7.32E+04	4.77E+04	5.23E+04	5.77E+04
31	655.4700	43.7	4.81E+04	3.28E+04	3.69E+04	3.93E+04	5.63E+03	4.69E+03	5.71E+03	5.35E+03
32	657.4889	44.3	3.96E+04	3.66E+04	3.93E+04	3.85E+04	8.40E+03	6.02E+03	8.33E+03	7.58E+03
33	659.5346	44.9	7.39E+04	5.41E+04	6.60E+04	6.47E+04	1.14E+04	5.02E+03	7.63E+03	8.01E+03
34	662.5667	44.6	1.32E+05	1.04E+05	8.53E+04	1.07E+05	1.43E+04	1.02E+04	1.58E+04	1.34E+04

#	m/z	RT (min)	Adjusted integrated mass ion intensity (aMSII)							
			EtOH-1	EtOH-2	EtOH-3	EtOH-avg	Con-1	Con-2	Con-3	Con-avg
35	664.6204	45.1	1.12E+05	9.71E+04	7.62E+04	9.51E+04	1.31E+04	1.18E+04	1.59E+04	1.36E+04
36	667.5271	44.6	3.60E+04	3.21E+04	3.29E+04	3.37E+04	5.91E+03	2.03E+03	2.83E+03	3.59E+03
37	816.7036	47.6	2.72E+05	2.35E+05	2.16E+05	2.41E+05	3.34E+04	2.71E+04	2.54E+04	2.86E+04
38	844.7360	47.8	1.79E+06	1.60E+06	1.50E+06	1.63E+06	3.96E+05	3.70E+05	3.45E+05	3.70E+05
39	860.7302	46.6	7.01E+04	4.70E+04	5.33E+04	5.68E+04	2.26E+03	2.67E+03	4.49E+03	3.14E+03
40	862.7455	46.9	1.60E+05	1.27E+05	1.58E+05	1.48E+05	2.98E+04	2.59E+04	4.03E+04	3.20E+04
41	864.7565	47.2	1.62E+05	1.53E+05	1.53E+05	1.56E+05	3.45E+04	3.66E+04	4.00E+04	3.70E+04
42	879.7409	46.5	5.55E+05	3.99E+05	4.95E+05	4.83E+05	0.00E+00	4.63E+04	4.30E+04	2.98E+04
43	886.7387	46.8	6.56E+05	4.55E+05	5.83E+05	5.65E+05	1.45E+05	7.24E+04	9.00E+04	1.02E+05
44	888.7606	47.1	9.14E+05	6.53E+05	7.37E+05	7.68E+05	9.74E+04	7.40E+04	1.11E+05	9.41E+04
45	890.7736	47.3	7.43E+05	5.89E+05	6.77E+05	6.70E+05	1.41E+05	1.12E+05	1.21E+05	1.25E+05
46	904.8319	49.0	1.72E+07	1.69E+07	1.61E+07	1.67E+07	3.98E+06	3.94E+06	3.31E+06	3.74E+06
47	906.8451	49.1	9.93E+06	9.89E+06	9.53E+06	9.78E+06	1.95E+06	2.07E+06	1.40E+06	1.81E+06
48	912.7626	46.9	8.70E+05	5.67E+05	5.97E+05	6.78E+05	6.58E+04	6.03E+04	5.52E+04	6.04E+04
49	914.7771	47.2	1.05E+06	7.29E+05	7.99E+05	8.58E+05	7.53E+04	7.08E+04	7.20E+04	7.27E+04
50	916.7929	47.5	8.11E+05	6.00E+05	6.79E+05	6.96E+05	5.81E+04	5.01E+04	1.29E+05	7.89E+04
51	918.8068	47.7	3.87E+05	2.99E+05	3.64E+05	3.50E+05	3.74E+04	3.47E+04	3.44E+04	3.55E+04
52	934.8749	49.5	1.34E+06	1.47E+06	1.34E+06	1.39E+06	3.47E+05	3.46E+05	2.56E+05	3.16E+05
53	990.9377	50.2	6.88E+06	6.56E+06	5.99E+06	6.48E+06	1.57E+06	1.88E+06	1.31E+06	1.59E+06
54	1002.9375	50.2	1.29E+06	1.17E+06	1.01E+06	1.16E+06	2.41E+05	2.62E+05	1.95E+05	2.33E+05
55	1004.9508	50.4	1.02E+06	9.07E+05	8.15E+05	9.14E+05	1.36E+05	1.46E+05	1.02E+05	1.28E+05
56	1018.9654	50.5	1.15E+06	1.10E+06	1.00E+06	1.08E+06	2.25E+05	2.71E+05	1.95E+05	2.30E+05
57	1231.9962	43.8	4.20E+04	3.21E+04	3.18E+04	3.53E+04	6.98E+03	4.08E+03	6.92E+03	5.99E+03
58	1234.0106	44.1	5.93E+04	5.65E+04	4.53E+04	5.37E+04	1.22E+04	7.20E+03	1.15E+04	1.03E+04
59	1236.0261	44.3	6.65E+04	6.19E+04	5.69E+04	6.18E+04	1.26E+04	8.33E+03	1.33E+04	1.14E+04
60	1238.0424	44.8	8.50E+04	8.97E+04	7.97E+04	8.48E+04	1.89E+04	9.81E+03	1.76E+04	1.54E+04
61	1255.9951	43.7	5.97E+04	4.39E+04	3.42E+04	4.59E+04	4.77E+03	2.66E+03	4.01E+03	3.81E+03
62	1260.0226	44.3	5.97E+04	6.20E+04	4.62E+04	5.60E+04	7.68E+03	4.92E+03	7.08E+03	6.56E+03
63	1264.0575	45.0	1.17E+05	1.30E+05	9.77E+04	1.15E+05	1.91E+04	1.09E+04	1.55E+04	1.52E+04

Table 3: Relative levels of identified ethanol-upregulated lipids and of other related lipids.

Lipid class and acyl chain	Ion	m/z	RT (min)	EtOH/con[a), b)]
Upregulated lipids in ethanol-treated extracellular samples				
Triacylglycerol (TAG)				
16:0/18:1/18:2	$[M + NH_4]^+$	874.7830	48.3	4.8*
18:1/18:2/18:2	$[M + NH_4]^+$	898.7839	48.1	6.6*
18:1/18:1/18:2	$[M + NH_4]^+$	900.7989	48.6	4.1†
18:1/18:1/18:1	$[M + NH_4]^+$	902.8136	48.7	7.7†
18:0/18:1/18:1	$[M + NH_4]^+$	904.8272	48.9	8.3†
Upregulated lipids in ethanol-treated intracellular samples				
Diacylglycerol (DAG)				
18:2/18:2	$[M + NH_4]^+$	634.5394	43.8	7.5*
18:1/18:2	$[M + NH_4]^+$	636.5550	44.4	6.7*
18:1/18:1	$[M + NH_4]^+$	638.5700	44.9	6.7†
18:0/18:1	$[M + NH_4]^+$	640.5815	45.3	8.7†
18:2/20:2	$[M + NH_4]^+$	662.5667	44.6	8.0*
18:2/20:1	$[M + NH_4]^+$	664.5833	45.1	7.0*
TAG				
12:0/18:2/18:2	$[M + NH_4]^+$	816.7036	47.6	8.4†
14:0/18:2/18:2	$[M + NH_4]^+$	844.7360	47.8	4.4‡
18:0/18:1/18:1	$[M + NH_4]^+$	904.8319	49.0	4.5§
18:0/18:0/18:1	$[M + NH_4]^+$	906.8451	49.1	5.4§
18:0/18:1/20:0	$[M + NH_4]^+$	934.8749	49.5	4.4§
18:0/18:1/24:0	$[M + NH_4]^+$	990.9377	50.2	4.1§
18:1/18:1/25:0	$[M + NH_4]^+$	1002.9375	50.2	5.0†
18:0/18:1/26:0	$[M + NH_4]^+$	1018.9654	50.5	4.7§
Hydroxy TAG (hTAG)				
16:0/16:1(OH)/18:2	$[M + NH_4]^+$	862.7455	46.9	4.6‡
16:0/16:0/18:2(OH)	$[M + NH_4]^+$	864.7565	47.2	4.2§
16:0/18:2/18:2(OH)	$[M + NH_4]^+$	888.7606	47.1	8.2*
16:0/18:1/18:2(OH)	$[M + NH_4]^+$	890.7736	47.3	5.4†
18:1/18:2(OH)/18:3	$[M + NH_4]^+$	912.7626	46.9	11.2*
18:1/18:2/18:2(OH)	$[M + NH_4]^+$	914.7771	47.2	11.8*
18:1/18:1/18:2(OH)	$[M + NH_4]^+$	916.7929	47.5	8.8‡
18:0/18:1/18:2(OH)	$[M + NH_4]^+$	918.8068	47.7	9.9†
Other intracellular lipids in the related pathways				
Fatty acid (FA)				
16:0	$[M - H]^-$	255.2317	18.6	1.6†

Lipid class and acyl chain	Ion	m/z	RT (min)	EtOH/con[a), b)]
18:2	$[M - H]^-$	279.2336	18.5	1.7†
18:1	$[M - H]^-$	281.2478	18.8	2.0‡
18:0	$[M - H]^-$	283.2624	19.2	1.5‡
Monoacylglycerol (MAG)				
16:0	$[M + Na]^+$	353.2656	34.0	2.4*
18:2	$[M + Na]^+$	377.2718	33.1	2.1
Phosphatidic acid (PA)				
16:0/18:2	$[M - H]^-$	671.4649	27.4	1.6
18:2/18:2	$[M - H]^-$	695.4647	26.8	2.3*
Phosphatidylethanolamine (PE)				
16:0/18:2	$[M - H]^-$	714.5023	39.0	1.0
18:2/18:2	$[M - H]^-$	738.5004	38.2	1.7
Phosphatidylserine (PS)				
16:0/18:2	$[M - H]^-$	758.4944	29.9	1.3
18:2/18:2	$[M - H]^-$	782.4946	29.3	1.5
Phosphatidylglycerol (PG)				
16:0/18:2	$[M - H]^-$	745.4976	34.4	1.4
18:2/18:2	$[M - H]^-$	769.4962	33.8	1.5
Phosphatidylinositol (PI)				
16:0/18:2	$[M - H]^-$	833.5160	34.0	1.2
18:2/18:2	$[M - H]^-$	857.5147	33.4	1.1
Phosphatidylcholine (PC)				
16:0/18:2	$[M + H]^+$	758.5726	41.7	0.8†
18:2/18:2	$[M + H]^+$	782.5751	41.3	1.8§

Abbreviations: mass-to-charge ratio (m/z) and retention time (RT)

[a)] EtOH/con value represents the ratio of the average mass ion intensity of ethanol-treated sample group and that of the control.

Table 4: Other lipids in the pathways found in intracellular *A. niger* samples. Lipids are shown in terms of their lipid class and acyl chain as (**a**) detected ion adduct, measured mass-to-charge ratio

(m/z), retention time (RT), MS/MS spectrum, (**b**) integrated mass ion intensity (MSII) and (**c**) adjusted mass ion intensity (aMSII). The MSII and aMSII data are shown for three *A. niger* samples without (Con-1–3) or with ethanol treatments (EtOH-1–3) and their respective averages (Con-avg and EtOH-avg, respectively).

(a) Other intracellular lipids in the pathways (ion, m/z, RT, MS/MS spectrum)

#	Lipid class acyl chain	Ions	m/z	RT (min)	MS/MS spectrum
	Fatty acid (FA)				
1	16:0	$[M - H]^-$	255.2317	18.6	-
2	18:2	$[M - H]^-$	279.2336	18.5	-
3	18:1	$[M - H]^-$	281.2478	18.8	-
4	18:0	$[M - H]^-$	283.2624	19.2	-
	Monoacylglycerol (MAG)				
3	16:0	$[M + Na]^+$	353.2656	34.0	-
4	18:2	$[M + Na]^+$	377.2718	33.1	-
	Phosphatidic acid (PA)				
5	16:0/18:2	$[M - H]^-$	671.4649	27.4	A32
6	18:2/18:2	$[M - H]^-$	695.4647	26.8	A33
	Phosphatidylethanolamine (PE)				
7	16:0/18:2	$[M - H]^-$	714.5023	39.0	A34
8	18:2/18:2	$[M - H]^-$	738.5004	38.2	A35
	Phosphatidylserine (PS)				
9	16:0/18:2	$[M - H]^-$	758.4944	29.9	A36
10	18:2/18:2	$[M - H]^-$	782.4946	29.3	A37
	Phosphatidylglycerol (PG)				
11	16:0/18:2	$[M - H]^-$	745.4976	34.4	A38
12	18:2/18:2	$[M - H]^-$	769.4962	33.8	A39
	Phosphatidylinositol (PI)				
13	16:0/18:2	$[M - H]^-$	833.5160	34.0	A40
14	18:2/18:2	$[M - H]^-$	857.5147	33.4	A41
	Phosphatidylcholine (PC)				
15	16:0/18:2	$[M + H]^+$	758.5726	41.7	A30
16	18:2/18:2	$[M + H]^+$	782.5751	41.3	A31

(b) Other intracellular lipids in the pathways (MSII)

#	Lipid class / acyl chain	Integrated mass ion intensity (MSII)							
		EtOH-1	EtOH-2	EtOH-3	EtOH-avg	Con-1	Con-2	Con-3	Con-avg
	Fatty acid (FA)								
1	16:0	2.26E+06	2.16E+06	1.99E+06	2.14E+06	2.43E+06	2.48E+06	2.53E+06	2.48E+06
2	18:2	1.48E+07	1.31E+07	1.38E+07	1.39E+07	1.56E+07	1.57E+07	1.57E+07	1.57E+07
3	18:1	7.86E+06	7.31E+06	6.94E+06	7.37E+06	7.03E+06	6.66E+06	7.33E+06	7.01E+06
4	18:0	1.51E+06	1.47E+06	1.36E+06	1.44E+06	1.91E+06	1.73E+06	1.77E+06	1.80E+06
	Monoacylglycerol (MAG)								
3	16:0	5.15E+05	4.80E+05	3.36E+05	4.44E+05	3.23E+05	5.30E+05	4.54E+05	4.36E+05
4	18:2	3.46E+05	1.88E+05	2.70E+05	2.68E+05	3.21E+05	3.07E+05	2.98E+05	3.09E+05
	Phosphatidic acid (PA)								
5	16:0/18:2	9.63E+05	1.32E+06	7.26E+05	1.00E+06	1.34E+06	1.18E+06	9.63E+05	1.16E+06
6	18:2/18:2	1.03E+06	1.47E+06	1.08E+06	1.20E+06	9.08E+05	1.04E+06	9.54E+05	9.68E+05
	Phosphatidylethanolamine (PE)								
7	16:0/18:2	3.62E+05	7.06E+05	4.47E+05	5.05E+05	1.03E+06	9.95E+05	8.92E+05	9.72E+05
8	18:2/18:2	2.77E+05	4.11E+05	3.38E+05	3.42E+05	3.80E+05	3.64E+05	3.75E+05	3.73E+05
	Phosphatidylserine (PS)								
9	16:0/18:2	1.08E+06	1.64E+06	1.35E+06	1.36E+06	2.30E+06	1.87E+06	1.64E+06	1.94E+06
10	18:2/18:2	3.07E+05	3.50E+05	4.30E+05	3.62E+05	4.76E+05	4.50E+05	4.35E+05	4.54E+05
	Phosphatidylglycerol (PG)								
11	16:0/18:2	1.03E+05	1.59E+05	1.11E+05	1.24E+05	1.89E+05	1.75E+05	1.49E+05	1.71E+05
12	18:2/18:2	2.22E+04	4.09E+04	2.56E+04	2.96E+04	4.18E+04	3.44E+04	3.51E+04	3.71E+04
	Phosphatidylinositol (PI)								
13	16:0/18:2	9.00E+05	1.20E+06	9.51E+05	1.02E+06	1.73E+06	1.65E+06	1.37E+06	1.59E+06
14	18:2/18:2	4.21E+05	5.89E+05	4.83E+05	4.98E+05	9.33E+05	8.45E+05	8.03E+05	8.60E+05
	Phosphatidylcholine (PC)								
15	16:0/18:2	4.97E+06	5.26E+06	4.69E+06	4.97E+06	1.21E+07	1.22E+07	1.10E+07	1.18E+07
16	18:2/18:2	2.06E+07	2.15E+07	2.00E+07	2.07E+07	2.25E+07	2.26E+07	2.13E+07	2.22E+07

(c) Other intracellular lipids in the pathways (aMSII)

#	Lipid class / acyl chain	Adjusted integrated mass ion intensity (aMSII)							
		EtOH-1	EtOH-2	EtOH-3	EtOH-avg	Con-1	Con-2	Con-3	Con-avg
	Fatty acid (FA)								
1	16:0	3.25E+06	3.11E+06	2.87E+06	3.08E+06	1.86E+06	1.90E+06	1.94E+06	1.90E+06
2	18:2	2.14E+07	1.89E+07	1.99E+07	2.01E+07	1.20E+07	1.20E+07	1.20E+07	1.20E+07
3	18:1	1.13E+07	1.05E+07	1.00E+07	1.06E+07	5.39E+06	5.10E+06	5.62E+06	5.37E+06
4	18:0	2.17E+06	2.11E+06	1.95E+06	2.08E+06	1.46E+06	1.33E+06	1.36E+06	1.38E+06

#	Lipid class acyl chain	Adjusted integrated mass ion intensity (aMSII)							
		EtOH-1	EtOH-2	EtOH-3	EtOH-avg	Con-1	Con-2	Con-3	Con-avg
	Monoacylglycerol (MAG)								
3	16:0	8.76E+05	8.16E+05	5.71E+05	7.54E+05	2.29E+05	3.76E+05	3.22E+05	3.09E+05
4	18:2	5.88E+05	3.19E+05	4.58E+05	4.55E+05	2.27E+05	2.17E+05	2.11E+05	2.19E+05
	Phosphatidic acid (PA)								
5	16:0/18:2	1.39E+06	1.91E+06	1.05E+06	1.45E+06	1.03E+06	9.02E+05	7.37E+05	8.88E+05
6	18:2/18:2	1.49E+06	2.12E+06	1.56E+06	1.72E+06	6.95E+05	7.98E+05	7.30E+05	7.41E+05
	Phosphatidylethanolamine (PE)								
7	16:0/18:2	5.21E+05	1.02E+06	6.44E+05	7.27E+05	7.89E+05	7.62E+05	6.83E+05	7.45E+05
8	18:2/18:2	4.00E+05	5.91E+05	4.86E+05	4.92E+05	2.91E+05	2.79E+05	2.87E+05	2.86E+05
	Phosphatidylserine (PS)								
9	16:0/18:2	1.56E+06	2.36E+06	1.94E+06	1.95E+06	1.76E+06	1.43E+06	1.26E+06	1.48E+06
10	18:2/18:2	4.42E+05	5.05E+05	6.19E+05	5.22E+05	3.65E+05	3.45E+05	3.33E+05	3.48E+05
	Phosphatidylglycerol (PG)								
11	16:0/18:2	1.48E+05	2.29E+05	1.59E+05	1.79E+05	1.45E+05	1.34E+05	1.14E+05	1.31E+05
12	18:2/18:2	3.19E+04	5.89E+04	3.69E+04	4.26E+04	3.20E+04	2.64E+04	2.69E+04	2.84E+04
	Phosphatidylinositol (PI)								
13	16:0/18:2	1.30E+06	1.73E+06	1.37E+06	1.46E+06	1.33E+06	1.26E+06	1.05E+06	1.21E+06
14	18:2/18:2	6.06E+05	8.48E+05	6.95E+05	7.17E+05	7.15E+05	6.47E+05	6.15E+05	6.59E+05
	Phosphatidylcholine (PC)								
15	16:0/18:2	7.16E+06	7.57E+06	6.76E+06	7.16E+06	9.24E+06	9.38E+06	8.41E+06	9.01E+06
16	18:2/18:2	2.96E+07	3.10E+07	2.88E+07	2.98E+07	1.73E+07	1.73E+07	1.63E+07	1.70E+07

Ethanol utilization by *A. niger* ES4

To survive on the wall of an ethanol tank, it might be necessary for *A. niger* strain ES4 to be capable of metabolizing ethanol for nutrients or incorporating ethanol into other molecules to reduce its toxicity. Because our metabolomics analyses above revealed the upregulation of DAG, TAG and hTAG in the ethanol-treated *A. niger* samples compared to the controls, we set out to trace the possible incorporation of ethanol or parts of ethanol into some of these lipids by using stable isotope labelling MS with ethanol-d_6.

The *A. niger* ES4 cultures were grown in MM in the presence of 4% (*v*/*v*) ethanol-d_6 (or non-labelled ethanol as controls) for 3 d, harvested for metabolites in the mycelia, and analyzed by LC–MS exactly as described earlier for metabolomics. The chromatograms were then inspected manually for the mass spectra of four representative metabolite ions: (i) DAG (18:2/18:2), (ii) TAG (18:0/18:1/18:1) (significantly elevated under ethanol treatment compared to the untreated controls), (iii) fatty acid (FA) (18:2) and (iv) phosphatidic acid (PA) (18:2/18:2) (in the related metabolic pathways but with unchanged levels). The data showed varying shift in the detected mass-to-charge

ratios (m/z) of all lipids in the ethanol-d_6 samples from the non-labelled controls (Figure 6). The monoisotopic peaks of all lipids, except for FA (18:2), in the non-labelled samples were no longer dominant peaks in the ethanol-d_6 samples. The m/z with the highest intensities were shifted by +3, +5 and +2 mass units for DAG (18:2/18:2), TAG (18:0/ 18:1/18:1) and PA (18:2/18:2) from those in the non-labelled samples, respectively. However, the m/z peaks at ± 1, ± 2 and ± 3 mass units from the dominant m/z peaks were not very different in intensities from those of the dominant m/z peaks for all investigated lipids in the ethanol-d_6 samples. Overall, the results support the metabolism of ethanol in *A. niger* ES4 into other metabolites.

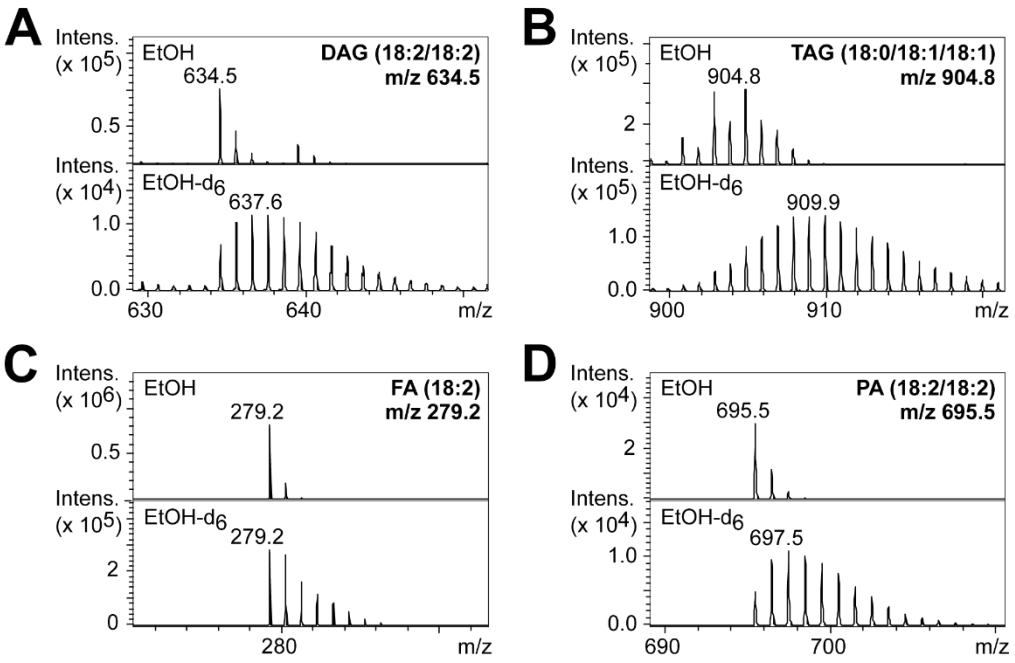

Figure 6 | Mass spectra of representative ions from stable isotope labelling MS experiments with ethanol-d_6. The *A. niger* ES4 was cultured in duplicate in the presence of 4% (*v*/*v*) either ethanol (EtOH)-d_6 or EtOH (as control) and analyzed for intracellular metabolites exactly as conducted in the untargeted metabolomics analysis. Mass spectra were extracted from the total ion chromatograms at the retention time (RT) of 43.8 min for **(A)** diacylglycerol (DAG) (18:2/18:2) and 49.0 min for **(B)** triacylglycerol (TAG) (18:0/18:1/18:1) in the positive ion mode, and at a RT of 18.5 min for **(C)** fatty acid (FA) (18:2) and 26.8 min for **(D)** phosphatidic acid (PA) (18:2/18:2) in the negative ion mode.

Discussion and Conclusions

The ability to tolerate chemicals present in cultures is one of the most essential traits of microorganisms for utilization in bioprocesses. In this study, we found *A. niger* ES4 capable of growing even in 5% (*v*/*v*) (or 4% (*w*/*v*)) ethanol with its growth amounting to approximately 30% of that of the ethanol-free control. Interestingly, this level of tolerance was comparable to that of the ethalogenic filamentous fungus *Fusarium oxysporum*[55] and higher than that of the natural ethanol-producing ascomycetous yeasts *Pichia stipites*, whose growth was inhibited at 3.4% (*w*/*v*) ethanol

when grown on glucose[56]. Assuming that the amount of ethanol produced by these ethalogenic microbes themselves stayed relatively low compared to that of the initially-added ethanol concentration, our results would indicate that *A. niger* strain ES4 had a relatively high resistance toward ethanol. However, as mentioned earlier, Dantigny and coworkers[25] also demonstrated the ability of the *A. niger* strain isolated from spoiled pastry products to grow on potato dextrose agar containing ethanol up to 4% (*w*/*w*) with about 50% reduction in its growth, which seemed to be higher than ethanol tolerance of *A. niger* ES4 in this study. Nevertheless, it was known that the choice of culture media and conditions could affect ethanol tolerance of microbes greatly, and thus, how tolerance *A. niger* ES4 is compared to other *A. niger* strains or other organisms remained to be proven in the future study.

The subsequent investigation into the response mechanisms of *A. niger* ES4 to ethanol using an untargeted metabolomics approach revealed the accumulation of neutral glycerolipids (extracellular TAG, and intracellular DAG, TAG and hTAG) under ethanol stress. DAG and TAG are interconnected in the glycerolipid metabolism (Figure 7). Functionally, DAG is known to play multiple roles from being a component of the cell membrane and an intermediate in lipid metabolism to a second messenger in lipid-mediated signaling cascades[57], whereas TAG is traditionally thought of as an energy storage lipid.

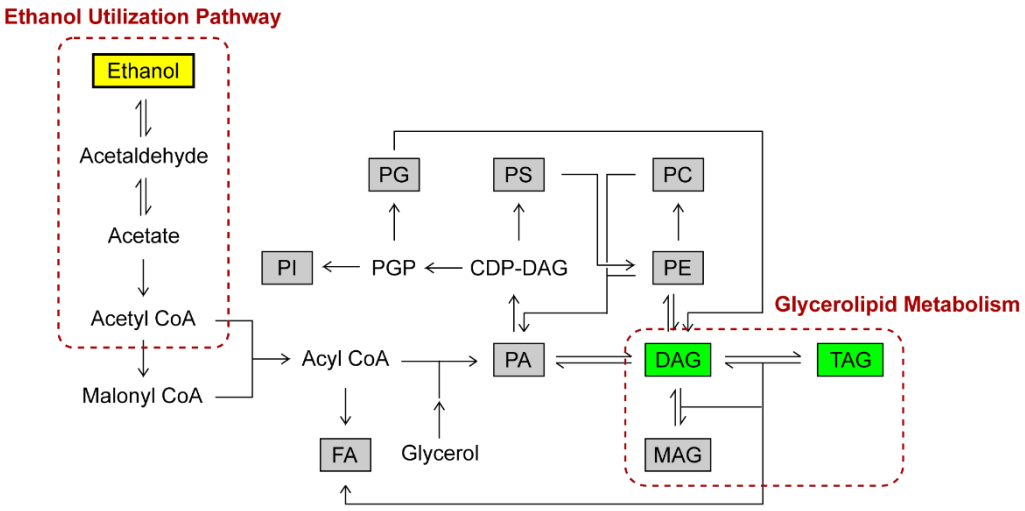

Figure 7 | Biosynthesis of glycerolipids and phospholipids in *A. niger*[58], starting from ethanol. The green boxes indicate lipids that had statistically significantly elevated levels, whereas the gray boxes show other lipids whose levels were quantitated in this study and the yellow box emphasizes where ethanol locates in the pathways. Glycerolipids include monoacylglycerol (MAG), diacylglycerol (DAG), and triacylglycerol (TAG), whereas phospholipids shown are phosphatidic acid (PA), phosphatidylethanolamine (PE), phosphatidylcholine (PC), phosphatidylserine (PS), phosphatidylglycerol (PG), and phosphatidylinositol (PI).

In terms of responses to stress, even though there have been no prior reports demonstrating the effect of upregulated DAG or TAG in the organic solvent tolerance of microbes, these neutral lipids were previously implicated in protecting plants from other abiotic stressors, such

as coldness[59] and darkness[60]. In the case of coldness, for example, *Arabidopsis* accumulated PA, DAG, and TAG during freezing stress where disruption in the genes encoding the enzymes acyl-coenzyme A: DAG acyltransferase and DAG kinase, which catalyze the conversion of DAG to TAG and PA, subsequently resulted in decreased and increased TAG levels and tolerance to coldness, respectively[59]. It is, therefore, possible that, with the unchanged levels of other phospholipids that are components of cell membranes (*e.g.*, PA, phosphatidylethanolamine (PE), and phosphatidylcholine (PC)[61]) found in this study, the elevated DAG and TAG levels as the novel responses to ethanol stress might play some roles in defending *A. niger* against the toxic effects of ethanol. Yet, because cold stress rigidifies cell membrane, the effect that is opposite to that of ethanol, further genetic data is needed to pinpoint the relevance of these glycerolipids on ethanol tolerance of *A. niger*. In addition, it remains to be determined whether the upregulation in glycerolipids following ethanol exposure is specific to *A. niger* ES4 or general for all *A. niger* isolates. Another class of metabolites elevated under ethanol stress was hTAGs, which have mainly been described in *Ricinus communis* castor oil[62], *Lesquerella* seed oil[63,64] and ergot oil from the fungus *Claviceps purpurea*[65]. As the detection and quantitation of hTAG in routine work has remained quite limited compared to other classes of lipids, there is no evidence to support or refute their relevance to various stresses. Yet, because their substrates, hydroxy fatty acids, are known for their specialized medical and industrial usages (*e.g.* lubricants, paints and coatings)[64,66], the discovery of upregulated hTAGs in this study suggested that, upon fully characterizing their structures, *A. niger* might be able to serve as another source of this industrially-important class of lipids as well.
One of the known metabolic responses of the yeast *Saccharomyces cerevisiae* toward ethanol involves an increase in the unsaturated-to-saturated fatty acids ratio, whereby the relative contents of FA (16:1) and FA (18:1) increase while those of FA (16:0) and FA (18:0) decrease[67]. Interestingly, our metabolomics studies showed only slight elevation in contents of all four most abundant fatty acids found in *A. niger* ES4 (*i.e.*, 16:0, 18:2, 18:1 and 18:0) under ethanol stress without an obvious shift in unsaturation index. The alteration in this index was also not immediately apparent in other lipid species, as most of the changing lipids contained both unsaturated and saturated acyl chains. The findings therefore suggested that *A. niger* might utilize different mechanisms to counteract toxicity of ethanol than *S. cerevisiae*. However, we could not rule out the possibilities that the observed effects might simply be specific to the choices of microbial strain, growth medium, or conditions depicted in this study.

The results from the stable isotope labelling MS showed that the isotopic patterns of all the molecular ions of representative lipids in the ethanol-d_6 samples differed from those in the non-labelled ethanol samples. Because the only isotope present at an unnaturally-high abundance in this case was deuterium, the finding indicated the incorporation of varying numbers of deuterium atoms into each lipid, which could potentially occur both via catabolism of ethanol-d_6 by *A. niger* and via deuterium exchanges with the deuteron on the hydroxyl group of ethanol-d_6 during the lipid biosynthesis. However, in this study, ethanol-d_6 was added into the cultures at 4% (*v*/*v*), which resulted in the mole ratio of proton to deuteron in the cultures being 100 to 0.58 (see Appendix 2 for

details on calculation). Assuming that all hydrogen atoms on each representative ion have equal chances to undergo deuterium exchanges, and disregarding any kinetics isotope effects of deuterium, the predicted isotopic ratios, M: M+1: M+2: M+3: M+4, when considering only deuterium exchanges and natural isotopic abundance of each element would be equal to 100: 84: 36: 10: 2 for DAG (18:2/18:2), 80: 100: 63: 27: 9 for TAG (18:0/18:1/18:1), 100: 38: 7: 1: <1 for FA (18:2), and 100: 82: 35: 10: 2 for PA (18:2/18:2) (Appendix 2). These ratios represent the highest probable signals of each isotope arisen from deuterium exchanges; yet, they alone still could not account for the observed high abundances of these isotopes, especially with M+2 and higher m/z species, in the ethanol-d_6 samples (Figure 6). The finding therefore suggested to us that *A. niger* ES4 was in fact capable of metabolizing ethanol-d_6 into other compounds in an existing metabolic pathway. Metabolically, the ethanol utilization pathway has been well studied in the closely-related fungus, *Aspergillus nidulans*[68]. In this pathway, ethanol is first oxidized to acetaldehyde by alcohol dehydrogenase I. Further oxidation of acetaldehyde by alcohol dehydrogenase then yields acetate, which subsequently is converted to acetyl CoA by acetyl CoA synthetase (Figure 7). In the form of acetyl CoA, these carbon and hydrogen atoms from ethanol can then enter into many metabolic pathways, along with the acetyl CoA synthesized from other carbon sources, such as glucose. For lipid synthesis, acetyl CoA is carboxylated to malonyl CoA and coupled with this product to yield acyl CoA, which is the substrate for production of fatty acids, phospholipids, and glycerolipids[58] (Figure 7). For *A. niger*, the genes encoding several homologs of alcohol dehydrogenases have been annotated in the genome of *A. niger* strain CBS513.88[17]. However, their activities in culture have not been confirmed. Our present data, therefore, represents the first piece of evidence to support the existence of this ethanol utilization pathway in *A. niger* ES4.

In total, by applying untargeted metabolomics to study the extracellular and intracellular hydrophobic components of the *A. niger* strain ES4 isolated from the wall of an ethanol tank, we demonstrated the upregulation of glycerolipids (*i.e.*, DAG, TAG and hTAG) as novel responses of microbes to ethanol stress. The subsequent stable isotope labelling MS with ethanol-d_6 also supported the utilization of ethanol by *A. niger* ES4. Future work will aim to determine the relevance of these upregulated changes in glycerolipid metabolism and the ethanol utilization pathway in the ethanol tolerance of *A. niger*, as well as to elucidate the structures, biosynthesis and functions of hTAG more thoroughly. More generally, we believe that untargeted metabolomics platforms and the overall approaches presented in this work will be powerful tools for the discovery of more novel responses of microbes to organic solvent stress, as well as to other external stimuli, in the future.

Output (Acknowledging the Thailand Research Fund)

1. International Journal Publication (see Appendix 3)

   Published 2 articles in 2 peer-reviewed international journals:

   1.1 **Vinayavekhin N***, Kongchai W, Piapukiew J, Chavasiri W (2020). *Aspergillus niger* upregulated glycerolipid metabolism and ethanol utilization pathway under ethanol stress. *MicrobiologyOpen* 9: e948. DOI: 10.1002/mbo3.948. Impact factor 2.738 in Quartile 2 of Scopus database

   1.2 **Vinayavekhin N***, Vangnai AS (2018). The effects of disruption in membrane lipid biosynthetic genes on 1-butanol tolerance of *Bacillus subtilis*. *Appl. Microbiol. Biotechnol.* 102: 9279–9289. Impact factor 3.670 in Quartile 1 of Scopus database

2. Research Utilization and Application

   Academic application – This project led to the novel discovery of metabolic responses of *A. niger* to ethanol. The knowledge can be applied for rationally engineering *A. niger* to have higher tolerance to ethanol in the future, which would be useful for processes involving ethanol, such as biocatalysis of ethanol. In addition, the knowledge also suggested metabolic pathways that might be disturbed to eliminate *A. niger* in unwanted situation, such as on the ethanol tank. This project was also used as a mean to train a Master student to do research in untargeted metabolomics.

3. Others (*e.g.*, national journal publication, proceeding, international conference, book chapter, patent)

   Published 1 proceeding article at the Research Administration Network Conference (RANC) 2018 on May 27–29, 2018 at Thumrin Thana Hotel, Trang. The article also received the best article award in the field of science and technology for development of community and better quality of life (บทความวิจัยดีเด่นสาขาวิทยาศาสตร์และเทคโนโลยี เพื่อพัฒนาชุมชนและคุณภาพชีวิต). The details of the article is as follows (see Appendix 4):

   > Wimonsiri Kongchai, Jittra Piapukiew, Warinthorn Chavasiri, Nawaporn Vinayavekhin* (2018), Targeted metabolomics analysis of *Aspergillus niger* ES4 under ethanol stress, p. 1114-1121. (วิมลสิริ กองไชย, จิตรตรา เพียภูเขียว, วรินทร ชวศิริ, นวพร วินยเวคิน (2018) “การวิเคราะห์เมตาโบโลมิกส์แบบมีเป้าหมายของ *Aspergillus niger* ES4 ภายใต้ความเครียดจากเอทานอล”, หน้า 1114-1121)

   1 Master student trained in untargeted metabolomics approaches and mass spectrometry

   Oral presentation in symposia and seminar classes, such as at National University of Singapore and at Department of Applied Chemistry, Faculty of Science, Maejo University.

References

1 Nicolaou, S. A., Gaida, S. M. & Papoutsakis, E. T. A comparative view of metabolite and substrate stress and tolerance in microbial bioprocessing: from biofuels and chemicals, to biocatalysis and bioremediation. *Metab. Eng.* 12, 307–331, doi:10.1016/j.ymben.2010.03.004 (2010).

2 Taylor, M., Tuffin, M., Burton, S., Eley, K. & Cowan, D. Microbial responses to solvent and alcohol stress. *Biotechnol J* 3, 1388–1397, doi:10.1002/biot.200800158 (2008).

3 Torres, S., Pandey, A. & Castro, G. R. Organic solvent adaptation of Gram positive bacteria: applications and biotechnological potentials. *Biotechnol. Adv.* 29, 442–452, doi:10.1016/j.biotechadv.2011.04.002 (2011).

4 Bohin, J. P., Rigomier, D. & Schaeffer, P. Ethanol sensitivity of sporulation in *Bacillus subtilis*: a new tool for the analysis of the sporulation process. *J. Bacteriol.* 127, 934–940 (1976).

5 Petersohn, A. *et al.* Global analysis of the general stress response of *Bacillus subtilis*. *J. Bacteriol.* 183, 5617–5631, doi:10.1128/JB.183.19.5617-5631.2001 (2001).

6 Aono, R., Tsukagoshi, N. & Yamamoto, M. Involvement of outer membrane protein TolC, a possible member of the mar-sox regulon, in maintenance and improvement of organic solvent tolerance of *Escherichia coli* K-12. *J. Bacteriol.* 180, 938–944 (1998).

7 Bustard, M. T., Whiting, S., Cowan, D. A. & Wright, P. C. Biodegradation of high-concentration isopropanol by a solvent-tolerant thermophile, *Bacillus pallidus*. *Extremophiles* 6, 319–323, doi:10.1007/s00792-001-0260-5 (2002).

8 Neumann, G. *et al.* Cells of *Pseudomonas putida* and *Enterobacter* sp. adapt to toxic organic compounds by increasing their size. *Extremophiles* 9, 163–168, doi:10.1007/s00792-005-0431-x (2005).

9 Aono, R. & Kobayashi, H. Cell surface properties of organic solvent-tolerant mutants of *Escherichia coli* K-12. *Appl Environ Microbiol* 63, 3637–3642 (1997).

10 Weber, F. J. & de Bont, J. A. Adaptation mechanisms of microorganisms to the toxic effects of organic solvents on membranes. *Biochim Biophys Acta* 1286, 225–245 (1996).

11 Kajiwara, S. *et al.* Polyunsaturated fatty acid biosynthesis in *Saccharomyces cerevisiae*: Expression of ethanol tolerance and the FAD2 gene from *Arabidopsis thaliana*. *Applied and Environmental Microbiology* 62, 4309–4313 (1996).

12 Kang, H. J. *et al.* Functional characterization of Hsp33 protein from *Bacillus psychrosaccharolyticus*; additional function of HSP33 on resistance to solvent stress. *Biochemical and Biophysical Research Communications* 358, 743–750, doi:10.1016/j.bbrc.2007.04.184 (2007).

13 Mahipant, G., Paemanee, A., Roytrakul, S., Kato, J. & Vangnai, A. S. The significance of proline and glutamate on butanol chaotropic stress in *Bacillus subtilis* 168. *Biotechnol Biofuels* 10, 122, doi:10.1186/s13068-017-0811-3 (2017).

14 Vinayavekhin, N. & Vangnai, A. S. The effects of disruption in membrane lipid biosynthetic genes on 1-butanol tolerance of *Bacillus subtilis*. *Appl Microbiol Biotechnol* 102, 9279–9289, doi:10.1007/s00253-018-9298-5 (2018).

15 Person, A. K., Chudgar, S. M., Norton, B. L., Tong, B. C. & Stout, J. E. *Aspergillus niger*: An unusual cause of invasive pulmonary aspergillosis. *J. Med. Microbiol.* 59, 834–838, doi:10.1099/jmm.0.018309-0 (2010).

16 Frisvad, J. C. *et al.* Fumonisin and ochratoxin production in industrial *Aspergillus niger* strains. *PLoS One* 6, e23496 doi:10.1371/journal.pone.0023496 (2011).

17 Pel, H. J. *et al.* Genome sequencing and analysis of the versatile cell factory *Aspergillus niger* CBS 513.88. *Nat. Biotechnol.* 25, 221–231, doi:10.1038/nbt1282 (2007).

18 Ramachandran, S., Fontanille, P., Pandey, A. & Larroche, C. Permeabilization and inhibition of the germination of spores of *Aspergillus niger* for gluconic acid production from glucose. *Bioresour. Technol.* 99, 4559–4565, doi:10.1016/j.biortech.2007.06.055 (2008).

19 Baker, S. E. *Aspergillus niger* genomics: Past, present and into the future. *Med. Mycol.* 44, S17–S21, doi:10.1080/13693780600921037 (2006).

20 Pariza, M. W. & Cook, M. Determining the safety of enzymes used in animal feed. *Regulatory Toxicology and Pharmacology* 56, 332–342, doi:10.1016/j.yrtph.2009.10.005 (2010).

21 Coulibaly, L., Naveau, H. & Agathos, S. N. A tanks-in-series bioreactor to simulate macromolecule-laden wastewater pretreatment under sewer conditions by *Aspergillus niger*. *Water Res.* 36, 3941–3948, doi:10.1016/S0043-1354(02)00117-3 (2002).

22 Srivastava, S. & Thakur, I. S. Evaluation of bioremediation and detoxification potentiality of *Aspergillus niger* for removal of hexavalent chromium in soil microcosm. *Soil Biol. Biochem.* 38, 1904–1911, doi:10.1016/j.soilbio.2005.12.016 (2006).

23 Lubertozzi, D. & Keasling, J. D. Developing *Aspergillus* as a host for heterologous expression. *Biotechnol. Adv.* 27, 53–75, doi:10.1016/j.biotechadv.2008.09.001 (2009).

24 Izmirlioglu, G. & Demirci, A. Simultaneous saccharification and fermentation of ethanol from potato waste by co-cultures of *Aspergillus niger* and *Saccharomyces cerevisiae* in biofilm reactors. *Fuel* 202, 260–270, doi:10.1016/j.fuel.2017.04.047 (2017).

25 Dantigny, P., Guilmart, A., Radoi, F., Bensoussan, M. & Zwietering, M. Modelling the effect of ethanol on growth rate of food spoilage moulds. *Int. J. Food Microbiol.* 98, 261–269, doi:10.1016/j.ijfoodmicro.2004.07.008 (2005).

26 O'Connell, M. J. & Kelly, J. M. Differences in the regulation of aldehyde dehydrogenase genes in *Aspergillus niger* and *Aspergillus nidulans*. *Curr. Genet.* 14, 95–103, doi:10.1007/BF00569332 (1988).

27 Mogensen, J., Nielsen, H. B., Hofmann, G. & Nielsen, J. Transcription analysis using high-density micro-arrays of *Aspergillus nidulans* wild-type and *creA* mutant during growth on glucose or ethanol. *Fungal Genet Biol* 43, 593–603, doi:10.1016/j.fgb.2006.03.003 (2006).

28 Vinayavekhin, N. & Saghatelian, A. Untargeted metabolomics. *Current protocols in molecular biology / edited by Frederick M. Ausubel ... [et al.]* **Chapter** 30, Unit 30 31 31–24, doi:10.1002/0471142727.mb3001s90 (2010).

29 Dawes, E. A. & Ribbons, D. W. Some aspects of the endogeneous metabolism of bacteria. *Bacteriol. Rev.* 28, 126–149, doi:Export Date 26 August 2013 (1964).

30 Parker, C. T. & Sperandio, V. Cell-to-cell signalling during pathogenesis. *Cell. Microbiol.* 11, 363–369, doi:Export Date 26 August 2013 (2009).

31 Price-Whelan, A., Dietrich, L. E. P. & Newman, D. K. Rethinking 'secondary' metabolism: Physiological roles for phenazine antibiotics. *Nat. Chem. Biol.* 2, 71–78, doi:Export Date 26 August 2013 (2006).

32 Wandersman, C. & Delepelaire, P. Bacterial iron sources: From siderophores to hemophores. *Annu. Rev. Microbiol.* 58, 611–647, doi:Export Date 26 August 2013 (2004).

33 Waters, C. M. & Bassler, B. L. Quorum sensing: Cell-to-cell communication in bacteria. *Annu. Rev. Cell. Dev. Biol.* 21, 319–346, doi:Export Date 26 August 2013 (2005).

34 Fisch, K. M. *et al.* Chemical induction of silent biosynthetic pathway transcription in *Aspergillus niger*. *J. Ind. Microbiol. Biotechnol.* 36, 1199–1213, doi:10.1007/s10295-009-0601-4 (2009).

35 Pettit, R. K. Small-molecule elicitation of microbial secondary metabolites. *Microb Biotechnol* 4, 471–478, doi:10.1111/j.1751-7915.2010.00196.x (2011).

36 Ingram, L. O. Adaptation of membrane lipids to alcohols. *J. Bacteriol.* 125, 670–678 (1976).

37 Beaven, M. J., Charpentier, C. & Rose, A. H. Production and tolerance of ethanol in relation to phospholipid fatty-acyl composition in *Saccharomyces cerevisiae* NCYC 431. *J. Gen. Microbiol.* 128, 1447–1455 (1982).

38 Rigomier, D., Bohin, J. P. & Lubochinsky, B. Effects of ethanol and methanol on lipid metabolism in *Bacillus subtilis*. *J. Gen. Microbiol.* 121, 139–149 (1980).

39 Borden, J. R. & Papoutsakis, E. T. Dynamics of genomic-library enrichment and identification of solvent tolerance genes for *Clostridium acetobutylicum*. *Appl. Environ. Microbiol.* 73, 3061–3068, doi:10.1128/AEM.02296-06 (2007).

40 Lepage, C., Fayolle, F., Hermann, M. & Vandecasteele, J. P. Changes in membrane lipid composition of *Clostridium acetobutylicum* during acetone-butanol fermentation: Effects of solvents, growth temperature and pH. *J. Gen. Microbiol.* 133, 103–110 (1987).

41 Sakaki, T. *et al.* Sterol glycosides and cerebrosides accumulate in *Pichia pastoris*, *Rhynchosporium secalis* and other fungi under normal conditions or under heat shock and ethanol stress. *Yeast* 18, 679–695, doi:10.1002/yea.720 (2001).

42 Chen, G., Wang, G. Y., Li, X., Waters, B. & Davies, J. Enhanced production of microbial metabolites in the presence of dimethyl sulfoxide. *J. Antibiot. (Tokyo)* 53, 1145–1153 (2000).

43 Doull, J. L., Singh, A. K., Hoare, M. & Ayer, S. W. Conditions for the production of jadomycin B by *Streptomyces venezuelae* ISP5230: Effects of heat-shock, ethanol treatment and phage infection. *J. Ind. Microbiol.* 13, 120–125, doi:Doi 10.1007/Bf01584109 (1994).

44 Gu, W. L., An, G. H. & Johnson, E. A. Ethanol increases carotenoid production in *Phaffia rhodozyma*. *J. Ind. Microbiol. Biotechnol.* 19, 114–117, doi:DOI 10.1038/sj.jim.2900425 (1997).

45 Abouzied, M. M. & Reddy, C. A. Direct fermentation of potato starch to ethanol by cocultures of *Aspergillus niger* and *Saccharomyces cerevisiae*. *Appl. Environ. Microbiol.* 52, 1055–1059 (1986).

46 Luo, L. H. *et al.* Improved ethanol tolerance in *Escherichia coli* by changing the cellular fatty acids composition through genetic manipulation. *Biotechnol. Lett.* 31, 1867–1871, doi:DOI 10.1007/s10529-009-0092-4 (2009).

47 Vinayavekhin, N., Homan, E. A. & Saghatelian, A. Exploring disease through metabolomics. *ACS Chem. Biol.* 5, 91–103, doi:10.1021/cb900271r (2009).

48 Vinayavekhin, N., Mahipant, G., Vangnai, A. S. & Sangvanich, P. Untargeted metabolomics analysis revealed changes in the composition of glycerolipids and phospholipids in *Bacillus subtilis* under 1-butanol stress. *Appl. Microbiol. Biotechnol.* 99, 5971–5983, doi:10.1007/s00253-015-6692-0 (2015).

49 Vinayavekhin, N. & Saghatelian, A. Regulation of alkyl-dihydrothiazole-carboxylates (ATCs) by iron and the pyochelin gene cluster in *Pseudomonas aeruginosa*. *ACS Chem. Biol.* 4, 617–623, doi:Export Date 26 August 2013 (2009).

50 Clark, D. S., Bordner, P., Galdrich, E. H., Kabler, P. W. & Huff, C. B. *Applied Microbiology*. (International Book Company, 1958).

51 Barratt, R. W., Johnson, G. B. & Ogata, W. N. Wild-type and mutant stocks of *Aspergillus nidulans*. *Genetics* 52, 233–246 (1965).

52 Vinayavekhin, N. *et al.* Serum lipidomics analysis of ovariectomized rats under *Curcuma comosa* treatment. *J. Ethnopharmacol.* 192, 273–282, doi:10.1016/j.jep.2016.07.054 (2016).

53 Vinayavekhin, N., Mahipant, G., Vangnai, A. S. & Sangvanich, P. Untargeted metabolomics analysis revealed changes in the composition of glycerolipids and phospholipids in *Bacillus subtilis* under 1-butanol stress. *Applied Microbiology and Biotechnology* 99, 5971–5983, doi:10.1007/s00253-015-6692-0 (2015).

54 Smith, C. A., Want, E. J., O'Maille, G., Abagyan, R. & Siuzdak, G. XCMS: Processing mass spectrometry data for metabolite profiling using nonlinear peak alignment, matching, and identification. *Anal. Chem.* 78, 779–787, doi:10.1021/ac051437y (2006).

55 Paschos, T., Xiros, C. & Christakopoulos, P. Ethanol effect on metabolic activity of the ethalogenic fungus Fusarium oxysporum. *BMC Biotechnol.* 15, 15, doi:10.1186/s12896-015-0130-3 (2015).

56 Meyrial, V., Delgenes, J. P., Romieu, C., Moletta, R. & Gounot, A. M. Ethanol tolerance and activity of plasma-membrane ATPase in *Pichia stipitis* grown on D-xylose or on D-glucose. *Enzyme and Microbial Technology* 17, 535–540, doi:10.1016/0141-0229(94)00065-Y (1995).

57 Carrasco, S. & Mérida, I. Diacylglycerol, when simplicity becomes complex. *Trends in Biochemical Sciences* 32, 27–36, doi:10.1016/j.tibs.2006.11.004 (2007).

58 Kanehisa, M. & Goto, S. KEGG: kyoto encyclopedia of genes and genomes. *Nucleic Acids Res.* 28, 27–30 (2000).

59 Tan, W. J. *et al.* Diacylglycerol acyltransferase and diacylglycerol kinase modulate triacylglycerol and phosphatidic acid production in the plant response to freezing stress. *Plant Physiol.* 177, 1303–1318, doi:10.1104/pp.18.00402 (2018).

60 Fan, J., Yu, L. & Xu, C. A central role for triacylglycerol in membrane lipid breakdown, fatty acid beta-oxidation, and plant survival under extended darkness. *Plant Physiol.* 174, 1517–1530, doi:10.1104/pp.17.00653 (2017).

61 Ianutsevich, E. A., Danilova, O. A., Groza, N. V. & Tereshina, V. M. Membrane lipids and cytosol carbohydrates in *Aspergillus niger* under osmotic, oxidative, and cold impact. *Microbiology* 85, 302–310, doi:10.1134/S0026261716030152 (2016).

62 Kim, H. U. *et al.* Endoplasmic reticulum-located PDAT1-2 from castor bean enhances hydroxy fatty acid accumulation in transgenic plants. *Plant Cell Physiol* 52, 983–993, doi:10.1093/pcp/pcr051 (2011).

63 Byrdwell, W. C. & Neff, W. E. Analysis of hydroxy-containing seed oils using atmospheric pressure chemical ionization mass spectrometry. *J. Liq. Chromatogr. Rel. Technol.* 21, 1485–1501, doi:10.1080/10826079808000529 (1998).

64 Hayes, D. G., Kleiman, R. & Phillips, B. S. The triglyceride composition, structure, and presence of estolides in the oils of *Lesquerella* and related species. *J. Am. Oil Chem. Soc.* 72, 559–569, doi:10.1007/Bf02638857 (1995).

65 Morris, L. J. & Hall, S. W. The structure of the glycerides of ergot oils. *Lipids* 1, 188–196, doi:10.1007/BF02531871 (1966).

66 Meesapyodsuk, D. & Qiu, X. An oleate hydroxylase from the fungus *Claviceps purpurea*: cloning, functional analysis, and expression in *Arabidopsis*. *Plant Physiol.* 147, 1325–1333, doi:10.1104/pp.108.117168 (2008).

67 Sajbidor, J., Ciesarova, Z. & Smogrovicova, D. Influence of ethanol on the lipid content and fatty acid composition of *Saccharomyces cerevisiae*. *Folia Microbiol. (Praha)* 40, 508–510 (1995).

68 Felenbok, B., Flipphi, M. & Nikolaev, I. Ethanol catabolism in *Aspergillus nidulans*: A model system for studying gene regulation. *Progress in Nucleic Acid Research and Molecular Biology* 69, 149–204, doi:10.1016/S0079-6603(01)69047-0 (2001).

Appendix 1

Figure A1. List of MS/MS Spectra (as referred to in Tables 1–2 and 4)

List of categories

List of Abbreviations

DAG	diacylglycerol
FA	fatty acid
hDAG	hydroxy-diacylglycerol
hTAG	hydroxy-triacylglycerol
LPA	lysophosphatidic acid
LPC	lysophosphatidylcholine
LPE	lysophosphatidylethanolamine
LPG	lysophosphatidylglycerol
LPI	lysophosphatidylinositol
MAG	monoacylglycerol
MF	molecular formula
PA	phosphatidic acid
PC	phosphatidylcholine
PE	phosphatidylethanolamine
PG	phosphatidylglycerol
PI	phosphatidylinositol
PS	phosphatidylserine
TAG	triacylglycerol

Upregulated positive-mode ions in ethanol-treated extracellular samples

m/z 874.7830 at 48.3 min – $[M + NH_4]^+$ of TAG (16:0/18:1/18:2)

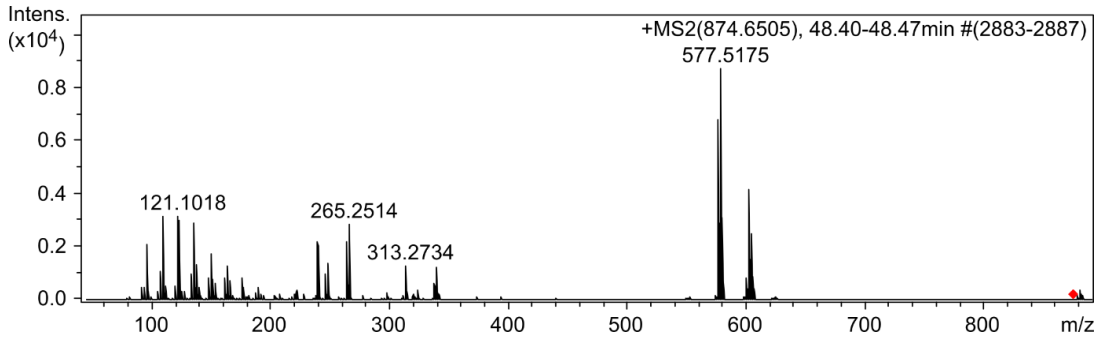

Measured m/z	Possible MF	Possible structural assignment
95.0861	$C_7H_{11}^+$	Fragment of acyl chains
109.1021	$C_8H_{13}^+$	Fragment of acyl chains
121.1018	$C_9H_{13}^+$	Fragment of acyl chains
123.1173	$C_9H_{15}^+$	Fragment of acyl chains
135.1181	$C_{10}H_{15}^+$	Fragment of acyl chains
149.1329	$C_{11}H_{17}^+$	Fragment of acyl chains
163.1471	$C_{12}H_{19}^+$	Fragment of acyl chains
175.1502	$C_{13}H_{19}^+$	Fragment of acyl chains
239.2371	$C_{16}H_{31}O^+$	Acylium ion from breakage of acyl chain C16:0
245.2253	$C_{18}H_{29}^+$	Fragment of acyl chains
247.2405	$C_{18}H_{31}^+$	Fragment of acyl chains
263.2353	$C_{18}H_{31}O^+$	Acylium ion from breakage of acyl chain C18:2
265.2514	$C_{18}H_{33}O^+$	Acylium ion from breakage of acyl chain C18:1
313.2734	$C_{19}H_{37}O_3^+$	MAG (16:0) – H_2O
339.2888	$C_{21}H_{39}O_3^+$	MAG (18:1) – H_2O
575.5033	$C_{37}H_{67}O_4^+$	DAG (16:0/18:2) – H_2O
577.5175	$C_{37}H_{69}O_4^+$	DAG (16:0/18:1) – H_2O
601.5177	$C_{39}H_{69}O_4^+$	DAG (18:1/18:2) – H_2O
603.5307	$C_{39}H_{71}O_4^+$	DAG (18:1/18:2) – H_2O + H_2

m/z 898.7839 at 48.1 min – $[M + NH_4]^+$ of TAG (18:1/18:2/18:2)

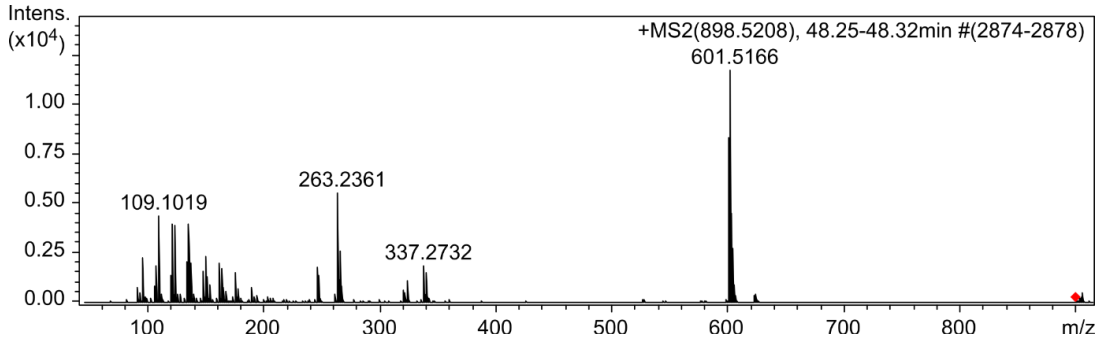

Measured m/z	Possible MF	Possible structural assignment
95.0855	$C_7H_{11}^+$	Fragment of acyl chains
109.1019	$C_8H_{13}^+$	Fragment of acyl chains
121.1026	$C_9H_{13}^+$	Fragment of acyl chains
123.1175	$C_9H_{15}^+$	Fragment of acyl chains
135.1177	$C_{10}H_{15}^+$	Fragment of acyl chains
149.1323	$C_{11}H_{17}^+$	Fragment of acyl chains
161.1323	$C_{12}H_{17}^+$	Fragment of acyl chains
163.1479	$C_{12}H_{19}^+$	Fragment of acyl chains
175.1480	$C_{13}H_{19}^+$	Fragment of acyl chains
245.2251	$C_{18}H_{29}^+$	Fragment of acyl chains
263.2361	$C_{18}H_{31}O^+$	Acylium ion from breakage of acyl chain C18:2
337.2732	$C_{21}H_{37}O_3^+$	MAG (18:2) – H_2O
599.5034	$C_{39}H_{67}O_4^+$	DAG (18:2/18:2) – H_2O
601.5166	$C_{39}H_{69}O_4^+$	DAG (18:1/18:2) – H_2O

m/z 900.7989 at 48.6 min – $[M + NH_4]^+$ of TAG (18:1/18:1/18:2)

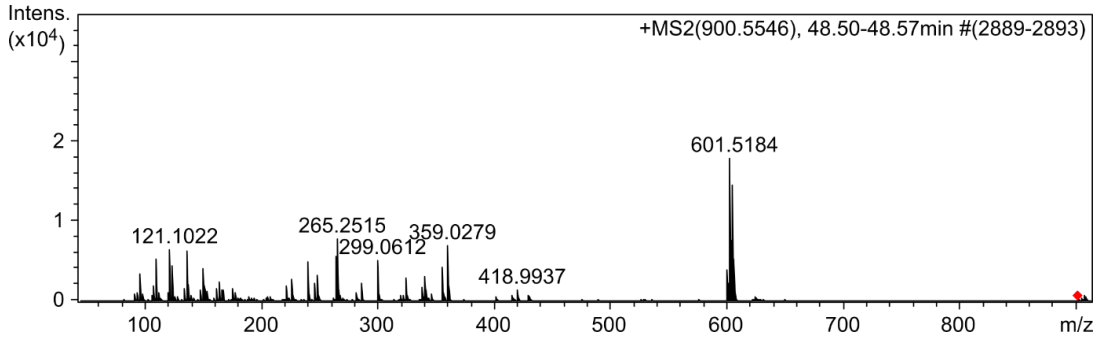

Measured m/z	Possible MF	Possible structural assignment
95.0858	$C_7H_{11}^+$	Fragment of acyl chains
109.1019	$C_8H_{13}^+$	Fragment of acyl chains
121.1022	$C_9H_{13}^+$	Fragment of acyl chains
123.1172	$C_9H_{15}^+$	Fragment of acyl chains
135.1173	$C_{10}H_{15}^+$	Fragment of acyl chains
149.1328	$C_{11}H_{17}^+$	Fragment of acyl chains
163.1481	$C_{12}H_{19}^+$	Fragment of acyl chains
175.1502	$C_{13}H_{19}^+$	Fragment of acyl chains
247.2412	$C_{18}H_{31}^+$	Fragment of acyl chains
265.2515	$C_{18}H_{33}O^+$	Acylium ion from breakage of acyl chain C18:1
601.5184	$C_{39}H_{69}O_4^+$	DAG (18:1/18:2) – H_2O
603.5334	$C_{39}H_{71}O_4^+$	DAG (18:1/18:1) – H_2O

m/z 902.8136 at 48.7 min – $[M + NH_4]^+$ of TAG (18:1/18:1/18:1)

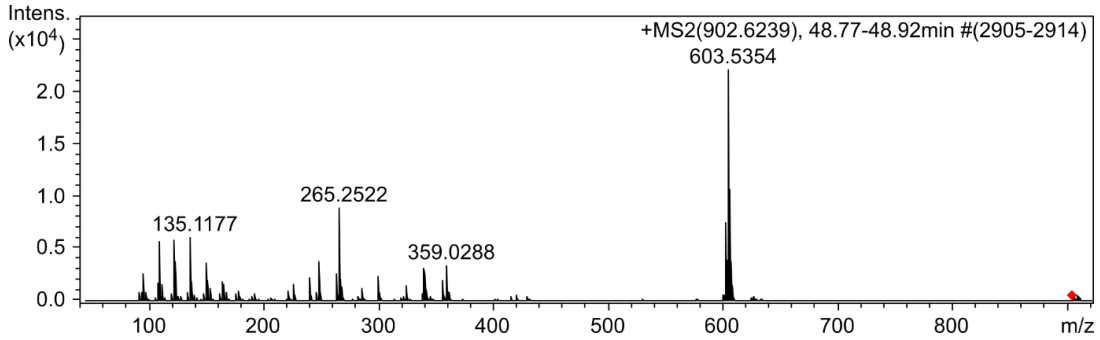

Measured m/z	Possible MF	Possible structural assignment
95.0861	$C_7H_{11}^+$	Fragment of acyl chains
109.1023	$C_8H_{13}^+$	Fragment of acyl chains
121.1019	$C_9H_{13}^+$	Fragment of acyl chains
135.1177	$C_{10}H_{15}^+$	Fragment of acyl chains
149.1330	$C_{11}H_{17}^+$	Fragment of acyl chains
247.2414	$C_{18}H_{31}^+$	Fragment of acyl chains
265.2522	$C_{18}H_{33}O^+$	Acylium ion from breakage of acyl chain C18:1
339.2900	$C_{21}H_{39}O_3^+$	MAG (18:1) – H_2O
601.5194	$C_{39}H_{69}O_4^+$	DAG (18:1/18:1) – H_2O – H_2
603.5354	$C_{39}H_{71}O_4^+$	DAG (18:1/18:1) – H_2O

m/z 904.8272 at 48.9 min – $[M + NH_4]^+$ of TAG (18:0/18:1/18:1)

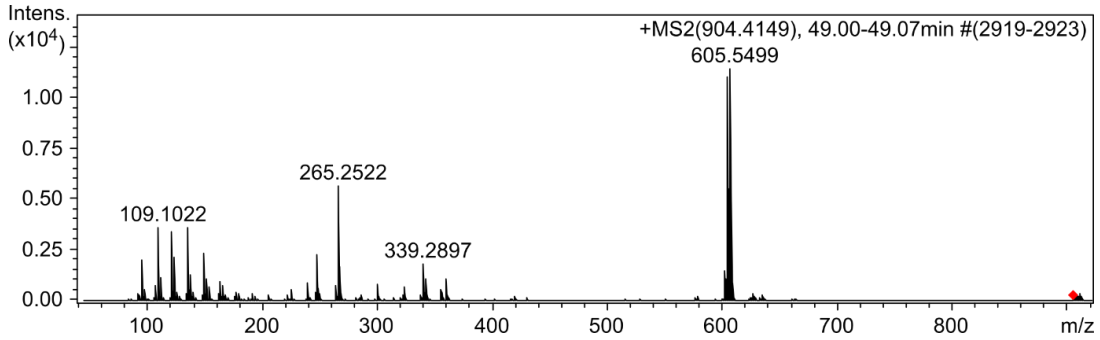

Measured m/z	Possible MF	Possible structural assignment
95.0861	$C_7H_{11}^+$	Fragment of acyl chains
109.1022	$C_8H_{13}^+$	Fragment of acyl chains
121.1023	$C_9H_{13}^+$	Fragment of acyl chains
135.1180	$C_{10}H_{15}^+$	Fragment of acyl chains
149.1334	$C_{11}H_{17}^+$	Fragment of acyl chains
247.2417	$C_{18}H_{31}^+$	Fragment of acyl chains
265.2522	$C_{18}H_{33}O^+$	Acylium ion from breakage of acyl chain C18:1
339.2897	$C_{21}H_{39}O_3^+$	MAG (18:1) – H_2O
603.5354	$C_{39}H_{71}O_4^+$	DAG (18:1/18:1) – H_2O
605.5499	$C_{39}H_{73}O_4^+$	DAG (18:0/18:1) – H_2O

Upregulated positive-mode ions in ethanol-treated intracellular samples

m/z 634.5394 at 43.8 min – $[M + NH_4]^+$ of DAG (18:2/18:2)

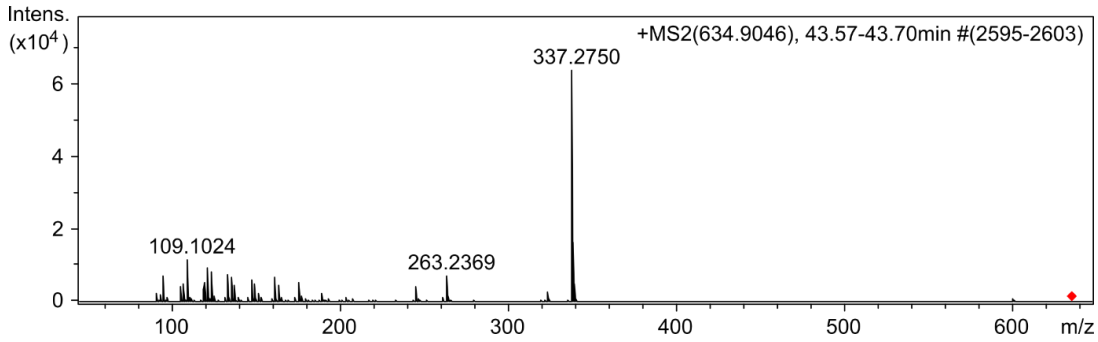

Measured m/z	Possible MF	Possible structural assignment
95.0858	$C_7H_{11}^+$	Fragment of acyl chains
109.1020	$C_8H_{13}^+$	Fragment of acyl chains
121.1020	$C_9H_{13}^+$	Fragment of acyl chains
123.1170	$C_9H_{15}^+$	Fragment of acyl chains
133.1020	$C_{10}H_{13}^+$	Fragment of acyl chains
135.1170	$C_{10}H_{15}^+$	Fragment of acyl chains
147.1170	$C_{11}H_{15}^+$	Fragment of acyl chains
161.1330	$C_{12}H_{17}^+$	Fragment of acyl chains
175.1490	$C_{13}H_{19}^+$	Fragment of acyl chains
189.1640	$C_{14}H_{21}^+$	Fragment of acyl chains
245.2260	$C_{18}H_{29}^+$	Fragment of acyl chains
263.2370	$C_{18}H_{31}O^+$	Acylium ion from breakage of acyl chain C18:2
337.2750	$C_{21}H_{37}O_3^+$	MAG (18:2) – H_2O

m/z 636.5550 at 44.4 min – $[M + NH_4]^+$ of DAG (18:1/18:2)

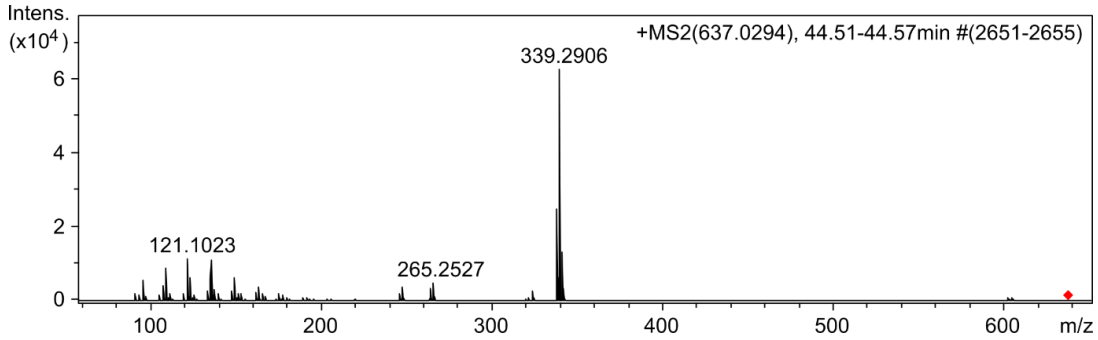

Measured m/z	Possible MF	Possible structural assignment
95.0863	$C_7H_{11}^+$	Fragment of acyl chains
109.1020	$C_8H_{13}^+$	Fragment of acyl chains
121.1020	$C_9H_{13}^+$	Fragment of acyl chains
135.1180	$C_{10}H_{15}^+$	Fragment of acyl chains
245.2260	$C_{18}H_{29}^+$	Fragment of acyl chains
247.2410	$C_{18}H_{31}^+$	Fragment of acyl chains
263.2360	$C_{18}H_{31}O^+$	Acylium ion from breakage of acyl chain C18:2
265.2530	$C_{18}H_{33}O^+$	Acylium ion from breakage of acyl chain C18:1
337.2750	$C_{21}H_{37}O_3^+$	MAG (18:2) – H_2O
339.2910	$C_{21}H_{39}O_3^+$	MAG (18:1) – H_2O

m/z 638.5700 at 44.9 min – $[M + NH_4]^+$ of DAG (18:1/18:1)

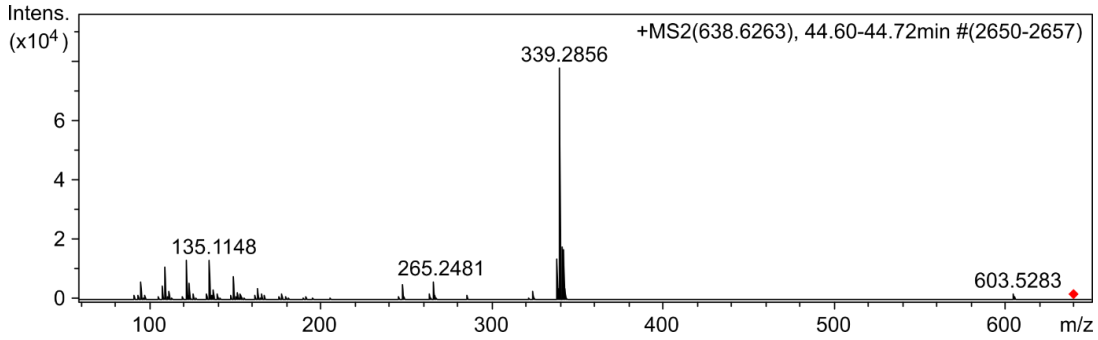

Measured m/z	Possible MF	Possible structural assignment
109.1000	$C_8H_{13}^+$	Fragment of acyl chains
121.0990	$C_9H_{13}^+$	Fragment of acyl chains
135.1150	$C_{10}H_{15}^+$	Fragment of acyl chains
149.1300	$C_{11}H_{17}^+$	Fragment of acyl chains
245.2260	$C_{18}H_{29}^+$	Fragment of acyl chains
247.2370	$C_{18}H_{31}^+$	Fragment of acyl chains
265.2480	$C_{18}H_{33}O^+$	Acylium ion from breakage of acyl chain C18:1
339.2860	$C_{21}H_{39}O_3^+$	MAG (18:1) – H_2O

m/z 640.5815 at 45.3 min – $[M + NH_4]^+$ of DAG (18:0/18:1)

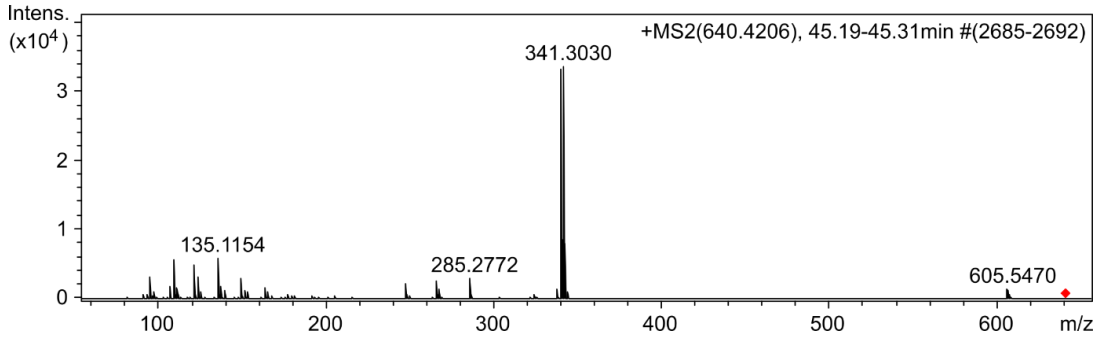

Measured m/z	Possible MF	Possible structural assignment
95.0848	$C_7H_{11}^+$	Fragment of acyl chains
109.1010	$C_8H_{13}^+$	Fragment of acyl chains
121.1010	$C_9H_{13}^+$	Fragment of acyl chains
135.1150	$C_{10}H_{15}^+$	Fragment of acyl chains
247.2400	$C_{18}H_{31}^+$	Fragment of acyl chains
265.2500	$C_{18}H_{33}O^+$	Acylium ion from breakage of acyl chain C18:1
267.2640	$C_{18}H_{35}O^+$	Acylium ion from breakage of acyl chain C18:0
339.2880	$C_{21}H_{39}O_3^+$	MAG (18:1) – H_2O
341.3030	$C_{21}H_{41}O_3^+$	MAG (18:0) – H_2O

m/z 662.5667 at 44.6 min – $[M + NH_4]^+$ of DAG (18:2/20:2)

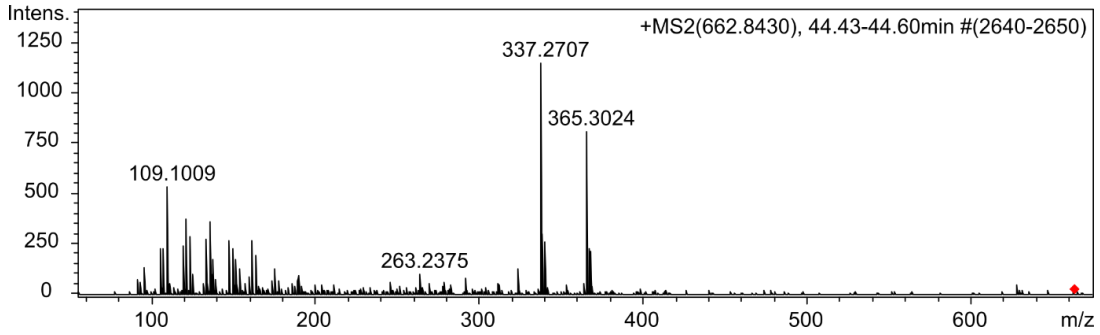

Measured m/z	Possible MF	Possible structural assignment
95.0846	$C_7H_{11}^+$	Fragment of acyl chains
109.1009	$C_8H_{13}^+$	Fragment of acyl chains
121.0997	$C_9H_{13}^+$	Fragment of acyl chains
135.1148	$C_{10}H_{15}^+$	Fragment of acyl chains
147.1149	$C_{11}H_{15}^+$	Fragment of acyl chains
161.1295	$C_{12}H_{17}^+$	Fragment of acyl chains
337.2707	$C_{21}H_{37}O_3^+$	MAG (18:2) – H_2O
365.3024	$C_{23}H_{41}O_3^+$	MAG (20:2) – H_2O

m/z 664.5833 at 45.1 min – $[M + NH_4]^+$ of DAG (18:2/20:1) and some DAG (18:1/20:2)

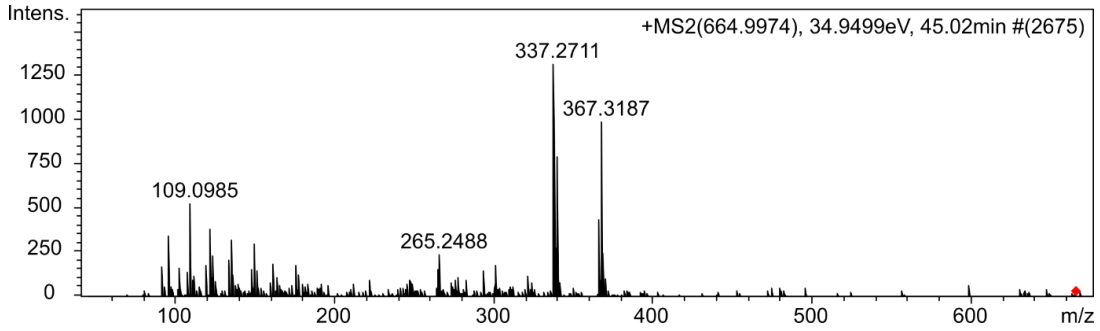

Measured m/z	Possible MF	Possible structural assignment
95.0836	$C_7H_{11}^+$	Fragment of acyl chains
109.0985	$C_8H_{13}^+$	Fragment of acyl chains
121.0996	$C_9H_{13}^+$	Fragment of acyl chains
135.1169	$C_{10}H_{15}^+$	Fragment of acyl chains
149.1286	$C_{11}H_{17}^+$	Fragment of acyl chains
161.1298	$C_{12}H_{17}^+$	Fragment of acyl chains
265.2488	$C_{18}H_{33}O^+$	Acylium ion from breakage of acyl chain C18:1
337.2711	$C_{21}H_{37}O_3^+$	MAG (18:2) – H_2O
339.2854	$C_{21}H_{39}O_3^+$	MAG (18:1) – H_2O
365.2987	$C_{23}H_{41}O_3^+$	MAG (20:2) – H_2O
367.3187	$C_{23}H_{43}O_3^+$	MAG (20:1) – H_2O

m/z 816.7036 at 47.6 min – $[M + NH_4]^+$ of TAG (12:0/18:2/18:2) and isomers

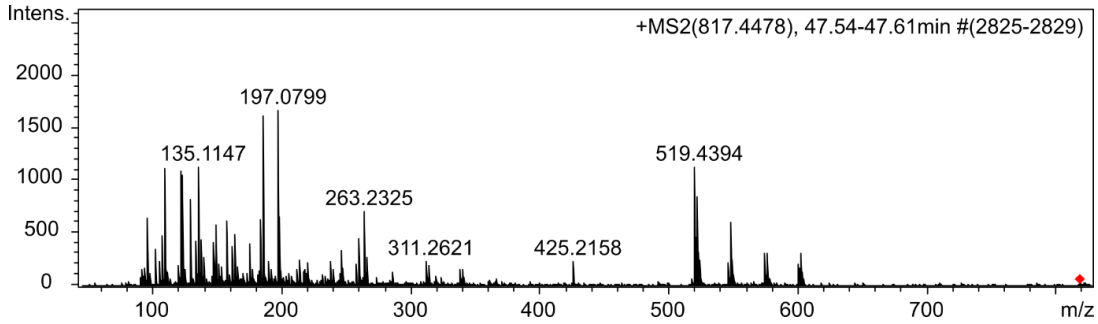

Measured m/z	Possible MF	Possible structural assignment
95.0835	$C_7H_{11}^+$	Fragment of acyl chains
109.1007	$C_8H_{13}^+$	Fragment of acyl chains
121.1000	$C_9H_{13}^+$	Fragment of acyl chains
123.1153	$C_9H_{15}^+$	Fragment of acyl chains
135.1147	$C_{10}H_{15}^+$	Fragment of acyl chains
263.2325	$C_{18}H_{31}O^+$	Acylium ion from breakage of acyl chain C18:2
311.2621	$C_{19}H_{35}O_3^+$	MAG (16:1) – H_2O
313.2708	$C_{19}H_{37}O_3^+$	MAG (16:0) – H_2O
337.2704	$C_{21}H_{37}O_3^+$	MAG (18:2) – H_2O
339.2812	$C_{21}H_{39}O_3^+$	MAG (18:1) – H_2O
519.4394	$C_{33}H_{59}O_4^+$	DAG (12:0/18:2) – H_2O
521.4539	$C_{33}H_{61}O_4^+$	DAG (12:0/18:1) – H_2O
547.4702	$C_{35}H_{63}O_4^+$	DAG (14:0/18:2) – H_2O
573.4778	$C_{37}H_{65}O_4^+$	DAG (16:0/18:3) – H_2O
575.4995	$C_{37}H_{67}O_4^+$	DAG (16:0/18:2) – H_2O
599.4956	$C_{39}H_{67}O_4^+$	DAG (18:2/18:2) – H_2O
601.5107	$C_{39}H_{69}O_4^+$	DAG (18:1/18:2) – H_2O

m/z 844.7360 at 47.8 min – $[M + NH_4]^+$ of TAG (14:0/18:2/18:2) and isomers

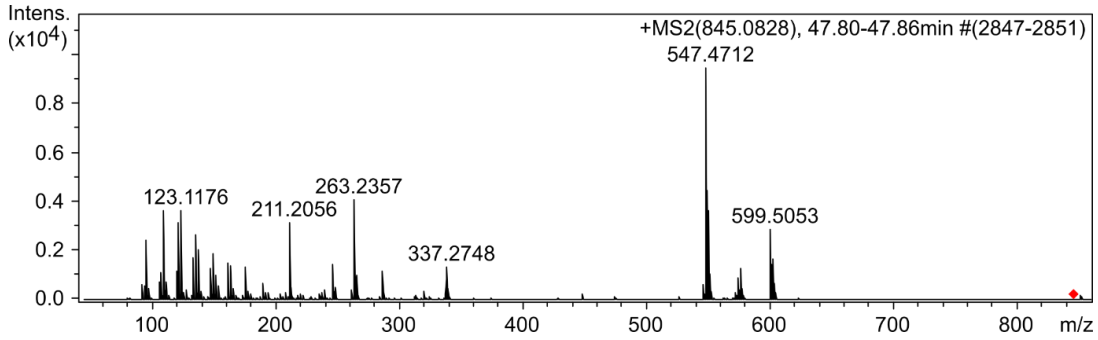

Measured m/z	Possible MF	Possible structural assignment
95.0857	$C_7H_{11}^+$	Fragment of acyl chains
109.1025	$C_8H_{13}^+$	Fragment of acyl chains
123.1176	$C_9H_{15}^+$	Fragment of acyl chains
135.1174	$C_{10}H_{15}^+$	Fragment of acyl chains
149.1335	$C_{11}H_{17}^+$	Fragment of acyl chains
161.1322	$C_{12}H_{17}^+$	Fragment of acyl chains
175.1481	$C_{13}H_{19}^+$	Fragment of acyl chains
211.2056	$C_{14}H_{27}O^+$	Acylium ion from breakage of acyl chain C14:0
245.2257	$C_{18}H_{29}^+$	Fragment of acyl chains
263.2357	$C_{18}H_{31}O^+$	Acylium ion from breakage of acyl chain C18:2
285.2414	$C_{17}H_{33}O_3^+$	MAG (14:0) – H_2O
337.2748	$C_{21}H_{37}O_3^+$	MAG (18:2) – H_2O
547.4712	$C_{35}H_{63}O_4^+$	DAG (14:0/18:2) – H_2O
573.4852	$C_{37}H_{65}O_4^+$	DAG (16:0/18:2) – H_2O – H_2
575.5025	$C_{37}H_{67}O_4^+$	DAG (16:0/18:2) – H_2O
599.5053	$C_{39}H_{67}O_4^+$	DAG (18:2/18:2) – H_2O

m/z 862.7455 at 46.9 min – $[M + NH_4]^+$ of hTAG (16:0/16:1(OH)/18:2)

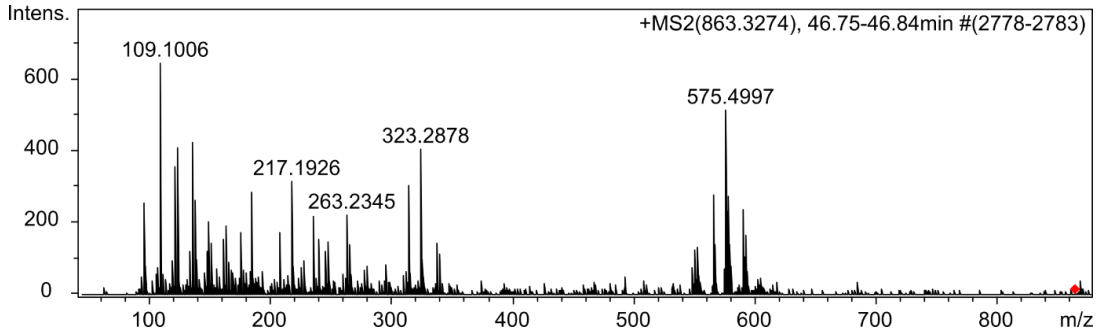

Measured m/z	Possible MF	Possible structural assignment
95.0828	$C_7H_{11}^+$	Fragment of acyl chains
109.1006	$C_8H_{13}^+$	Fragment of acyl chains
121.0990	$C_9H_{13}^+$	Fragment of acyl chains
123.1150	$C_9H_{15}^+$	Fragment of acyl chains
135.1148	$C_{10}H_{15}^+$	Fragment of acyl chains
149.1301	$C_{11}H_{17}^+$	Fragment of acyl chains
163.1445	$C_{12}H_{19}^+$	Fragment of acyl chains
175.1471	$C_{13}H_{19}^+$	Fragment of acyl chains
217.1926	$C_{16}H_{25}^+$	Fragment of acyl chains
235.2011	$C_{16}H_{27}O^+$	Acylium ion of hydroxy fatty acyl chain C16:1 – H_2O
239.2337	$C_{16}H_{31}O^+$	Acylium ion from breakage of acyl chain C16:0
263.2345	$C_{18}H_{31}O^+$	Acylium ion from breakage of acyl chain C18:2
313.2715	$C_{19}H_{37}O_3^+$	MAG (16:0) – H_2O
323.2878	$C_{21}H_{39}O_2^+$	MAG (18:1) – $2H_2O$ (?)
337.2700	$C_{21}H_{37}O_3^+$	MAG (18:2) – H_2O
549.4886	$C_{35}H_{65}O_4^+$	DAG (16:1/16:0) – H_2O
551.4956	$C_{35}H_{67}O_4^+$	DAG (16:1/16:0) – H_2O + H_2
565.4776	$C_{35}H_{65}O_5^+$	hDAG (16:0/16:1) – H_2O
575.4997	$C_{37}H_{67}O_4^+$	DAG (16:0/18:2) – H_2O
577.5119	$C_{37}H_{69}O_4^+$	DAG (16:0/18:2) – H_2O + H_2
589.4740	$C_{37}H_{65}O_5^+$	hDAG (16:1/18:2) – H_2O
591.4946	$C_{37}H_{67}O_5^+$	hDAG (16:1/18:2) – H_2O + H_2

m/z 864.7565 at 47.2 min – $[M + NH_4]^+$ of hTAG (16:0/16:0/18:2(OH))

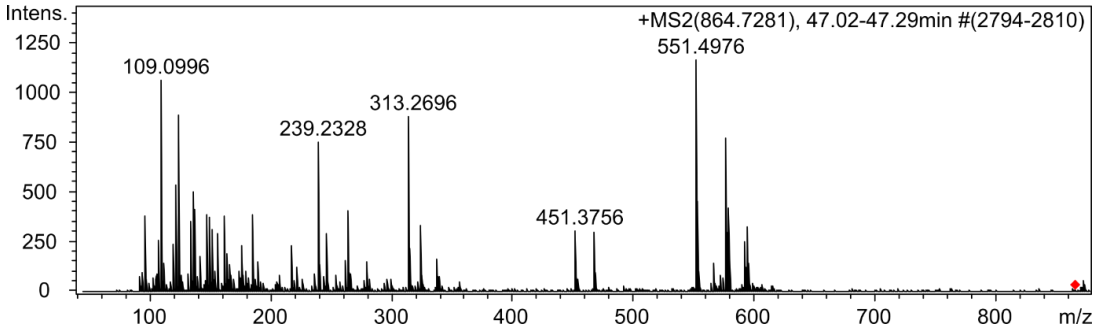

Measured m/z	Possible MF	Possible structural assignment
95.0842	$C_7H_{11}^+$	Fragment of acyl chains
109.0996	$C_8H_{13}^+$	Fragment of acyl chains
123.1146	$C_9H_{15}^+$	Fragment of acyl chains
135.1151	$C_{10}H_{15}^+$	Fragment of acyl chains
147.1147	$C_{11}H_{15}^+$	Fragment of acyl chains
161.1311	$C_{12}H_{17}^+$	Fragment of acyl chains
217.1916	$C_{16}H_{25}^+$	Fragment of acyl chains
239.2328	$C_{16}H_{31}O^+$	Acylium ion from breakage of acyl chain C16:0
263.2312	$C_{18}H_{31}O^+$	Acylium ion from breakage of acyl chain C18:2
279.2285	$C_{18}H_{31}O_2^+$	Acylium ion of hydroxy fatty acyl chain C18:2
313.2696	$C_{19}H_{37}O_3^+$	MAG (16:0) – H_2O
551.4976	$C_{35}H_{67}O_4^+$	DAG (16:0/16:0) – H_2O
575.4985	$C_{37}H_{67}O_4^+$	DAG (16:0/18:2) – H_2O
577.5123	$C_{37}H_{69}O_4^+$	DAG (16:0/18:2) – H_2O + H_2
591.4927	$C_{37}H_{67}O_5^+$	hDAG (16:0/18:2) – H_2O
593.5117	$C_{37}H_{69}O_5^+$	hDAG (16:0/18:2) – H_2O + H_2

m/z 888.7606 at 47.1 min – $[M + NH_4]^+$ of hTAG (16:0/18:2/18:2(OH))

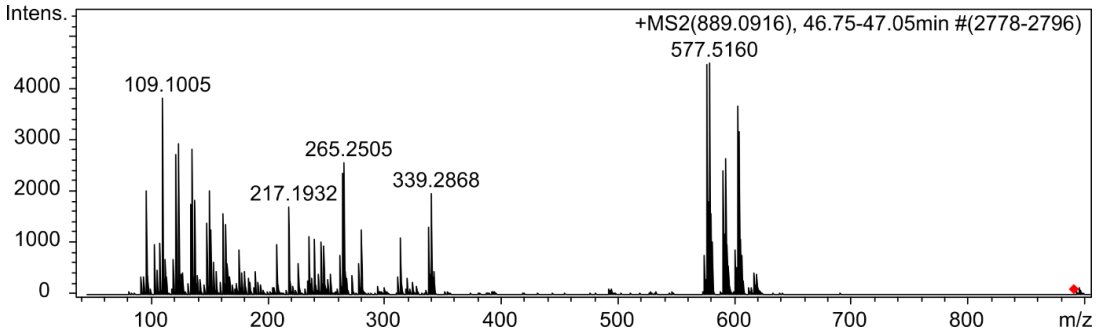

Measured m/z	Possible MF	Possible structural assignment
95.0842	$C_7H_{11}^+$	Fragment of acyl chains
109.1005	$C_8H_{13}^+$	Fragment of acyl chains
121.1004	$C_9H_{13}^+$	Fragment of acyl chains
123.1154	$C_9H_{15}^+$	Fragment of acyl chains
135.1155	$C_{10}H_{15}^+$	Fragment of acyl chains
149.1304	$C_{11}H_{17}^+$	Fragment of acyl chains
161.1306	$C_{12}H_{17}^+$	Fragment of acyl chains
175.1455	$C_{13}H_{19}^+$	Fragment of acyl chains
217.1932	$C_{16}H_{25}^+$	Fragment of acyl chains
263.2350	$C_{18}H_{31}O^+$	Acylium ion from breakage of acyl chain C18:2
265.2505	$C_{18}H_{33}O^+$	Acylium ion from breakage of acyl chain C18:1
279.2291	$C_{18}H_{31}O_2^+$	Acylium ion of hydroxy fatty acyl chain C18:2
313.2717	$C_{19}H_{37}O_3^+$	MAG (16:0) – H_2O
337.2706	$C_{21}H_{37}O_3^+$	MAG (18:2) – H_2O
339.2868	$C_{21}H_{39}O_3^+$	MAG (18:1) – H_2O
575.5004	$C_{37}H_{67}O_4^+$	DAG (16:0/18:2) – H_2O
577.5160	$C_{37}H_{69}O_4^+$	DAG (16:0/18:1) – H_2O
589.4800	$C_{37}H_{65}O_5^+$	hDAG (16:0/18:2) – H_2O – H_2
591.4943	$C_{37}H_{67}O_5^+$	hDAG (16:0/18:2) – H_2O
601.5162	$C_{39}H_{69}O_4^+$	DAG (18:1/18:2) – H_2O (?)
603.5304	$C_{39}H_{71}O_4^+$	DAG (18:0/18:2) – H_2O (?)
615.4941	$C_{39}H_{67}O_5^+$	hDAG (18:2/18:2) – H_2O
617.5096	$C_{39}H_{69}O_5^+$	hDAG (18:1/18:2) – H_2O

m/z 890.7736 at 47.3 min – $[M + NH_4]^+$ of hTAG (16:0/18:1/18:2(OH))

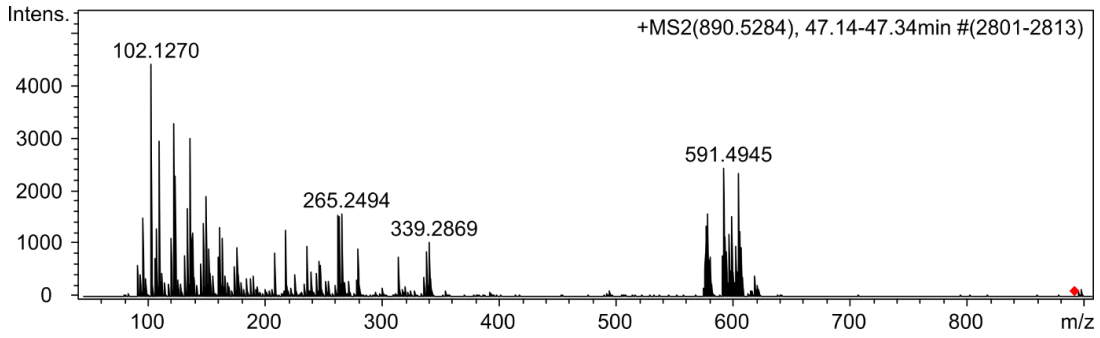

Measured m/z	Possible MF	Possible structural assignment
95.0837	$C_7H_{11}^+$	Fragment of acyl chains
109.1008	$C_8H_{13}^+$	Fragment of acyl chains
121.1008	$C_9H_{13}^+$	Fragment of acyl chains
135.1156	$C_{10}H_{15}^+$	Fragment of acyl chains
149.1315	$C_{11}H_{17}^+$	Fragment of acyl chains
161.1314	$C_{12}H_{17}^+$	Fragment of acyl chains
217.1918	$C_{16}H_{25}^+$	Fragment of acyl chains
263.2346	$C_{18}H_{31}O^+$	Acylium ion from breakage of acyl chain C18:2
265.2494	$C_{18}H_{33}O^+$	Acylium ion from breakage of acyl chain C18:1
279.2280	$C_{18}H_{31}O_2^+$	Acylium ion of hydroxy fatty acyl chain C18:2
313.2697	$C_{19}H_{37}O_3^+$	MAG (16:0) – H_2O
337.2708	$C_{21}H_{37}O_3^+$	MAG (18:2) – H_2O
339.2869	$C_{21}H_{39}O_3^+$	MAG (18:1) – H_2O
575.4987	$C_{37}H_{67}O_4^+$	DAG (16:0/18:2) – H_2O
577.5132	$C_{37}H_{69}O_4^+$	DAG (16:0/18:1) – H_2O
591.4945	$C_{37}H_{67}O_5^+$	hDAG (16:0/18:2) – H_2O
603.5342	$C_{39}H_{71}O_4^+$	DAG (18:0/18:2) – H_2O (?)
617.5115	$C_{39}H_{69}O_5^+$	hDAG (18:1/18:2) – H_2O

m/z 904.8319 at 49.0 min – $[M + NH_4]^+$ of TAG (18:0/18:1/18:1)

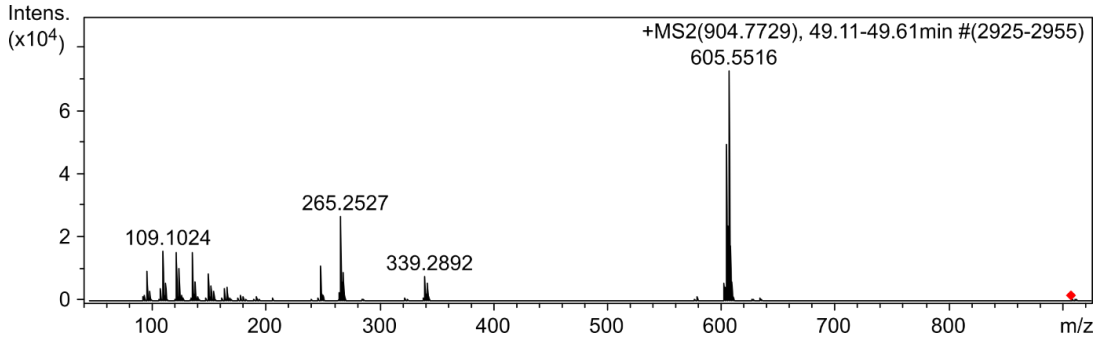

Measured m/z	Possible MF	Possible structural assignment
95.0860	$C_7H_{11}^+$	Fragment of acyl chains
109.1024	$C_8H_{13}^+$	Fragment of acyl chains
121.1023	$C_9H_{13}^+$	Fragment of acyl chains
135.1178	$C_{10}H_{15}^+$	Fragment of acyl chains
149.1330	$C_{11}H_{17}^+$	Fragment of acyl chains
163.1477	$C_{12}H_{19}^+$	Fragment of acyl chains
247.2415	$C_{18}H_{31}^+$	Fragment of acyl chains
265.2527	$C_{18}H_{33}O^+$	Acylium ion from breakage of acyl chain C18:1
339.2892	$C_{21}H_{39}O_3^+$	MAG (18:1) – H_2O
341.3047	$C_{21}H_{41}O_3^+$	MAG (18:0) – H_2O
603.5362	$C_{39}H_{71}O_4^+$	DAG (18:1/18:1) – H_2O
605.5516	$C_{39}H_{73}O_4^+$	DAG (18:0/18:1) – H_2O

m/z 906.8451 at 49.1 min – $[M + NH_4]^+$ of TAG (18:0/18:0/18:1)

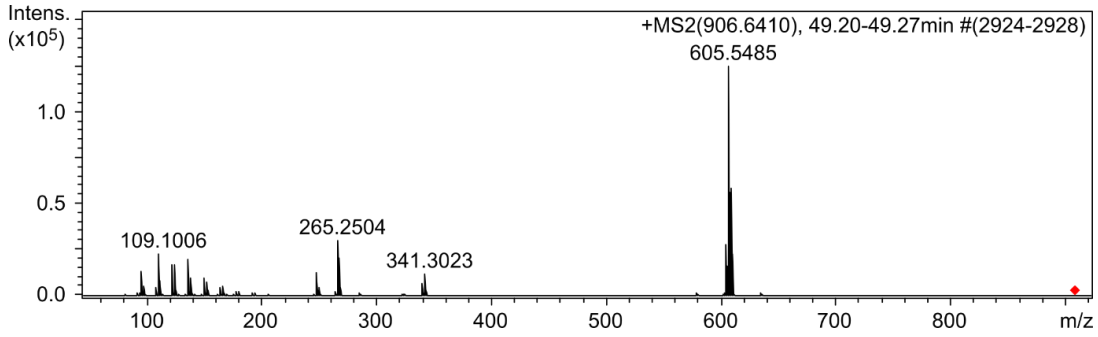

Measured m/z	Possible MF	Possible structural assignment
95.0841	$C_7H_{11}^+$	Fragment of acyl chains
109.1006	$C_8H_{13}^+$	Fragment of acyl chains
121.1005	$C_9H_{13}^+$	Fragment of acyl chains
123.1160	$C_9H_{15}^+$	Fragment of acyl chains
135.1156	$C_{10}H_{15}^+$	Fragment of acyl chains
149.1312	$C_{11}H_{17}^+$	Fragment of acyl chains
247.2394	$C_{18}H_{31}^+$	Fragment of acyl chains
265.2504	$C_{18}H_{33}O^+$	Acylium ion from breakage of acyl chain C18:1
267.2657	$C_{18}H_{35}O^+$	Acylium ion from breakage of acyl chain C18:0
339.2866	$C_{21}H_{39}O_3^+$	MAG (18:1) – H_2O
341.3023	$C_{21}H_{41}O_3^+$	MAG (18:0) – H_2O
603.5319	$C_{39}H_{71}O_4^+$	DAG (18:1/18:1) – H_2O
605.5485	$C_{39}H_{73}O_4^+$	DAG (18:0/18:1) – H_2O
607.5612	$C_{39}H_{75}O_4^+$	DAG (18:0/18:0) – H_2O

m/z 912.7626 at 46.9 min – $[M + NH_4]^+$ of hTAG (18:1/18:2(OH)/18:3) and isomers

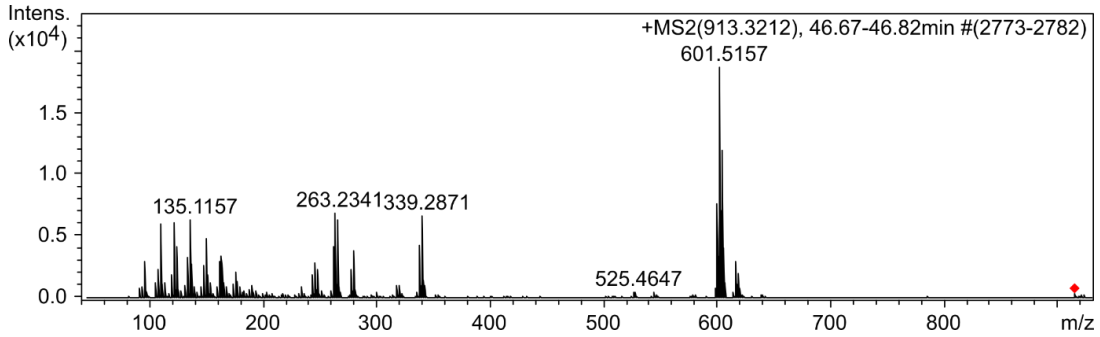

Measured m/z	Possible MF	Possible structural assignment
95.0842	$C_7H_{11}^+$	Fragment of acyl chains
109.1003	$C_8H_{13}^+$	Fragment of acyl chains
121.1003	$C_9H_{13}^+$	Fragment of acyl chains
123.1158	$C_9H_{15}^+$	Fragment of acyl chains
135.1157	$C_{10}H_{15}^+$	Fragment of acyl chains
149.1305	$C_{11}H_{17}^+$	Fragment of acyl chains
161.1309	$C_{12}H_{17}^+$	Fragment of acyl chains
163.1450	$C_{12}H_{19}^+$	Fragment of acyl chains
243.2076	$C_{18}H_{27}^+$	Fragment of acyl chains
245.2236	$C_{18}H_{29}^+$	Fragment of acyl chains
247.2391	$C_{18}H_{31}^+$	Fragment of acyl chains
261.2181	$C_{18}H_{29}O^+$	Acylium ion from breakage of acyl chain C18:3
263.2344	$C_{18}H_{31}O^+$	Acylium ion from breakage of acyl chain C18:2
265.2499	$C_{18}H_{33}O^+$	Acylium ion from breakage of acyl chain C18:1
277.2148	$C_{18}H_{29}O_2^+$	Acylium ion of hydroxy fatty acyl chain C18:3
279.2287	$C_{18}H_{31}O_2^+$	Acylium ion of hydroxy fatty acyl chain C18:2
337.2701	$C_{21}H_{37}O_3^+$	MAG (18:2) – H_2O
339.2871	$C_{21}H_{39}O_3^+$	MAG (18:1) – H_2O
599.4994	$C_{39}H_{67}O_4^+$	DAG (18:1/18:3) – H_2O
601.5157	$C_{39}H_{69}O_4^+$	DAG (18:1/18:2) – H_2O
603.5314	$C_{39}H_{71}O_4^+$	DAG (18:0/18:2) – H_2O (?)
615.4940	$C_{39}H_{67}O_5^+$	hDAG (18:2/18:2) – H_2O
617.5106	$C_{39}H_{69}O_5^+$	hDAG (18:1/18:2) – H_2O

m/z 914.7771 at 47.2 min – $[M + NH_4]^+$ of hTAG (18:1/18:2/18:2(OH))

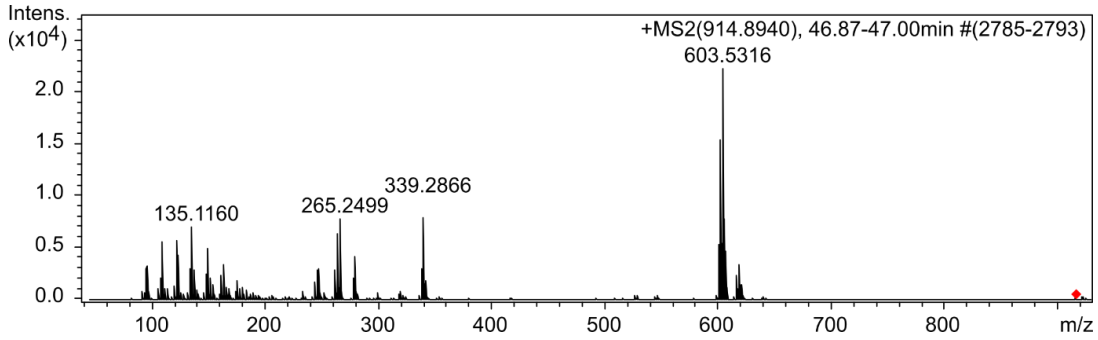

Measured m/z	Possible MF	Possible structural assignment
95.0841	$C_7H_{11}^+$	Fragment of acyl chains
109.1003	$C_8H_{13}^+$	Fragment of acyl chains
121.1004	$C_9H_{13}^+$	Fragment of acyl chains
135.1160	$C_{10}H_{15}^+$	Fragment of acyl chains
149.1307	$C_{11}H_{17}^+$	Fragment of acyl chains
163.1450	$C_{12}H_{19}^+$	Fragment of acyl chains
245.2241	$C_{18}H_{29}^+$	Fragment of acyl chains
247.2396	$C_{18}H_{31}^+$	Fragment of acyl chains
263.2344	$C_{18}H_{31}O^+$	Acylium ion from breakage of acyl chain C18:2
265.2499	$C_{18}H_{33}O^+$	Acylium ion from breakage of acyl chain C18:1
279.2294	$C_{18}H_{31}O_2^+$	Acylium ion of hydroxy fatty acyl chain C18:2
339.2866	$C_{21}H_{39}O_3^+$	MAG (18:1) – H_2O
599.5011	$C_{39}H_{67}O_4^+$	hDAG (18:1/18:2) – $2H_2O$
601.5164	$C_{39}H_{69}O_4^+$	DAG (18:1/18:2) – H_2O
603.5316	$C_{39}H_{71}O_4^+$	DAG (18:0/18:2) – H_2O (?)
615.4950	$C_{39}H_{67}O_5^+$	hDAG (18:2/18:2) – H_2O
617.5100	$C_{39}H_{69}O_5^+$	hDAG (18:1/18:2) – H_2O

m/z 916.7929 at 47.5 min – $[M + NH_4]^+$ of hTAG (18:1/18:1/18:2(OH))

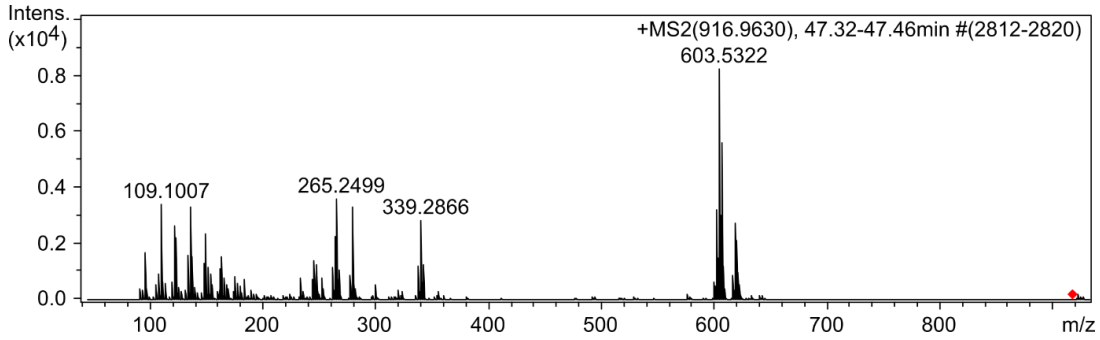

Measured m/z	Possible MF	Possible structural assignment
95.0843	$C_7H_{11}^+$	Fragment of acyl chains
109.1007	$C_8H_{13}^+$	Fragment of acyl chains
121.1006	$C_9H_{13}^+$	Fragment of acyl chains
135.1166	$C_{10}H_{15}^+$	Fragment of acyl chains
149.1306	$C_{11}H_{17}^+$	Fragment of acyl chains
175.1455	$C_{13}H_{19}^+$	Fragment of acyl chains
245.2233	$C_{18}H_{29}^+$	Fragment of acyl chains
247.2393	$C_{18}H_{31}^+$	Fragment of acyl chains
263.2348	$C_{18}H_{31}O^+$	Acylium ion from breakage of acyl chain C18:2
265.2499	$C_{18}H_{33}O^+$	Acylium ion from breakage of acyl chain C18:1
279.2307	$C_{18}H_{31}O_2^+$	Acylium ion of hydroxy fatty acyl chain C18:2
337.2713	$C_{21}H_{37}O_3^+$	MAG (18:2) – H_2O
339.2866	$C_{21}H_{39}O_3^+$	MAG (18:1) – H_2O
341.3017	$C_{21}H_{41}O_3^+$	MAG (18:0) – H_2O
601.5167	$C_{39}H_{69}O_4^+$	DAG (18:1/18:2) – H_2O
603.5322	$C_{39}H_{71}O_4^+$	DAG (18:1/18:1) – H_2O
605.5475	$C_{39}H_{73}O_4^+$	DAG (18:0/18:1) – H_2O (?)
617.5099	$C_{39}H_{69}O_5^+$	hDAG (18:1/18:2) – H_2O
619.5271	$C_{39}H_{71}O_5^+$	hDAG (18:0/18:2) – H_2O (?)

m/z 918.8068 at 47.7 min – $[M + NH_4]^+$ of hTAG (18:0/18:1/18:2(OH))

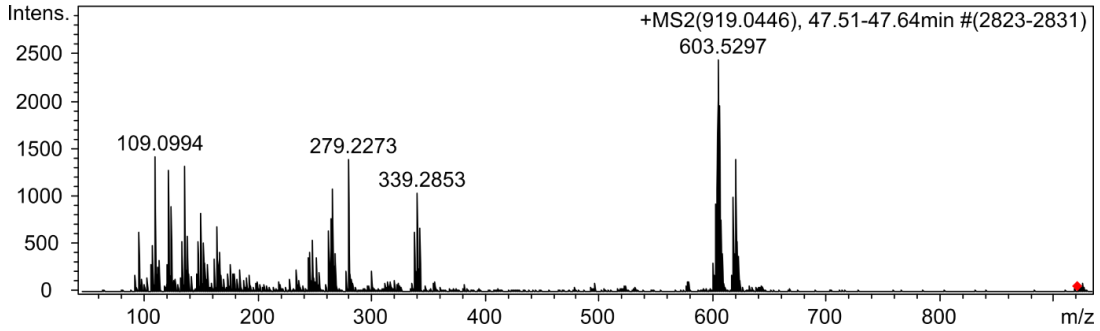

Measured m/z	Possible MF	Possible structural assignment
95.0845	$C_7H_{11}^+$	Fragment of acyl chains
109.0994	$C_8H_{13}^+$	Fragment of acyl chains
121.0993	$C_9H_{13}^+$	Fragment of acyl chains
135.1146	$C_{10}H_{15}^+$	Fragment of acyl chains
149.1303	$C_{11}H_{17}^+$	Fragment of acyl chains
247.2390	$C_{18}H_{31}^+$	Fragment of acyl chains
263.2329	$C_{18}H_{31}O^+$	Acylium ion from breakage of acyl chain C18:2
265.2503	$C_{18}H_{33}O^+$	Acylium ion from breakage of acyl chain C18:1
279.2273	$C_{18}H_{31}O_2^+$	Acylium ion of hydroxy fatty acyl chain C18:2
337.2688	$C_{21}H_{37}O_3^+$	MAG (18:2) – H_2O
339.2853	$C_{21}H_{39}O_3^+$	MAG (18:1) – H_2O
341.3026	$C_{21}H_{41}O_3^+$	MAG (18:0) – H_2O
603.5297	$C_{39}H_{71}O_4^+$	DAG (18:0/18:2) – H_2O
605.5459	$C_{39}H_{73}O_4^+$	DAG (18:0/18:1) – H_2O
617.5079	$C_{39}H_{69}O_5^+$	hDAG (18:1/18:2) – H_2O
619.5252	$C_{39}H_{71}O_5^+$	hDAG (18:0/18:2) – H_2O

m/z 934.8749 at 49.5 min – $[M + NH_4]^+$ of TAG (18:0/18:1/20:0) and other isomers

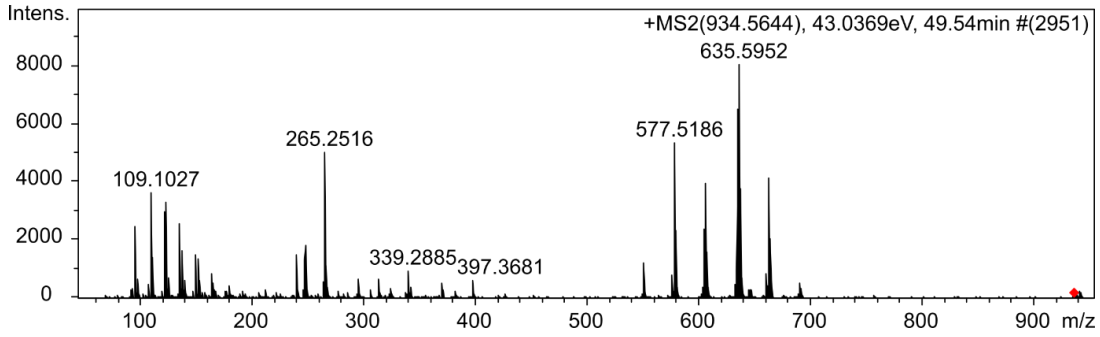

Measured m/z	Possible MF	Possible structural assignment
95.0855	$C_7H_{11}^+$	Fragment of acyl chains
109.1027	$C_8H_{13}^+$	Fragment of acyl chains
121.1025	$C_9H_{13}^+$	Fragment of acyl chains
123.1179	$C_9H_{15}^+$	Fragment of acyl chains
135.1175	$C_{10}H_{15}^+$	Fragment of acyl chains
149.1326	$C_{11}H_{17}^+$	Fragment of acyl chains
163.1449	$C_{12}H_{19}^+$	Fragment of acyl chains
239.2379	$C_{16}H_{31}O^+$	Acylium ion from breakage of acyl chain C16:0
247.2420	$C_{18}H_{31}^+$	Fragment of acyl chains
265.2516	$C_{18}H_{33}O^+$	Acylium ion from breakage of acyl chain C18:1
295.3001	$C_{20}H_{39}O^+$	Acylium ion from breakage of acyl chain C20:0
313.2730	$C_{19}H_{37}O_3^+$	MAG (16:0) – H_2O
339.2885	$C_{21}H_{39}O_3^+$	MAG (18:1) – H_2O
369.3348	$C_{23}H_{45}O_3^+$	MAG (20:0) – H_2O
397.3681	$C_{25}H_{49}O_3^+$	MAG (22:0) – H_2O
549.4848	$C_{35}H_{65}O_4^+$	DAG (16:0/16:1) – H_2O
577.5186	$C_{37}H_{69}O_4^+$	DAG (16:0/18:1) – H_2O
605.5504	$C_{39}H_{73}O_4^+$	DAG (18:0/18:1) – H_2O
635.5952	$C_{41}H_{79}O_4^+$	DAG (18:0/20.0) – H_2O
661.6102	$C_{43}H_{81}O_4^+$	DAG (18:1/22:0) – H_2O
689.6420	$C_{45}H_{85}O_4^+$	DAG (20:1/22:0) – H_2O

m/z 990.9377 at 50.2 min – $[M + NH_4]^+$ of TAG (18:0/18:1/24:0)

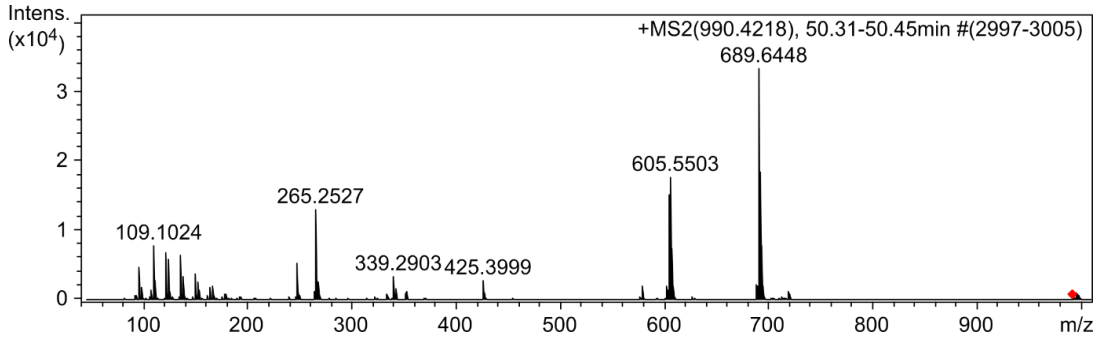

Measured m/z	Possible MF	Possible structural assignment
95.0862	$C_7H_{11}^+$	Fragment of acyl chains
109.1024	$C_8H_{13}^+$	Fragment of acyl chains
121.1021	$C_9H_{13}^+$	Fragment of acyl chains
135.1174	$C_{10}H_{15}^+$	Fragment of acyl chains
149.1329	$C_{11}H_{17}^+$	Fragment of acyl chains
247.2414	$C_{18}H_{31}^+$	Fragment of acyl chains
265.2527	$C_{18}H_{33}O^+$	Acylium ion from breakage of acyl chain C18:1
339.2903	$C_{21}H_{39}O_3^+$	MAG (18:1) – H_2O
425.3999	$C_{27}H_{53}O_3^+$	MAG (24:0) – H_2O
603.5343	$C_{39}H_{71}O_4^+$	DAG (18:0/18:1) – H_2O – H_2
605.5503	$C_{39}H_{73}O_4^+$	DAG (18:0/18:1) – H_2O
689.6448	$C_{45}H_{85}O_4^+$	DAG (18:1/24:0) – H_2O
691.6571	$C_{45}H_{87}O_4^+$	DAG (18:0/24:0) – H_2O

m/z 1002.9375 at 50.2 min – $[M + NH_4]^+$ of TAG (18:1/18:1/25:0)

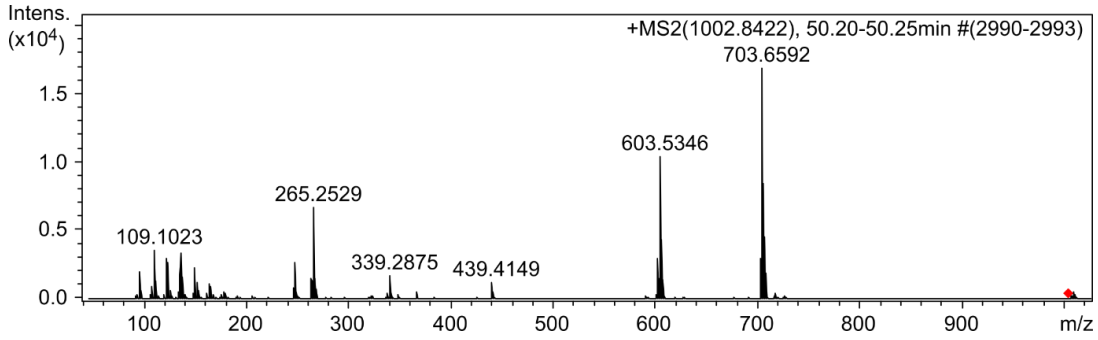

Measured m/z	Possible MF	Possible structural assignment
95.0864	$C_7H_{11}^+$	Fragment of acyl chains
109.1023	$C_8H_{13}^+$	Fragment of acyl chains
121.1018	$C_9H_{13}^+$	Fragment of acyl chains
135.1177	$C_{10}H_{15}^+$	Fragment of acyl chains
149.1329	$C_{11}H_{17}^+$	Fragment of acyl chains
247.2425	$C_{18}H_{31}^+$	Fragment of acyl chains
339.2875	$C_{21}H_{39}O_3^+$	MAG (18:1) – H_2O
439.4149	$C_{28}H_{55}O_3^+$	MAG (25:0) – H_2O
601.5191	$C_{39}H_{69}O_4^+$	DAG (18:1/18:1) – H_2O – H_2
603.5346	$C_{39}H_{71}O_4^+$	DAG (18:1/18:1) – H_2O
701.6445	$C_{46}H_{85}O_4^+$	DAG (18:1/25:0) – H_2O – H_2
703.6592	$C_{46}H_{87}O_4^+$	DAG (18:1/25:0) – H_2O

m/z 1018.9654 at 50.5 min – $[M + NH_4]^+$ of TAG (18:0/18:1/26:0)

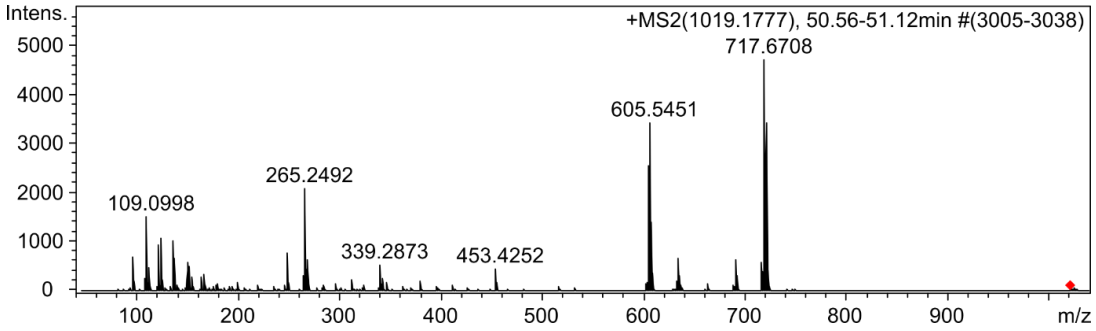

Measured m/z	Possible MF	Possible structural assignment
95.0829	$C_7H_{11}^+$	Fragment of acyl chains
109.0998	$C_8H_{13}^+$	Fragment of acyl chains
123.1143	$C_9H_{13}^+$	Fragment of acyl chains
135.1151	$C_{10}H_{15}^+$	Fragment of acyl chains
137.1302	$C_{10}H_{17}^+$	Fragment of acyl chains
149.1312	$C_{11}H_{17}^+$	Fragment of acyl chains
247.2399	$C_{18}H_{31}^+$	Fragment of acyl chains
265.2492	$C_{18}H_{33}O^+$	Acylium ion from breakage of acyl chain C18:1
339.2873	$C_{21}H_{39}O_3^+$	MAG (18:1) – H_2O
453.4252	$C_{29}H_{57}O_3^+$	MAG (26:0) – H_2O
603.5294	$C_{39}H_{71}O_4^+$	DAG (18:0/18:1) – H_2O – H_2
605.5451	$C_{39}H_{73}O_4^+$	DAG (18:0/18:1) – H_2O
717.6708	$C_{47}H_{89}O_4^+$	DAG (18:1/26:0) – H_2O
719.6843	$C_{47}H_{91}O_4^+$	DAG (18:0/26:0) – H_2O

Other intracellular lipids in the pathways in the positive ion modes

m/z 758.5726 at 41.7 min – $[M + H]^+$ of PC (16:0/18:2)

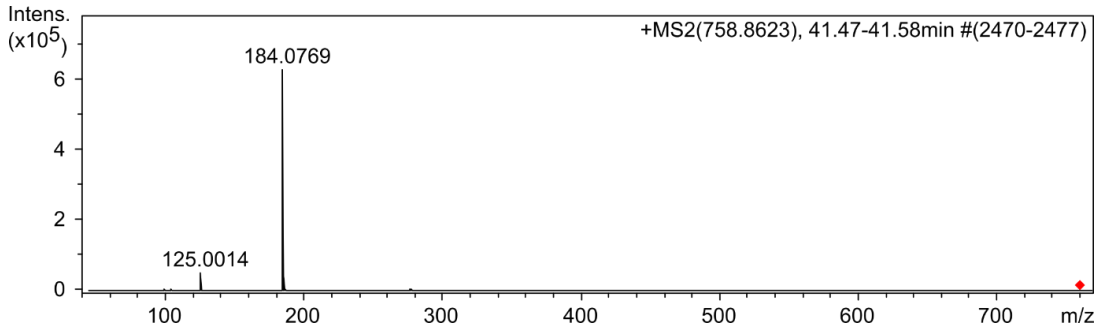

Zoom in

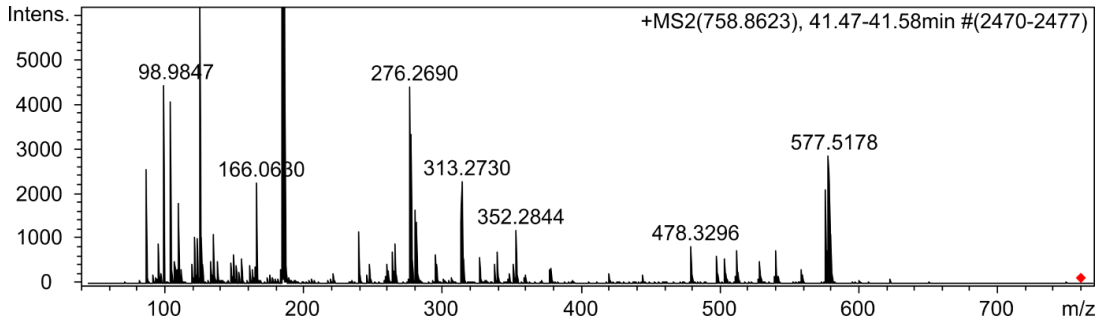

Measured m/z	Possible MF	Possible structural assignment
98.9847	$H_4O_4P^+$	Phosphate
125.0014	$C_2H_6O_4P^+$	Phosphocholine – $N(CH_3)_3$
166.0630	$C_5H_{13}NO_3P^+$	Phosphocholine – H_2O
184.0769	$C_5H_{15}NO_4P^+$	Phosphocholine
239.2359	$C_{16}H_{31}O^+$	Acylium ion from breakage of acyl chain C16:0
263.2401	$C_{18}H_{31}O^+$	Acylium ion from breakage of acyl chain C18:2
265.2517	$C_{18}H_{33}O^+$	Acylium ion from breakage of acyl chain C18:1
313.2730	$C_{19}H_{37}O_3^+$	MAG (16:0) – H_2O
337.2741	$C_{21}H_{37}O_3^+$	MAG (18:2) – H_2O
339.2878	$C_{21}H_{39}O_3^+$	MAG (18:1) – H_2O
478.3296	$C_{24}H_{49}NO_6P^+$	LPC (16:0) – H_2O
496.3378	$C_{24}H_{51}NO_7P^+$	LPC (16:0)
502.3281	$C_{26}H_{49}NO_6P^+$	LPC (18:2) – H_2O
575.5029	$C_{37}H_{67}O_4^+$	DAG (16:0/18:2) – H_2O
577.5178	$C_{37}H_{69}O_4^+$	DAG (16:0/18:1) – H_2O

m/z 782.5751 at 41.3 min – $[M + H]^+$ of PC (18:2/18:2)

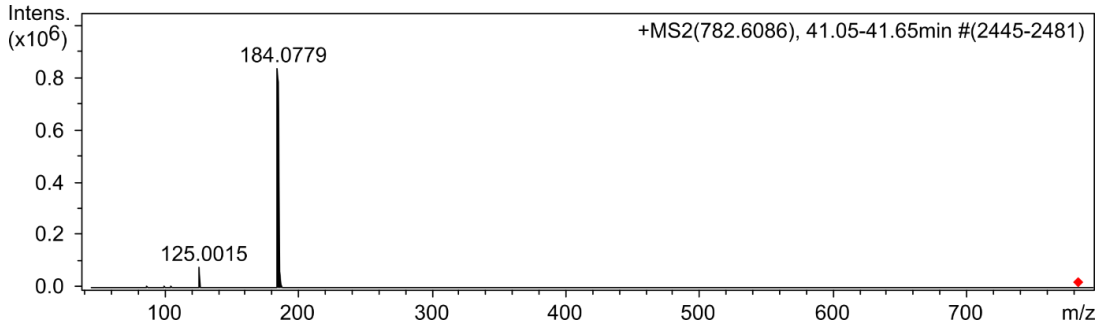

Zoom in

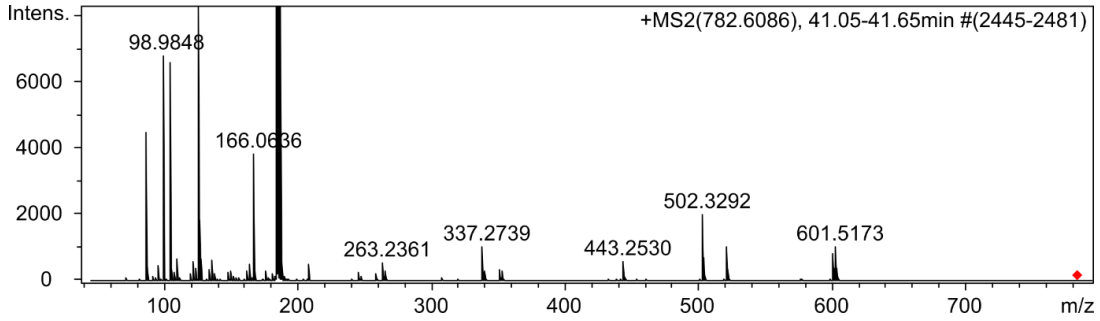

Measured m/z	Possible MF	Possible structural assignment
98.9848	$H_4O_4P^+$	Phosphate
125.0015	$C_2H_6O_4P^+$	Phosphocholine – $N(CH_3)_3$
166.0636	$C_5H_{13}NO_3P^+$	Phosphocholine – H_2O
184.0779	$C_5H_{15}NO_4P^+$	Phosphocholine
263.2361	$C_{18}H_{31}O^+$	Acylium ion from breakage of acyl chain C18:2
337.2739	$C_{21}H_{37}O_3^+$	MAG (18:2) – H_2O
443.2530	$C_{23}H_{40}O_6P^+$	LPC (18:2) – H_2O – $N(CH_3)_3$
502.3292	$C_{26}H_{49}NO_6P^+$	LPC (18:2) – H_2O
520.3410	$C_{26}H_{51}NO_7P^+$	LPC (18:2)
599.5051	$C_{39}H_{67}O_4^+$	DAG (18:2/18:2) – H_2O
601.5173	$C_{39}H_{69}O_4^+$	DAG (18:1/18:2) – H_2O

Other intracellular lipids in the pathways in the negative ion modes

m/z 671.4649 at 27.4 min – $[M - H]^-$ of PA (16:0/18:2)

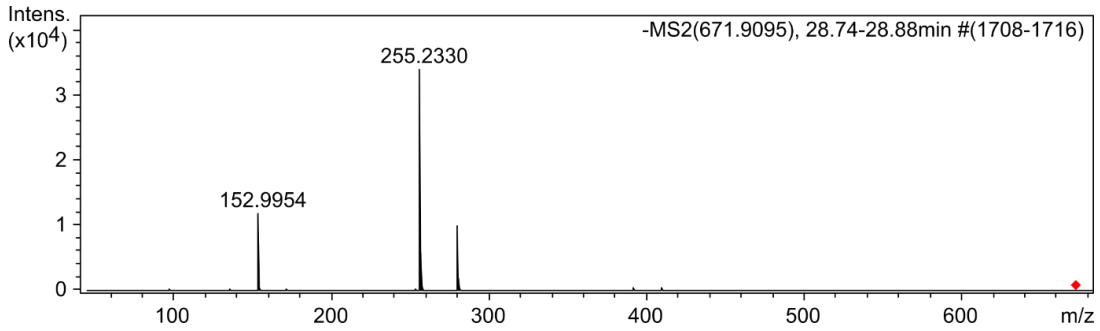

Zoom in

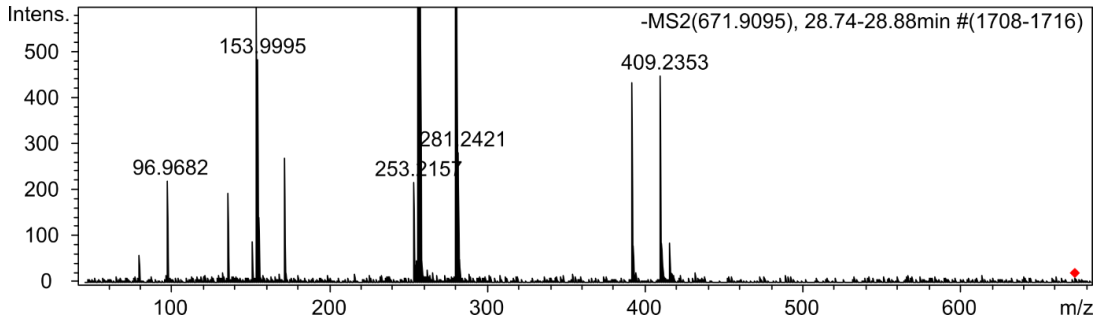

Measured m/z	Possible MF	Possible structural assignment
96.9682	$H_2O_4P^-$	Phosphate
134.9859	$C_3H_4O_4P^-$	Glycerol phosphate – $2H_2O$
152.9954	$C_3H_6O_5P^-$	Glycerol phosphate – H_2O
171.0060	$C_3H_8O_6P^-$	Glycerol phosphate
255.2330	$C_{16}H_{31}O_2^-$	FA (16:0)
279.2331	$C_{18}H_{31}O_2^-$	FA (18:2)
391.2294	$C_{19}H_{36}O_6P^-$	LPA (16:0) – H_2O
409.2353	$C_{19}H_{38}O_7P^-$	LPA (16:0)

m/z 695.4647 at 26.8 min – $[M - H]^-$ of PA (18:2/18:2)

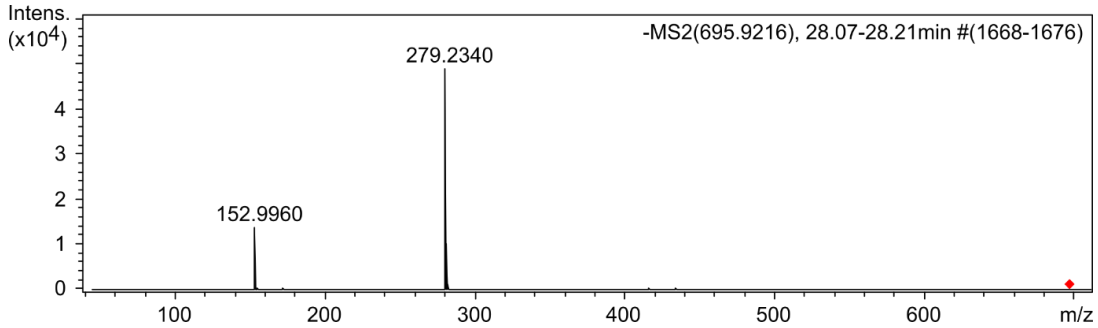

Zoom in

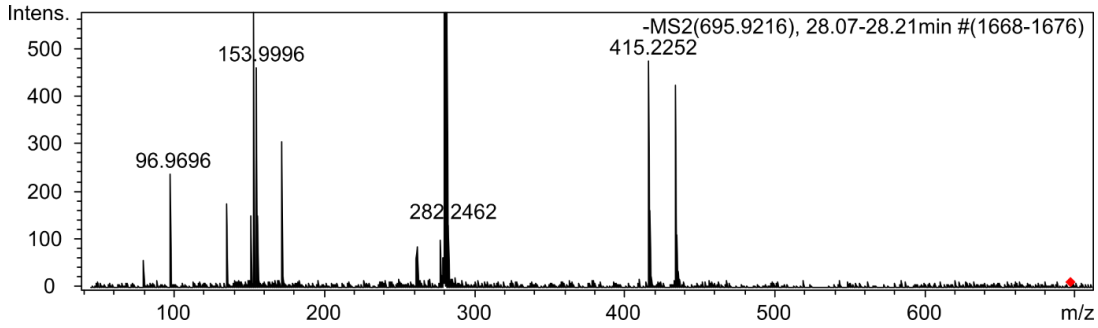

Measured m/z	Possible MF	Possible structural assignment
96.9696	$H_2O_4P^-$	Phosphate
134.9855	$C_3H_4O_4P^-$	Glycerol phosphate – $2H_2O$
152.9960	$C_3H_6O_5P^-$	Glycerol phosphate – H_2O
171.0070	$C_3H_8O_6P^-$	Glycerol phosphate
279.2340	$C_{18}H_{31}O_2^-$	FA (18:2)
415.2252	$C_{21}H_{36}O_6P^-$	LPA (18:2) – H_2O
433.2347	$C_{21}H_{38}O_7P^-$	LPA (18:2)

m/z 714.5023 at 39.0 min – $[M - H]^-$ of PE (16:0/18:2)

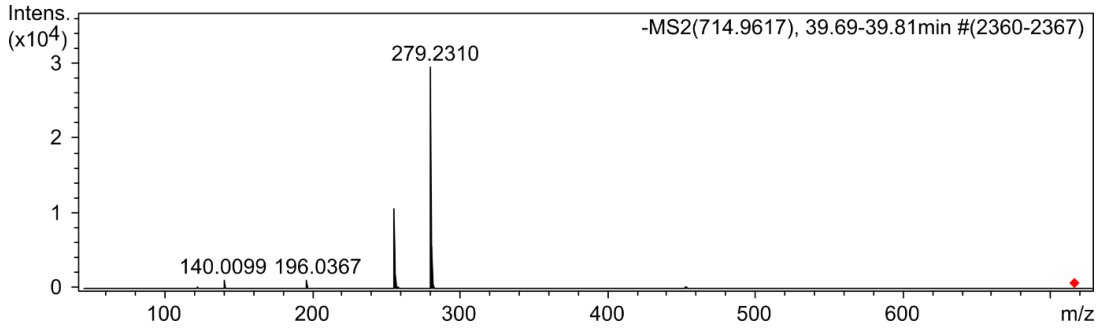

Zoom in

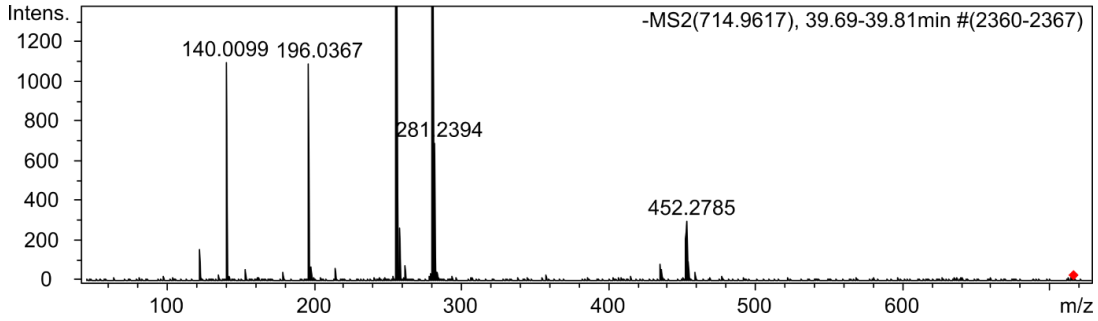

Measured m/z	Possible MF	Possible structural assignment
122.0001	$C_2H_5NO_3P^-$	Ethanolamine phosphate – H_2O
140.0099	$C_2H_7NO_4P^-$	Ethanolamine phosphate
196.0367	$C_5H_{11}NO_5P^-$	Glycerophosphorylethanolamine
255.2310	$C_{16}H_{31}O_2^-$	FA (16:0)
279.2310	$C_{18}H_{31}O_2^-$	FA (18:2)
452.2785	$C_{21}H_{43}NO_7P^-$	LPE (16:0)

m/z 738.5004 at 38.2 min – $[M - H]^-$ of PE (18:2/18:2)

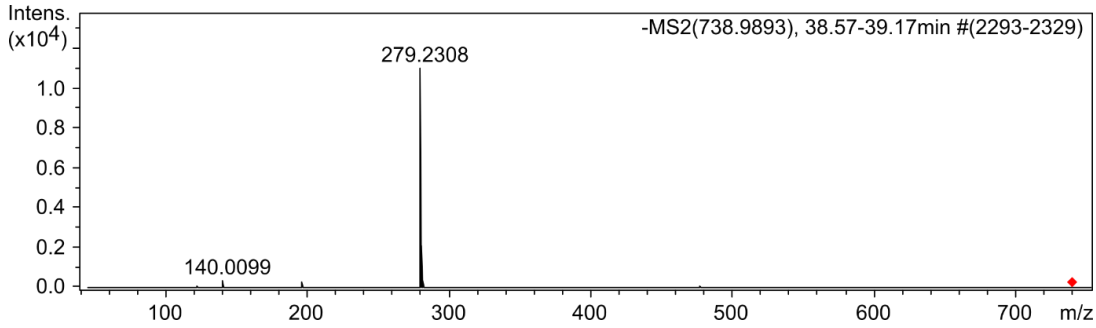

Zoom in

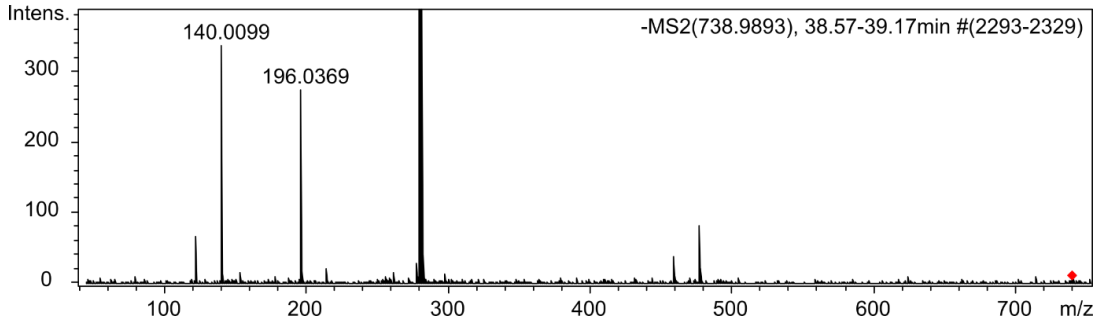

Measured m/z	Possible MF	Possible structural assignment
121.9997	$C_2H_5NO_3P^-$	Ethanolamine phosphate – H_2O
140.0099	$C_2H_7NO_4P^-$	Ethanolamine phosphate
196.0369	$C_5H_{11}NO_5P^-$	Glycerophosphorylethanolamine
279.2308	$C_{18}H_{31}O_2^-$	FA (18:2)
458.2627	$C_{23}H_{41}NO_6P^-$	LPE (18:2) – H_2O
476.2690	$C_{23}H_{43}NO_7P^-$	LPE (18:2)

m/z 758.4944 at 29.9 min – $[M - H]^-$ of PS (16:0/18:2)

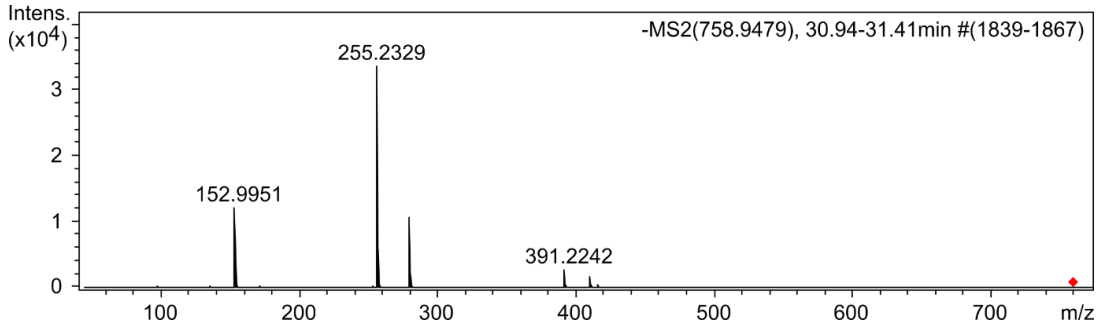

Measured m/z	Possible MF	Possible structural assignment
152.9951	$C_3H_6O_5P^-$	Glycerol phosphate – H_2O
255.2329	$C_{16}H_{31}O_2^-$	FA (16:0)
279.2331	$C_{18}H_{31}O_2^-$	FA (18:2)
391.2294	$C_{19}H_{36}O_6P^-$	LPA (16:0) – H_2O
409.2353	$C_{19}H_{38}O_7P^-$	LPA (16:0)

m/z 782.4946 at 29.3 min – $[M - H]^-$ of PS (18:2/18:2)

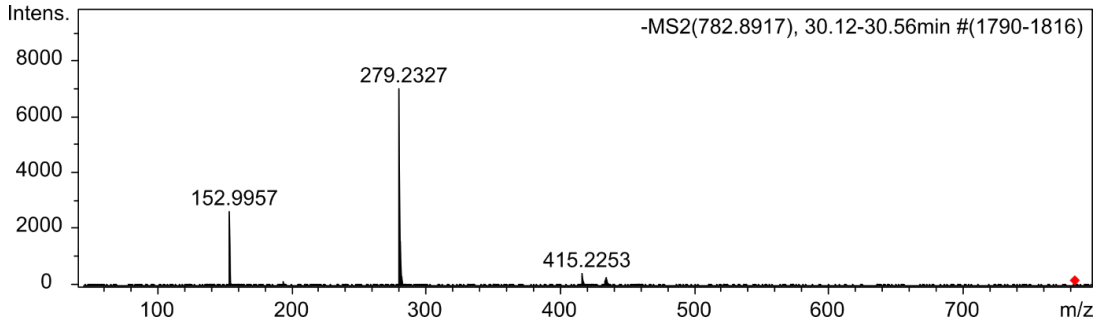

Measured m/z	Possible MF	Possible structural assignment
152.9957	$C_3H_6O_5P^-$	Glycerol phosphate – H_2O
279.2327	$C_{18}H_{31}O_2^-$	FA (18:2)
415.2253	$C_{21}H_{36}O_6P^-$	LPA (18:2) – H_2O
433.2379	$C_{21}H_{38}O_7P^-$	LPA (18:2)

m/z 745.4976 at 34.4 min – $[M - H]^-$ of PG (16:0/18:2)

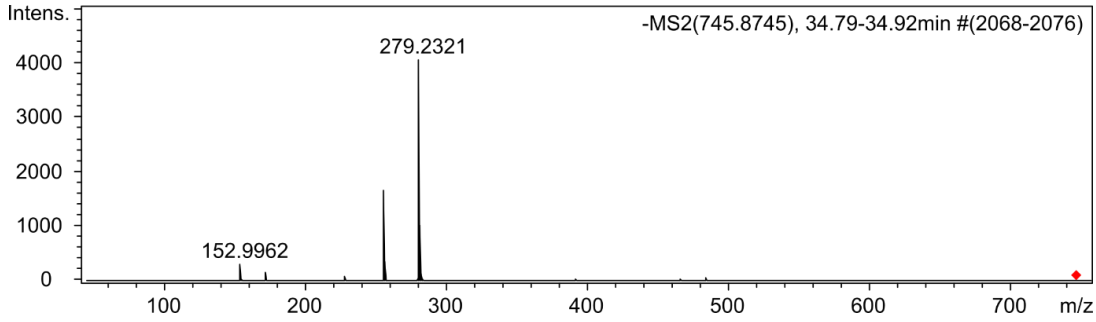

Measured m/z	Possible MF	Possible structural assignment
152.9962	$C_3H_6O_5P^-$	Glycerol phosphate – H_2O
171.0062	$C_3H_8O_6P^-$	Glycerol phosphate
255.2323	$C_{16}H_{31}O_2^-$	FA (16:0)
279.2321	$C_{18}H_{31}O_2^-$	FA (18:2)
465.2532	$C_{22}H_{42}O_8P^-$	LPG (16:0) – H_2O
483.2832	$C_{22}H_{44}O_9P^-$	LPG (16:0)

m/z 769.4962 at 33.8 min – $[M - H]^-$ of PG (18:2/18:2)

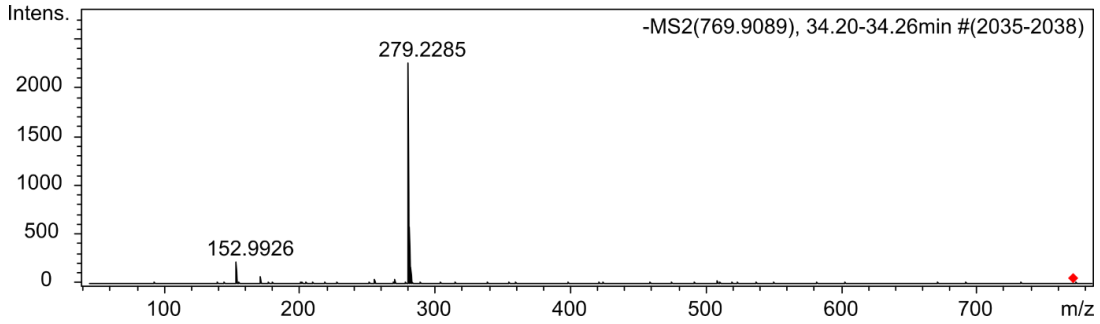

Measured m/z	Possible MF	Possible structural assignment
152.9926	$C_3H_6O_5P^-$	Glycerol phosphate – H_2O
279.2285	$C_{18}H_{31}O_2^-$	FA (18:2)

m/z 833.5160 at 34.0 min – $[M - H]^-$ of PI (16:0/18:2)

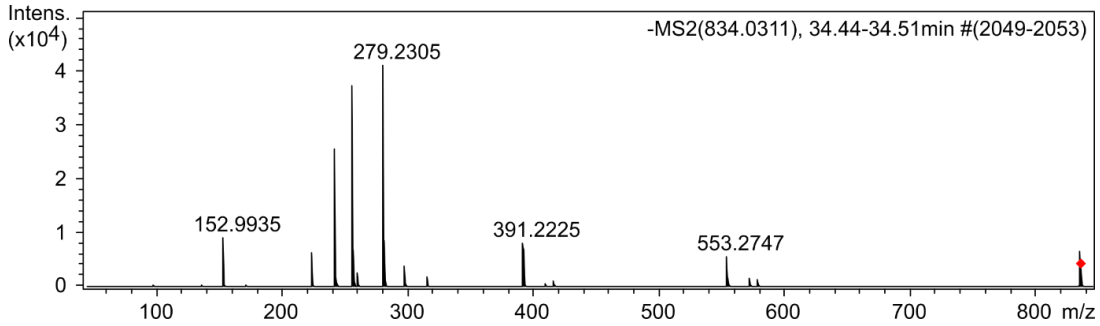

Measured m/z	Possible MF	Possible structural assignment
152.9935	$C_3H_6O_5P^-$	Glycerol phosphate – H_2O
241.0096	$C_6H_{10}O_8P^-$	Inositol phosphate – H_2O
255.2304	$C_{16}H_{31}O_2^-$	FA (16:0)
279.2305	$C_{18}H_{31}O_2^-$	FA (18:2)
391.2225	$C_{19}H_{36}O_6P^-$	LPA (16:0) – H_2O
409.2321	$C_{19}H_{38}O_7P^-$	LPA (16:0)
553.2747	$C_{25}H_{46}O_{11}P^-$	LPI (16:0) – H_2O
571.2860	$C_{25}H_{48}O_{12}P^-$	LPI (16:0)

m/z 857.5147 at 33.4 min – $[M - H]^-$ of PI (18:2/18:2)

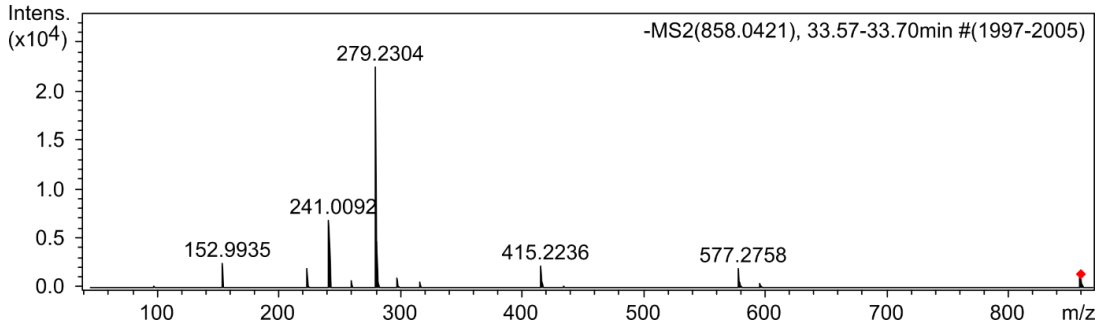

Measured m/z	Possible MF	Possible structural assignment
152.9935	$C_3H_6O_5P^-$	Glycerol phosphate – H_2O
241.0092	$C_6H_{10}O_8P^-$	Inositol phosphate – H_2O
279.2304	$C_{18}H_{31}O_2^-$	FA (18:2)
415.2236	$C_{21}H_{36}O_6P^-$	LPA (18:2) – H_2O
577.2758	$C_{27}H_{46}O_{11}P^-$	LPI (18:2) – H_2O

Calculation and predicted isotopic patterns on the mass spectra of representative ions in the ethanol-d_6 samples when taking into account only deuterium exchanges of all hydrogens on the representative ions and natural abundances of elements.

Base calculation:

As ethanol-d_6 (or CD_3CD_2OD) was added to the culture at the concentration of 4% (v/v), the medium had the following ratios of H_2O to CD_3CD_2OD:

By volume	96: 4
By mass (At 25°C, density of H_2O = 0.99707 g/mL and of ethanol = 0.78522 g/mL)	95.7: 3.1
By mole (MW of H_2O = 18.01528 g/mol and of CD_3CD_2OD = 52.10541 g/mol)	5.3: 0.060

Since H_2O has 2 protons, while CD_3CD_2OD has 1 deuteron, the mole ratio of proton (and some deuteron from water) to deuteron (from ethanol-d_6) is equal to 10.6: 0.060. However, considering that natural abundances of hydrogen and deuterium are 99.9844% and 0.0156%, respectively, the mole ratio of proton to deuteron then becomes 10.6: 0.062, which is equal to 100: 0.58.

(a) Diacylglycerol (DAG) (18:2/18:2)

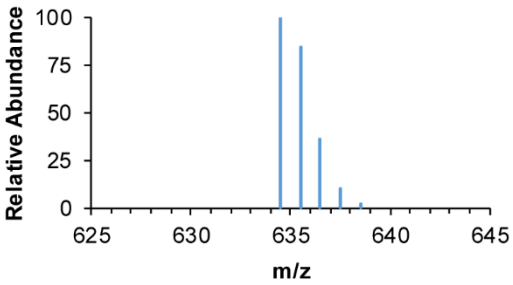

Calculation:

$[M + NH_4]^+$ has the molecular formula of $C_{39}H_{72}NO_5^+$.

The highest probability of each isotope when considering only deuterium exchanges and natural isotopic abundance of each element is then equal to the following:

(Note: Terms with relatively small contribution are ignored below.)

M: $P(M) = P(0\ D)$

$$= {}^{72}C_0\left(\frac{0.58}{100}\right)^0\left(\frac{100}{100}\right)^{72}$$

$$= 1.00$$

M+1: $P(M+1) = P(1\ D) + P(1\ {}^{13}C)$

$$= {}^{72}C_1\left(\frac{0.58}{100}\right)^1\left(\frac{100}{100}\right)^{71} + {}^{39}C_1\left(\frac{1.08}{100}\right)^1\left(\frac{100}{100}\right)^{38}$$

$$= 0.84$$

M+2: $P(M+2) = P(2\ D) + P(2\ {}^{13}C) + P(1\ D\ \&\ 1\ {}^{13}C) + P(1\ {}^{18}O)$

$$= {}^{72}C_2\left(\frac{0.58}{100}\right)^2\left(\frac{100}{100}\right)^{70} + {}^{39}C_2\left(\frac{1.08}{100}\right)^2\left(\frac{100}{100}\right)^{37} +$$

$$P(1\ D)\cdot P(1\ {}^{13}C) + {}^{5}C_1\left(\frac{0.20}{100}\right)^1\left(\frac{100}{100}\right)^4$$

$$= 0.36$$

M+3: $P(M+3) = P(3\ D) + P(3\ ^{13}C) + P(2\ D\ \&\ 1\ ^{13}C) + P(1\ D\ \&\ 2\ ^{13}C) +$

$P(1\ D\ \&\ 1\ ^{18}O) + P(1\ ^{13}C\ \&\ 1\ ^{18}O)$

$$= {}^{72}C_3\left(\frac{0.58}{100}\right)^3\left(\frac{100}{100}\right)^{69} + {}^{39}C_3\left(\frac{1.08}{100}\right)^3\left(\frac{100}{100}\right)^{36} +$$

$P(2\ D)\cdot P(1\ ^{13}C) + P(1\ D)\cdot P(2\ ^{13}C) + P(1\ D)\cdot P(1\ ^{18}O) +$

$P(1\ ^{13}C)\cdot P(1\ ^{18}O)$

$= 0.10$

M+4: $P(M+4) = P(4\ D) + P(4\ ^{13}C) + P(3\ D\ \&\ 1\ ^{13}C) + P(2\ D\ \&\ 2\ ^{13}C) +$

$P(1\ D\ \&\ 3\ ^{13}C) + P(2\ D\ \&\ 1\ ^{18}O) + P(2\ ^{13}C\ \&\ 1\ ^{18}O) +$

$P(1\ D\ \&\ 1\ ^{13}C + 1\ ^{18}O)$

$$= {}^{72}C_4\left(\frac{0.58}{100}\right)^4\left(\frac{100}{100}\right)^{68} + {}^{39}C_4\left(\frac{1.08}{100}\right)^4\left(\frac{100}{100}\right)^{35} +$$

$P(3\ D)\cdot P(1\ ^{13}C) + P(2\ D)\cdot P(2\ ^{13}C) + P(1\ D)\cdot P(3\ ^{13}C) +$

$P(2\ D)\cdot P(1\ ^{18}O) + P(2\ ^{13}C)\cdot P(1\ ^{18}O) + P(1\ D)\cdot P(1\ ^{13}C)\cdot P(1\ ^{18}O)$

$= 0.02$

Thus, M: M+1: M+2: M+3: M+4 = 100: 84: 36: 10: 2.

(b) Triacylglycerol (TAG) (18:0/18:1/18:1)

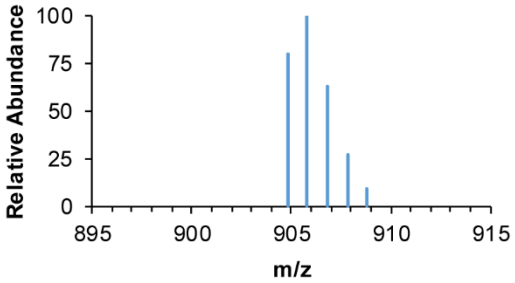

Calculation:

$[M + NH_4]^+$ has the molecular formula of $C_{57}H_{110}NO_6^+$.

The highest probability of each isotope when considering only deuterium exchanges and natural isotopic abundance of each element is then equal to the following:

(Note: Terms with relatively small contribution are ignored below.)

M: $P(M) = P(0\ D)$

$$= {}^{110}C_0 \left(\frac{0.58}{100}\right)^0 \left(\frac{100}{100}\right)^{110}$$

$$= 1.00$$

M+1: $P(M+1) = P(1\ D) + P(1\ {}^{13}C)$

$$= {}^{110}C_1 \left(\frac{0.58}{100}\right)^1 \left(\frac{100}{100}\right)^{109} + {}^{57}C_1 \left(\frac{1.08}{100}\right)^1 \left(\frac{100}{100}\right)^{56}$$

$$= 1.26$$

M+2: $P(M+2) = P(2\ D) + P(2\ {}^{13}C) + P(1\ D\ \&\ 1\ {}^{13}C) + P(1\ {}^{18}O)$

$$= {}^{110}C_2 \left(\frac{0.58}{100}\right)^2 \left(\frac{100}{100}\right)^{108} + {}^{57}C_2 \left(\frac{1.08}{100}\right)^2 \left(\frac{100}{100}\right)^{55} +$$

$$P(1\ D)\cdot P(1\ {}^{13}C) + {}^{6}C_1 \left(\frac{0.20}{100}\right)^1 \left(\frac{100}{100}\right)^5$$

$$= 0.80$$

M+3: $P(M+3) = P(3\ D) + P(3\ {}^{13}C) + P(2\ D\ \&\ 1\ {}^{13}C) + P(1\ D\ \&\ 2\ {}^{13}C) +$

$$P(1\ D\ \&\ 1\ {}^{18}O) + P(1\ {}^{13}C\ \&\ 1\ {}^{18}O)$$

$$= {}^{110}C_3 \left(\frac{0.58}{100}\right)^3 \left(\frac{100}{100}\right)^{107} + {}^{57}C_3 \left(\frac{1.08}{100}\right)^3 \left(\frac{100}{100}\right)^{54} +$$

$$P(2\ D)\cdot P(1\ {}^{13}C) + P(1\ D)\cdot P(2\ {}^{13}C) + P(1\ D)\cdot P(1\ {}^{18}O) +$$

$$P(1\ {}^{13}C)\cdot P(1\ {}^{18}O)$$

$$= 0.34$$

M+4: P(M+4) = P(4 D) + P(4 ^{13}C) + P(3 D & 1 ^{13}C) + P(2 D & 2 ^{13}C) +

P(1 D & 3 ^{13}C) + P(2 D & 1 ^{18}O) + P(2 ^{13}C & 1 ^{18}O) +

P(1 D & 1 ^{13}C + 1 ^{18}O)

$$= {}^{110}C_4\left(\frac{0.58}{100}\right)^4\left(\frac{100}{100}\right)^{106} + {}^{57}C_4\left(\frac{1.08}{100}\right)^4\left(\frac{100}{100}\right)^{53} +$$

P(3 D)·P(1 ^{13}C) + P(2 D)·P(2 ^{13}C) + P(1 D)·P(3 ^{13}C) +

P(2 D)·P(1 ^{18}O) + P(2 ^{13}C)·P(1 ^{18}O) + P(1 D)·P(1 ^{13}C)·P(1 ^{18}O)

= 0.11

Thus, M: M+1: M+2: M+3: M+4 = 80: 100: 63: 27: 9.

(c) Fatty acid (FA) (18:2)

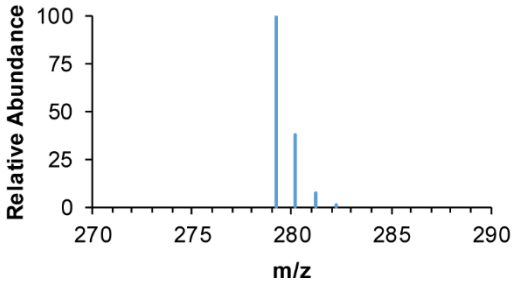

Calculation:

$[M - H]^-$ has the molecular formula of $C_{18}H_{31}O_2^-$.

The highest probability of each isotope when considering only deuterium exchanges and natural isotopic abundance of each element is then equal to the following:

(Note: Terms with relatively small contribution are ignored below.)

M: P(M) = P(0 D)

$$= {}^{31}C_0\left(\frac{0.58}{100}\right)^0\left(\frac{100}{100}\right)^{31}$$

= 1.00

M+1: P(M+1) = P(1 D) + P(1 ^{13}C)

$$= {}^{31}C_1\left(\frac{0.58}{100}\right)^1\left(\frac{100}{100}\right)^{30} + {}^{18}C_1\left(\frac{1.08}{100}\right)^1\left(\frac{100}{100}\right)^{17}$$

= 0.38

M+2: P(M+2) = P(2 D) + P(2 ^{13}C) + P(1 D & 1 ^{13}C) + P(1 ^{18}O)

$$= {}^{31}C_2\left(\frac{0.58}{100}\right)^2\left(\frac{100}{100}\right)^{29} + {}^{18}C_2\left(\frac{1.08}{100}\right)^2\left(\frac{100}{100}\right)^{16} +$$

$$P(1\ D)\cdot P(1\ {}^{13}C) + {}^{2}C_1\left(\frac{0.20}{100}\right)^1\left(\frac{100}{100}\right)^1$$

= 0.07

M+3: P(M+3) = P(3 D) + P(3 ^{13}C) + P(2 D & 1 ^{13}C) + P(1 D & 2 ^{13}C) +

P(1 D & 1 ^{18}O) + P(1 ^{13}C & 1 ^{18}O)

$$= {}^{31}C_3\left(\frac{0.58}{100}\right)^3\left(\frac{100}{100}\right)^{28} + {}^{18}C_3\left(\frac{1.08}{100}\right)^3\left(\frac{100}{100}\right)^{15} +$$

$$P(2\ D)\cdot P(1\ {}^{13}C) + P(1\ D)\cdot P(2\ {}^{13}C) + P(1\ D)\cdot P(1\ {}^{18}O) +$$

$$P(1\ {}^{13}C)\cdot P(1\ {}^{18}O)$$

= 0.01

Thus, M: M+1: M+2: M+3 = 100: 38: 7: 1.

(d) Phosphatidic acid (PA) (18:2/18:2)

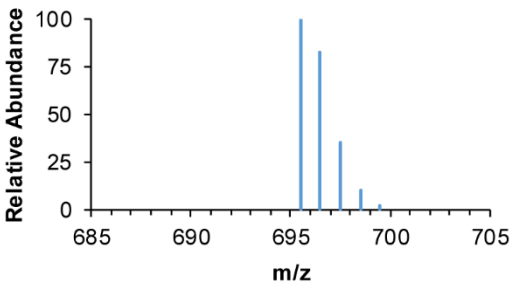

Calculation:

$[M - H]^-$ has the molecular formula of $C_{39}H_{68}O_8P^-$.

The highest probability of each isotope when considering only deuterium exchanges and natural isotopic abundance of each element is then equal to the following:

(Note: Terms with relatively small contribution are ignored below.)

M: $P(M) = P(0\ D)$

$$= {}^{68}C_0\left(\frac{0.58}{100}\right)^0\left(\frac{100}{100}\right)^{68}$$

$$= 1.00$$

M+1: $P(M+1) = P(1\ D) + P(1\ {}^{13}C)$

$$= {}^{68}C_1\left(\frac{0.58}{100}\right)^1\left(\frac{100}{100}\right)^{67} + {}^{39}C_1\left(\frac{1.08}{100}\right)^1\left(\frac{100}{100}\right)^{38}$$

$$= 0.82$$

M+2: $P(M+2) = P(2\ D) + P(2\ {}^{13}C) + P(1\ D\ \&\ 1\ {}^{13}C) + P(1\ {}^{18}O)$

$$= {}^{68}C_2\left(\frac{0.58}{100}\right)^2\left(\frac{100}{100}\right)^{66} + {}^{39}C_2\left(\frac{1.08}{100}\right)^2\left(\frac{100}{100}\right)^{37} +$$

$$P(1\ D)\cdot P(1\ {}^{13}C) + {}^{8}C_1\left(\frac{0.20}{100}\right)^1\left(\frac{100}{100}\right)^{7}$$

$$= 0.35$$

M+3: $P(M+3) = P(3\ D) + P(3\ {}^{13}C) + P(2\ D\ \&\ 1\ {}^{13}C) + P(1\ D\ \&\ 2\ {}^{13}C) +$

$P(1\ D\ \&\ 1\ {}^{18}O) + P(1\ {}^{13}C\ \&\ 1\ {}^{18}O)$

$$= {}^{68}C_3\left(\frac{0.58}{100}\right)^3\left(\frac{100}{100}\right)^{65} + {}^{39}C_3\left(\frac{1.08}{100}\right)^3\left(\frac{100}{100}\right)^{36} +$$

$P(2\ D)\cdot P(1\ {}^{13}C) + P(1\ D)\cdot P(2\ {}^{13}C) + P(1\ D)\cdot P(1\ {}^{18}O) +$

$P(1\ {}^{13}C)\cdot P(1\ {}^{18}O)$

= 0.10

M+4: P(M+4) = P(4 D) + P(4 ^{13}C) + P(3 D & 1 ^{13}C) + P(2 D & 2 ^{13}C) +

P(1 D & 3 ^{13}C) + P(2 D & 1 ^{18}O) + P(2 ^{13}C & 1 ^{18}O) +

P(1 D & 1 ^{13}C + 1 ^{18}O)

$$= {}^{68}C_4\left(\frac{0.58}{100}\right)^4\left(\frac{100}{100}\right)^{64} + {}^{39}C_4\left(\frac{1.08}{100}\right)^4\left(\frac{100}{100}\right)^{35} +$$

P(3 D)·P(1 ^{13}C) + P(2 D)·P(2 ^{13}C) + P(1 D)·P(3 ^{13}C) +

P(2 D)·P(1 ^{18}O) + P(2 ^{13}C)·P(1 ^{18}O) + P(1 D)·P(1 ^{13}C)·P(1 ^{18}O)

= 0.02

Thus, M: M+1: M+2: M+3: M+4 = 100: 82: 35: 10: 2.

Received: 24 February 2019 | Revised: 24 September 2019 | Accepted: 27 September 2019

DOI: 10.1002/mbo3.948

ORIGINAL ARTICLE

MicrobiologyOpen Open Access WILEY

Aspergillus niger upregulated glycerolipid metabolism and ethanol utilization pathway under ethanol stress

Nawaporn Vinayavekhin[1,2] | Wimonsiri Kongchai[1] | Jittra Piapukiew[2,3] | Warinthorn Chavasiri[1]

[1]Center of Excellence in Natural Products Chemistry, Department of Chemistry, Faculty of Science, Chulalongkorn University, Bangkok, Thailand

[2]Biocatalyst and Environmental Biotechnology Research Unit, Faculty of Science, Chulalongkorn University, Bangkok, Thailand

[3]Department of Botany, Faculty of Science, Chulalongkorn University, Bangkok, Thailand

Correspondence
Nawaporn Vinayavekhin, Department of Chemistry, Faculty of Science, Chulalongkorn University, Bangkok 10330, Thailand.
Email: nawaporn.v@chula.ac.th

Funding information
Thailand Research Fund, Grant/Award Number: MRG6180002; Office of the Higher Education Commission, Thailand

Abstract

The knowledge of how *Aspergillus niger* responds to ethanol can lead to the design of strains with enhanced ethanol tolerance to be utilized in numerous industrial bioprocesses. However, the current understanding about the response mechanisms of *A. niger* toward ethanol stress remains quite limited. Here, we first applied a cell growth assay to test the ethanol tolerance of *A. niger* strain ES4, which was isolated from the wall near a chimney of an ethanol tank of a petroleum company, and found that it was capable of growing in 5% (v/v) ethanol to 30% of the ethanol-free control level. Subsequently, the metabolic responses of this strain toward ethanol were investigated using untargeted metabolomics, which revealed the elevated levels of triacylglycerol (TAG) in the extracellular components, and of diacylglycerol, TAG, and hydroxy-TAG in the intracellular components. Lastly, stable isotope labeling mass spectrometry with ethanol-d_6 showed altered isotopic patterns of molecular ions of lipids in the ethanol-d_6 samples, compared with the nonlabeled ethanol controls, suggesting the ability of *A. niger* ES4 to utilize ethanol as a carbon source. Together, the studies revealed the upregulation of glycerolipid metabolism and ethanol utilization pathway as novel response mechanisms of *A. niger* ES4 toward ethanol stress, thereby underlining the utility of untargeted metabolomics and the overall approaches as tools for elucidating new biological insights.

KEYWORDS

Aspergillus niger, ethanol response, ethanol utilization pathway, glycerolipid metabolism, metabolomics

1 | INTRODUCTION

Organic solvent-tolerant microbes play key roles in many industrial bioprocesses, such as biofuel production, biocatalysis, and bioremediation (Nicolaou, Gaida, & Papoutsakis, 2010). To obtain strains with tolerance to these solvents, an approach involves genetically engineering selected strains based on the knowledge of organic solvent-induced stresses and responses (Taylor, Tuffin, Burton, Eley, & Cowan, 2008; Torres, Pandey, & Castro, 2011), which include repression or activation of sporulation (Bohin, Rigomier, & Schaeffer, 1976), induction of stress proteins (Petersohn et al., 2001), biodegradation or secretion of toxic organic solvents (Aono, Tsukagoshi, & Yamamoto, 1998; Bustard, Whiting, Cowan, & Wright, 2002), alteration in cell morphology (Neumann et al., 2005), and adaptation of the cell surface and cell membrane (Aono & Kobayashi, 1997; Weber & de Bont, 1996). Because these responses might be triggered to

counteract chemical toxins, the elevation in their levels might lead to the development of tolerance traits in these microorganisms (Kajiwara et al., 1996; Kang et al., 2007; Mahipant, Paemanee, Roytrakul, Kato, & Vangnai, 2017; Vinayavekhin & Vangnai, 2018).

Aspergillus niger is a filamentous ascomycete fungus, which can be found in almost every environment. It is known as the black mold on rotting fruits and vegetables. Yet, despite these common views of *A. niger* as an undesirable contaminant, it rarely causes disease in humans (Person, Chudgar, Norton, Tong, & Stout, 2010). In fact, it has the GRAS (generally regarded as safe) status for many of its processes (Frisvad et al., 2011) and is one of the most economically useful fungi in the biotechnological industry (Pel et al., 2007). It has been applied in the fermentation process for the production of organic acids, such as gluconic (Ramachandran, Fontanille, Pandey, & Larroche, 2008) and citric acids, with production of the latter exceeding one million metric tons annually (Baker, 2006), and of various extracellular enzymes, including α-amylase or β-glucosidase (Pariza & Cook, 2010). Apart from these industrial usages, *A. niger* has also been utilized in bioremediation processes (Coulibaly, Naveau, & Agathos, 2002; Srivastava & Thakur, 2006), as heterologous hosts for proteins and secondary metabolites production (Lubertozzi & Keasling, 2009) and as a cofermentation partner with *Saccharomyces cerevisiae* for the simultaneous saccharification and fermentation in bioethanol production (Izmirlioglu & Demirci, 2017). The further studies and usages of *A. niger* have also been facilitated by the availability of the genome sequence of three different *A. niger* strains (NRRL3, ATCC1015, and CBS513.88) (Baker, 2006; Pel et al., 2007).

Recently, one of the black spots found on the roof and outside upper wall of an ethanol tank of a petroleum company was investigated and identified as a living organism, *A. niger* strain ES4. The black spots could be found most densely near the valved chimney of the tank where ethanol was allowed to evaporate, which indicated the preference of this strain of *A. niger* for ethanol. This finding was rather surprising, as most non-ethanol-producing species are not capable of tolerating a high concentration of ethanol.

Relating to ethanol tolerance, *A. niger* isolated from spoiled pastry products was shown previously to be able to grow on potato dextrose agar containing ethanol up to about 3% (*w*/*w*) with almost no growth defect and up to 4% (*w*/*w*) with about 50% reduction in its growth (Dantigny, Guilmart, Radoi, Bensoussan, & Zwietering, 2005). Another unrelated study also exhibited the capabilities of *A. niger* to grow weakly on a plate containing 1% ethanol as a sole carbon source (O'Connell & Kelly, 1988). However, while *A. niger* was demonstrated to be capable of tolerating some concentrations of ethanol in many cases, and while a transcriptomic analysis of its closely related fungus *Aspergillus nidulans* revealed a 10-fold and twofold upregulation of alcohol dehydrogenase *alcA* and *aldA* genes in minimal medium containing ethanol compared with glucose, respectively (Mogensen, Nielsen, Hofmann, & Nielsen, 2006), there have so far been no reports on the metabolic responses of *A. niger* toward ethanol. The knowledge of which would allow for the engineering of the strain to have either higher tolerance toward ethanol for utilization in biotechnological industry or for designing novel methods for eradication of the strain in unwanted situations, such as in food spoilage or on a wall of an ethanol tank. We therefore decided to study the metabolic responses of *A. niger* ES4 toward ethanol further.

In this study, ethanol tolerance of *A. niger* ES4 was first examined. Then, to understand its metabolic responses toward ethanol, untargeted metabolomics analysis was conducted to assay extracellular and intracellular hydrophobic compound changes in *A. niger* ES4 when put under ethanol stress. Lastly, since it was possible that this strain of *A. niger* might intake ethanol for nutrients or substrates for production of some metabolites, the incorporation of ethanol into its metabolites was interrogated by stable isotope labeling mass spectrometry (MS) experiments using ethanol-d_6.

2 | MATERIALS AND METHODS

2.1 | Fungal strain and growth conditions

Aspergillus niger strain ES4 was isolated from a black spot on the outside upper wall of an ethanol tank of a petroleum company by the serial dilution method (Clark, Bordner, Galdrich, Kabler, & Huff, 1958). It was identified based on morphological characteristics and then confirmed using molecular technique. The nucleotide sequence data were submitted into the DDBJ/EMBL/GenBank nucleotide sequence databases with accession number MK621333.

The fungus was grown on potato dextrose agar for 7 days, before three agar plugs were inoculated in 20 ml of potato dextrose broth and shaken at 180 rpm, room temperature for 3 days. The culture was then diluted 20-fold into 20 ml of minimal medium (MM; per liter: 6 g $NaNO_3$, 0.52 g KCl, 0.52 g $MgSO_4.7H_2O$, 1.52 g KH_2PO_4, 10 g glucose, 2 ml Hutner's trace elements, pH 6.8) (Barratt, Johnson, & Ogata, 1965) with ethanol (Merck, absolute, ≥99.9%), water (as control), or ethanol-d_6 (Merck, deuteration degree ≥ 99%; for stable isotope labeling MS) at the indicated concentrations and shaken further until the predetermined time.

2.2 | Determination of the dry weight

Mycelia from three 20-ml cultures were combined and collected on a dry, preweighed Whatman paper no. 1 by vacuum filtration. They were then washed with distilled water (4 × 5 ml, then 2 × 20 ml) and dried on the filter paper at 70°C until at a constant weight (dry weight [DW]).

2.3 | Metabolites extraction and analysis

Mycelia and supernatant from the 3-day-old 20-ml *A. niger* culture were separated by gravity filtration through a cotton ball. A mixture of 10 ml of chloroform and 5 ml of methanol was added to the supernatant, while mycelia were washed once with 10 ml of distilled water and soaked overnight in a mixture of 3 ml of chloroform and 1.5 ml of methanol, before 1.5 ml of MM without glucose was added to them. Subsequently, all mixtures were shaken vigorously, and centrifuged

at 1500 *g*, room temperature for 3 min to separate the organic layer (bottom) from the aqueous layer (top). The organic layer was transferred to another glass vial, evaporated to dryness under a steam of nitrogen, and placed at −20°C for storage. The extracts were reconstituted in 200 µl of chloroform prior to analysis by liquid chromatography (LC)–MS.

For LC–MS and LC–MS/MS analyses, 40 µl of each sample was quantitated on an Ultimate DGP-3600SD LC coupled to a Bruker MicrOTOF Q-II MS instrument, both in the positive and negative ion modes, as described previously (Vinayavekhin et al., 2016).

2.4 | LC–MS untargeted data analysis

The total ion chromatograms from each sample group (i.e., control vs. ethanol treatment) were obtained in triplicate. The total of six chromatograms for mycelia samples and six chromatograms for supernatant samples were then subjected to comparative data analyses separately as previously described (Vinayavekhin, Mahipant, Vangnai, & Sangvanich, 2015), except that (a) the data were normalized by the average DW of the cultures instead of the optical density at 600 nm and (b) the minimum integrated mass ion intensity (MSII) was set at 5,000 instead of 30,000.

2.5 | Stable isotope labeling MS with ethanol-d_6

Intracellular metabolites from *A. niger* cultures treated with ethanol-d_6 were extracted and analyzed by LC–MS exactly as described above in the section "2.3 Metabolites extraction and analysis." The resulting chromatograms were then inspected manually to obtain the mass spectra of the indicated ions.

3 | RESULTS

3.1 | Ethanol tolerance of *A. niger* ES4

Since *A. niger* ES4 was isolated from the outside upper wall of an ethanol tank, we first assessed its ethanol tolerance. It, however, was not possible to monitor the growth of *A. niger* on the solid agar medium containing ethanol, which best mimicked its growth on the wall of the tank, because its spore interfered with the radial growth (data not shown). We therefore determined its ethanol tolerance using a cell growth assay in a defined liquid medium instead (Mahipant et al., 2017). In this assay, *A. niger* ES4 mycelia (60 ml) were cultured in MM adapted slightly from that used by Barratt et al. (1965) for culturing *Aspergillus nidulans*, and with ethanol added at concentrations up to 5% (*v*/*v*). Then, their growth was monitored daily over a 5-day period by measuring the DW of mycelia.

The *A. niger* strain ES4 was able to grow in ethanol at all tested concentrations (2%–5% [*v*/*v*]), although at slower growth rates than the no-ethanol control (Figure 1). Increasing ethanol concentrations decreased the DW at each measured time point in a dose-dependent manner and became lowest at 5% (*v*/*v*) ethanol. The DW amounted to 78%, 65%, 49%, and 30% of that of the ethanol-free control at 2%, 3%, 4%, and 5% (*v*/*v*) ethanol, respectively, at day 4 when the cells were solidly in the stationary phase. Overall, the data revealed some degree of tolerance toward ethanol by the *A. niger* ES4 strain.

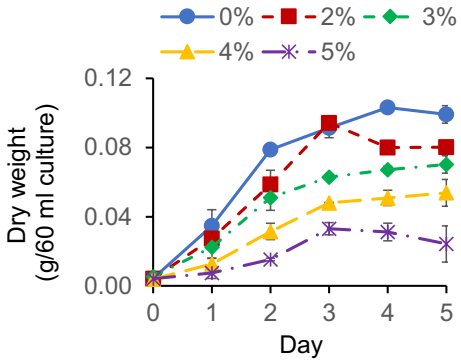

FIGURE 1 Growth curves of *A. niger* ES4 in MM with concentrations of ethanol from 0% to 5% (*v*/*v*). Data are shown as the average DW of mycelia from a 60-ml culture ± standard error of the mean for triplicate experiments per concentration

3.2 | Metabolomics of *A. niger* under ethanol stress

To further characterize the microbe and understand the responses of *A. niger* toward ethanol, metabolomics analysis was performed on both the extracellular and intracellular components of *A. niger* ES4 cultures in the presence and absence of 4% (*v*/*v*) ethanol at day 3, which was the condition that induced moderate stress levels to the fungi (i.e., 52% growth of that without ethanol) and at the day the cells entered early stationary phase (Figure 1). The mycelia or culture supernatant was then extracted for analysis of the hydrophobic metabolites using a 2:1 (*v*/*v*) ratio of chloroform:methanol, and the extracts were concentrated and analyzed by LC–MS using a previously developed untargeted metabolomics platform (Vinayavekhin et al., 2015).

To identify differential metabolites related to ethanol stress responses, the XCMS program (Smith, Want, O'Maille, Abagyan, & Siuzdak, 2006) was used to obtain an MSII value for each detectable metabolite ion in each LC–MS chromatogram, and the MSII values were normalized by the DW to account for the differences in fungal growth. Ions were then regarded as potential responses to ethanol stress only if they were up- or downregulated by fourfold or more with statistical significance (Student's *t* test with $p < .05$) in the ethanol-treated samples compared with the controls, and only if they also met these criteria in another set of independent experimental repeat. Using these criteria, the unbiased comparative analyses revealed 68 and 7 upregulated ions and 1 and 1 downregulated ions in the supernatant, and 322 and 29 upregulated ions and 14 and 24 downregulated ions in the mycelia under ethanol stress in the positive and negative ion modes, respectively (Figure 2).

Next, the structural characterization of these ions with altered levels following ethanol treatment was undertaken manually using the combined clues from the accurate mass, previously reported retention time (RT) (Vinayavekhin et al., 2015, 2016), and tandem mass

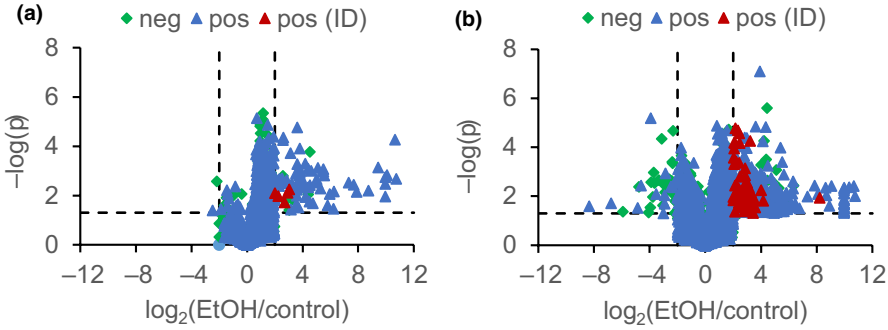

FIGURE 2 Volcano plots of metabolite changes in *A. niger* ES4 at day 3 caused by 4% (*v*/*v*) ethanol. Each (a) extracellular and (b) intracellular metabolite ion in the hydrophobic components with an average MSII above 5,000 counts is plotted as its statistical significance (*p*-value) against the fold change of ethanol (EtOH) over the control. The ions that locate above the horizontal dash line and outside the two vertical dash lines have a *p*-value of less than 0.05 and a fold change of greater than 4, respectively. Each plot contains data from both negative (neg) and positive (pos) ion modes. However, only some positive-mode MS ions with $p < .05$ could be identified (pos (ID)) in this study

spectra (Appendix 1: Tables A1 and A2, and Figure S1). Structures could be assigned to five extracellular and 63 intracellular upregulated positive-mode ions. All of these ions were in the family of triacylglycerol (TAG) for the extracellular components, and the families of diacylglycerol (DAG), TAG, and hydroxy-(h)TAG for the intracellular components (Table 1, and Appendix 1: Tables A1 and A2 with the *sn*-1, *sn*-2 and *sn*-3 side chains written in random order and exact positions of the hydroxyl groups on hTAG unspecified). The most commonly found acyl chains in these altered lipids were 16:0, 18:0, 18:1, and 18:2. The remaining uncharacterized changed ions could not be grouped into the same families as other changed ions, were detected at relatively lower MSII, or were potentially classified as ion fragments or adducts of other smaller or larger molecules. As references, we also performed targeted analyses of other lipids in the biosynthetic pathways of DAG and TAG, such as phospholipids (see Figure 3 for details), and found their levels under ethanol stress more or less undifferentiated from those of the controls (Table 1, Appendix 1: Table A3, and Figure S1). Together, the untargeted metabolomics analysis suggested the involvement of glycerolipids in response to ethanol stress in *A. niger* ES4.

3.3 | Ethanol utilization by *A. niger* ES4

To survive on the wall of an ethanol tank, it might be necessary for *A. niger* strain ES4 to be capable of metabolizing ethanol for nutrients or incorporating ethanol into other molecules to reduce its toxicity. Because our metabolomics analyses above revealed the upregulation of DAG, TAG, and hTAG in the ethanol-treated *A. niger* samples compared with the controls, we set out to trace the possible incorporation of ethanol or parts of ethanol into some of these lipids by using stable isotope labeling MS with ethanol-d_6.

The *A. niger* ES4 cultures were grown in MM in the presence of 4% (*v*/*v*) ethanol-d_6 (or nonlabeled ethanol as controls) for 3 days, harvested for metabolites in the mycelia, and analyzed by LC–MS exactly as described earlier for metabolomics. The chromatograms were then inspected manually for the mass spectra of four representative metabolite ions: (a) DAG (18:2/18:2), (b) TAG (18:0/18:1/18:1) (significantly elevated under ethanol treatment compared to the untreated controls), (c) fatty acid (FA) (18:2), and (d) phosphatidic acid (PA) (18:2/18:2) (in the related metabolic pathways but with unchanged levels). The data showed varying shift in the detected mass-to-charge ratios (m/z) of all lipids in the ethanol-d_6 samples from the nonlabeled controls (Figure 4). The monoisotopic peaks of all lipids, except for FA (18:2), in the nonlabeled samples were no longer dominant peaks in the ethanol-d_6 samples. The m/z with the highest intensities were shifted by +3, +5, and +2 mass units for DAG (18:2/18:2), TAG (18:0/18:1/18:1), and PA (18:2/18:2) from those in the nonlabeled samples, respectively. However, the m/z peaks at ±1, ±2, and ±3 mass units from the dominant m/z peaks were not very different in intensities from those of the dominant m/z peaks for all investigated lipids in the ethanol-d_6 samples. Overall, the results support the metabolism of ethanol in *A. niger* ES4 into other metabolites.

4 | DISCUSSION

The ability to tolerate chemicals present in cultures is one of the most essential traits of microorganisms for utilization in bioprocesses. In this study, we found *A. niger* ES4 capable of growing even in 5% (*v*/*v*) (or 4% [*w*/*v*]) ethanol with its growth amounting to approximately 30% of that of the ethanol-free control. Interestingly, this level of tolerance was comparable with that of the ethalogenic filamentous fungus *Fusarium oxysporum* (Paschos, Xiros, & Christakopoulos, 2015) and higher than that of the natural ethanol-producing ascomycetous yeasts *Pichia stipites*, whose growth was inhibited at 3.4% (*w*/*v*) ethanol when grown on glucose (Meyrial, Delgenes, Romieu, Moletta, & Gounot, 1995). Assuming that the amount of ethanol produced by these ethalogenic microbes themselves stayed relatively low compared with that of the initially added ethanol concentration, our results would indicate that *A. niger* strain ES4 had a relatively high resistance toward ethanol. However, as mentioned earlier, Dantigny et al. (2005) also demonstrated the ability of the *A. niger*

TABLE 1 Relative levels of identified ethanol-upregulated lipids and of other related lipids

Lipid class and acyl chain	Ion	m/z	RT (min)	EtOH/con[a,b]
Upregulated lipids in ethanol-treated extracellular samples				
Triacylglycerol (TAG)				
16:0/18:1/18:2	$[M + NH_4]^+$	874.7830	48.3	4.8*
18:1/18:2/18:2	$[M + NH_4]^+$	898.7839	48.1	6.6*
18:1/18:1/18:2	$[M + NH_4]^+$	900.7989	48.6	4.1†
18:1/18:1/18:1	$[M + NH_4]^+$	902.8136	48.7	7.7†
18:0/18:1/18:1	$[M + NH_4]^+$	904.8272	48.9	8.3†
Upregulated lipids in ethanol-treated intracellular samples				
Diacylglycerol (DAG)				
18:2/18:2	$[M + NH_4]^+$	634.5394	43.8	7.5*
18:1/18:2	$[M + NH_4]^+$	636.5550	44.4	6.7*
18:1/18:1	$[M + NH_4]^+$	638.5700	44.9	6.7†
18:0/18:1	$[M + NH_4]^+$	640.5815	45.3	8.7†
18:2/20:2	$[M + NH_4]^+$	662.5667	44.6	8.0*
18:2/20:1	$[M + NH_4]^+$	664.5833	45.1	7.0*
TAG				
12:0/18:2/18:2	$[M + NH_4]^+$	816.7036	47.6	8.4†
14:0/18:2/18:2	$[M + NH_4]^+$	844.7360	47.8	4.4‡
18:0/18:1/18:1	$[M + NH_4]^+$	904.8319	49.0	4.5§
18:0/18:0/18:1	$[M + NH_4]^+$	906.8451	49.1	5.4§
18:0/18:1/20:0	$[M + NH_4]^+$	934.8749	49.5	4.4§
18:0/18:1/24:0	$[M + NH_4]^+$	990.9377	50.2	4.1§
18:1/18:1/25:0	$[M + NH_4]^+$	1,002.9375	50.2	5.0†
18:0/18:1/26:0	$[M + NH_4]^+$	1,018.9654	50.5	4.7§
Hydroxy-TAG (hTAG)				
16:0/16:1(OH)/18:2	$[M + NH_4]^+$	862.7455	46.9	4.6‡
16:0/16:0/18:2(OH)	$[M + NH_4]^+$	864.7565	47.2	4.2§
16:0/18:2/18:2(OH)	$[M + NH_4]^+$	888.7606	47.1	8.2*
16:0/18:1/18:2(OH)	$[M + NH_4]^+$	890.7736	47.3	5.4†
18:1/18:2(OH)/18:3	$[M + NH_4]^+$	912.7626	46.9	11.2*
18:1/18:2/18:2(OH)	$[M + NH_4]^+$	914.7771	47.2	11.8*
18:1/18:1/18:2(OH)	$[M + NH_4]^+$	916.7929	47.5	8.8‡
18:0/18:1/18:2(OH)	$[M + NH_4]^+$	918.8068	47.7	9.9†
Other intracellular lipids in the related pathways				
Fatty acid (FA)				
16:0	$[M - H]^-$	255.2317	18.6	1.6†
18:2	$[M - H]^-$	279.2336	18.5	1.7†
18:1	$[M - H]^-$	281.2478	18.8	2.0‡
18:0	$[M - H]^-$	283.2624	19.2	1.5‡
Monoacylglycerol (MAG)				
16:0	$[M + Na]^+$	353.2656	34.0	2.4*
18:2	$[M + Na]^+$	377.2718	33.1	2.1
Phosphatidic acid (PA)				
16:0/18:2	$[M-H]^-$	671.4649	27.4	1.6
18:2/18:2	$[M-H]^-$	695.4647	26.8	2.3*

(Continues)

TABLE 1 (Continued)

Lipid class and acyl chain	Ion	m/z	RT (min)	EtOH/con[a,b]
Phosphatidylethanolamine (PE)				
16:0/18:2	$[M - H]^-$	714.5023	39.0	1.0
18:2/18:2	$[M - H]^-$	738.5004	38.2	1.7
Phosphatidylserine (PS)				
16:0/18:2	$[M - H]^-$	758.4944	29.9	1.3
18:2/18:2	$[M - H]^-$	782.4946	29.3	1.5
Phosphatidylglycerol (PG)				
16:0/18:2	$[M - H]^-$	745.4976	34.4	1.4
18:2/18:2	$[M - H]^-$	769.4962	33.8	1.5
Phosphatidylinositol (PI)				
16:0/18:2	$[M - H]^-$	833.5160	34.0	1.2
18:2/18:2	$[M - H]^-$	857.5147	33.4	1.1
Phosphatidylcholine (PC)				
16:0/18:2	$[M + H]^+$	758.5726	41.7	0.8†
18:2/18:2	$[M + H]^+$	782.5751	41.3	1.8§

Abbreviations: m/z, mass-to-charge ratio; RT, retention time.
[a]EtOH/con value represents the ratio of the average mass ion intensity of ethanol-treated sample group and that of the control.
[b]Student's *t* test: *, $p < .05$; †, $p < .01$; ‡, $p < .005$; §, $p < .001$; $N = 3$.

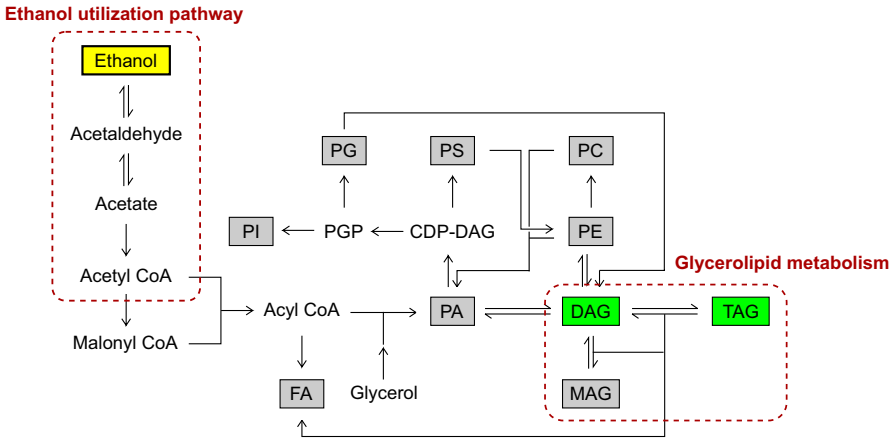

FIGURE 3 Biosynthesis of glycerolipids and phospholipids in *A. niger* (Kanehisa & Goto, 2000), starting from ethanol. The *green boxes* indicate lipids that had statistically significantly elevated levels, whereas the *gray boxes* show other lipids whose levels were quantitated in this study and the *yellow box* emphasizes where ethanol locates in the pathways. Glycerolipids include monoacylglycerol (MAG), diacylglycerol (DAG), and triacylglycerol (TAG), whereas phospholipids shown are phosphatidic acid (PA), phosphatidylethanolamine (PE), phosphatidylcholine (PC), phosphatidylserine (PS), phosphatidylglycerol (PG), and phosphatidylinositol (PI)

strain isolated from spoiled pastry products to grow on potato dextrose agar containing ethanol up to 4% (*w*/*w*) with about 50% reduction in its growth, which seemed to be higher than ethanol tolerance of *A. niger* ES4 in this study. Nevertheless, it was known that the choice of culture media and conditions could affect ethanol tolerance of microbes greatly, and thus, how tolerance *A. niger* ES4 is compared to other *A. niger* strains or other organisms remained to be proven in the future study.

The subsequent investigation into the response mechanisms of *A. niger* ES4 to ethanol using an untargeted metabolomics approach revealed the accumulation of neutral glycerolipids (extracellular TAG, and intracellular DAG, TAG, and hTAG) under ethanol stress. DAG and TAG are interconnected in the glycerolipid metabolism (Figure 4). Functionally, DAG is known to play multiple roles from being a component of the cell membrane and an intermediate in lipid metabolism to a second messenger in lipid-mediated signaling cascades (Carrasco & Mérida, 2007), whereas TAG is traditionally thought of as an energy storage lipid.

In terms of responses to stress, even though there have been no prior reports demonstrating the effect of upregulated DAG or TAG in the organic solvent tolerance of microbes, these neutral lipids were previously implicated in protecting plants from other abiotic

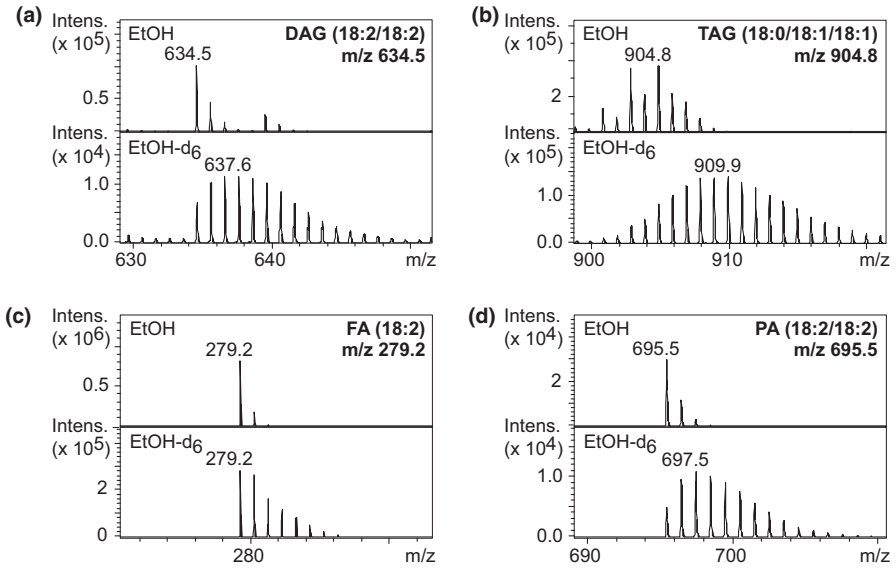

FIGURE 4 Mass spectra of representative ions from stable isotope labeling MS experiments with ethanol-d_6. The *A. niger* ES4 was cultured in duplicate in the presence of 4% (v/v) either ethanol (EtOH)-d_6 or EtOH (as control) and analyzed for intracellular metabolites exactly as conducted in the untargeted metabolomics analysis. Mass spectra were extracted from the total ion chromatograms at the retention time (RT) of 43.8 min for (a) diacylglycerol (DAG) (18:2/18:2) and 49.0 min for (b) triacylglycerol (TAG) (18:0/18:1/18:1) in the positive ion mode, and at a RT of 18.5 min for (c) fatty acid (FA) (18:2) and 26.8 min for (d) phosphatidic acid (PA) (18:2/18:2) in the negative ion mode

stressors, such as coldness (Tan et al., 2018) and darkness (Fan, Yu, & Xu, 2017). In the case of coldness, for example, *Arabidopsis* accumulated PA, DAG, and TAG during freezing stress where disruption in the genes encoding the enzymes acyl-coenzyme A: DAG acyltransferase and DAG kinase, which catalyze the conversion of DAG to TAG and PA, subsequently resulted in decreased and increased TAG levels and tolerance to coldness, respectively (Tan et al., 2018). It is, therefore, possible that, with the unchanged levels of other phospholipids that are components of cell membranes (e.g., PA, phosphatidylethanolamine (PE), and phosphatidylcholine (PC) [Ianutsevich, Danilova, Groza, & Tereshina, 2016]) found in this study, the elevated DAG and TAG levels as the novel responses to ethanol stress might play some roles in defending *A. niger* against the toxic effects of ethanol. Yet, because cold stress rigidifies cell membrane, the effect that is opposite to that of ethanol, further genetic data are needed to pinpoint the relevance of these glycerolipids on ethanol tolerance of *A. niger*. In addition, it remains to be determined whether the upregulation in glycerolipids following ethanol exposure is specific to *A. niger* ES4 or general for all *A. niger* isolates.

Another class of metabolites elevated under ethanol stress was hTAGs, which have mainly been described in *Ricinus communis* castor oil (Kim et al., 2011), *Lesquerella* seed oil (Byrdwell & Neff, 1998; Hayes, Kleiman, & Phillips, 1995), and ergot oil from the fungus *Claviceps purpurea* (Morris & Hall, 1966). As the detection and quantitation of hTAG in routine work have remained quite limited compared with other classes of lipids, there is no evidence to support or refute their relevance to various stresses. Yet, because their substrates, hydroxy fatty acids, are known for their specialized medical and industrial usages (e.g. lubricants, paints, and coatings) (Hayes et al., 1995; Meesapyodsuk & Qiu, 2008), the discovery of upregulated hTAGs in this study suggested that, upon fully characterizing their structures, *A. niger* might be able to serve as another source of this industrially important class of lipids as well.

One of the known metabolic responses of the yeast *Saccharomyces cerevisiae* toward ethanol involves an increase in the unsaturated-to-saturated fatty acids ratio, whereby the relative contents of FA (16:1) and FA (18:1) increase while those of FA (16:0) and FA (18:0) decrease (Sajbidor, Ciesarova, & Smogrovicova, 1995). Interestingly, our metabolomics studies showed only slight elevation in contents of all four most abundant fatty acids found in *A. niger* ES4 (i.e., 16:0, 18:2, 18:1 and 18:0) under ethanol stress without an obvious shift in unsaturation index. The alteration in this index was also not immediately apparent in other lipid species, as most of the changing lipids contained both unsaturated and saturated acyl chains. The findings therefore suggested that *A. niger* might utilize different mechanisms to counteract toxicity of ethanol than *S. cerevisiae*. However, we could not rule out the possibilities that the observed effects might simply be specific to the choices of microbial strain, growth medium, or conditions depicted in this study.

The results from the stable isotope labeling MS showed that the isotopic patterns of all the molecular ions of representative lipids in the ethanol-d_6 samples differed from those in the nonlabeled ethanol samples. Because the only isotope present at an unnaturally high abundance in this case was deuterium, the finding indicated the incorporation of varying numbers of deuterium atoms into each lipid, which could potentially occur both via catabolism of ethanol-d_6 by *A. niger* and via deuterium exchanges with the deuteron on the hydroxyl group of ethanol-d_6 during the lipid biosynthesis.

However, in this study, ethanol-d_6 was added into the cultures at 4% (*v*/*v*), which resulted in the mole ratio of proton to deuteron in the cultures being 100 to 0.58 (see Appendix 2 for details on calculation). Assuming that all hydrogen atoms on each representative ion have equal chances to undergo deuterium exchanges, and disregarding any kinetics isotope effects of deuterium, the predicted isotopic ratios, M:M + 1:M + 2:M + 3:M + 4, when considering only deuterium exchanges and natural isotopic abundance of each element would be equal to 100:84:36:10:2 for DAG (18:2/18:2), 80:100:63:27:9 for TAG (18:0/18:1/18:1), 100:38:7:1:<1 for FA (18:2), and 100:82:35:10:2 for PA (18:2/18:2) (Appendix 2). These ratios represent the highest probable signals of each isotope arisen from deuterium exchanges; yet, they alone still could not account for the observed high abundances of these isotopes, especially with M + 2 and higher m/z species, in the ethanol-d_6 samples (Figure 3). The finding therefore suggested to us that *A. niger* ES4 was in fact capable of metabolizing ethanol-d_6 into other compounds in an existing metabolic pathway.

Metabolically, the ethanol utilization pathway has been well studied in the closely related fungus, *Aspergillus nidulans* (Felenbok, Flipphi, & Nikolaev, 2001). In this pathway, ethanol is first oxidized to acetaldehyde by alcohol dehydrogenase I. Further oxidation of acetaldehyde by alcohol dehydrogenase then yields acetate, which subsequently is converted to acetyl CoA by acetyl CoA synthetase (Figure 3). In the form of acetyl CoA, these carbon and hydrogen atoms from ethanol can then enter into many metabolic pathways, along with the acetyl CoA synthesized from other carbon sources, such as glucose. For lipid synthesis, acetyl CoA is carboxylated to malonyl CoA and coupled with this product to yield acyl CoA, which is the substrate for production of fatty acids, phospholipids, and glycerolipids (Figure 3) (Kanehisa & Goto, 2000). For *A. niger*, the genes encoding several homologs of alcohol dehydrogenases have been annotated in the genome of *A. niger* strain CBS513.88 (Pel et al., 2007). However, their activities in culture have not been confirmed. Our present data, therefore, represent the first piece of evidence to support the existence of this ethanol utilization pathway in *A. niger* ES4.

5 | CONCLUSIONS

In total, by applying untargeted metabolomics to study the extracellular and intracellular hydrophobic components of the *A. niger* strain ES4 isolated from the wall of an ethanol tank, we demonstrated the upregulation of glycerolipids (i.e., DAG, TAG and hTAG) as novel responses of microbes to ethanol stress. The subsequent stable isotope labeling MS with ethanol-d_6 also supported the utilization of ethanol by *A. niger* ES4. Future work will aim to determine the relevance of these upregulated changes in glycerolipid metabolism and the ethanol utilization pathway in the ethanol tolerance of *A. niger*, as well as to elucidate the structures, biosynthesis, and functions of hTAG more thoroughly. More generally, we believe that untargeted metabolomics platforms and the overall approaches presented in this work will be powerful tools for the discovery of more novel responses of microbes to organic solvent stress, as well as to other external stimuli, in the future.

ACKNOWLEDGEMENTS

We thank Dr. Robert Douglas John Butcher (Research Clinic Unit, Office of Research Affairs, Chulalongkorn University) for editorial help in preparing this manuscript. This research was supported by the Office of the Higher Education Commission and the Thailand Research Fund (MRG6180002). The opinions expressed in this paper are the sole responsibility of the authors and do not necessarily reflect those of the funding agencies or Chulalongkorn University.

CONFLICT OF INTEREST

None declared.

AUTHOR CONTRIBUTIONS

Nawaporn Vinayavekhin coordinated the experiments, analyzed the data, drafted, and revised the manuscript. Wimonsiri Kongchai conducted the experiments and analyzed the data. Jittra Piapukiew and Warinthorn Chavasiri discussed the experiments and revised the manuscript. All authors read and approved the final version of the manuscript.

ETHICAL APPROVAL

None required.

DATA AVAILABILITY STATEMENT

The nucleotide sequence data were deposited into the DDBJ/EMBL/GenBank nucleotide sequence databases with accession number MK621333. Other data generated or analyzed during this study are included in this published article and its Supporting Information file.

ORCID

Nawaporn Vinayavekhin https://orcid.org/0000-0002-1525-0382

Jittra Piapukiew https://orcid.org/0000-0003-0116-590X

Warinthorn Chavasiri https://orcid.org/0000-0001-5201-1324

REFERENCES

Aono, R., & Kobayashi, H. (1997). Cell surface properties of organic solvent-tolerant mutants of *Escherichia coli* K-12. *Applied and Environmental Microbiology*, *63*(9), 3637–3642.

Aono, R., Tsukagoshi, N., & Yamamoto, M. (1998). Involvement of outer membrane protein TolC, a possible member of the mar-sox regulon,

in maintenance and improvement of organic solvent tolerance of *Escherichia coli* K-12. *Journal of Bacteriology*, *180*(4), 938–944.

Baker, S. E. (2006). *Aspergillus niger* genomics: Past, present and into the future. *Medical Mycology*, *44*, S17–S21. https://doi.org/10.1080/13693780600921037

Barratt, R. W., Johnson, G. B., & Ogata, W. N. (1965). Wild-type and mutant stocks of *Aspergillus nidulans*. *Genetics*, *52*(1), 233–246.

Bohin, J. P., Rigomier, D., & Schaeffer, P. (1976). Ethanol sensitivity of sporulation in *Bacillus subtilis*: A new tool for the analysis of the sporulation process. *Journal of Bacteriology*, *127*(2), 934–940.

Bustard, M. T., Whiting, S., Cowan, D. A., & Wright, P. C. (2002). Biodegradation of high-concentration isopropanol by a solvent-tolerant thermophile. *Bacillus Pallidus*. *Extremophiles*, *6*(4), 319–323. https://doi.org/10.1007/s00792-001-0260-5

Byrdwell, W. C., & Neff, W. E. (1998). Analysis of hydroxy-containing seed oils using atmospheric pressure chemical ionization mass spectrometry. *Journal of Liquid Chromatography & Related Technologies*, *21*(10), 1485–1501. https://doi.org/10.1080/10826079808000529

Carrasco, S., & Mérida, I. (2007). Diacylglycerol, when simplicity becomes complex. *Trends in Biochemical Sciences*, *32*(1), 27–36. https://doi.org/10.1016/j.tibs.2006.11.004

Clark, D. S., Bordner, P., Galdrich, E. H., Kabler, P. W., & Huff, C. B. (1958). *Applied Microbiology*. New York, NY: International Book Company.

Coulibaly, L., Naveau, H., & Agathos, S. N. (2002). A tanks-in-series bioreactor to simulate macromolecule-laden wastewater pretreatment under sewer conditions by *Aspergillus niger*. *Water Research*, *36*(16), 3941–3948. https://doi.org/10.1016/S0043-1354(02)00117-3

Dantigny, P., Guilmart, A., Radoi, F., Bensoussan, M., & Zwietering, M. (2005). Modelling the effect of ethanol on growth rate of food spoilage moulds. *International Journal of Food Microbiology*, *98*(3), 261–269. https://doi.org/10.1016/j.ijfoodmicro.2004.07.008

Fan, J., Yu, L., & Xu, C. (2017). A central role for triacylglycerol in membrane lipid breakdown, fatty acid beta-oxidation, and plant survival under extended darkness. *Plant Physiology*, *174*(3), 1517–1530. https://doi.org/10.1104/pp.17.00653

Felenbok, B., Flipphi, M., & Nikolaev, I. (2001). Ethanol catabolism in *Aspergillus nidulans*: A model system for studying gene regulation. *Progress in Nucleic Acid Research and Molecular Biology*, *69*, 149–204. https://doi.org/10.1016/S0079-6603(01)69047-0

Frisvad, J. C., Larsen, T. O., Thrane, U., Meijer, M., Varga, J., Samson, R. A., & Nielsen, K. F. (2011). Fumonisin and ochratoxin production in industrial *Aspergillus niger* strains. *PLoS ONE*, *6*(8), e23496. https://doi.org/10.1371/journal.pone.0023496

Hayes, D. G., Kleiman, R., & Phillips, B. S. (1995). The triglyceride composition, structure, and presence of estolides in the oils of *Lesquerella* and related species. *Journal of the American Oil Chemists Society*, *72*(5), 559–569. https://doi.org/10.1007/Bf02638857

Ianutsevich, E. A., Danilova, O. A., Groza, N. V., & Tereshina, V. M. (2016). Membrane lipids and cytosol carbohydrates in *Aspergillus niger* under osmotic, oxidative, and cold impact. *Microbiology*, *85*(3), 302–310. https://doi.org/10.1134/S0026261716030152

Izmirlioglu, G., & Demirci, A. (2017). Simultaneous saccharification and fermentation of ethanol from potato waste by co-cultures of *Aspergillus niger* and *Saccharomyces cerevisiae* in biofilm reactors. *Fuel*, *202*, 260–270. https://doi.org/10.1016/j.fuel.2017.04.047

Kajiwara, S., Shirai, A., Fujii, T., Toguri, T., Nakamura, K., & Ohtaguchi, K. (1996). Polyunsaturated fatty acid biosynthesis in *Saccharomyces cerevisiae*: Expression of ethanol tolerance and the FAD2 gene from *Arabidopsis thaliana*. *Applied and Environmental Microbiology*, *62*(12), 4309–4313.

Kanehisa, M., & Goto, S. (2000). KEGG: Kyoto encyclopedia of genes and genomes. *Nucleic Acids Research*, *28*(1), 27–30. https://doi.org/10.1093/nar/28.1.27

Kang, H.-J., Heo, D.-H., Choi, S.-W., Kim, K.-N., Shim, J., Kim, C.-W., … Yun, C.-W. (2007). Functional characterization of Hsp33 protein from *Bacillus psychrosaccharolyticus*; additional function of HSP33 on resistance to solvent stress. *Biochemical and Biophysical Research Communications*, *358*(3), 743–750. https://doi.org/10.1016/j.bbrc.2007.04.184

Kim, H. U., Lee, K. R., Go, Y. S., Jung, J. H., Suh, M. C., & Kim, J. B. (2011). Endoplasmic reticulum-located PDAT1-2 from castor bean enhances hydroxy fatty acid accumulation in transgenic plants. *Plant and Cell Physiology*, *52*(6), 983–993. https://doi.org/10.1093/pcp/pcr051

Lubertozzi, D., & Keasling, J. D. (2009). Developing *Aspergillus* as a host for heterologous expression. *Biotechnology Advances*, *27*(1), 53–75. https://doi.org/10.1016/j.biotechadv.2008.09.001

Mahipant, G., Paemanee, A., Roytrakul, S., Kato, J., & Vangnai, A. S. (2017). The significance of proline and glutamate on butanol chaotropic stress in *Bacillus subtilis* 168. *Biotechnology for Biofuels*, *10*, 122. https://doi.org/10.1186/s13068-017-0811-3

Meesapyodsuk, D., & Qiu, X. (2008). An oleate hydroxylase from the fungus *Claviceps purpurea*: Cloning, functional analysis, and expression in *Arabidopsis*. *Plant Physiology*, *147*(3), 1325–1333. https://doi.org/10.1104/pp.108.117168

Meyrial, V., Delgenes, J. P., Romieu, C., Moletta, R., & Gounot, A. M. (1995). Ethanol tolerance and activity of plasma-membrane ATPase in *Pichia stipitis* grown on D-xylose or on D-glucose. *Enzyme and Microbial Technology*, *17*(6), 535–540. https://doi.org/10.1016/0141-0229(94)00065-Y

Mogensen, J., Nielsen, H. B., Hofmann, G., & Nielsen, J. (2006). Transcription analysis using high-density micro-arrays of *Aspergillus nidulans* wild-type and *creA* mutant during growth on glucose or ethanol. *Fungal Genetics and Biology*, *43*(8), 593–603. https://doi.org/10.1016/j.fgb.2006.03.003

Morris, L. J., & Hall, S. W. (1966). The structure of the glycerides of ergot oils. *Lipids*, *1*(3), 188–196. https://doi.org/10.1007/BF02531871

Neumann, G., Veeranagouda, Y., Karegoudar, T. B., Sahin, O., Mäusezahl, I., Kabelitz, N., … Heipieper, H. J. (2005). Cells of *Pseudomonas putida* and *Enterobacter* sp. adapt to toxic organic compounds by increasing their size. *Extremophiles*, *9*(2), 163–168. https://doi.org/10.1007/s00792-005-0431-x

Nicolaou, S. A., Gaida, S. M., & Papoutsakis, E. T. (2010). A comparative view of metabolite and substrate stress and tolerance in microbial bioprocessing: From biofuels and chemicals, to biocatalysis and bioremediation. *Metabolic Engineering*, *12*(4), 307–331. https://doi.org/10.1016/j.ymben.2010.03.004

O'Connell, M. J., & Kelly, J. M. (1988). Differences in the regulation of aldehyde dehydrogenase genes in *Aspergillus niger* and *Aspergillus nidulans*. *Current Genetics*, *14*(2), 95–103. https://doi.org/10.1007/BF00569332

Pariza, M. W., & Cook, M. (2010). Determining the safety of enzymes used in animal feed. *Regulatory Toxicology and Pharmacology*, *56*(3), 332–342. https://doi.org/10.1016/j.yrtph.2009.10.005

Paschos, T., Xiros, C., & Christakopoulos, P. (2015). Ethanol effect on metabolic activity of the ethalogenic fungus Fusarium oxysporum. *BMC Biotechnology*, *15*, 15. https://doi.org/10.1186/s12896-015-0130-3

Pel, H. J., de Winde, J. H., Archer, D. B., Dyer, P. S., Hofmann, G., Schaap, P. J., … Stam, H. (2007). Genome sequencing and analysis of the versatile cell factory *Aspergillus niger* CBS 513.88. *Nature Biotechnology*, *25*(2), 221–231. https://doi.org/10.1038/nbt1282

Person, A. K., Chudgar, S. M., Norton, B. L., Tong, B. C., & Stout, J. E. (2010). *Aspergillus niger*: An unusual cause of invasive pulmonary aspergillosis. *Journal of Medical Microbiology*, *59*(Pt 7), 834–838. https://doi.org/10.1099/jmm.0.018309-0

Petersohn, A., Brigulla, M., Haas, S., Hoheisel, J. D., Volker, U., & Hecker, M. (2001). Global analysis of the general stress response of *Bacillus subtilis*. *Journal of Bacteriology*, *183*(19), 5617–5631. https://doi.org/10.1128/JB.183.19.5617-5631.2001

Ramachandran, S., Fontanille, P., Pandey, A., & Larroche, C. (2008). Permeabilization and inhibition of the germination of spores of *Aspergillus niger* for gluconic acid production from glucose. *Bioresource Technology*, *99*(11), 4559–4565. https://doi.org/10.1016/j.biortech.2007.06.055

Sajbidor, J., Ciesarova, Z., & Smogrovicova, D. (1995). Influence of ethanol on the lipid content and fatty acid composition of *Saccharomyces cerevisiae*. *Folia Microbiologica*, *40*(5), 508–510.

Smith, C. A., Want, E. J., O'Maille, G., Abagyan, R., & Siuzdak, G. (2006). XCMS: Processing mass spectrometry data for metabolite profiling using nonlinear peak alignment, matching, and identification. *Analytical Chemistry*, *78*(3), 779–787. https://doi.org/10.1021/ac051437y

Srivastava, S., & Thakur, I. S. (2006). Evaluation of bioremediation and detoxification potentiality of *Aspergillus niger* for removal of hexavalent chromium in soil microcosm. *Soil Biology & Biochemistry*, *38*(7), 1904–1911. https://doi.org/10.1016/j.soilbio.2005.12.016

Tan, W.-J., Yang, Y.-C., Zhou, Y., Huang, L.-P., Xu, L. E., Chen, Q.-F., … Xiao, S. (2018). Diacylglycerol acyltransferase and diacylglycerol kinase modulate triacylglycerol and phosphatidic acid production in the plant response to freezing stress. *Plant Physiology*, *177*(3), 1303–1318. https://doi.org/10.1104/pp.18.00402

Taylor, M., Tuffin, M., Burton, S., Eley, K., & Cowan, D. (2008). Microbial responses to solvent and alcohol stress. *Biotechnology Journal*, *3*(11), 1388–1397. https://doi.org/10.1002/biot.200800158

Torres, S., Pandey, A., & Castro, G. R. (2011). Organic solvent adaptation of Gram positive bacteria: Applications and biotechnological potentials. *Biotechnology Advances*, *29*(4), 442–452. https://doi.org/10.1016/j.biotechadv.2011.04.002

Vinayavekhin, N., Mahipant, G., Vangnai, A. S., & Sangvanich, P. (2015). Untargeted metabolomics analysis revealed changes in the composition of glycerolipids and phospholipids in *Bacillus subtilis* under 1-butanol stress. *Applied Microbiology and Biotechnology*, *99*(14), 5971–5983. https://doi.org/10.1007/s00253-015-6692-0

Vinayavekhin, N., Sueajai, J., Chaihad, N., Panrak, R., Chokchaisiri, R., Sangvanich, P., … Piyachaturawat, P. (2016). Serum lipidomics analysis of ovariectomized rats under *Curcuma comosa* treatment. *Journal of Ethnopharmacology*, *192*, 273–282. https://doi.org/10.1016/j.jep.2016.07.054

Vinayavekhin, N., & Vangnai, A. S. (2018). The effects of disruption in membrane lipid biosynthetic genes on 1-butanol tolerance of *Bacillus subtilis*. *Applied Microbiology and Biotechnology*, *102*(21), 9279–9289. https://doi.org/10.1007/s00253-018-9298-5

Weber, F. J., & de Bont, J. A. (1996). Adaptation mechanisms of microorganisms to the toxic effects of organic solvents on membranes. *Biochimica Et Biophysica Acta (BBA) - Reviews on Biomembranes*, *1286*(3), 225–245. https://doi.org/10.1016/S0304-4157(96)00010-X

SUPPORTING INFORMATION

Additional supporting information may be found online in the Supporting Information section at the end of the article.

How to cite this article: Vinayavekhin N, Kongchai W, Piapukiew J, Chavasiri W. *Aspergillus niger* upregulated glycerolipid metabolism and ethanol utilization pathway under ethanol stress. *MicrobiologyOpen*. 2019;00:e948. https://doi.org/10.1002/mbo3.948

APPENDIX 1

TABLE A1: Identified positive-mode ions with statistically significantly elevated levels in ethanol-treated extracellular *A. niger* samples compared to the untreated control showing the mass-to-charge ratio (*m/z*), retention time (RT) and (a) potential identification and MS/MS spectrum, (b) integrated mass ion intensity (MSII) and (c) adjusted mass ion intensity (aMSII). The MSII and aMSII data are shown for three *A. niger* samples without (Con-1–3) or with ethanol treatment (EtOH-1–3) and their respective averages (Con-avg and EtOH-avg, respectively)

(a) Identified significantly elevated positive-mode ions in ethanol-treated extracellular *A. niger* samples (potential identification and MS/MS spectrum)

No.	*m/z*	RT (min)	Ion	Potential identification	MS/MS spectrum
1	874.7830	48.3	$[M + NH_4]^+$	TAG (16:0/18:1/18:2)	SI, p. S3
2	898.7839	48.1	$[M + NH_4]^+$	TAG (18:1/18:2/18:2)	SI, p. S4
3	900.7989	48.6	$[M + NH_4]^+$	TAG (18:1/18:1/18:2)	SI, p. S5
4	902.8136	48.7	$[M + NH_4]^+$	TAG (18:1/18:1/18:1)	SI, p. S6
5	904.8272	48.9	$[M + NH_4]^+$	TAG (18:0/18:1/18:1)	SI, p. S7

(b) Identified significantly elevated positive-mode ions in ethanol-treated extracellular *A. niger* samples (MSII)

			Integrated mass ion intensity (MSII)							
No.	*m/z*	RT (min)	EtOH-1	EtOH-2	EtOH-3	EtOH-avg	Con-1	Con-2	Con-3	Con-avg
1	874.7830	48.3	3.27E+06	2.51E+06	2.47E+06	2.75E+06	1.30E+06	1.02E+06	9.02E+05	1.07E+06
2	898.7839	48.1	1.01E+07	7.88E+06	6.70E+06	8.24E+06	2.79E+06	2.21E+06	2.08E+06	2.36E+06
3	900.7989	48.6	1.17E+07	8.98E+06	8.84E+06	9.85E+06	8.84E+06	2.66E+06	2.16E+06	4.55E+06
4	902.8136	48.7	7.59E+06	5.94E+06	5.82E+06	6.45E+06	2.02E+06	1.55E+06	1.18E+06	1.58E+06
5	904.8272	48.9	4.85E+06	3.76E+06	4.10E+06	4.23E+06	1.17E+06	9.80E+05	7.42E+05	9.64E+05

(c) Identified significantly elevated positive-mode ions in ethanol-treated extracellular *A. niger* samples (aMSII)

			Adjusted integrated mass ion intensity (aMSII)							
No.	*m/z*	RT (min)	EtOH-1	EtOH-2	EtOH-3	EtOH-avg	Con-1	Con-2	Con-3	Con-avg
1	874.7830	48.3	4.71E+06	3.62E+06	3.55E+06	3.96E+06	9.95E+05	7.83E+05	6.91E+05	8.23E+05
2	898.7839	48.1	1.46E+07	1.13E+07	9.65E+06	1.19E+07	2.14E+06	1.69E+06	1.59E+06	1.81E+06
3	900.7989	48.6	1.69E+07	1.29E+07	1.27E+07	1.42E+07	6.77E+06	2.04E+06	1.65E+06	3.49E+06
4	902.8136	48.7	1.09E+07	8.56E+06	8.38E+06	9.29E+06	1.55E+06	1.19E+06	9.04E+05	1.21E+06
5	904.8272	48.9	6.98E+06	5.41E+06	5.90E+06	6.10E+06	8.95E+05	7.51E+05	5.68E+05	7.38E+05

TABLE A2: Identified positive-mode ions with statistically significantly elevated levels in ethanol-treated intracellular *A. niger* samples compared to the untreated control showing the mass-to-charge ratio (*m/z*), retention time (RT) and (a) potential identification and MS/MS spectrum, (b) integrated mass ion intensity (MSII) and (c) adjusted mass ion intensity (aMSII). The MSII and aMSII data are shown for three *A. niger* samples without (Con-1–3) or with ethanol treatments (EtOH-1–3) and their respective averages (Con-avg and EtOH-avg, respectively)

(a) Identified significantly elevated positive-mode ions in ethanol-treated intracellular *A. niger* samples (potential identification and MS/MS spectrum)

No.	*m/z*	RT (min)	Ion	Potential identification	MS/MS spectrum
1	243.2090	43.8	–	Fragment of DAG (18:2/18:2)	–
2	261.2182	43.8	–	Fragment of DAG (18:2/18:2)	–
3	263.2362	44.0	–	Fragment of DAG (16:0/18:2)	–
4	299.2571	44.2	–	Fragment of DAG (16:0/18:2)	–
5	331.2789	44.0	–	Fragment of DAG (16:0/18:2)	–
6	337.2740	44.0	–	Fragment of DAG (16:0/18:2)	–
7	339.2896	44.6	–	Fragment of DAG (18:2/20:2)	–
8	357.2972	44.4	–	Fragment of DAG (18:1/18:2)	–
9	505.3885	43.8	–	Fragment of DAG (18:2/18:2) (?)	–
10	577.5185	44.6	$[M - H_2O + H]^+$	DAG (16:0/18:1)	–
11	593.5154	44.1	$[M + H]^+$	DAG (16:0/18:2)	–
12	595.5281	44.6	$[M + H]^+$	DAG (16:0/18:1)	–
13	599.5026	43.8	$[M - H_2O + H]^+$	DAG (18:2/18:2)	–
14	601.5186	44.4	$[M - H_2O + H]^+$	DAG (18:1/18:2)	–
15	603.5334	44.9	$[M - H_2O + H]^+$	DAG (18:1/18:1)	–
16	605.5484	44.0	$[M - H_2O + C_2H_6 + H]^+$	DAG (16:0/18:2)	–
17	617.5133	43.7	$[M + H]^+$	DAG (18:2/18:2)	–
18	617.5101	44.7	$[M - H_2 + H]^+$	DAG (18:1/18:2)	–
19	619.5266	44.4	$[M + H]^+$	DAG (18:1/18:2)	–
20	621.5416	44.9	$[M + H]^+$	DAG (18:1/18:1)	–
21	631.5539	44.2	$[M - H_2O + C_2H_6 + H_2 + H]^+$	DAG (18:2/18:2)	–
22	633.5441	44.6	$[M + CH_2 + H]^+$	DAG (18:1/18:2)	–
23	634.5394	43.8	$[M + NH_4]^+$	DAG (18:2/18:2)	SI, p. S8
24	636.5550	44.4	$[M + NH_4]^+$	DAG (18:1/18:2)	SI, p. S9
25	638.5700	44.9	$[M + NH_4]^+$	DAG (18:1/18:1)	SI, p. S10
26	639.4951	43.8	$[M + Na]^+$	DAG (18:2/18:2)	–
27	640.5815	45.3	$[M + NH_4]^+$	DAG (18:0/18:1)	SI, p. S11
28	641.5108	44.3	$[M + Na]^+$	DAG (18:1/18:2)	–
29	643.5256	44.9	$[M + Na]^+$	DAG (18:1/18:1)	–
30	645.5386	45.4	$[M + Na]^+$	DAG (18:0/18:1)	–
31	655.4700	43.7	$[M + K]^+$	DAG (18:2/18:2)	–
32	657.4889	44.3	$[M + K]^+$	DAG (18:1/18:2)	–
33	659.5346	44.9	$[M + K]^+$	DAG (18:1/18:1)	–
34	662.5667	44.6	$[M + NH_4]^+$	DAG (18:2/20:2)	SI, p. S12
35	664.6204	45.1	$[M + NH_4]^+$	DAG (18:2/20:1) and some DAG (18:1/20:2)	SI, p. S13
36	667.5271	44.6	$[M + Na]^+$	DAG (18:2/20:2)	–
37	816.7036	47.6	$[M + NH_4]^+$	TAG (12:0/18:2/18:2) and isomers	SI, p. S14
38	844.7360	47.8	$[M + NH_4]^+$	TAG (14:0/18:2/18:2) and isomers	SI, p. S15

(Continues)

TABLE A2: (Continued)

(a) Identified significantly elevated positive-mode ions in ethanol-treated intracellular *A. niger* samples (potential identification and MS/MS spectrum)

No.	*m/z*	RT (min)	Ion	Potential identification	MS/MS spectrum
39	860.7302	46.6	$[M + NH_4]^+$	hTAG (16:1/16:1(OH)/18:2) (?)	–
40	862.7455	46.9	$[M + NH_4]^+$	hTAG (16:0/16:1(OH)/18:2)	SI, p. S16
41	864.7565	47.2	$[M + NH_4]^+$	hTAG (16:0/16:0/18:2(OH))	SI, p. S17
42	879.7409	46.5	$[M + H]^+$	TAG (18:2/18:2/18:2)	–
43	886.7387	46.8	$[M + NH_4]^+$	hTAG (16:0/18:2(OH)/18:3) (?)	–
44	888.7606	47.1	$[M + NH_4]^+$	hTAG (16:0/18:2/18:2(OH))	SI, p. S18
45	890.7736	47.3	$[M + NH_4]^+$	hTAG (16:0/18:1/18:2(OH))	SI, p. S19
46	904.8319	49.0	$[M + NH_4]^+$	TAG (18:0/18:1/18:1)	SI, p. S20
47	906.8451	49.1	$[M + NH_4]^+$	TAG (18:0/18:0/18:1)	SI, p. S21
48	912.7626	46.9	$[M + NH_4]^+$	hTAG (18:1/18:2(OH)/18:3) and isomers	SI, p. S22
49	914.7771	47.2	$[M + NH_4]^+$	hTAG (18:1/18:2/18:2(OH))	SI, p. S23
50	916.7929	47.5	$[M + NH_4]^+$	hTAG (18:1/18:1/18:2(OH))	SI, p. S24
51	918.8068	47.7	$[M + NH_4]^+$	hTAG (18:0/18:1/18:2(OH))	SI, p. S25
52	934.8749	49.5	$[M + NH_4]^+$	TAG (18:0/18:1/20:0) and other isomers	SI, p. S26
53	990.9377	50.2	$[M + NH_4]^+$	TAG (18:0/18:1/24:0)	SI, p. S27
54	1,002.9375	50.2	$[M + NH_4]^+$	TAG (18:1/18:1/25:0)	SI, p. S28
55	1,004.9508	50.4	$[M + NH_4]^+$	TAG (18:0/18:1/25:0) (?)	–
56	1,018.9654	50.5	$[M + NH_4]^+$	TAG (18:0/18:1/26:0)	SI, p. S29
57	1,231.9962	43.8	$[2M - H_2 + H]^+$	DAG (18:2/18:2)	–
58	1,234.0106	44.1	$[2M + H]^+$	DAG (18:2/18:2) (?)	–
59	1,236.0261	44.3	$[2M - H_2 + H]^+$	DAG (18:1/18:2)	–
60	1,238.0424	44.8	$[M + H]^+$	DAG (18:1/18:1) + DAG (18:2/18:2)	–
61	1,255.9951	43.7	$[2M + Na]^+$	DAG (18:2/18:2)	–
62	1,260.0226	44.3	$[2M + Na]^+$	DAG (18:1/18:2)	–
63	1264.0575	45.0	$[2M + Na]^+$	DAG (18:1/18:1)	–

(b) Identified significantly elevated positive-mode ions in ethanol-treated intracellular *A. niger* samples (MSII)

NO.	*m/z*	RT (min)	Integrated mass ion intensity (MSII)							
			EtOH-1	EtOH-2	EtOH-3	EtOH-avg	Con-1	Con-2	Con-3	Con-avg
1	243.2090	43.8	6.14E+04	4.25E+04	4.54E+04	4.98E+04	1.68E+04	1.42E+04	1.86E+04	1.65E+04
2	261.2182	43.8	3.14E+05	2.07E+05	2.35E+05	2.52E+05	8.54E+04	6.46E+04	1.16E+05	8.86E+04
3	263.2362	44.0	9.81E+05	7.13E+05	8.18E+05	8.37E+05	3.26E+05	2.60E+05	4.16E+05	3.34E+05
4	299.2571	44.2	1.72E+04	2.82E+04	2.56E+04	2.37E+04	7.81E+03	8.39E+03	8.35E+03	8.18E+03
5	331.2789	44.0	1.87E+05	1.27E+05	1.54E+05	1.56E+05	7.13E+04	5.52E+04	9.16E+04	7.27E+04
6	337.2740	44.0	1.18E+07	8.40E+06	9.33E+06	9.86E+06	2.82E+06	2.33E+06	3.69E+06	2.95E+06
7	339.2896	44.6	1.09E+07	9.04E+06	9.03E+06	9.67E+06	2.18E+06	1.64E+06	2.92E+06	2.25E+06
8	357.2972	44.4	8.13E+04	6.16E+04	6.28E+04	6.86E+04	1.91E+04	1.51E+04	2.27E+04	1.89E+04
9	505.3885	43.8	6.89E+04	3.99E+04	4.40E+04	5.10E+04	1.32E+04	1.17E+04	1.58E+04	1.35E+04
10	577.5185	44.6	2.10E+06	1.80E+06	2.14E+06	2.02E+06	8.52E+05	6.66E+05	1.19E+06	9.04E+05
11	593.5154	44.1	3.19E+05	2.27E+05	2.70E+05	2.72E+05	1.25E+05	1.01E+05	1.56E+05	1.28E+05
12	595.5281	44.6	1.90E+05	1.73E+05	1.70E+05	1.78E+05	7.65E+04	6.12E+04	1.03E+05	8.01E+04

(Continues)

TABLE A2: (Continued)

(b) Identified significantly elevated positive-mode ions in ethanol-treated intracellular *A. niger* samples (MSII)

NO.	*m/z*	RT (min)	Integrated mass ion intensity (MSII)							
			EtOH-1	EtOH-2	EtOH-3	EtOH-avg	Con-1	Con-2	Con-3	Con-avg
13	599.5026	43.8	2.80E+06	1.70E+06	1.90E+06	2.13E+06	5.39E+05	4.38E+05	5.83E+05	5.20E+05
14	601.5186	44.4	4.16E+06	3.46E+06	3.26E+06	3.63E+06	9.62E+05	7.49E+05	1.16E+06	9.58E+05
15	603.5334	44.9	3.49E+06	3.09E+06	2.97E+06	3.18E+06	8.51E+05	6.37E+05	9.90E+05	8.26E+05
16	605.5484	44.0	8.82E+05	9.92E+05	1.22E+06	1.03E+06	0.00E+00	3.30E+05	3.98E+05	2.42E+05
17	617.5133	43.7	6.33E+06	3.80E+06	4.06E+06	4.73E+06	1.14E+06	9.60E+05	1.34E+06	1.15E+06
18	617.5101	44.7	5.45E+04	7.25E+04	1.01E+05	7.59E+04	4.26E+04	2.30E+04	3.19E+04	3.25E+04
19	619.5266	44.4	2.09E+06	1.66E+06	1.57E+06	1.77E+06	4.97E+05	3.95E+05	6.40E+05	5.11E+05
20	621.5416	44.9	5.78E+05	5.25E+05	4.47E+05	5.17E+05	1.34E+05	1.05E+05	1.84E+05	1.41E+05
21	631.5539	44.2	5.90E+04	6.91E+04	8.55E+04	7.12E+04	0.00E+00	0.00E+00	1.34E+03	4.47E+02
22	633.5441	44.6	1.14E+04	2.51E+04	2.37E+04	2.01E+04	0.00E+00	4.73E+03	5.80E+03	3.51E+03
23	634.5394	43.8	3.66E+06	2.28E+06	2.11E+06	2.68E+06	7.41E+05	5.42E+05	7.47E+05	6.77E+05
24	636.5550	44.4	2.82E+06	2.21E+06	1.89E+06	2.30E+06	6.98E+05	4.98E+05	7.58E+05	6.51E+05
25	638.5700	44.9	2.01E+06	1.78E+06	1.49E+06	1.76E+06	5.18E+05	3.72E+05	5.97E+05	4.96E+05
26	639.4951	43.8	1.03E+06	7.02E+05	8.05E+05	8.45E+05	1.82E+05	1.16E+05	2.06E+05	1.68E+05
27	640.5815	45.3	6.84E+05	6.19E+05	4.95E+05	5.99E+05	1.32E+05	1.02E+05	1.54E+05	1.29E+05
28	641.5108	44.3	7.54E+05	7.40E+05	8.55E+05	7.83E+05	2.20E+05	1.42E+05	2.41E+05	2.01E+05
29	643.5256	44.9	5.60E+05	6.48E+05	6.90E+05	6.33E+05	2.65E+05	1.51E+05	2.12E+05	2.09E+05
30	645.5386	45.4	2.36E+05	3.23E+05	3.02E+05	2.87E+05	9.56E+04	6.22E+04	6.83E+04	7.53E+04
31	655.4700	43.7	3.34E+04	2.28E+04	2.56E+04	2.73E+04	7.36E+03	6.12E+03	7.46E+03	6.98E+03
32	657.4889	44.3	2.75E+04	2.54E+04	2.73E+04	2.67E+04	1.10E+04	7.86E+03	1.09E+04	9.90E+03
33	659.5346	44.9	5.13E+04	3.76E+04	4.59E+04	4.49E+04	1.48E+04	6.56E+03	9.97E+03	1.05E+04
34	662.5667	44.6	9.14E+04	7.21E+04	5.92E+04	7.42E+04	1.87E+04	1.33E+04	2.06E+04	1.75E+04
35	664.6204	45.1	7.79E+04	6.74E+04	5.29E+04	6.61E+04	1.70E+04	1.54E+04	2.07E+04	1.77E+04
36	667.5271	44.6	2.50E+04	2.23E+04	2.28E+04	2.34E+04	7.71E+03	2.65E+03	3.69E+03	4.68E+03
37	816.7036	47.6	1.89E+05	1.63E+05	1.50E+05	1.68E+05	4.36E+04	3.54E+04	3.32E+04	3.74E+04
38	844.7360	47.8	1.24E+06	1.11E+06	1.04E+06	1.13E+06	5.17E+05	4.83E+05	4.51E+05	4.84E+05
39	860.7302	46.6	4.87E+04	3.27E+04	3.70E+04	3.94E+04	2.95E+03	3.49E+03	5.87E+03	4.10E+03
40	862.7455	46.9	1.11E+05	8.84E+04	1.09E+05	1.03E+05	3.89E+04	3.38E+04	5.26E+04	4.18E+04
41	864.7565	47.2	1.13E+05	1.06E+05	1.06E+05	1.08E+05	4.50E+04	4.77E+04	5.22E+04	4.83E+04
42	879.7409	46.5	3.85E+05	2.77E+05	3.44E+05	3.35E+05	0.00E+00	6.04E+04	5.62E+04	3.89E+04
43	886.7387	46.8	4.56E+05	3.16E+05	4.05E+05	3.92E+05	1.89E+05	9.46E+04	1.17E+05	1.34E+05
44	888.7606	47.1	6.34E+05	4.53E+05	5.12E+05	5.33E+05	1.27E+05	9.66E+04	1.45E+05	1.23E+05
45	890.7736	47.3	5.16E+05	4.09E+05	4.70E+05	4.65E+05	1.84E+05	1.46E+05	1.58E+05	1.63E+05
46	904.8319	49.0	1.20E+07	1.17E+07	1.12E+07	1.16E+07	5.20E+06	5.14E+06	4.32E+06	4.89E+06
47	906.8451	49.1	6.89E+06	6.87E+06	6.62E+06	6.79E+06	2.54E+06	2.70E+06	1.83E+06	2.36E+06
48	912.7626	46.9	6.04E+05	3.94E+05	4.14E+05	4.71E+05	8.59E+04	7.87E+04	7.21E+04	7.89E+04
49	914.7771	47.2	7.27E+05	5.06E+05	5.55E+05	5.96E+05	9.83E+04	9.24E+04	9.40E+04	9.49E+04
50	916.7929	47.5	5.63E+05	4.16E+05	4.71E+05	4.84E+05	7.59E+04	6.54E+04	1.68E+05	1.03E+05
51	918.8068	47.7	2.68E+05	2.07E+05	2.53E+05	2.43E+05	4.88E+04	4.53E+04	4.49E+04	4.63E+04
52	934.8749	49.5	9.33E+05	1.02E+06	9.33E+05	9.62E+05	4.54E+05	4.52E+05	3.34E+05	4.13E+05
53	990.9377	50.2	4.77E+06	4.56E+06	4.16E+06	4.50E+06	2.04E+06	2.45E+06	1.71E+06	2.07E+06
54	1,002.9375	50.2	8.96E+05	8.10E+05	7.02E+05	8.02E+05	3.15E+05	3.43E+05	2.54E+05	3.04E+05
55	1,004.9508	50.4	7.08E+05	6.30E+05	5.66E+05	6.34E+05	1.78E+05	1.91E+05	1.33E+05	1.67E+05

(Continues)

TABLE A2: (Continued)

(b) Identified significantly elevated positive-mode ions in ethanol-treated intracellular *A. niger* samples (MSII)

NO.	*m/z*	RT (min)	Integrated mass ion intensity (MSII)							
			EtOH-1	EtOH-2	EtOH-3	EtOH-avg	Con-1	Con-2	Con-3	Con-avg
56	1,018.9654	50.5	7.98E+05	7.61E+05	6.96E+05	7.52E+05	2.94E+05	3.54E+05	2.54E+05	3.01E+05
57	1,231.9962	43.8	2.92E+04	2.23E+04	2.21E+04	2.45E+04	9.12E+03	5.33E+03	9.03E+03	7.83E+03
58	1,234.0106	44.1	4.12E+04	3.93E+04	3.15E+04	3.73E+04	1.59E+04	9.40E+03	1.51E+04	1.35E+04
59	1,236.0261	44.3	4.62E+04	4.30E+04	3.95E+04	4.29E+04	1.65E+04	1.09E+04	1.74E+04	1.49E+04
60	1,238.0424	44.8	5.91E+04	6.23E+04	5.54E+04	5.89E+04	2.47E+04	1.28E+04	2.30E+04	2.02E+04
61	1,255.9951	43.7	4.14E+04	3.05E+04	2.37E+04	3.19E+04	6.23E+03	3.47E+03	5.24E+03	4.98E+03
62	1,260.0226	44.3	4.14E+04	4.31E+04	3.21E+04	3.89E+04	1.00E+04	6.42E+03	9.24E+03	8.56E+03
63	1,264.0575	45.0	8.14E+04	9.04E+04	6.78E+04	7.99E+04	2.49E+04	1.43E+04	2.03E+04	1.98E+04

(c) Identified significantly elevated positive-mode ions in ethanol-treated intracellular *A. niger* samples (aMSII)

No.	*m/z*	RT (min)	Adjusted integrated mass ion intensity (aMSII)							
			EtOH-1	EtOH-2	EtOH-3	EtOH-avg	Con-1	Con-2	Con-3	Con-avg
1	243.2090	43.8	8.85E+04	6.12E+04	6.54E+04	7.17E+04	1.29E+04	1.09E+04	1.42E+04	1.27E+04
2	261.2182	43.8	4.52E+05	2.99E+05	3.39E+05	3.63E+05	6.54E+04	4.95E+04	8.86E+04	6.78E+04
3	263.2362	44.0	1.41E+06	1.03E+06	1.18E+06	1.21E+06	2.50E+05	1.99E+05	3.18E+05	2.56E+05
4	299.2571	44.2	2.47E+04	4.07E+04	3.68E+04	3.41E+04	5.98E+03	6.42E+03	6.39E+03	6.27E+03
5	331.2789	44.0	2.70E+05	1.83E+05	2.22E+05	2.25E+05	5.46E+04	4.23E+04	7.02E+04	5.57E+04
6	337.2740	44.0	1.71E+07	1.21E+07	1.34E+07	1.42E+07	2.16E+06	1.78E+06	2.83E+06	2.26E+06
7	339.2896	44.6	1.58E+07	1.30E+07	1.30E+07	1.39E+07	1.67E+06	1.25E+06	2.23E+06	1.72E+06
8	357.2972	44.4	1.17E+05	8.87E+04	9.04E+04	9.87E+04	1.46E+04	1.15E+04	1.74E+04	1.45E+04
9	505.3885	43.8	9.92E+04	5.75E+04	6.34E+04	7.34E+04	1.01E+04	8.93E+03	1.21E+04	1.04E+04
10	577.5185	44.6	3.03E+06	2.60E+06	3.08E+06	2.90E+06	6.53E+05	5.10E+05	9.14E+05	6.92E+05
11	593.5154	44.1	4.59E+05	3.27E+05	3.89E+05	3.92E+05	9.60E+04	7.73E+04	1.20E+05	9.77E+04
12	595.5281	44.6	2.73E+05	2.49E+05	2.45E+05	2.56E+05	5.86E+04	4.69E+04	7.86E+04	6.14E+04
13	599.5026	43.8	4.04E+06	2.45E+06	2.74E+06	3.07E+06	4.13E+05	3.35E+05	4.46E+05	3.98E+05
14	601.5186	44.4	5.99E+06	4.98E+06	4.70E+06	5.22E+06	7.37E+05	5.74E+05	8.92E+05	7.34E+05
15	603.5334	44.9	5.03E+06	4.45E+06	4.28E+06	4.59E+06	6.52E+05	4.88E+05	7.58E+05	6.33E+05
16	605.5484	44.0	1.27E+06	1.43E+06	1.76E+06	1.49E+06	0.00E+00	2.52E+05	3.05E+05	1.86E+05
17	617.5133	43.7	9.12E+06	5.47E+06	5.85E+06	6.81E+06	8.77E+05	7.35E+05	1.03E+06	8.79E+05
18	617.5101	44.7	7.85E+04	1.04E+05	1.45E+05	1.09E+05	3.26E+04	1.76E+04	2.44E+04	2.49E+04
19	619.5266	44.4	3.00E+06	2.39E+06	2.26E+06	2.55E+06	3.81E+05	3.03E+05	4.90E+05	3.91E+05
20	621.5416	44.9	8.32E+05	7.56E+05	6.44E+05	7.44E+05	1.03E+05	8.02E+04	1.41E+05	1.08E+05
21	631.5539	44.2	8.49E+04	9.96E+04	1.23E+05	1.03E+05	0.00E+00	0.00E+00	1.03E+03	3.43E+02
22	633.5441	44.6	1.64E+04	3.62E+04	3.42E+04	2.89E+04	0.00E+00	3.62E+03	4.44E+03	2.69E+03
23	634.5394	43.8	5.27E+06	3.28E+06	3.04E+06	3.86E+06	5.67E+05	4.15E+05	5.72E+05	5.18E+05
24	636.5550	44.4	4.06E+06	3.18E+06	2.73E+06	3.32E+06	5.34E+05	3.82E+05	5.81E+05	4.99E+05
25	638.5700	44.9	2.89E+06	2.56E+06	2.15E+06	2.53E+06	3.97E+05	2.85E+05	4.58E+05	3.80E+05
26	639.4951	43.8	1.48E+06	1.01E+06	1.16E+06	1.22E+06	1.40E+05	8.91E+04	1.57E+05	1.29E+05
27	640.5815	45.3	9.84E+05	8.91E+05	7.12E+05	8.62E+05	1.01E+05	7.84E+04	1.18E+05	9.92E+04
28	641.5108	44.3	1.09E+06	1.07E+06	1.23E+06	1.13E+06	1.69E+05	1.09E+05	1.85E+05	1.54E+05
29	643.5256	44.9	8.07E+05	9.34E+05	9.94E+05	9.11E+05	2.03E+05	1.16E+05	1.63E+05	1.60E+05
30	645.5386	45.4	3.39E+05	4.65E+05	4.35E+05	4.13E+05	7.32E+04	4.77E+04	5.23E+04	5.77E+04
31	655.4700	43.7	4.81E+04	3.28E+04	3.69E+04	3.93E+04	5.63E+03	4.69E+03	5.71E+03	5.35E+03
32	657.4889	44.3	3.96E+04	3.66E+04	3.93E+04	3.85E+04	8.40E+03	6.02E+03	8.33E+03	7.58E+03
33	659.5346	44.9	7.39E+04	5.41E+04	6.60E+04	6.47E+04	1.14E+04	5.02E+03	7.63E+03	8.01E+03

(Continues)

TABLE A2: (Continued)

(c) Identified significantly elevated positive-mode ions in ethanol-treated intracellular *A. niger* samples (aMSII)										
			Adjusted integrated mass ion intensity (aMSII)							
No.	*m/z*	RT (min)	EtOH-1	EtOH-2	EtOH-3	EtOH-avg	Con-1	Con-2	Con-3	Con-avg
34	662.5667	44.6	1.32E+05	1.04E+05	8.53E+04	1.07E+05	1.43E+04	1.02E+04	1.58E+04	1.34E+04
35	664.6204	45.1	1.12E+05	9.71E+04	7.62E+04	9.51E+04	1.31E+04	1.18E+04	1.59E+04	1.36E+04
36	667.5271	44.6	3.60E+04	3.21E+04	3.29E+04	3.37E+04	5.91E+03	2.03E+03	2.83E+03	3.59E+03
37	816.7036	47.6	2.72E+05	2.35E+05	2.16E+05	2.41E+05	3.34E+04	2.71E+04	2.54E+04	2.86E+04
38	844.7360	47.8	1.79E+06	1.60E+06	1.50E+06	1.63E+06	3.96E+05	3.70E+05	3.45E+05	3.70E+05
39	860.7302	46.6	7.01E+04	4.70E+04	5.33E+04	5.68E+04	2.26E+03	2.67E+03	4.49E+03	3.14E+03
40	862.7455	46.9	1.60E+05	1.27E+05	1.58E+05	1.48E+05	2.98E+04	2.59E+04	4.03E+04	3.20E+04
41	864.7565	47.2	1.62E+05	1.53E+05	1.53E+05	1.56E+05	3.45E+04	3.66E+04	4.00E+04	3.70E+04
42	879.7409	46.5	5.55E+05	3.99E+05	4.95E+05	4.83E+05	0.00E+00	4.63E+04	4.30E+04	2.98E+04
43	886.7387	46.8	6.56E+05	4.55E+05	5.83E+05	5.65E+05	1.45E+05	7.24E+04	9.00E+04	1.02E+05
44	888.7606	47.1	9.14E+05	6.53E+05	7.37E+05	7.68E+05	9.74E+04	7.40E+04	1.11E+05	9.41E+04
45	890.7736	47.3	7.43E+05	5.89E+05	6.77E+05	6.70E+05	1.41E+05	1.12E+05	1.21E+05	1.25E+05
46	904.8319	49.0	1.72E+07	1.69E+07	1.61E+07	1.67E+07	3.98E+06	3.94E+06	3.31E+06	3.74E+06
47	906.8451	49.1	9.93E+06	9.89E+06	9.53E+06	9.78E+06	1.95E+06	2.07E+06	1.40E+06	1.81E+06
48	912.7626	46.9	8.70E+05	5.67E+05	5.97E+05	6.78E+05	6.58E+04	6.03E+04	5.52E+04	6.04E+04
49	914.7771	47.2	1.05E+06	7.29E+05	7.99E+05	8.58E+05	7.53E+04	7.08E+04	7.20E+04	7.27E+04
50	916.7929	47.5	8.11E+05	6.00E+05	6.79E+05	6.96E+05	5.81E+04	5.01E+04	1.29E+05	7.89E+04
51	918.8068	47.7	3.87E+05	2.99E+05	3.64E+05	3.50E+05	3.74E+04	3.47E+04	3.44E+04	3.55E+04
52	934.8749	49.5	1.34E+06	1.47E+06	1.34E+06	1.39E+06	3.47E+05	3.46E+05	2.56E+05	3.16E+05
53	990.9377	50.2	6.88E+06	6.56E+06	5.99E+06	6.48E+06	1.57E+06	1.88E+06	1.31E+06	1.59E+06
54	1,002.9375	50.2	1.29E+06	1.17E+06	1.01E+06	1.16E+06	2.41E+05	2.62E+05	1.95E+05	2.33E+05
55	1,004.9508	50.4	1.02E+06	9.07E+05	8.15E+05	9.14E+05	1.36E+05	1.46E+05	1.02E+05	1.28E+05
56	1,018.9654	50.5	1.15E+06	1.10E+06	1.00E+06	1.08E+06	2.25E+05	2.71E+05	1.95E+05	2.30E+05
57	1,231.9962	43.8	4.20E+04	3.21E+04	3.18E+04	3.53E+04	6.98E+03	4.08E+03	6.92E+03	5.99E+03
58	1,234.0106	44.1	5.93E+04	5.65E+04	4.53E+04	5.37E+04	1.22E+04	7.20E+03	1.15E+04	1.03E+04
59	1,236.0261	44.3	6.65E+04	6.19E+04	5.69E+04	6.18E+04	1.26E+04	8.33E+03	1.33E+04	1.14E+04
60	1,238.0424	44.8	8.50E+04	8.97E+04	7.97E+04	8.48E+04	1.89E+04	9.81E+03	1.76E+04	1.54E+04
61	1,255.9951	43.7	5.97E+04	4.39E+04	3.42E+04	4.59E+04	4.77E+03	2.66E+03	4.01E+03	3.81E+03
62	1,260.0226	44.3	5.97E+04	6.20E+04	4.62E+04	5.60E+04	7.68E+03	4.92E+03	7.08E+03	6.56E+03
63	1,264.0575	45.0	1.17E+05	1.30E+05	9.77E+04	1.15E+05	1.91E+04	1.09E+04	1.55E+04	1.52E+04

TABLE A3: Other lipids in the pathways found in intracellular *A. niger* samples. Lipids are shown in terms of their lipid class and acyl chain as (a) detected ion adduct, measured mass-to-charge ratio (*m/z*), retention time (RT), MS/MS spectrum, (b) integrated mass ion intensity (MSII) and (c) adjusted mass ion intensity (aMSII). The MSII and aMSII data are shown for three *A. niger* samples without (Con-1–3) or with ethanol treatments (EtOH-1–3) and their respective averages (Con-avg and EtOH-avg, respectively)

(a) Other intracellular lipids in the pathways (ion, *m/z*, RT, MS/MS spectrum)					
	Lipid class				
No.	Acyl chain	Ions	*m/z*	RT (min)	MS/MS spectrum
	Fatty acid (FA)				
1	16:0	$[M-H]^-$	255.2317	18.6	–
2	18:2	$[M-H]^-$	279.2336	18.5	–
3	18:1	$[M-H]^-$	281.2478	18.8	–
4	18:0	$[M-H]^-$	283.2624	19.2	–
	Monoacylglycerol (MAG)				

(Continues)

TABLE A3: (Continued)

(a) Other intracellular lipids in the pathways (ion, *m/z*, RT, MS/MS spectrum)

No.	Lipid class: Acyl chain	Ions	*m/z*	RT (min)	MS/MS spectrum
3	16:0	$[M + Na]^+$	353.2656	34.0	–
4	18:2	$[M + Na]^+$	377.2718	33.1	–
	Phosphatidic acid (PA)				
5	16:0/18:2	$[M - H]^-$	671.4649	27.4	SI, p. S32
6	18:2/18:2	$[M - H]^-$	695.4647	26.8	SI, p. S33
	Phosphatidylethanolamine (PE)				
7	16:0/18:2	$[M - H]^-$	714.5023	39.0	SI, p. S34
8	18:2/18:2	$[M - H]^-$	738.5004	38.2	SI, p. S35
	Phosphatidylserine (PS)				
9	16:0/18:2	$[M - H]^-$	758.4944	29.9	SI, p. S36
10	18:2/18:2	$[M - H]^-$	782.4946	29.3	SI, p. S37
	Phosphatidylglycerol (PG)				
11	16:0/18:2	$[M - H]^-$	745.4976	34.4	SI, p. S38
12	18:2/18:2	$[M - H]^-$	769.4962	33.8	SI, p. S39
	Phosphatidylinositol (PI)				
13	16:0/18:2	$[M - H]^-$	833.5160	34.0	SI, p. S40
14	18:2/18:2	$[M - H]^-$	857.5147	33.4	SI, p. S41
	Phosphatidylcholine (PC)				
15	16:0/18:2	$[M + H]^+$	758.5726	41.7	SI, p. S30
16	18:2/18:2	$[M + H]^+$	782.5751	41.3	SI, p. S31

(b) Other intracellular lipids in the pathways (MSII)

No.	Lipid class: Acyl chain	Integrated mass ion intensity (MSII): EtOH-1	EtOH-2	EtOH-3	EtOH-avg	Con-1	Con-2	Con-3	Con-avg
	Fatty acid (FA)								
1	16:0	2.26E+06	2.16E+06	1.99E+06	2.14E+06	2.43E+06	2.48E+06	2.53E+06	2.48E+06
2	18:2	1.48E+07	1.31E+07	1.38E+07	1.39E+07	1.56E+07	1.57E+07	1.57E+07	1.57E+07
3	18:1	7.86E+06	7.31E+06	6.94E+06	7.37E+06	7.03E+06	6.66E+06	7.33E+06	7.01E+06
4	18:0	1.51E+06	1.47E+06	1.36E+06	1.44E+06	1.91E+06	1.73E+06	1.77E+06	1.80E+06
	Monoacylglycerol (MAG)								
3	16:0	5.15E+05	4.80E+05	3.36E+05	4.44E+05	3.23E+05	5.30E+05	4.54E+05	4.36E+05
4	18:2	3.46E+05	1.88E+05	2.70E+05	2.68E+05	3.21E+05	3.07E+05	2.98E+05	3.09E+05
	Phosphatidic acid (PA)								
5	16:0/18:2	9.63E+05	1.32E+06	7.26E+05	1.00E+06	1.34E+06	1.18E+06	9.63E+05	1.16E+06
6	18:2/18:2	1.03E+06	1.47E+06	1.08E+06	1.20E+06	9.08E+05	1.04E+06	9.54E+05	9.68E+05
	Phosphatidylethanolamine (PE)								
7	16:0/18:2	3.62E+05	7.06E+05	4.47E+05	5.05E+05	1.03E+06	9.95E+05	8.92E+05	9.72E+05
8	18:2/18:2	2.77E+05	4.11E+05	3.38E+05	3.42E+05	3.80E+05	3.64E+05	3.75E+05	3.73E+05
	Phosphatidylserine (PS)								
9	16:0/18:2	1.08E+06	1.64E+06	1.35E+06	1.36E+06	2.30E+06	1.87E+06	1.64E+06	1.94E+06
10	18:2/18:2	3.07E+05	3.50E+05	4.30E+05	3.62E+05	4.76E+05	4.50E+05	4.35E+05	4.54E+05
	Phosphatidylglycerol (PG)								

(Continues)

TABLE A3: (Continued)

(b) Other intracellular lipids in the pathways (MSII)									
	Lipid class	Integrated mass ion intensity (MSII)							
No.	Acyl chain	EtOH-1	EtOH-2	EtOH-3	EtOH-avg	Con-1	Con-2	Con-3	Con-avg
11	16:0/18:2	1.03E+05	1.59E+05	1.11E+05	1.24E+05	1.89E+05	1.75E+05	1.49E+05	1.71E+05
12	18:2/18:2	2.22E+04	4.09E+04	2.56E+04	2.96E+04	4.18E+04	3.44E+04	3.51E+04	3.71E+04
	Phosphatidylinositol (PI)								
13	16:0/18:2	9.00E+05	1.20E+06	9.51E+05	1.02E+06	1.73E+06	1.65E+06	1.37E+06	1.59E+06
14	18:2/18:2	4.21E+05	5.89E+05	4.83E+05	4.98E+05	9.33E+05	8.45E+05	8.03E+05	8.60E+05
	Phosphatidylcholine (PC)								
15	16:0/18:2	4.97E+06	5.26E+06	4.69E+06	4.97E+06	1.21E+07	1.22E+07	1.10E+07	1.18E+07
16	18:2/18:2	2.06E+07	2.15E+07	2.00E+07	2.07E+07	2.25E+07	2.26E+07	2.13E+07	2.22E+07

(c) Other intracellular lipids in the pathways (aMSII)									
	Lipid class	Adjusted integrated mass ion intensity (aMSII)							
No.	Acyl chain	EtOH-1	EtOH-2	EtOH-3	EtOH-avg	Con-1	Con-2	Con-3	Con-avg
	Fatty acid (FA)								
1	16:0	3.25E+06	3.11E+06	2.87E+06	3.08E+06	1.86E+06	1.90E+06	1.94E+06	1.90E+06
2	18:2	2.14E+07	1.89E+07	1.99E+07	2.01E+07	1.20E+07	1.20E+07	1.20E+07	1.20E+07
3	18:1	1.13E+07	1.05E+07	1.00E+07	1.06E+07	5.39E+06	5.10E+06	5.62E+06	5.37E+06
4	18:0	2.17E+06	2.11E+06	1.95E+06	2.08E+06	1.46E+06	1.33E+06	1.36E+06	1.38E+06
	Monoacylglycerol (MAG)								
3	16:0	8.76E+05	8.16E+05	5.71E+05	7.54E+05	2.29E+05	3.76E+05	3.22E+05	3.09E+05
4	18:2	5.88E+05	3.19E+05	4.58E+05	4.55E+05	2.27E+05	2.17E+05	2.11E+05	2.19E+05
	Phosphatidic acid (PA)								
5	16:0/18:2	1.39E+06	1.91E+06	1.05E+06	1.45E+06	1.03E+06	9.02E+05	7.37E+05	8.88E+05
6	18:2/18:2	1.49E+06	2.12E+06	1.56E+06	1.72E+06	6.95E+05	7.98E+05	7.30E+05	7.41E+05
	Phosphatidylethanolamine (PE)								
7	16:0/18:2	5.21E+05	1.02E+06	6.44E+05	7.27E+05	7.89E+05	7.62E+05	6.83E+05	7.45E+05
8	18:2/18:2	4.00E+05	5.91E+05	4.86E+05	4.92E+05	2.91E+05	2.79E+05	2.87E+05	2.86E+05
	Phosphatidylserine (PS)								
9	16:0/18:2	1.56E+06	2.36E+06	1.94E+06	1.95E+06	1.76E+06	1.43E+06	1.26E+06	1.48E+06
10	18:2/18:2	4.42E+05	5.05E+05	6.19E+05	5.22E+05	3.65E+05	3.45E+05	3.33E+05	3.48E+05
	Phosphatidylglycerol (PG)								
11	16:0/18:2	1.48E+05	2.29E+05	1.59E+05	1.79E+05	1.45E+05	1.34E+05	1.14E+05	1.31E+05
12	18:2/18:2	3.19E+04	5.89E+04	3.69E+04	4.26E+04	3.20E+04	2.64E+04	2.69E+04	2.84E+04
	Phosphatidylinositol (PI)								
13	16:0/18:2	1.30E+06	1.73E+06	1.37E+06	1.46E+06	1.33E+06	1.26E+06	1.05E+06	1.21E+06
14	18:2/18:2	6.06E+05	8.48E+05	6.95E+05	7.17E+05	7.15E+05	6.47E+05	6.15E+05	6.59E+05
	Phosphatidylcholine (PC)								
15	16:0/18:2	7.16E+06	7.57E+06	6.76E+06	7.16E+06	9.24E+06	9.38E+06	8.41E+06	9.01E+06
16	18:2/18:2	2.96E+07	3.10E+07	2.88E+07	2.98E+07	1.73E+07	1.73E+07	1.63E+07	1.70E+07

APPENDIX 2:

Calculation and predicted isotopic patterns on the mass spectra of representative ions in the ethanol-d_6 samples when taking into account only deuterium exchanges of all hydrogens on the representative ions and natural abundances of elements.

BASE CALCULATION

As ethanol-d_6 (or CD_3CD_2OD) was added to the culture at the concentration of 4% (*v*/*v*), the medium had the following ratios of H_2O to CD_3CD_2OD:

By volume	96: 4
By mass (At 25°C, density of H_2O = 0.99707 g/ml and of ethanol = 0.78522 g/ml)	95.7: 3.1
By mole (MW of H_2O = 18.01528 g/mol and of CD_3CD_2OD = 52.10541 g/mol)	5.3: 0.060

Since H_2O has 2 protons, while CD_3CD_2OD has 1 deuteron, the mole ratio of proton (and some deuteron from water) to deuteron (from ethanol-d_6) is equal to 10.6: 0.060. However, considering that natural abundances of hydrogen and deuterium are 99.9844% and 0.0156%, respectively, the mole ratio of proton to deuteron then becomes 10.6: 0.062, which is equal to 100: 0.58.

(A) DIACYLGLYCEROL (DAG) (18:2/18:2)

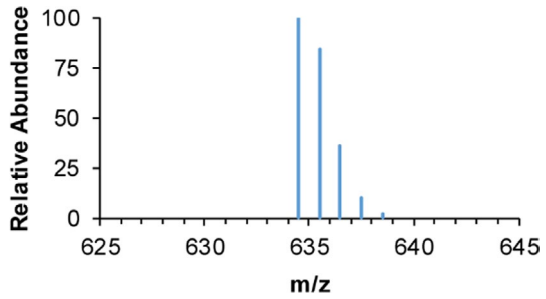

CALCULATION

$[M + NH_4]^+$ has the molecular formula of $C_{39}H_{72}NO_5^+$.

The highest probability of each isotope when considering only deuterium exchanges and natural isotopic abundance of each element is then equal to the following:

(Note: Terms with relatively small contribution are ignored below.)

$$M:\quad P(M)=P(0D)$$
$$={}^{72}C_0\left(\frac{0.58}{100}\right)^0\left(\frac{100}{100}\right)^{72}$$
$$=1.00$$

$$M+1:\quad P(M+1)=P(1D)+P\left(1^{13}C\right)$$
$$={}^{72}C_1\left(\frac{0.58}{100}\right)^1\left(\frac{100}{100}\right)^{71}+{}^{39}C_1\left(\frac{1.08}{100}\right)^1\left(\frac{100}{100}\right)^{38}$$
$$=0.84$$

$$M+2:\quad P(M+2)=P(2D)+P\left(2^{13}C\right)+P\left(1D\&1^{13}C\right)+P\left(1^{18}O\right)$$
$$={}^{72}C_2\left(\frac{0.58}{100}\right)^2\left(\frac{100}{100}\right)^{70}+{}^{39}C_2\left(\frac{1.08}{100}\right)^2\left(\frac{100}{100}\right)^{37}+P(1D)\cdot P\left(1^{13}C\right)+$$
$${}^{5}C_1\left(\frac{0.20}{100}\right)^1\left(\frac{100}{100}\right)^4$$
$$=0.36$$

$$M+3:\quad P(M+3)=P(3D)+P\left(3^{13}C\right)+P\left(2D\&1^{13}C\right)+P\left(1D\&2^{13}C\right)$$
$$+P\left(1D\&1^{18}O\right)+P\left(1^{13}C\&1^{18}O\right)$$
$$={}^{72}C_3\left(\frac{0.58}{100}\right)^3\left(\frac{100}{100}\right)^{69}+{}^{39}C_3\left(\frac{1.08}{100}\right)^3\left(\frac{100}{100}\right)^{36}$$
$$+P(2D)\cdot P\left(1^{13}C\right)$$
$$+P(1D)\cdot P\left(2^{13}C\right)+P(1D)\cdot P\left(1^{18}O\right)+P\left(1^{13}C\right)\cdot P\left(1^{18}O\right)$$
$$=0.10$$

$$M+4:\quad P(M+4)=P(4D)+P\left(4^{13}C\right)+P\left(3D\&1^{13}C\right)+P\left(2D\&2^{13}C\right)$$
$$+P\left(1D\&3^{13}C\right)+P\left(2D\&1^{18}O\right)+P\left(2^{13}C\&1^{18}O\right)$$
$$+P\left(1D\&1^{13}C+1^{18}O\right)={}^{72}C_4\left(\frac{0.58}{100}\right)^4\left(\frac{100}{100}\right)^{68}+{}^{39}C_4\left(\frac{1.08}{100}\right)^4\left(\frac{100}{100}\right)^{35}$$
$$+P(3D)\cdot P\left(1^{13}C\right)+P(2D)\cdot P\left(2^{13}C\right)+P(1D)\cdot P\left(3^{13}C\right)$$
$$+P(2D)\cdot P\left(1^{18}O\right)+P\left(2^{13}C\right)\cdot P\left(1^{18}O\right)$$
$$+P(1D)\cdot P\left(1^{13}C\right)\cdot P\left(1^{18}O\right)=0.02$$

Thus, *M*: *M* + 1: *M* + 2: *M* + 3: *M* + 4 = 100: 84: 36: 10: 2.

(B) TRIACYLGLYCEROL (TAG) (18:0/18:1/18:1)

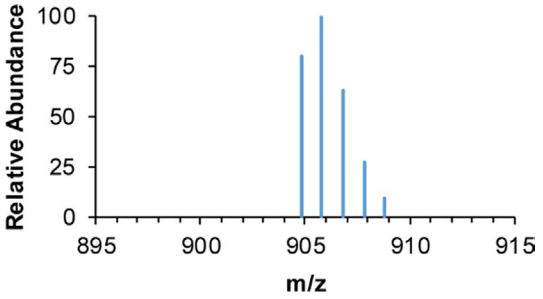

CALCULATION

$[M + NH_4]^+$ has the molecular formula of $C_{57}H_{110}NO_6^+$.

The highest probability of each isotope when considering only deuterium exchanges and natural isotopic abundance of each element is then equal to the following:

(Note: Terms with relatively small contribution are ignored below.)

$$M:\quad P(M)=P(0D)$$
$$={}^{110}C_0\left(\frac{0.58}{100}\right)^0\left(\frac{100}{100}\right)^{110}$$
$$=1.00$$

$$M+1:\quad P(M+1)=P(1D)+P\left(1^{13}C\right)$$
$$={}^{110}C_1\left(\frac{0.58}{100}\right)^1\left(\frac{100}{100}\right)^{109}+{}^{57}C_1\left(\frac{1.08}{100}\right)^1\left(\frac{100}{100}\right)^{56}$$
$$=1.26$$

$$M+2:\quad P(M+2)=P(2D)+P\left(2^{13}C\right)+P\left(1D\&1^{13}C\right)+P\left(1^{18}O\right)$$
$$={}^{110}C_2\left(\frac{0.58}{100}\right)^2\left(\frac{100}{100}\right)^{108}+{}^{57}C_2\left(\frac{1.08}{100}\right)^2\left(\frac{100}{100}\right)^{55}$$
$$+P(1D)\cdot P\left(1^{13}C\right)+{}^{6}C_1\left(\frac{0.20}{100}\right)^1\left(\frac{100}{100}\right)^5$$
$$=0.80$$

$$M+3:\quad P(M+3)=P(3D)+P\left(3^{13}C\right)+P\left(2D\&1^{13}C\right)$$
$$+P\left(1D\&2^{13}C\right)+P\left(1D\&1^{18}O\right)+P\left(1^{13}C\&1^{18}O\right)$$
$$={}^{110}C_3\left(\frac{0.58}{100}\right)^3\left(\frac{100}{100}\right)^{107}+{}^{57}C_3\left(\frac{1.08}{100}\right)^3\left(\frac{100}{100}\right)^{54}$$
$$+P(2D)\cdot P\left(1^{13}C\right)+P(1D)\cdot P\left(2^{13}C\right)+P(1D)\cdot P\left(1^{18}O\right)$$
$$+P\left(1^{13}C\right)\cdot P\left(1^{18}O\right)$$
$$=0.34$$

$$M+4:\quad P(M+4)=P(4D)+P\left(4^{13}C\right)+P\left(3D\&1^{13}C\right)$$
$$+P\left(2D\&2^{13}C\right)+P\left(1D\&3^{13}C\right)+P\left(2D\&1^{18}O\right)+P\left(2^{13}C\&1^{18}O\right)$$
$$+P\left(1D\&1^{13}C+1^{18}O\right)={}^{110}C_4\left(\frac{0.58}{100}\right)^4\left(\frac{100}{100}\right)^{106}$$
$$+{}^{57}C_4\left(\frac{1.08}{100}\right)^4\left(\frac{100}{100}\right)^{53}+P(3D)\cdot P\left(1^{13}C\right)+$$
$$P(2D)\cdot P\left(2^{13}C\right)+P(1D)\cdot P\left(3^{13}C\right)+P(2D)\cdot P\left(1^{18}O\right)+$$
$$P\left(2^{13}C\right)\cdot P\left(1^{18}O\right)+P(1D)\cdot P\left(1^{13}C\right)\cdot P\left(1^{18}O\right)$$
$$=0.11$$

Thus, M: $M+1$: $M+2$: $M+3$: $M+4$ = 80: 100: 63: 27: 9.

(C) FATTY ACID (FA) (18:2)

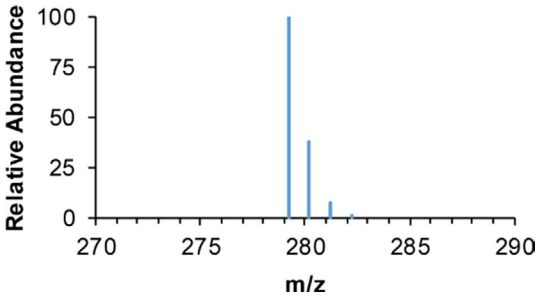

CALCULATION

$[M - H]^-$ has the molecular formula of $C_{18}H_{31}O_2^-$.

The highest probability of each isotope when considering only deuterium exchanges and natural isotopic abundance of each element is then equal to the following:

(Note: Terms with relatively small contribution are ignored below.)

$$M:\quad P(M)=P(0D)$$
$$={}^{31}C_0\left(\frac{0.58}{100}\right)^0\left(\frac{100}{100}\right)^{31}$$
$$=1.00$$

$$M+1:\quad P(M+1)=P(1D)+P\left(1^{13}C\right)$$
$$={}^{31}C_1\left(\frac{0.58}{100}\right)^1\left(\frac{100}{100}\right)^{30}+{}^{18}C_1\left(\frac{1.08}{100}\right)^1\left(\frac{100}{100}\right)^{17}$$
$$=0.38$$

$$M+2:\quad P(M+2)=P(2D)+P\left(2^{13}C\right)+P\left(1D\&1^{13}C\right)+$$
$$P\left(1^{18}O\right)={}^{31}C_2\left(\frac{0.58}{100}\right)^2\left(\frac{100}{100}\right)^{29}+{}^{18}C_2\left(\frac{1.08}{100}\right)^2\left(\frac{100}{100}\right)^{16}+$$
$$P(1D)\cdot P\left(1^{13}C\right)+{}^{2}C_1\left(\frac{0.20}{100}\right)^1\left(\frac{100}{100}\right)^1$$
$$=0.07$$

$$M+3:\quad P(M+3)=P(3D)+P\left(3^{13}C\right)+P\left(2D\&1^{13}C\right)+$$
$$P\left(1D\&2^{13}C\right)+P\left(1D\&1^{18}O\right)+P\left(1^{13}C\&1^{18}O\right)$$
$$={}^{31}C_3\left(\frac{0.58}{100}\right)^3\left(\frac{100}{100}\right)^{28}+{}^{18}C_3\left(\frac{1.08}{100}\right)^3\left(\frac{100}{100}\right)^{15}+$$
$$P(2D)\cdot P\left(1^{13}C\right)+P(1D)\cdot P\left(2^{13}C\right)+$$
$$P(1D)\cdot P\left(1^{18}O\right)+P\left(1^{13}C\right)\cdot P\left(1^{18}O\right)$$
$$=0.01$$

Thus, M: $M+1$: $M+2$: $M+3$ = 100: 38: 7: 1.

(D) PHOSPHATIDIC ACID (PA) (18:2/18:2)

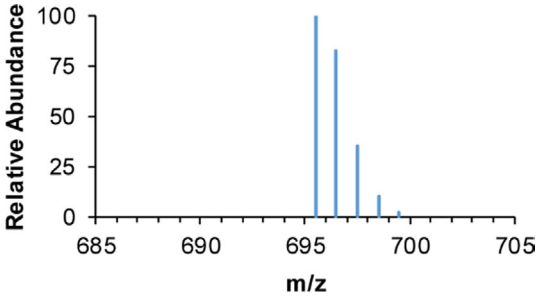

CALCULATION

$[M - H]^-$ has the molecular formula of $C_{39}H_{68}O_8P^-$.

The highest probability of each isotope when considering only deuterium exchanges and natural isotopic abundance of each element is then equal to the following:

(Note: Terms with relatively small contribution are ignored below.)

$$M:\quad P(M)=P(0D)$$
$$={}^{68}C_0\left(\frac{0.58}{100}\right)^0\left(\frac{100}{100}\right)^{68}$$
$$=1.00$$

$$M+1:\quad P(M+1)=P(1D)+P\left(1^{13}C\right)$$
$$={}^{68}C_1\left(\frac{0.58}{100}\right)^1\left(\frac{100}{100}\right)^{67}+{}^{39}C_1\left(\frac{1.08}{100}\right)^1\left(\frac{100}{100}\right)^{38}$$
$$=0.82$$

$$M+2:\quad P(M+2)=P(2D)+P\left(2^{13}C\right)+P\left(1D\&1^{13}C\right)+P\left(1^{18}O\right)$$
$$={}^{68}C_2\left(\frac{0.58}{100}\right)^2\left(\frac{100}{100}\right)^{66}+{}^{39}C_2\left(\frac{1.08}{100}\right)^2\left(\frac{100}{100}\right)^{37}+P(1D)\cdot P\left(1^{13}C\right)+$$
$${}^{8}C_1\left(\frac{0.20}{100}\right)^1\left(\frac{100}{100}\right)^{7}$$
$$=0.35$$

$$M+3:\quad P(M+3)=P(3D)+P\left(3^{13}C\right)+P\left(2D\&1^{13}C\right)+$$
$$P\left(1D\&2^{13}C\right)+P\left(1D\&1^{18}O\right)+P\left(1^{13}C\&1^{18}O\right)$$
$$={}^{68}C_3\left(\frac{0.58}{100}\right)^3\left(\frac{100}{100}\right)^{65}+{}^{39}C_3\left(\frac{1.08}{100}\right)^3\left(\frac{100}{100}\right)^{36}+$$
$$P(2D)\cdot P\left(1^{13}C\right)+P(1D)\cdot P\left(2^{13}C\right)+$$
$$P(1D)\cdot P\left(1^{18}O\right)+P\left(1^{13}C\right)\cdot P\left(1^{18}O\right)$$
$$=0.10$$

$$M+4:\quad P(M+4)=P(4D)+P\left(4^{13}C\right)+P\left(3D\&1^{13}C\right)+P\left(2D\&2^{13}C\right)+$$
$$P\left(1D\&3^{13}C\right)+P\left(2D\&1^{18}O\right)+P\left(2^{13}C\&1^{18}O\right)+$$
$$P\left(1D\&1^{13}C+1^{18}O\right)={}^{68}C_4\left(\frac{0.58}{100}\right)^4\left(\frac{100}{100}\right)^{64}+$$
$${}^{39}C_4\left(\frac{1.08}{100}\right)^4\left(\frac{100}{100}\right)^{35}+P(3D)\cdot P\left(1^{13}C\right)+$$
$$P(2D)\cdot P\left(2^{13}C\right)+P(1D)\cdot P\left(3^{13}C\right)+P(2D)\cdot P\left(1^{18}O\right)+$$
$$P\left(2^{13}C\right)\cdot P\left(1^{18}O\right)+P(1D)\cdot P\left(1^{13}C\right)\cdot P\left(1^{18}O\right)$$
$$=0.02$$

Thus, M: $M+1$: $M+2$: $M+3$: $M+4$ = 100: 82: 35: 10: 2.

Applied Microbiology and Biotechnology (2018) 102:9279–9289
https://doi.org/10.1007/s00253-018-9298-5

APPLIED GENETICS AND MOLECULAR BIOTECHNOLOGY

The effects of disruption in membrane lipid biosynthetic genes on 1-butanol tolerance of *Bacillus subtilis*

Nawaporn Vinayavekhin[1,3] · Alisa S. Vangnai[2,3,4]

Received: 13 March 2018 / Revised: 23 July 2018 / Accepted: 2 August 2018 / Published online: 23 August 2018

Abstract

Microbes with enhanced 1-butanol tolerance have the potentials to be utilized in various biotechnological processes. To achieve the rational design of such strains, we previously conducted an untargeted metabolomics analysis of *Bacillus subtilis* under 1-butanol stress and uncovered a novel type of microbial responses as the alterations in the glycerolipid and phospholipid composition. However, the current knowledge about the relevance of these changes on 1-butanol tolerance remains quite limited. Here, we constructed the *B. subtilis* mutants with disruption in the *pssA*, *ugtP* (U), *mprF* (M), *yfnI*, and *yfnI*/*mprF* genes in the membrane lipid biosynthetic pathways. The 1-butanol tolerance test indicated markedly increased and decreased 1-butanol resistance in M and U compared to the wild-type strain, respectively, and slight effects in other strains under high stress level. Further examination of the lipid contents of these strains in the presence of 1-butanol by liquid chromatography–mass spectrometry demonstrated an elevated ratio of neutral and anionic to cationic lipids in direct relation with an improved 1-butanol tolerance. Last, cell morphological studies showed the shortening of only the U cells, compared to the wild-type. All strains including U were capable of elongating by 14–24% under 1-butanol stress. Together, the studies indicated the involvement of membrane lipid biosynthetic genes, which regulated glycerolipid and phospholipid composition, on 1-butanol tolerance and allowed for the procurement of M with enhanced 1-butanol tolerance trait, highlighting the usefulness of the overall approaches on discovery of novel biological insights and engineering of microorganisms with desired resistance characteristics.

Keywords *Bacillus subtilis* · 1-butanol tolerance · Glycerolipids · Phospholipids · Membrane lipids
Liquid chromatography–mass spectrometry

Introduction

1-butanol is a linear short-chain alcohol, which finds wide industrial usages as a solvent, a stabilizer, and an intermediate for the production of butyl esters in the manufacture of paints, polymers, and plastics (Green 2011). With its many advantageous properties over ethanol, such as its higher energy density and performance, 1-butanol is also an attractive renewable biofuel (Fortman et al. 2008).

Industrially, the production of 1-butanol can be achieved via oxidation of propylene, the precursor from petroleum feedstock (Chauvel and Lefebvre 1989). However, the increasing concerns about the diminishing supply of petroleum oil and other environmental issues associated with petroleum have led many countries to recently adopt manufacturing plants using the greener acetone-butanol-ethanol (ABE) fermentation process, which converts starch or sugar molasses into 1-butanol using *Clostridium acetobutylicum*, a natural 1-butanol-producing host (Durre 2011; Green 2011; Ni and Sun 2009). Apart from this industrial process, several attempts have also been made in recent years to engineer other microbes that have more easily manipulated biological pathways, such as *Escherichia coli* and *Bacillus subtilis*, to synthesize 1-butanol (Connor and Liao 2009; Nielsen et al. 2009). Nevertheless, the low product concentrations arising from the

✉ Nawaporn Vinayavekhin
nawaporn.v@chula.ac.th

[1] Department of Chemistry, Faculty of Science, Chulalongkorn University, Bangkok 10330, Thailand

[2] Department of Biochemistry, Faculty of Science, Chulalongkorn University, Bangkok 10330, Thailand

[3] Biocatalyst and Environmental Biotechnology Research Unit, Faculty of Science, Chulalongkorn University, Bangkok 10330, Thailand

[4] Center of Excellence on Hazardous Substance Management (HSM), Chulalongkorn University, Bangkok 10330, Thailand

toxicity of 1-butanol remain one of the key challenges to overcome in these systems (Liu and Qureshi 2009). In fact, during the industrial ABE fermentation using the wild-type *Clostridium acetobutylicum* strain, the feedback inhibition prevents 1-butanol product from accumulating to greater than 1.3% (*w*/*v*) (Jones and Woods 1986), and the growth of its solvent-tolerant strain is inhibited at only about 2% (*w*/*v*) of 1-butanol (Lin and Blaschek 1983).

Our prior work attempted to give clues for unraveling this challenge in *Bacillus subtilis* by evaluating its metabolic responses under 1-butanol stress (Vinayavekhin et al. 2015). Our choice of *B. subtilis* was from the fact that *B. subtilis* exhibited the highest tolerance toward 1-butanol anaerobically among seven common biofuel-producing hosts (Fischer et al. 2008) and that *B. subtilis* strain GRSW2-B1 was isolated in the search for microorganisms with higher resistance toward 1-butanol (Kataoka et al. 2011). Moreover, the non-pathogenic Gram-positive *B. subtilis* has also been thoroughly characterized and frequently used for industrial heterologous enzyme production (Kunst et al. 1997).

The results from our previous untargeted metabolomics analysis of *B. subtilis* strain 168 (a laboratory strain) indicated changes in levels of glycerolipids and phospholipids in the membrane lipid biosynthetic pathways in response to 1-butanol stress (Fig. 1) (Vinayavekhin et al. 2015). Specifically, the cells were shown to have elevated levels of phosphatidylethanolamine (PE), diglucosyldiacylglycerol (DGDAG), and phosphatidylserine (PS) and decreased levels of diacylglycerol (DAG) and lysylphosphatidylglycerol (lysylPG) upon treatment with 1% (*v*/*v*) 1-butanol for 6 h in Spizizen's minimal media (SMM). The subsequent analysis of the gene transcript levels in the pathways also revealed elevation in levels of *ywiE* transcripts and the reduction in levels of *cdsA*, *pgsA*, *mprF*, *clsA*, and *yfnI* transcripts under similar conditions. Moreover, the cell morphological analysis demonstrated the elongation of cells by almost twofold after being exposed to 1.4% (*v*/*v*) 1-butanol for 12 h in Luria-Bertani (LB) medium. Since the mutations in some genes in the pathways, such as the *ugtP* and *yflE* genes, have been reported previously to result in alterations in the cell lengths (Salzberg and Helmann 2008; Schirner et al. 2009), the overall studies highly pointed to the involvement of these membrane lipid biosynthetic pathways in response to 1-butanol.

Yet, while these previous findings provided novel knowledge of the responses of *B. subtilis* toward 1-butanol stress, it did not prove the relevance of these changes in glycerolipid and phospholipid levels or in cell lengths on the development of 1-butanol tolerance traits. As parts of evolutionary adaptation, one would expect these responses to provide protection against chemical toxins, thereby conferring tolerance on the cells (Nicolaou et al. 2010). However, the as-yet limited examples on literature render it elusive to predict which responses eventually lead to these benefits, especially with novel gene targets.

With an endeavor to probe the mechanisms and the relevance of glycerolipid and phospholipid composition on 1-butanol tolerance of *B. subtilis*, we therefore set out to

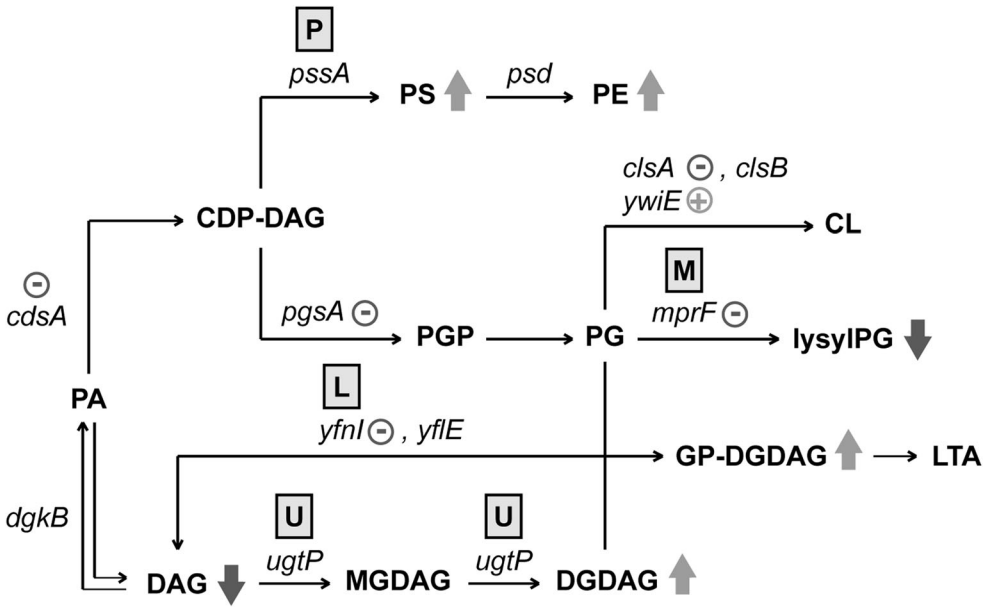

Fig. 1 Membrane lipid biosynthetic pathways in *B. subtilis*. The block arrows and the arithmetic symbols indicate lipids and gene transcripts with increased (upward arrows and pluses) or decreased (downward arrows and minuses) levels under 1-butanol stress as found in the previous metabolomics and qrtRT-PCR analysis, respectively (Vinayavekhin et al. 2015). The letters in the filled frames represent the *B. subtilis* mutants with mutation in the genes written beneath them. Abbreviations: phosphatidic acid (PA), cytidine diphosphate-diacylglycerol (CDP-DAG), phosphatidylserine (PS), phosphatidylethanolamine (PE), phosphatidylglycerol phosphate (PGP), phosphatidylglycerol (PG), cardiolipin (CL), lysylphosphatidylglycerol (lysylPG), diacylglycerol (DAG), monoglucosyldiacylglycerol (MGDAG), diglucosyldiacylglycerol (DGDAG), lipoteichoic acid (LTA)

manipulate the following genes in the membrane lipid biosynthetic pathways of *B. subtilis* strain 168 in this work: *pssA* (P), *ugtP* (U), *mprF* (M), *yfnI* (L), and *yfnI* and *mprF* (LM) (Table 1 and Fig. 1). These mutants were then tested for their abilities to tolerate 1-butanol, compared to that of the wild-type (WT) 168 strain. Subsequently, levels of all lipids in the pathways, as well as cell morphologies, of the WT and mutant strains were examined both in the presence and absence of 1-butanol. In this last step, these findings were assimilated together to pinpoint the factors that potentially affect the tolerance of *B. subtilis* toward 1-butanol.

Materials and methods

Bacterial strains and growth conditions

All *Bacillus subtilis* strains in this study (Table 1) were derivatives of the strain 168 provided by the Bacillus Genetic Stock Center (BGSC; Columbus, OH, USA). The *Escherichia coli* strain DH5α was employed for standard cloning procedures. All bacteria were grown aerobically at 200 rpm, 37 °C. For cloning, cultures were cultivated in LB medium supplemented with the following antibiotics when appropriate: 100 μg mL^{-1} of ampicillin for *E. coli*, 5 μg mL^{-1} of chloramphenicol for *B. subtilis*, 20 μg mL^{-1} of tetracycline for *B. subtilis*, and 100 μg mL^{-1} of spectinomycin for *B. subtilis* (Kataoka et al. 2011). For experiments with 1-butanol, *B. subtilis* (20 mL) was cultured in SMM as previously described (Vinayavekhin et al. 2015) and treated with 0, 1, or 1.4% (*v*/*v*) of 1-butanol as indicated when the optical density at 600 nm (OD_{600}) of the cultures reached 0.2–0.3. Growth curves were generated by measuring OD_{600} of each culture every 3 h after addition of 1-butanol. For quantitation of lipids and cell morphology studies, *B. subtilis* cells were harvested at 6 h after treatment with 1% (*v*/*v*) of 1-butanol.

Table 1 Bacterial strains used in this study and their predicted tolerance. The symbols − and + represent decreased and elevated tolerance against 1-butanol

Strain[a]	Abbrev.	Genotype	Predicted tolerance
PS561	P	168 *pssA*::*cat*	–
UGT31	U	168 *ugtP*::*spc*	–
LPG31	M	168 *mprF*::*cat*	+
LTA31	L	168 *yfnI*::*spc*	+
LM31	LM	168 *yfnI*::*spc mprF*::*cat*	+

[a] The strains were sequence verified at the disrupted positions upon deposit at the BIOTEC Culture Collection, National Center for Genetic Engineering and Biotechnology (Pathumthani, Thailand) under the codes TBRC 2-54–TBRC 2-58

Construction of mutants

Primers used for the construction of mutants are listed in Table 2. All target gene fragments were amplified from *B. subtilis* strain 168 chromosomal DNA, except for the *cat* and *spc* genes, which were sourced to pHT01 and pIC333, respectively (Mahipant et al. 2017). They were then digested by the restriction enzyme pairs shown on the primer names.

For construction of P, the *pssA* gene fragments (containing the *pssA* gene along with the DNA sequences ~1000 bp upstream and downstream) were inserted into the pBluescript II SK(−) plasmid. The resulting plasmid was then digested by *Acc*I/*Hin*dIII to remove some parts of the *pssA* gene and replaced by the *cat* gene. The gene cassette on the pBluescript II SK(−) plasmid was subsequently subcloned into a pHYA *E. coli-B. subtilis* shuttle vector, which contained the sequence 5′-GGTACCCTCGAGAGATCTGCATGCGCTAGCCG GCCGCATAT-3′ in place of the sequence 5′-CTGT TATAAAAAAAG-3′ after the *Eco*RI site in a pHY300PLK vector (Ishiwa and Shibahara 1985). The plasmid carrying the disrupted gene was electroporated into *B. subtilis* 168 (Kataoka et al. 2011), and the homologous recombinant strain was selected on LB agar plates supplemented with tetracycline or chloramphenicol.

L was constructed analogously to P, except that part of the *yfnI* gene on the pBluescript II SK(−) plasmid was removed by *Hin*dIII/*Sal*I before being replaced by the *spc* gene cassette. The resulting pBluescript II SK(−) plasmid was also transformed directly into *B. subtilis* 168 using the protocol similarly to that described previously (Kunst and Rapoport 1995). Briefly, *B. subtilis* cells were grown in modified GCHE medium containing 100 mM potassium phosphate buffer (pH 7), 3 mM trisodium citrate, 3 mM $MgSO_4$, 2% (*w*/*v*) glucose, 0.2% (*w*/*v*) potassium glutamate, 0.1% (*w*/*v*) tryptone, 22 μg mL^{-1} of ferric ammonium citrate, and 50 μg mL^{-1} of tryptophan, until its OD_{600} reached ~0.6. 1 mL of the culture was then incubated with the plasmid at 200 rpm, 37 °C for 2 h, before it was plated on LB agar plate supplemented with appropriate antibiotic.

For construction of U and M, the gene fragments were cloned into the pBluescript II SK(−) plasmid in the order of upstream (U), antibiotic, and downstream (D) sequences. The transformation of the plasmids carrying the disrupted genes into *B. subtilis* 168 was carried out analogously to L. Last, a double-mutant LM was also constructed by transforming the pBluescript II SK(−) plasmid carrying the disrupted *mprF* gene into L using the latter transformation protocol.

Quantitation of lipids

Cell pellets of each bacterial strain ($N = 3$) were collected, extracted for metabolites, and analyzed by LC–MS exactly as reported earlier for the metabolomics studies

Table 2 Oligonucleotides used for construction of mutants in this study

Strain	Gene	Primer name	Primer sequence (5′ to 3′)
P	pssA	F-pssA-XbaI	AGTCTCTAGAAAAGACAAATTGTGGCGGGC
		R-pssA-KpnI	AGTCGGTACCCGGGTATGAGCGATTTCCGA
	cat	F-cat-AccI	ATGCGTATACACAAACGAAAATTGGATAAAGTG
		R-cat-HindIII	ATGCAAGCTTTTATAAAAGCCAGTCATTAGGCCT
U	U*ugtP*	F-UugtP-SmaI	ATGCCCCGGGAACGATATGAGCGTCAGTTCA
		R-UugtP-EcoRI	ATGCGAATTCCACCTCAATGTAATCAACAACAAGC
	spc	F-spc-EcoRI	ATGCGAATTCAACGAGGTGAAATCATGAGC
		R-spc-XhoI	ATGCCTCGAGTAAATTAAAGTAATAAAGCGTTCTCT AATTTC
	D*ugtP*	F-DugtP-ApaI	ATGCGGGCCCCAATCGGGAAACAGTTTTATCG
		R-DugtP-KpnI	ATGCGGTACCTTACGATAGCACTTTGGCTT
M	U*mprF*	F-UmprF-KpnI	AGTCGGTACCACCAAGTCCGAACAGGCAAA
		R-UmprF-HindIII	AGTCAAGCTTTAGTTCGATCCTCTCCCCCA
	cat	F-cat-HindIII	ATGCAAGCTTACAAACGAAAATTGGATAAAGTG
		R-cat-EcoRI	ATGCGAATTCTTATAAAAGCCAGTCATTAGGCCT
	D*mprF*	F-DmprF-EcoRI	AGTCGAATTCCGGAGTGGCGAGGGAAATAC
		R-DmprF-BamHI	AGTCGGATCCAGTTCAAGCAACAGCGAGGT
L	yfnI	F-yfnI-EcoRI	ATGCGAATTCCGAATACAGGGGTGTGGCAT
		R-yfnI-XhoI	ATGCCTCGAGCAAGTCCTCAAGAGAGCCCC
	spc	F-spc-HindIII	ATGCAAGCTTAACGAGGTGAAATCATGAGC
		R-spc-SalI	ATGCGTCGACTAAATTAAAGTAATAAAGCGTTCTCT AATTTC

(Vinayavekhin et al. 2015), except that the LC–MS analysis was performed on an Ultimate DGP-3600SD LC coupled to a Bruker MicrOTOF Q-II MS instruments instead.

For data analysis, all LC–MS chromatograms in each ion mode were first simultaneously analyzed by the XCMS program (Smith et al. 2006) to obtain a list of all detected metabolite ions in terms of average mass-to-charge ratio (m/z), average retention time (rt), and integrated mass ion intensities (peak area; MSII). The obtained MSII was then normalized by OD_{600} value and averaged within each set of samples (fMSII). Fold changes were calculated by taking the ratios between fMSII's of each data pair in question, and statistical significance was determined by a two-tailed Student's *t* test. Last, ions of lipids of interest were selected from these lists based on the previously reported m/z and rt (Vinayavekhin et al. 2015).

Cell morphology

B. subtilis cells (1 mL) were collected by centrifugation at 8000×*g* for 2 min and fixed by resuspension in 1 mL of cold 2.5% (*v*/*v*) glutaraldehyde in 0.1 M phosphate buffer (pH 7.2), which allowed them to be stable for a week at 4 °C. The cells were then prepared for and examined by SEM analysis as described previously (Vinayavekhin et al. 2015), except that cells were not fixed again after the solution was filtered through a 0.4-μm polycarbonate membrane. The obtained electron micrograph images were then used for examining the length of bacterial cells by using the SemAfore program, and the values were reported as an average from 60 individual bacterial cells.

Results

Glycerolipid and phospholipid composition in *B. subtilis* mutants

Our prior metabolomics and qrtRT-PCR analyses inferred the potential involvement of glycerolipids and phospholipids in the membrane lipid biosynthetic pathways in the defense against 1-butanol toxicity of *B. subtilis* (Fig. 1) (Vinayavekhin et al. 2015). To test the relevance of these lipids on 1-butanol tolerance, we therefore constructed *B. subtilis* mutants with possible alterations in levels of these lipids around the previous data here by replacing the whole or part of the specified gene with the *cat* or *spc* antibiotic cassette. Specifically, we inactivated the *pssA* gene in P and the *ugtP* gene in U, which were expected from the pathways to result in the depletion of PS and PE, and the downregulation of monoglucosyldiacylglycerol (MGDAG), DGDAG, and glycerophosphodiglucosyldiacylglycerol (GP-DGDAG) and the upregulation of DAG, respectively. These effects on metabolites opposed those of the WT *B. subtilis* under 1-butanol stress, and

thus, P and U were predicted to have lower tolerance toward 1-butanol (Table 1). On the other hand, inactivation of the *mprF* gene in M should lead to the reduction in levels of lysylPG (Salzberg and Helmann 2008), which was also observed when cells were put under 1-butanol stress, and therefore the disruption should result in an improved 1-butanol tolerance. For L, even though it was unclear what the metabolic consequences of inactivating the *yfnI* gene might be from the many associated genes and the looped pathways, the mutation in L was based on our previous findings on the gene transcript levels of *B. subtilis* which showed downregulation of the *yfnI* gene under 1-butanol treatment and therefore should also result in an increased tolerance toward 1-butanol. Last, the double mutant in the *yfnI* and *mprF* gene, LM, should receive the additive benefits from both mutations and have the highest 1-butanol tolerance among all tested strains.

Because it was possible that these mutations might lead to alterations in other lipids in the pathways aside from their immediate substrates or products, the glycerolipid and phospholipid composition in these *B. subtilis* mutants was quantitated. Here, each strain was cultured in SMM without addition of 1-butanol, extracted for metabolites with chloroform and methanol mixture, and analyzed for the following lipid composition with the acyl chains 15:0/15:0, 16:0/15:0, and 17:0/15:0 by the LC–MS platforms developed previously for the metabolomics analysis (Vinayavekhin et al. 2015): PE, DGDAG, GP-DGDAG, DAG, lysylPG, cardiolipin (CL), phosphatidic acid (PA), phosphatidylglycerol (PG), and MGDAG. Notably, we did not include the quantitation for PS, cytidine diphosphate (CDP)-DAG, and phosphatidylglycerol phosphate (PGP) here, because they were detected at approximately the limit of detection of the instrument, rendering the comparison unreliable.

The results showed the anticipated absence of PE and lysylPG in P and M, respectively (Table 3). We also could not detect the signals of DGDAG and GP-DGDAG in U. However, in this strain, MGDAG could still be found at 7- and 17-fold reduction in signals, and the levels of DAG were unchanged compared to the WT. For L, only the levels of its immediate product GP-DGDAG were statistically significantly diminished from those of WT. Finally, the LM strain contained the combined lipid composition of L and M with some reduced amount of GP-DGDAG and no lysylPG. Together, the data provided phenotypic evidences for the disruption of the *pssA*, *ugtP*, *mprF*, *yfnI*, and *yfnI*/*mprF* genes and confirmed the alterations in glycerolipid and phospholipid composition of the constructed *B. subtilis* mutants compared to the WT.

Growth of the *B. subtilis* mutants with and without 1-butanol treatment

We then assessed the tolerance toward 1-butanol of the *B. subtilis* mutants by using cell growth assay (Mahipant et al. 2017), the same assay used for finding conditions for performing the prior metabolomics analysis (Vinayavekhin et al. 2015). Here, each *B. subtilis* strain was treated with 1-butanol (or water for controls) in SMM during late lag phase (OD_{600} ~ 0.25) and monitored for its OD_{600} every 3 h as a measure of tolerance.

Using this method, all of the recombinant strains showed similar cell growth as WT in the absence of 1-butanol (Fig. 2), consistent with those in the previous report for P, U, and M on a CU1065 background by Salzberg and Helmann (2008). Knowing that the differences in growth of these mutants, if any, were not derived from the differing lipid composition itself, we proceeded to subject them to varying degrees of 1-butanol stress: 1% (*v*/*v*) and 1.4% (*v*/*v*) of 1-butanol for moderate and high stress levels with the OD_{600} of WT decreased to 65 and 19% of those of the untreated samples at 12 h exposure, respectively. To our surprise, at 1% (*v*/*v*) of 1-butanol where the metabolic responses were previously derived constituting the basis for our current studies, U was the only tested strains with slightly reduced cell growth compared to WT; the other strains grew non-differentially.

The distinction in growth of mutant strains was clearly evidenced when *B. subtilis* cells were exposed to 1.4% (*v*/*v*) of 1-butanol (Fig. 2), however. At this concentration, U did not grow at all, while M could proliferate at a somewhat faster rate and to a higher density than WT with specific growth rate of 0.17 ± 0.04 h^{-1} (vs. 0.12 ± 0.04 h^{-1} of WT; insignificant with $p \geq 0.05$) and OD_{600} at 12 h exposure of 0.53 ± 0.01 (vs. 0.41 ± 0.02 of WT; $p < 0.01$). The rest of the strains only had slight differential cell growth from WT; P and L cells grew slightly worse, whereas LM cells grew marginally better than the WT strain. Overall, the data on the cell growth of the varying strains suggested a correlation between some glycerolipid and phospholipid composition and 1-butanol tolerance of *B. subtilis* under high stress level.

Levels of glycerolipids and phospholipids in 1-butanol-treated *B. subtilis* mutant samples

Next, we attempted to investigate potential factors contributing to 1-butanol tolerance of *B. subtilis*. Particularly, we questioned if any glycerolipids or phospholipids, or their ratios, might be responsible for the observed increase or decrease in the tolerance of varying *B. subtilis* mutant strains. We therefore set out to quantitate levels of glycerolipids and phospholipids of all recombinant strains in SMM in the presence of 1% (*v*/*v*) of 1-butanol after 6 h exposure, which was the same condition used in the prior metabolomics analysis to facilitate the direct comparison between results.

The data indicated that, except for the lipids depleted by inactivation of genes in each strain as mentioned above, *B. subtilis* mutant strains under treatment contained almost all lipids at similar levels to those of the 1-butanol-treated WT samples (Table 3). P was absent of PE and PS; however, though the latter was statistically insignificant ($p \geq 0.05$), it

Table 3 Levels of representative membrane lipids in various *B. subtilis* mutants relative to WT

Lipid class	m/z	Fold[a, b] (/WT)						Fold[a, b] (/WT-B)				
Acyl chain		WT-B	P	U	M	L	LM	P-B	U-B	M-B	L-B	LM-B
Lipids previously reported to be increased in 1-BuOH-treated samples[c]												
PE												
15:0/15:0	664.5	6.8§	*≥84.3*§	1.1	1.3	1.0	1.3	*266.3*§	2.2*	1.0	1.0	*1.1*
16:0/15:0	678.5	11.3§	*≥87.5*‡	1.1	1.4*	1.3	1.6	*185.0*§	1.5	1.0	1.0	1.0
17:0/15:0	692.5	4.9§	*128.0*‡	1.1	1.3	1.1	1.6	*318.1*§	1.6	1.0	*1.1*	1.1
DGDAG												
15:0/15:0	887.6	8.7§	1.0	*≥68.3**	1.0	1.1	1.6	1.8*	*191.1*§	*1.1*	1.1	1.2
16:0/15:0	901.6	8.0‡	1.2	*≥17.4*‡	*1.2*	*1.1*	1.2	3.6*	*≥140.1*‡	*1.1*	1.2	1.3
PS												
15:0/15:0	706.5	≥10.3§	n.a.	n.a.	n.a.	n.a.	n.a.	*≥10.3*§	*2.9*‡	1.2	1.0	*1.4*
16:0/15:0	720.5	≥23.2‡	n.a.	n.a.	n.a.	n.a.	n.a.	*≥23.2*‡	*2.9*†	1.0	*1.2*	*1.4*
17:0/15:0	734.5	≥13.4‡	n.a.	n.a.	n.a.	n.a.	n.a.	*≥13.4*‡	*2.5**	*1.1*	*1.3*	*1.4*
GP-DGDAG												
15:0/15:0	1017.6	2.2§	1.1	*≥35.1*§	1.4	*5.8*‡	*6.0*‡	1.0	*≥76.4*§	*1.2*	*9.5*§	*9.4*§
16:0/15:0	1031.6	3.9§	*1.4*	*≥14.5*†	1.3	*6.6**	*7.1*†	1.1	*≥56.0*§	*1.2*	*12.8*§	*11.1*§
17:0/15:0	1045.6	2.9§	*1.2*	*≥16.6*‡	1.4	*6.3*†	*5.2*†	1.1	*≥47.4*§	*1.2*	*10.4*§	*8.6*§
Lipids previously reported to be decreased in 1-BuOH-treated samples[c]												
DAG												
15:0/15:0	558.5	*9.8*‡	2.0	1.1	1.5	1.8	1.7	1.3	*1.1*	1.8	*1.1*	*1.4*
16:0/15:0	572.5	*7.1*†	1.3	*1.2*	1.7	1.9	1.8	1.4	*1.3*	2.2	1.0	*1.3*
17:0/15:0	586.5	*9.3*‡	1.5	*1.1*	1.8	1.7	2.0	1.3	*1.1*	1.8	1.0	*1.1*
LysylPG												
15:0/15:0	823.6	*32.5*‡	1.6	2.7	*≥1130*§	1.2	*≥1130*§	6.1	8.8	*≥34.8*†	1.3	*≥34.8*†
16:0/15:0	837.6	*25.8*‡	*1.3*	1.6	*≥1243*‡	*1.2*	*≥1243*‡	7.6	9.2	*≥48.2**	1.2	*≥48.2**
17:0/15:0	851.6	*16.4*§	*1.4*	2.1	*≥694*§	*1.2*	*≥694*§	6.4	10.6	*≥42.4*†	1.0	*≥42.4*†
Other lipids												
CL												
16:0/16:0/15:0/15:0	1323.9	*1.4**	*1.1*	*1.9*‡	1.1	1.1	1.2	1.1	*1.8**	1.6	1.5	1.4
17:0/17:0/15:0/15:0	1352.0	1.0	*1.1*	*2.3*§	1.5‡	1.1	1.7	1.0	*1.2*	1.7*	1.5	1.7
PA												
16:0/15:0	633.5	3.1†	*1.1*	1.0	*1.2*	1.1	*1.1*	*1.7**	*1.2*	*1.1*	*1.4*	*1.3*
17:0/15:0	647.5	2.4*	1.0	1.2	*1.2*	1.1	*1.0*	*1.5*	*1.0*	*1.3*	*1.5*	*1.3*
PG												
16:0/15:0	707.5	*1.2*	1.1	1.2	*1.1*	1.1	1.1	1.3	*1.2*	1.0	1.1	1.1
17:0/15:0	721.5	*1.3*	1.2	1.4	*1.1*	1.0	1.2	1.3	1.0	*1.2*	1.0	1.1
MGDAG												
16:0/15:0	739.5	*1.1*	1.4	*6.5*§	1.1	1.0	*1.1*	4.6	*7.5*§	*1.1*	*1.1*	*1.3*
17:0/15:0	753.5	1.5	1.3	*16.6*‡	1.4	1.3	1.6	1.2	*27.6*‡	*1.2*	*1.4*	*1.3*

m/z mass-to-charge ratio, *-B* 1-BuOH-treated, *n.a.* not available

[a] Fold value represents the ratio of the average normalized mass ion intensity (fMSII) of indicated sample group and that of untreated (WT) or 1-BuOH-treated (WT-B) wild-type group and vice versa (in italics). When the mass ion intensity was below 3000 counts, the ratio was calculated by assuming the value of 3000 and reported as greater than or equal to the obtained value

[b] Student's *t* test: *, $p < 0.05$; †, $p < 0.01$; ‡, $p < 0.005$; §, $p < 0.001$; $N = 3$

[c] See Vinayavekhin et al. (2015)

[d] The ion with m/z 1031.6 was found previously in the metabolomics studies to be elevated in 1-BuOH-treated samples, but it was not identified in the previous work. Here, GP-DGDAG was detected as $[M–H]^-$ ions at the retention time of 31.1, 32.0, and 32.8 min for m/z 1017.6, 1031.6, and 1045.6, respectively

also had an unanticipated 1.8–3.6-fold and 6.1–7.6-fold increases in DGDAG and lysylPG, respectively. For U, not only were DGDAG and GP-DGDAG undetectable and MGDAG was declined as predicted, but it also contained 2.5–2.9-fold reduction in PS and 8.8–10.6-fold elevation in lysylPG as well, although the change in lysylPG was again statistically insignificant. Last, M was deficit in only lysylPG, and L was downregulated in only GP-DGDAG, while LM was depleted in both lipids. Although the levels of some lipids, such as lysylPG and PS, were only escalated or reduced in the 1-butanol-resistant or sensitive strains, their levels were found to be unchanged in some other strains with altered 1-butanol tolerance, such as L. Therefore, the data suggested that these individual lipids might not affect 1-butanol tolerance of *B. subtilis* directly by themselves, but only when considered collectively (see the "Discussion" section for more details).

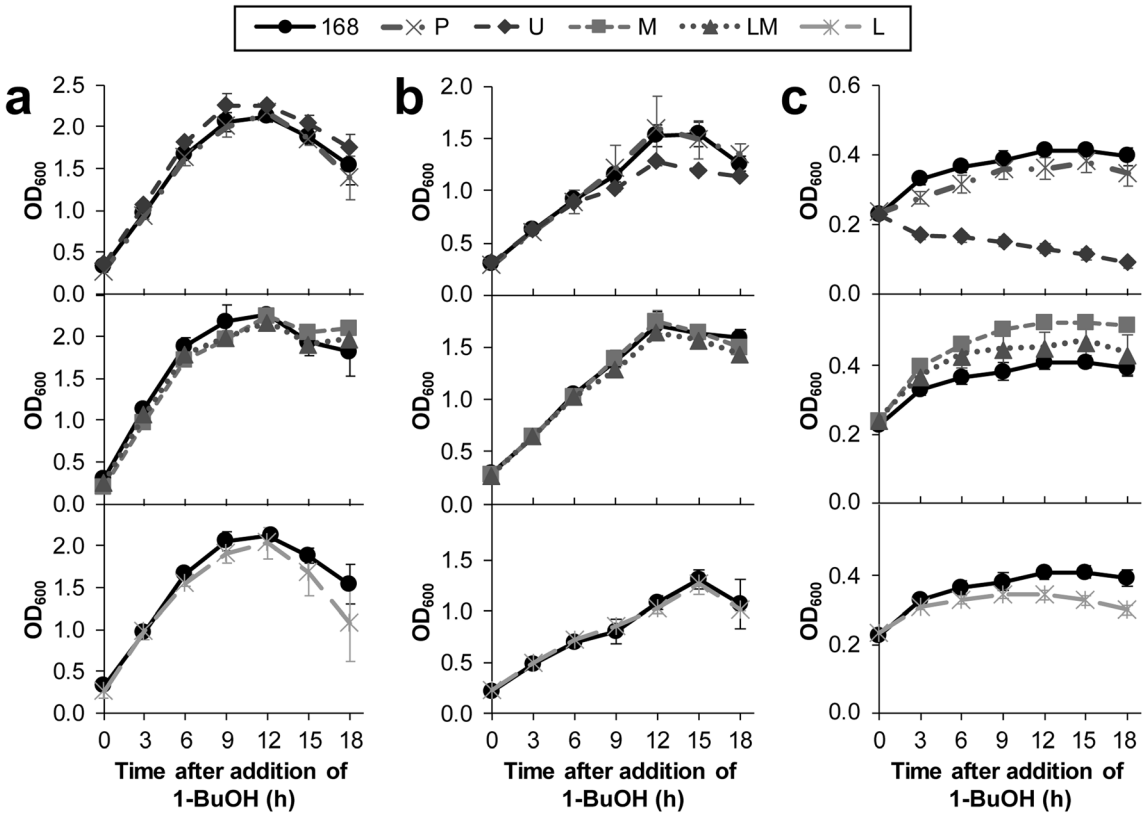

Fig. 2 Growth curves of *B. subtilis* wild-type (168, circles with solid lines) and mutant (P, crosses with dash-dot lines; U, diamonds with dashed lines; M, squares with short dashed lines; LM, triangles with dotted lines; and L, asterisks with long dashed lines) strains in SMM **a** without 1-butanol, and with **b** 1% and **c** 1.4% (*v*/*v*) of 1-butanol. Each data point is represented as the average OD_{600} ± standard error of the mean from three to five experimental replicates

Cell morphologies of the *B. subtilis* mutants with and without 1-butanol

Our previous work found that cells elongated almost twofold in length, compared to the controls, when they were treated with 1.4% (*v*/*v*) of 1-butanol for 12 h in LB (Vinayavekhin et al. 2015). Hypothesized that alterations in cell length might affect 1-butanol tolerance, we studied morphologies of the *B. subtilis* mutant cells grown under the exact same conditions as the above analysis of lipids by SEM. Under these conditions, 168 WT cells markedly lengthened under 1-butanol stress (1.73 ± 0.05 vs. 1.46 ± 0.03 μm of the WT unexposed controls; Fig. 3). When not treated with 1-butanol, all *B. subtilis* mutants, except U, had cell lengths indistinctive from the WT with the measured lengths of 1.38 ± 0.03, 1.37 ± 0.04, 1.34 ± 0.03, and 1.36 ± 0.04 μm for P, M, L, and LM, respectively, consistent with those previously described for P, M, and L (Salzberg and Helmann 2008; Schirner et al. 2009). The P, M, and L cells remained nondistinctive from the WT under 1-butanol treatment (1.71 ± 0.05, 1.70 ± 0.05, and 1.65 ± 0.05 μm, respectively), whereas the LM cells elongated but to a slightly lesser extent (1.56 ± 0.04 μm). For U, consistent with the previous report (Salzberg and Helmann 2008), we found their cells to be evidently shorter than those of the WT under no 1-butanol treatment (1.12 ± 0.03 μm). Their cells also lengthened slightly when exposed to 1-butanol (1.29 ± 0.03 μm), although they were still apparently shorter than other strains. Considering that the gene disruption in U had the adverse effects on 1-butanol tolerance and that only the U cells were shortened both with and without 1-butanol exposure, cell length might be another factor affecting 1-butanol tolerance of the U strain, but not of other tested strains.

Discussion

Organic solvent tolerance is one of the desired properties of bacteria for utilization in industrial bioprocesses, such as biofuel and chemical production, bioremediation, and biocatalysis (Nicolaou et al. 2010). A powerful approach to obtain strains with tolerance to these solvents is to focus on elucidating the mechanisms of the microbial responses (Torres et al. 2011). These responses generally involve activation or inhibition of sporulation (Bohin et al. 1976), biodegradation of organic solvents (Bustard et al. 2002), induction of stress proteins (Kang et al. 2007; Petersohn et al. 2001), changes in cell morphology (Neumann et al. 2005), modification of cell membrane and cell

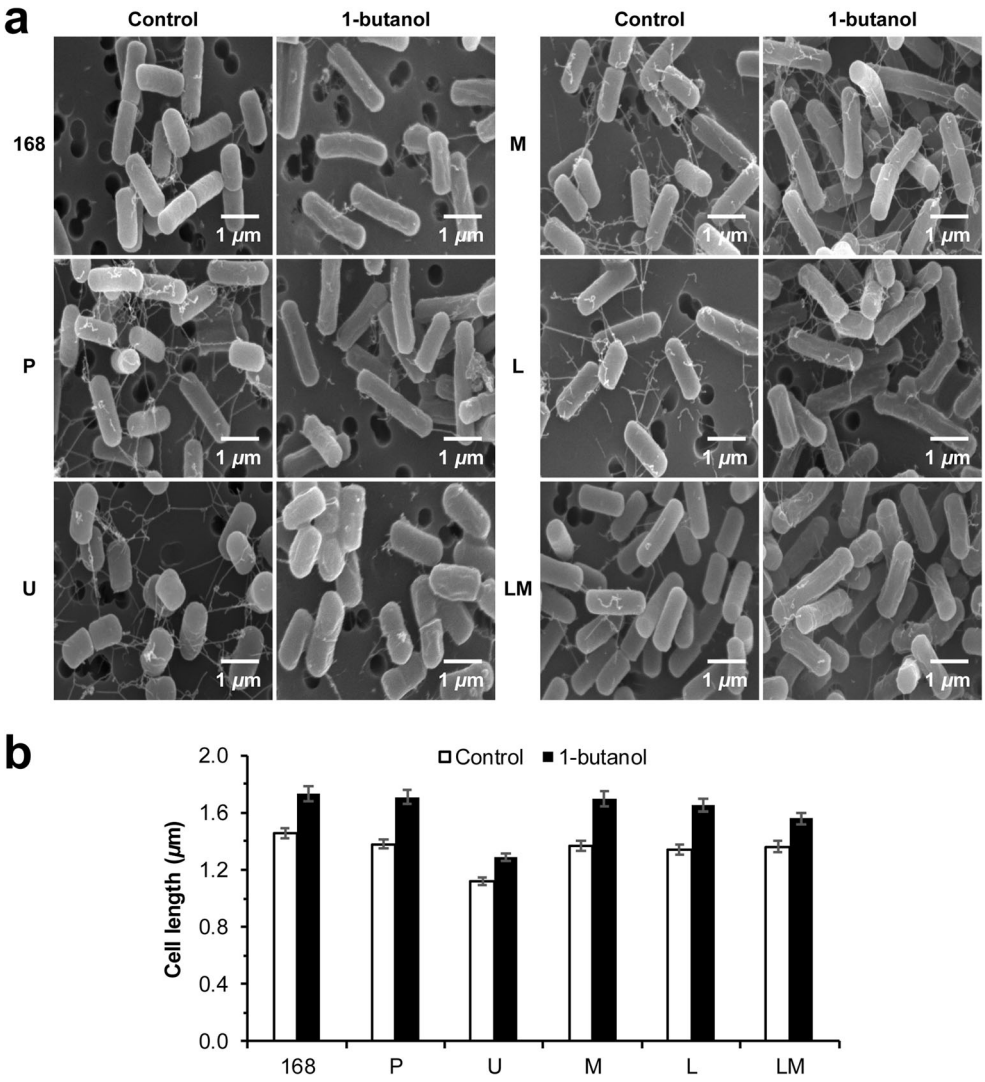

Fig. 3 Morphologies of *B. subtilis* cells in SMM in the absence (control; white bars) or presence of 1% (*v*/*v*) 1-butanol (1-butanol; black bars). **a** Representative SEM images of *B. subtilis* wild-type (168) and mutant (P, U, M, L, and LM) strains shown at ×15,000 magnification with a scale bar of 1 μm. **b** Cell lengths were then measured from the SEM images, and data were shown as the average cell lengths ± standard error of the mean from 60 individual bacterial cells

surface (Aono and Kobayashi 1997; Ingram 1976; Weber and de Bont 1996), and secretion of solvent through efflux pumps (Aono et al. 1998). Because these responses might be triggered to counteract the toxic effects of chemicals, they have the potential to provide cellular protection to microbes, thereby allowing the engineered strains with elevated levels of such responses to possess enhanced tolerance characteristics (Zingaro and Papoutsakis 2012).

Our prior work on untargeted metabolomics analysis of *B. subtilis* under 1-butanol stress uncovered a novel type of metabolic responses of the microbes toward 1-butanol through changes in glycerolipid and phospholipid composition in the membrane lipid biosynthetic pathways (Vinayavekhin et al. 2015). However, the issue of whether these responses translate to defense against 1-butanol and hence mechanisms of 1-butanol tolerance remained unresolved. The present study was therefore aimed at dissecting this potential connection by investigating physical and morphological characteristics of the *B. subtilis* mutants with disruption in genes in the membrane lipid biosynthetic pathways.

The 1-butanol tolerance test identified two *B. subtilis* mutants with markedly increased and decreased resistance toward 1-butanol as M and U, respectively. However, these tolerance differences were detected mostly when *B. subtilis* was grown in the presence of 1.4% (*v*/*v*; high stress level), but not 1% (*v*/*v*; moderate stress level) of 1-butanol. While the reasons behind the observation were still unclear, the recent transcriptomics and proteomics analyses of *Clostridium acetobutylicum* under butyrate and butanol at low, medium, and high stress levels indicated that high stress levels accentuated the features distinctive of each stress condition (Venkataramanan et al. 2015). Since at 1% (*v*/*v*) of 1-butanol, U had slightly reduced growth when compared to the untreated control, it was possible that the high stress level at 1.4% (*v*/*v*) of 1-butanol might simply render the effects more prominent, and thus detectable, for M and U.

Our studies also attempted to understand the metabolic basis contributing to 1-butanol tolerance of *B. subtilis*. Ideally, the lipid analyses should be performed with the 1.4% (*v*/*v*) of 1-butanol samples, as this concentration allowed for the observation of altered growth tolerance. Nevertheless, the analyses at this concentration were limited by the fact that *B. subtilis* grew to much lower OD_{600} values under this condition than under the no 1-butanol control, resulting in the potentially dissimilar background in the LC–MS chromatograms between treated and untreated samples which obscured the accurate quantitative comparison between them. We therefore chose to quantitate the lipids in the 1% (*v*/*v*) of 1-butanol samples instead by assuming from the above finding by Venkataramanan et al. (2015) that the metabolic shifts potentially occurred under the 1.4% (*v*/*v*) of 1-butanol condition would be similar to those found under the 1% (*v*/*v*) of 1-butanol condition, but with amplified magnitude.

In the presence of 1% (*v*/*v*) of 1-butanol, M metabolically differs from the WT under 1-butanol stress in that it lacked the positively charged lysylPG. U, on the other hand, comprised elevated levels of the cationic lysylPG, but depleted levels of the neutral MGDAG, the neutral DGDAG, the neutral PS, and the anionic GP-DGDAG, compared to the treated WT. Assuming that the total cellular lipid contents measured in this work were directly proportional to those found on the microbial membranes, this meant that the ratio of neutral and anionic to cationic lipids was escalated in the case of M but reduced in the case of U. The elevation in this ratio also matched well with that observed when WT was put under 1-butanol stress (Vinayavekhin et al. 2015). For other mutants, as P was deficient in the zwitterionic PE and the neutral PS but abundant in the neutral DGDAG and the cationic lysylPG, whereas L did not contain the negatively charged GP-DGDAG, P and L with slightly lower resistance also demonstrated the decrease in this ratio as well but to the lesser extent than U. For LM, it lacked both the anionic GP-DGDAG and the cationic lysylPG. Thus, this ratio of neutral and anionic to cationic lipids remained similar to that of the exposed WT, which might explain why it only had a slight improvement on its 1-butanol tolerance. While it was not yet apparent why maintaining this ratio might be beneficial to the organism, the increase in this ratio via the enhanced anionic phospholipid contents was shown in the past to facilitate the adaptation of *B. subtilis* in a high-salinity environment (Lopez et al. 2006). We therefore postulated that this benefit might be extended to *B. subtilis* placed under intense 1-butanol toxicity as well, thereby explaining how the change in glycerolipid and phospholipid composition constituted a novel mechanism of 1-butanol tolerance.

Apart from the effects of the *ugtP* disruption in U on the ratio of neutral and anionic to cationic lipids, the gene inactivation also affects the synthesis of the downstream LTA, the main polymer on the cell wall of most Gram-positive bacteria. Incapable of producing DGDAG as the LTA precursor, U achieves the synthesis of LTA by anchoring the glycerol phosphate polymer to DAG instead (Salzberg and Helmann 2008). Notably, this use of DAG for LTA production likely explained our finding that the level of DAG was unaltered, instead of elevated, in U, compared to the WT. The loss of the uncharged diglucosyl group on the LTA structure alone should not attract 1-butanol to the cells more favorably or increase its sensitivity to the uncharged 1-butanol, however.

The other mutant that might be related to the LTA synthesis or structures in this study is the *yfnI* mutant, or L. Along with YflE, YfnI was one of the two LTA synthase orthologs that could be detected in the *B. subtilis* culture in the previous proteomics studies (Hirose et al. 2000). The *yfnI* expression is regulated by the sigma factor σ^M, which suggests its involvement in specific stress resistance, such as high salt, low pH, heat, and antibiotics (Eiamphungporn and Helmann 2008; Jervis et al. 2007). The previous report, however, described no effects of the mutant on salt stress (Schirner et al. 2009). Interestingly, our data showed otherwise with the somewhat decreased tolerance of L. While its tolerance went in the reverse direction from that predicted by the transcript responses, the results provided supporting evidence for the σ^M-controlled *yfnI* transcription, especially under 1-butanol stress.

Another phenotype unique to U in this study was the shortening of cells from the WT strain. Some microbes, such as *Pseudomonas putida* and *Enterobacter* sp., were reported to adapt to organic solvent toxicity by increasing their cell sizes (Neumann et al. 2005) such that their surface-to-volume ratios were decreased, thereby reducing their direct contacts with organic solvents. It was thus possible that the observed adverse 1-butanol resistance found in U might be rooted from the shortening of cells. Interestingly, our data indicated that these shortened cells were still capable of extending their length by 15% when placed under 1-butanol stress, which was closed to the changes in length of other strains (14–24%) in this study. If the altered cell length truly constituted the cause of increased solvent sensitivity in U, one would expect the gene disruption to block its ability to lengthen, thereby becoming incapable of protecting itself from toxin. However, because our findings demonstrated otherwise, and because other strains with differential tolerance, such as M, still had similar lengths compared to WT both in the presence and absence of 1-butanol, while cell length might affect 1-butanol tolerance of U, we doubted that the cell elongation morphologies was the key mechanism of 1-butanol tolerance that provided protection to *B. subtilis* under the tested conditions.

In summary, by conducting 1-butanol tolerance test with the *B. subtilis* mutants with disruption in genes in the membrane lipid biosynthetic pathways, we demonstrated the correlation between some changes in glycerolipid and phospholipid composition as metabolic responses to 1-butanol stress and 1-butanol tolerance. The subsequent detailed investigation into lipid contents of each strain pointed to the importance of the

elevated ratio of neutral and anionic to cationic lipids on the protection of *B. subtilis* cells against 1-butanol, whereas the cell morphological studies suggested the potential effects of cell shortening on the increased 1-butanol sensitivity of the U strain, even though it might not constitute the key mechanism of 1-butanol resistance. Together, this study indicated the involvement of membrane lipid biosynthetic genes, which regulated glycerolipid and phospholipid composition, on 1-butanol tolerance in *B. subtilis* and led to the obtainment of the M strain with enhanced tolerance toward 1-butanol. Future work will extend the approaches to study responses and tolerance to other stressors and microorganisms (e.g., a solventogenic *Clostidium*) to probe the generalizations of this mechanism. More generally, the findings underlined the power of untargeted metabolomic approaches and the downstream experiments in discovery of novel mechanism of 1-butanol response and tolerance, as well as the attainment of strains with improved resistance for further use in biotechnological applications.

Acknowledgments We thank Dr. Andrew King (Department of Chemistry, Faculty of Science, Chulalongkorn University) for editorial help in preparing this manuscript, and Pensuphat Thongkachok for her initial help with the project.

Funding This research was supported by the Asahi Glass Foundation, the Office of the Higher Education Commission, and the Thailand Research Fund (MRG6180002). The opinions expressed in this paper are the sole responsibility of the authors and do not necessarily reflect those of the funding agencies or Chulalongkorn University.

Compliance with ethical standards

Conflict of interest The authors declare that they have no conflict of interest.

Ethical approval This article does not contain any studies with human participants or animals performed by any of the authors.

References

Aono R, Kobayashi H (1997) Cell surface properties of organic solvent-tolerant mutants of *Escherichia coli* K-12. Appl Environ Microbiol 63(9):3637–3642

Aono R, Tsukagoshi N, Yamamoto M (1998) Involvement of outer membrane protein TolC, a possible member of the mar-sox regulon, in maintenance and improvement of organic solvent tolerance of *Escherichia coli* K-12. J Bacteriol 180(4):938–944

Bohin JP, Rigomier D, Schaeffer P (1976) Ethanol sensitivity of sporulation in *Bacillus subtilis*: a new tool for the analysis of the sporulation process. J Bacteriol 127(2):934–940

Bustard MT, Whiting S, Cowan DA, Wright PC (2002) Biodegradation of high-concentration isopropanol by a solvent-tolerant thermophile, *Bacillus pallidus*. Extremophiles 6(4):319–323. https://doi.org/10.1007/s00792-001-0260-5

Chauvel A, Lefebvre G (1989) Petrochemical processes: technical and economic characteristics (trans: Marshall N), Technip edn. Imprimerie Nouvelle, France

Connor MR, Liao JC (2009) Microbial production of advanced transportation fuels in non-natural hosts. Curr Opin Biotechnol 20(3):307–315. https://doi.org/10.1016/j.copbio.2009.04.002

Durre P (2011) Fermentative production of butanol—the academic perspective. Curr Opin Biotechnol 22(3):331–336. https://doi.org/10.1016/j.copbio.2011.04.010

Eiamphungporn W, Helmann JD (2008) The *Bacillus subtilis* sigma (M) regulon and its contribution to cell envelope stress responses. Mol Microbiol 67(4):830–848. https://doi.org/10.1111/j.1365-2958.2007.06090.x

Fischer CR, Klein-Marcuschamer D, Stephanopoulos G (2008) Selection and optimization of microbial hosts for biofuels production. Metab Eng 10(6):295–304. https://doi.org/10.1016/j.ymben.2008.06.009

Fortman JL, Chhabra S, Mukhopadhyay A, Chou H, Lee TS, Steen E, Keasling JD (2008) Biofuel alternatives to ethanol: pumping the microbial well. Trends Biotechnol 26(7):375–381. https://doi.org/10.1016/j.tibtech.2008.03.008

Green EM (2011) Fermentative production of butanol—the industrial perspective. Curr Opin Biotechnol 22(3):337–343. https://doi.org/10.1016/j.copbio.2011.02.004

Hirose I, Sano K, Shioda I, Kumano M, Nakamura K, Yamane K (2000) Proteome analysis of *Bacillus subtilis* extracellular proteins: a two-dimensional protein electrophoretic study. Microbiology 146(Pt 1):65–75. https://doi.org/10.1099/00221287-146-1-65

Ingram LO (1976) Adaptation of membrane lipids to alcohols. J Bacteriol 125(2):670–678

Ishiwa H, Shibahara H (1985) New shuttle vectors for *Escherichia coli* and *Bacillus subtilis*. II. Plasmid pHY300PLK, a multipurpose cloning vector with a polylinker, derived from pHY460. Jpn J Genet 60:235–243. https://doi.org/10.1266/jjg.60.235

Jervis AJ, Thackray PD, Houston CW, Horsburgh MJ, Moir A (2007) SigM-responsive genes of *Bacillus subtilis* and their promoters. J Bacteriol 189(12):4534–4538. https://doi.org/10.1128/Jb.00130-07

Jones DT, Woods DR (1986) Acetone-butanol fermentation revisited. Microbiol Rev 50(4):484–524

Kang HJ, Heo DH, Choi SW, Kim KN, Shim J, Kim CW, Sung HC, Yun CW (2007) Functional characterization of Hsp33 protein from *Bacillus psychrosaccharolyticus*; additional function of HSP33 on resistance to solvent stress. Biochem Biophys Res Commun 358(3):743–750. https://doi.org/10.1016/j.bbrc.2007.04.184

Kataoka N, Tajima T, Kato J, Rachadech W, Vangnai AS (2011) Development of butanol-tolerant *Bacillus subtilis* strain GRSW2-B1 as a potential bioproduction host. AMB Express 1:Artn 10. https://doi.org/10.1186/2191-0855-1-10

Kunst F, Rapoport G (1995) Salt stress is an environmental signal affecting degradative enzyme synthesis in *Bacillus subtilis*. J Bacteriol 177(9):2403–2407

Kunst F, Ogasawara N, Moszer I, Albertini AM, Alloni G, Azevedo V, Bertero MG, Bessieres P, Bolotin A, Borchert S, Borriss R, Boursier L, Brans A, Braun M, Brignell SC, Bron S, Brouillet S, Bruschi CV, Caldwell B, Capuano V, Carter NM, Choi SK, Codani JJ, Connerton IF, Cummings NJ, Daniel RA, Denizot F, Devine KM, Dusterhoft A, Ehrlich SD, Emmerson PT, Entian KD, Errington J, Fabret C, Ferrari E, Foulger D, Fritz C, Fujita M, Fujita Y, Fuma S, Galizzi A, Galleron N, Ghim SY, Glaser P, Goffeau A, Golightly EJ, Grandi G, Guiseppi G, Guy BJ, Haga K, Haiech J, Harwood CR, Henaut A, Hilbert H, Holsappel S, Hosono S, Hullo MF, Itaya M, Jones L, Joris B, Karamata D, Kasahara Y, Klaerr-Blanchard M, Klein C, Kobayashi Y, Koetter P, Koningstein G, Krogh S, Kumano M, Kurita K, Lapidus A, Lardinois S, Lauber J, Lazarevic V, Lee SM, Levine A, Liu H, Masuda S, Mauel C, Medigue C, Medina N, Mellado RP, Mizuno M, Moestl D, Nakai S, Noback M, Noone D, O'Reilly M, Ogawa K, Ogiwara A, Oudega B, Park SH, Parro V, Pohl TM, Portetelle D, Porwollik S, Prescott AM, Presecan E, Pujic P, Purnelle B, Rapoport G, Rey M, Reynolds S, Rieger M, Rivolta C, Rocha E, Roche B, Rose M, Sadaie Y, Sato T, Scanlan E,

Schleich S, Schroeter R, Scoffone F, Sekiguchi J, Sekowska A, Seror SJ, Serror P, Shin BS, Soldo B, Sorokin A, Tacconi E, Takagi T, Takahashi H, Takemaru K, Takeuchi M, Tamakoshi A, Tanaka T, Terpstra P, Tognoni A, Tosato V, Uchiyama S, Vandenbol M, Vannier F, Vassarotti A, Viari A, Wambutt R, Wedler E, Wedler H, Weitzenegger T, Winters P, Wipat A, Yamamoto H, Yamane K, Yasumoto K, Yata K, Yoshida K, Yoshikawa HF, Zumstein E, Yoshikawa H, Danchin A (1997) The complete genome sequence of the gram-positive bacterium *Bacillus subtilis*. Nature 390(6657): 249–256

Lin YL, Blaschek HP (1983) Butanol production by a butanol-tolerant strain of *Clostridium acetobutylicum* in extruded corn broth. Appl Environ Microbiol 45(3):966–973

Liu S, Qureshi N (2009) How microbes tolerate ethanol and butanol. New Biotechnol 26(3–4):117–121. https://doi.org/10.1016/j.nbt.2009.06.984

Lopez CS, Alice AF, Heras H, Rivas EA, Sanchez-Rivas C (2006) Role of anionic phospholipids in the adaptation of *Bacillus subtilis* to high salinity. Microbiology 152(Pt 3):605–616. https://doi.org/10.1099/mic.0.28345-0

Mahipant G, Paemanee A, Roytrakul S, Kato J, Vangnai AS (2017) The significance of proline and glutamate on butanol chaotropic stress in *Bacillus subtilis* 168. Biotechnol Biofuels 10:122. https://doi.org/10.1186/s13068-017-0811-3

Neumann G, Veeranagouda Y, Karegoudar TB, Sahin O, Mausezahl I, Kabelitz N, Kappelmeyer U, Heipieper HJ (2005) Cells of *Pseudomonas putida* and *Enterobacter* sp. adapt to toxic organic compounds by increasing their size. Extremophiles 9(2):163–168. https://doi.org/10.1007/s00792-005-0431-x

Ni Y, Sun Z (2009) Recent progress on industrial fermentative production of acetone-butanol-ethanol by *Clostridium acetobutylicum* in China. Appl Microbiol Biotechnol 83(3):415–423. https://doi.org/10.1007/s00253-009-2003-y

Nicolaou SA, Gaida SM, Papoutsakis ET (2010) A comparative view of metabolite and substrate stress and tolerance in microbial bioprocessing: from biofuels and chemicals, to biocatalysis and bioremediation. Metab Eng 12(4):307–331. https://doi.org/10.1016/j.ymben.2010.03.004

Nielsen DR, Leonard E, Yoon SH, Tseng HC, Yuan C, Prather KL (2009) Engineering alternative butanol production platforms in heterologous bacteria. Metab Eng 11(4–5):262–273. https://doi.org/10.1016/j.ymben.2009.05.003

Petersohn A, Brigulla M, Haas S, Hoheisel JD, Volker U, Hecker M (2001) Global analysis of the general stress response of *Bacillus subtilis*. J Bacteriol 183(19):5617–5631. https://doi.org/10.1128/JB.183.19.5617-5631.2001

Salzberg LI, Helmann JD (2008) Phenotypic and transcriptomic characterization of *Bacillus subtilis* mutants with grossly altered membrane composition. J Bacteriol 190(23):7797–7807. https://doi.org/10.1128/JB.00720-08

Schirner K, Marles-Wright J, Lewis RJ, Errington J (2009) Distinct and essential morphogenic functions for wall- and lipo-teichoic acids in *Bacillus subtilis*. EMBO J 28(7):830–842. https://doi.org/10.1038/emboj.2009.25

Smith CA, Want EJ, O'Maille G, Abagyan R, Siuzdak G (2006) XCMS: processing mass spectrometry data for metabolite profiling using nonlinear peak alignment, matching, and identification. Anal Chem 78(3):779–787. https://doi.org/10.1021/ac051437y

Torres S, Pandey A, Castro GR (2011) Organic solvent adaptation of gram positive bacteria: applications and biotechnological potentials. Biotechnol Adv 29(4):442–452. https://doi.org/10.1016/j.biotechadv.2011.04.002

Venkataramanan KP, Min L, Hou S, Jones SW, Ralston MT, Lee KH, Papoutsakis ET (2015) Complex and extensive post-transcriptional regulation revealed by integrative proteomic and transcriptomic analysis of metabolite stress response in *Clostridium acetobutylicum*. Biotechnol Biofuels 8:81. https://doi.org/10.1186/s13068-015-0260-9

Vinayavekhin N, Mahipant G, Vangnai AS, Sangvanich P (2015) Untargeted metabolomics analysis revealed changes in the composition of glycerolipids and phospholipids in *Bacillus subtilis* under 1-butanol stress. Appl Microbiol Biotechnol 99(14):5971–5983. https://doi.org/10.1007/s00253-015-6692-0

Weber FJ, de Bont JA (1996) Adaptation mechanisms of microorganisms to the toxic effects of organic solvents on membranes. Biochim Biophys Acta 1286(3):225–245

Zingaro KA, Papoutsakis ET (2012) Toward a semisynthetic stress response system to engineer microbial solvent tolerance. mBio 3(5). https://doi.org/10.1128/mBio.00308-12

การวิเคราะห์เมตาโบโลมิกส์แบบมีเป้าหมายของ *Aspergillus niger* ES4 ภายใต้ความเครียดจากเอทานอล

Targeted metabolomics analysis of *Aspergillus niger* ES4 under ethanol stress

วิมลสิริ กองไชย[1], จิตรตรา เพียภูเขียว[2], วรินทร ชวศิริ[3], นวพร วินยเวคิน[3*]
Wimonsiri Kongchai[1], Jittra Piapukiew[2], Warinthorn Chavasiri[3], Nawaporn Vinayavekhin[4*]

บทคัดย่อ

Aspergillus niger ES4 เป็นราที่แยกมาจากผนังด้านบนของถังเก็บเอทานอลของบริษัทปิโตรเลียมแห่งหนึ่ง เนื่องจากโดยปกติจุลินทรีย์จะไม่สามารถทนต่อเอทานอลในปริมาณสูงได้ การโตของ *A. niger* ES4 บนถังเก็บเอทานอล จึงบ่งชี้ถึงคุณสมบัติพิเศษของราสายพันธุ์นี้ในการตอบสนองต่อเอทานอล งานวิจัยนี้จึงสนใจศึกษาผลของเอทานอลต่อ *A. niger* ES4 โดยศึกษาการผลิตสารเมแทบอไลต์ประเภทไขมันภายในเซลล์ เมื่อเลี้ยง *A. niger* ES4 ในอาหารเลี้ยงเชื้อ minimal media ที่มีเอทานอลเข้มข้น 4% เป็นเวลา 3 วัน ไขมัน 2 ชนิด ได้แก่ ไดเอซิล-กลีเซอรอล และไตรเอซิลกลีเซอรอล มีปริมาณเพิ่มขึ้นอย่างมีนัยสำคัญทางสถิติ เมื่อเทียบกับภาวะที่ไม่มีเอทานอล ในขณะที่ไขมันอื่นๆ ได้แก่ กรดไขมัน กรดฟอสฟาติดิก ฟอสฟาติดิลเอทาโนลามีน ฟอสฟาติดิลเซอรีน ฟอสฟาติดิล-กลีเซอรอล และฟอสฟาติดิลอินโนซิทอล มีปริมาณเปลี่ยนแปลงเพียงเล็กน้อยหรือไม่เปลี่ยนแปลง สารเหล่านี้อาจเกี่ยวข้องกับการทนทานเอทานอลของ *A. niger* ES4 ซึ่งอาจนำไปสู่การใช้ประโยชน์ในอุตสาหกรรมที่เกี่ยวข้องกับเอทานอล หรือเป็นวิธีใหม่ในการกำจัดราต่อไป

คำสำคัญ: *Aspergillus niger*, เอทานอล, เมตาโบโลมิกส์, เมแทบอไลต์, ไขมัน

Abstract

Aspergillus niger ES4 is a fungus isolated from the top wall of an ethanol tank of a petroleum company. Because normally, microorganism cannot tolerate high amount of ethanol, the growth of *A. niger* ES4 on the ethanol tank indicates the special properties of this fungal strain in response to ethanol. This research was therefore aimed at studying the effects of ethanol on *A. niger* ES4 by studying the production of various lipophilic metabolites within the cells. When *A. niger* ES4 cultures were grown in minimal media containing 4% of ethanol for 3 days, two lipids, including diacylglycerol and triacylglycerol, were statistically-significantly elevated when compared with no ethanol conditions, while other lipids, such as fatty acid, phosphatidic acid, phosphatidylethanolamine, phosphatidylserine, phosphatidylglycerol, and phosphatidylinositol, remained unaltered. These metabolites might be related to the tolerance of *A. niger* ES4, potentially benefiting ethanol-related industries or leading to discovery of the novel methods to eliminate mold in the future.

Keyword: *Aspergillus niger*, Ethanol, Metabolomics, Metabolites, Lipids

[1]นิสิตปริญญาโท ภาควิชาเคมี คณะวิทยาศาสตร์ จุฬาลงกรณ์มหาวิทยาลัย
[2]ผู้ช่วยศาสตราจารย์ ภาควิชาพฤกษศาสตร์ คณะวิทยาศาสตร์ จุฬาลงกรณ์มหาวิทยาลัย
[3]ผู้ช่วยศาสตราจารย์ ภาควิชาเคมี คณะวิทยาศาสตร์ จุฬาลงกรณ์มหาวิทยาลัย
***Corresponding author, E-mail: nawaporn.v@chula.ac.th**

บทนำ

Aspergillus niger เป็นราที่มีสปอร์สีดำ (conidial head) มีเส้นใยสีขาว ภายในเส้นใยมีผนังกั้นเป็นช่วงๆ (septate hyphae) แตกแขนงเป็นกิ่งก้านสาขา (Shahlaei และคณะ, 2013) โดยทั่วไปเรามักพบราชนิดนี้ปนเปื้อนอยู่ในผักและผลไม้ เช่น องุ่น แอปริคอท หัวหอม และถั่ว (Samson และคณะ, 2001) หรือพบในดินและสภาพแวดล้อมในร่ม (Frisvad และคณะ, 2011) ราสปีชีส์นี้มีประโยชน์ในทางเทคโนโลยีชีวภาพ และอุตสาหกรรมหลายประเภท โดยเฉพาะในการผลิตกรดซิตริก กรดกลูโคนิก กรดออกซาลิก และเอนไซม์ต่างๆ ได้แก่ อะไมเลส ไลเปส เพคติเนส และอะไมโลกลูโคซิเดส (Samson และคณะ, 2010) ในทางการแพทย์ *A. niger* ใช้ในการผลิตเอนไซม์ prolyl endoprotease ซึ่งใช้ในการรักษาโรคลำไส้อักเสบได้ (Tack และคณะ, 2013)

จากการทดลองที่ผ่านมา คณะวิจัยได้แยก *A. niger* ES4 จากผนังด้านบนของถังเก็บเอทานอลของบริษัทปิโตรเลียมแห่งหนึ่ง เนื่องจากปกติแล้วราจะไม่สามารถทนต่อเอทานอลในปริมาณสูงได้ การโตของราสายพันธุ์นี้บนถังเก็บเอทานอลจึงบ่งชี้ถึงคุณสมบัติพิเศษบางประการในการอยู่รอดหรือการตอบสนองต่อเอทานอล

เนื่องจากงานวิจัยที่ผ่านมา พบว่า จุลินทรีย์หลายชนิดตอบสนองต่อความเครียดจากตัวทำละลายอินทรีย์โดยการเปลี่ยนแปลงชนิดของกรดไขมันบนเยื่อหุ้มเซลล์ (Nicolaou และคณะ, 2010) คณะวิจัยจึงสนใจศึกษาผลของเอทานอลต่อ *A. niger* ES4 โดยการศึกษาการเปลี่ยนแปลงปริมาณของไขมันชนิดต่างๆ ได้แก่ กรดไขมัน (fatty acid; FFA) ไดเอซิลกลีเซอรอล (diacylglycerol; DAG) ไตรกลีเซอรอล (triacylglycerol; TAG) กรดฟอสฟาติดิก (phosphatidic acid; PA) ฟอสฟาติดิลเอทาโนลามีน (phosphatidylethanolamine; PE) ฟอสฟาติดิลเซอรีน (phosphatidylserine; PS) ฟอสฟาติดิลกลีเซอรอล (phosphatidylglycerol; PG) และฟอสฟาติดิลอินโนซิทอล (phosphatidylinositol; PI) ด้วยวิธีการเมตาโบโลมิกส์แบบมีเป้าหมาย โดยใช้เทคนิคลิควิดโครมาโทกราฟี-แมสสเปกโทรเมตรี (liquid chromatography–mass spectrometry; LC–MS)

วัตถุประสงค์ของการวิจัย

เพื่อศึกษาผลของเอทานอลต่อการผลิตสารเมแทบอไลต์ประเภทไขมันภายในเซลล์ของ *A. niger* ES4

แนวคิด ทฤษฎี กรอบแนวคิด

ราเป็นจุลินทรีย์ประเภทยูแคริโอตที่สืบพันธุ์ได้ทั้งแบบอาศัยเพศและไม่อาศัยเพศ เรามักพบราปนเปื้อนอยู่ในอาหาร ในดิน หรือตามสภาพแวดล้อมในร่ม (Frisvad และคณะ, 2011) ปกติแล้วราจะไม่สามารถทนต่อเอทานอลในปริมาณสูงได้ การโตของ *A. niger* สายพันธุ์ ES4 บนถังเก็บเอทานอลจึงบ่งชี้ถึงคุณสมบัติพิเศษบางประการในการอยู่รอดหรือการตอบสนองต่อเอทานอล

เอทานอลเป็นตัวทำละลายอินทรีย์ที่มีพิษค่อนข้างสูงต่อจุลินทรีย์ เอทานอลทำให้ดีเอ็นเอในไมโทคอนเดรีย (mitochondria DNA) เสียหาย และทำให้เอนไซม์บางชนิด เช่น เฮกโซไคเนส และดีไฮโดรจีเนสทำงานผิดปกติ ส่งผลต่อสมดุลในกระบวนการเมแทบอลิซึมในเซลล์ (Pettit, 2011) และต่อการเจริญเติบโตของมัน ในปี 1998 Walters และคณะศึกษาการเจริญเติบโตของ *Pyrenophora avenae* ที่แยกมาจากโรคพืช โดยวัดน้ำหนักของ *P. avenae* ที่เจริญเติบโตในอาหารเหลว potato dextrose broth ในภาวะที่มีเอทานอลเข้มข้น 1% 3% และ 6% เทียบกับภาวะปกติที่ไม่มีเอทานอล คณะวิจัยพบว่า น้ำหนักของ *P. avenae* ในภาวะที่มีเอทานอลเข้มข้น 1% 3% และ 6% เท่ากับ 18.0 9.8 และ 1.1 กรัม ตามลำดับ ซึ่งลดลงเรื่อยๆ ตามความเข้มข้นของเอทานอลที่เพิ่มมากขึ้นจากภาวะปกติ ซึ่งมีน้ำหนักเท่ากับ 22.3 กรัม

จากความเป็นพิษของเอทานอลนี้ จุลินทรีย์จึงอยู่ภายใต้ภาวะความเครียดและต้องปรับตัวเพื่อให้อยู่รอด โดยกลไกหนึ่งในการตอบสนองต่อเอทานอลหรือตัวทำละลายอินทรีย์ต่างๆ คือการปรับเปลี่ยนไขมัน ซึ่งเป็นองค์ประกอบของเยื่อหุ้มเซลล์ ดังแสดงในตัวอย่างต่อไปนี้

You และคณะ (2003) รายงานว่า ความเครียดจากเอทานอลส่งผลต่อองค์ประกอบของกรดไขมันไม่อิ่มตัวในเยื่อหุ้มเซลล์ของ *Saccharomyces cerevisiae* ที่ผ่านการตัดต่อยีนมาแล้ว (TniNPVE transformant

strain) เมื่อเลี้ยง *S. cerevisiae* ในอาหารเหลว YPD ที่มีเอทานอลเข้มข้น 5% You และคณะพบว่า กรดโอเลอิกมีปริมาณเพิ่มขึ้นอย่างมีนัยสำคัญทางสถิติ ในขณะที่กรดไขมันอื่นๆ ได้แก่ กรดปาล์มิติก กรดสเตียริก และกรดปาล์มิโตเลอิกมีปริมาณลดลง

Vinayavekhin และคณะ (2015) วิเคราะห์เมตาโบโลมิกส์แบบไม่มีเป้าหมายของ *Bacillus subtilis* ภายใต้ความเครียดจาก 1-บิวทานอล พบว่า การผลิตสารเมแทบอไลต์ประเภทไขมันของ *B. subtilis* มีการเปลี่ยนแปลงไปเป็นอย่างมากในอาหารเหลว Spizizen's minimal media ที่มี 1-บิวทานอลเข้มข้น 1% ซึ่งไขมัน 3 ชนิด ได้แก่ ฟอสฟาติดิลเอทาโนลามีน ฟอสฟาติดิลเซอรีน และไดกลูโคซิลไดเอซิลกลีเซอรอลมีปริมาณเพิ่มขึ้น ในขณะที่ไขมันอื่นๆ ได้แก่ ไดเอซิลกลีเซอรอล และไลซิลฟอสฟาติดิลกลีเซอรอลมีปริมาณลดลง

วิธีดำเนินการวิจัย

1. สายพันธุ์และการเพาะเลี้ยง *A. niger*

แยก *A. niger* สายพันธุ์ ES4 มาจากผนังด้านบนของถังเก็บเอทานอลของบริษัทปิโตรเลียมแห่งหนึ่ง เพาะเลี้ยง *A. niger* ES4 บนอาหารแข็ง potato dextrose agar เป็นเวลา 7 วัน ก่อนตัดชิ้นส่วนเล็กๆ จำนวน 3 ชิ้น มาใช้เป็นเชื้อเริ่มต้นในอาหารเหลว potato dextrose broth (PDB) ปริมาตร 20 มิลลิลิตร เขย่าอย่างต่อเนื่องที่อุณหภูมิห้องเป็นเวลา 3 วัน จากนั้น ปิเปต *A. niger* ES4 ใน PDB ปริมาตร 1 มิลลิลิตร ลงในอาหารเหลว minimal medium (MM; $NaNO_3$ 6 กรัมต่อลิตร, KCl 0.52 กรัมต่อลิตร, $MgSO_4.7H_2O$ 0.52 กรัมต่อลิตร, KH_2PO_4 1.52 กรัมต่อลิตร, D-glucose 10 กรัมต่อลิตร, $ZnSO_4.7H_2O$ 22 กรัมต่อลิตร, H_3BO_3 11 กรัมต่อลิตร, $MnCl_2.4H_2O$ 5 กรัมต่อลิตร, $FeSO_4.7H_2O$ 5 กรัมต่อลิตร, $CoCl_2.6H_2O$ 1.6 กรัมต่อลิตร, $CuSO_4.5H_2O$ 1.6 กรัมต่อลิตร, $(NH_4)Mo_7O_{24}.4H_2O$ 1.1 กรัมต่อลิตร และ EDTA 50 กรัมต่อลิตร, pH 6.8) (Barratt และคณะ, 1965) ปริมาตร 20 มิลลิลิตร ที่มีเอทานอลเข้มข้น 0% (ชุดควบคุม) หรือ 4% เขย่าอย่างต่อเนื่องที่อุณหภูมิห้องเป็นเวลา 3 วัน

2. การเจริญเติบโตของ *A. niger* ES4 ในอาหารเหลว MM ที่มีเอทานอล

เพาะเลี้ยง *A. niger* ในอาหารเหลว MM ที่มีเอทานอลเข้มข้น 0% หรือ 4% ดังข้อ 1 จากนั้น กรองเชื้อผ่านกระดาษกรอง Whatman เบอร์ 1 (เส้นผ่านศูนย์กลางขนาด 110 มิลลิเมตร) ที่อบแห้งและทราบน้ำหนักคงที่แล้ว ด้วยวิธีกรองแบบสุญญากาศ เพื่อแยกเส้นใยและอาหารเหลวออกจากกัน ล้างเส้นใยด้วยน้ำกลั่นปริมาตร 5 มิลลิลิตร จำนวน 4 ครั้ง และปริมาตร 20 มิลลิลิตร จำนวน 2 ครั้ง นำเส้นใยไปอบให้แห้งที่อุณหภูมิ 70 องศาเซลเซียส จนกระทั่งเส้นใยแห้งมีน้ำหนักคงที่ บันทึกน้ำหนักแห้ง ทำทั้งหมด 3 ซ้ำสำหรับแต่ละความเข้มข้น

จากการเพาะเลี้ยง *A. niger* ในอาหารเหลว MM ที่มีเอทานอลเข้มข้น 0% หรือ 4% เป็นเวลา 3 วัน ซึ่งเป็นช่วงเวลาที่ *A. niger* มีการเจริญเติบโตอยู่ในเฟสเริ่มคงที่ (early stationary phase) พบว่าค่าเฉลี่ยของน้ำหนักแห้งของเส้นใยจากภาวะที่ไม่มีเอทานอลเท่ากับ 0.0897±0.0026 กรัม และในภาวะที่มีเอทานอลเข้มข้น 4% เท่ากับ 0.0374±0.0007 กรัม แสดงให้เห็นว่า *A. niger* ในภาวะที่มีเอทานอลโตลดลงจากภาวะที่ไม่มีเอทานอลอยู่ 2.4 เท่า

3. การสกัดสารเมแทบอไลต์

เพาะเลี้ยง *A. niger* ในอาหารเหลว MM ที่มีเอทานอลเข้มข้น 0% หรือ 4% ดังข้อ 1 กรองเชื้อผ่านสำลีเพื่อเก็บเส้นใย แช่เส้นใยในสารละลายผสมระหว่างคลอโรฟอร์ม 3 มิลลิลิตร และเมทานอล 1.5 มิลลิลิตร เป็นเวลา 1 วัน จากนั้นเติมอาหารเลี้ยงเชื้อ MM แบบไม่มีกลูโคสลงไป 1.5 มิลลิลิตร เขย่า นำไปปั่นเหวี่ยงที่ความเร็ว 1500g เป็นเวลา 3 นาที ที่อุณหภูมิห้อง แยกชั้นคลอโรฟอร์มใสในขวดเก็บสารขนาด 4 มิลลิลิตร ระเหยตัวทำละลายภายใต้แก๊สไนโตรเจน เก็บสารสกัดหยาบ (crude extract) ที่ -20 องศาเซลเซียส ก่อนละลายในคลอโรฟอร์ม 200 ไมโครลิตร เพื่อวิเคราะห์ด้วย LC–MS หรือลิควิดโครมาโทกราฟี-แทนเดมแมสสเปกโทรเมตรี (liquid chromatography–tandem mass spectrometry; LC–MS/MS)

4. การวิเคราะห์สารเมแทบอไลต์ด้วยเทคนิค LC–MS และ LC–MS/MS

วิเคราะห์สารเมแทบอไลต์ที่สกัดจากเส้นใยของ *A. niger* ES4 ด้วยเทคนิค LC–MS และ LC–MS/MS ในโหมดไอออนบวก (positive ion mode) และโหมดไอออนลบ (negative ion mode) ดังรายงานโดย Vinayavekhin และคณะ (2016) ยกเว้นใช้เครื่อง Ultimate DGP 3600SD LC ต่อกับ Bruker MicrOTOF Q-II MS แทน

5. การวิเคราะห์ข้อมูลด้วยวิธีการเมตาโบโลมิกส์แบบมีเป้าหมาย

วิเคราะห์เมตาโบโลมิกส์แบบมีเป้าหมายของ FFA DAG TAG PA PE PS PG และ PI คำนวณพื้นที่ใต้กราฟของไอออนของสารที่สนใจในโครมาโตแกรมแต่ละโครมาโตแกรม นอร์มัลไลซ์ (normalize) โดยหารค่าที่ได้ด้วยน้ำหนักแห้งของเส้นใยในภาวะที่มีเอทานอลเข้มข้น 0% หรือ 4% จากนั้น หาค่าเฉลี่ยของพื้นที่ใต้กราฟที่ได้รับการนอร์มัลไลซ์แล้วในตัวอย่างแต่ละกลุ่ม (เช่น ชุดควบคุม) ทดสอบความแตกต่างของค่าเฉลี่ยด้วยการทดสอบที (*t*-test) โดยกำหนดระดับนัยสำคัญที่ 0.05 และเปรียบเทียบอัตราส่วนการเปลี่ยนแปลงของพื้นที่ใต้กราฟนี้ของตัวอย่างที่ใส่เอทานอลเข้มข้น 4% เทียบกับชุดควบคุม

ทั้งนี้ สำหรับจำนวนคาร์บอนในสายโซ่ของไขมันที่เป็นเป้าหมายในการวิเคราะห์เหล่านี้ ผู้วิจัยเลือกวิเคราะห์ไขมันที่มีสายโซ่ C16:0 C18:0 C18:1 และ C18:2 เพราะกรดไขมัน (FFA) ที่มีสายโซ่เหล่านี้เป็นกรดไขมันที่ให้ค่าพื้นที่ใต้กราฟในโครมาโตแกรมสูงที่สุด เมื่อเทียบกับกรดไขมันที่มีจำนวนคาร์บอนหรือจำนวนพันธะคู่อื่นๆ เนื่องจากจุลินทรีย์ใช้กรดไขมันเป็นสารตั้งต้นในกระบวนการสังเคราะห์ไขมันชนิดอื่น เช่น DAG TAG และ PA เราจึงน่าจะพบสายโซ่เหล่านี้มากในไขมันเป้าหมายชนิดอื่นเช่นกัน

จากการทดลอง พบปริมาณของ DAG และ TAG ในตัวอย่างที่เลี้ยงในภาวะที่มีเอทานอล 4% เพิ่มขึ้นเป็น 8-15 เท่า และ 4-9 เท่าของภาวะที่ไม่มีเอทานอล ตามลำดับ ในขณะที่ไขมันอื่นๆ ได้แก่ FFA PA PE PS PG และ PI มีปริมาณเปลี่ยนแปลงเพียงเล็กน้อยหรือไม่เปลี่ยนแปลง (ตาราง 1 และภาพ 1)

ตาราง 1 ปริมาณของไขมันประเภทต่างๆ ในเซลล์ของ *A. niger* ES4 ในภาวะที่มีเอทานอลเข้มข้น 4% เทียบกับภาวะที่ไม่มีเอทานอล

ชนิดของไขมัน	ไอออน	มวลต่อประจุ (m/z)	Retention time (min)	Ethanol/Control[a,b]
ไขมันที่เพิ่มขึ้นในภาวะที่มีเอทานอล 4 %				
DAG				
16:0/18:1	$[M + NH_4]^+$	612.5	44.6	8.0*
16:0/18:2	$[M + NH_4]^+$	610.5	44.0	7.0***
18:2/18:2	$[M + NH_4]^+$	634.5	43.7	12.7***
18:2/18:1	$[M + NH_4]^+$	636.5	44.3	14.7***
TAG				
16:0/16:0/18:1	$[M + NH_4]^+$	850.7	48.5	4.4***
18:2/18:2/18:2	$[M + NH_4]^+$	896.7	48.0	8.4***
18:2/18:2/18:1	$[M + NH_4]^+$	898.7	48.3	8.8***
18:1/18:1/18:1	$[M + NH_4]^+$	902.8	48.7	9.1***
ไขมันอื่นๆ (Ethanol/Control < 4 หรือ $p > 0.05$)				
FFA				
16:0	$[M - H]^-$	255.2	19.0	1.3**
18:1	$[M - H]^-$	281.2	19.4	1.0
18:0	$[M - H]^-$	283.2	19.9	0.5*
PA				
16:0/18:1	$[M - H]^-$	673.4	32.4	2.5***
16:0/18:2	$[M - H]^-$	671.4	31.2	2.2***

ชนิดของไขมัน	ไอออน	มวลต่อประจุ (m/z)	Retention time (min)	Ethanol/Control[a,b]
18:2/18:2	[M - H]$^-$	695.4	30.6	3.0***
18:2/18:1	[M - H]$^-$	697.4	31.8	3.6***
PE				
16:0/18:1	[M - H]$^-$	716.5	42.4	1.9***
16:0/18:2	[M - H]$^-$	714.5	41.4	1.3**
18:2/18:2	[M - H]$^-$	738.5	40.7	2.2***
18:2/18:1	[M - H]$^-$	740.5	41.8	2.5***
PS				
16:0/18:1	[M - H]$^-$	760.5	34.9	2.2***
16:0/18:2	[M - H]$^-$	758.4	33.8	2.0***
18:2/18:2	[M - H]$^-$	782.4	33.1	1.2*
18:2/18:1	[M - H]$^-$	784.5	34.2	2.4***
PG				
16:0/18:1	[M - H]$^-$	747.5	37.5	0.9
16:0/18:2	[M - H]$^-$	745.4	36.6	1.0
PI				
16:0/18:1	[M - H]$^-$	835.5	37.2	1.6**
16:0/18:2	[M - H]$^-$	833.5	36.2	1.7***
18:2/18:2	[M - H]$^-$	857.5	35.6	1.8*
18:2/18:1	[M - H]$^-$	859.5	36.6	2.2***

[a]Ethanol/Control คืออัตราส่วนของค่าเฉลี่ยพื้นที่ใต้กราฟที่ได้รับการนอร์มัลไลซ์แล้วของเมแทบอไลต์ไอออนที่พบในตัวอย่างภาวะเอทานอลเข้มข้น 4% เทียบกับภาวะที่ไม่มีเอทานอล

[b]Student's *t* test: *$p < 0.05$; ** $p < 0.01$; ***$p < 0.005$; $N = 3$

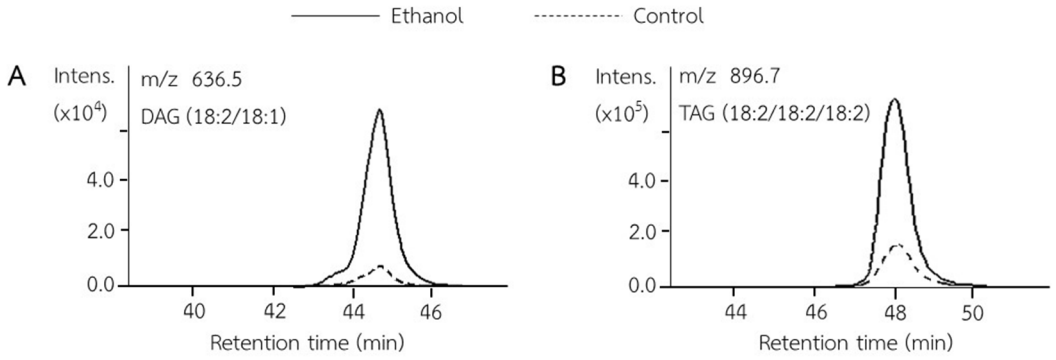

ภาพ 1 ตัวอย่าง extracted ion chromatogram ของ (A) DAG (18:2/18:1) และ (B) TAG (18:2/18:2/18:2) ในเซลล์ของ *A. niger* ES4 ในภาวะที่มีเอทานอล (Ethanol) เทียบกับภาวะที่ไม่มีเอทานอล (Control)

สรุปผลการทดลอง

จากการศึกษา *A. niger* ES4 ที่แยกมาจากผนังด้านบนของถังเก็บเอทานอลของบริษัทปิโตรเลียมแห่งหนึ่ง ด้วยวิธีการเมตาโบโลมิกส์แบบมีเป้าหมาย โดยวิเคราะห์ไขมันที่มีสายโซ่ C16:0 C18:0 C18:1 และ C18:2 พบว่า *A. niger* ES4 ตอบสนองต่อความเครียดจากเอทานอลความเข้มข้น 4% ณ วันที่ 3 ในอาหารเลี้ยงเชื้อ MM โดยการเพิ่มปริมาณ DAG และ TAG ภายในเซลล์ เมื่อเทียบกับภาวะที่ไม่มีเอทานอล ในขณะที่ไขมันอื่นๆ ได้แก่ FFA PA PE PS PG และ PI มีปริมาณไม่เปลี่ยนแปลง สารเหล่านี้อาจเกี่ยวข้องกับความทนทานของ *A. niger* ES4 ต่อเอทานอล ซึ่งอาจนำไปสู่การใช้ประโยชน์ในอุตสาหกรรมที่เกี่ยวข้องกับเอทานอล หรือเป็นวิธีใหม่ในการกำจัดราต่อไปในอนาคต

อภิปรายผลการวิจัย

ตัวทำละลายอินทรีย์มีความเป็นพิษค่อนข้างสูงต่อจุลินทรีย์ จุลินทรีย์จึงมีกลไลการปรับตัวเพื่อการอยู่รอด (Nicolaou และคณะ 2010) เช่น มีการยับยั้งการทำงานของเอนไซม์เอทีพีเอส (ATPases) ทำให้การสลายพลังงานในเซลล์ลดลง ส่งผลให้ระดับของ ATP สูงขึ้น และสามารถซ่อมแซมเซลล์ที่ได้รับความเสียหายได้ (Segura และคณะ , 2005) นอกจากนี้ โปรตีนที่แทรกอยู่ในเยื่อหุ้มเซลล์ (efflux pump) จะทำหน้าที่ช่วยขับตัวทำละลายที่เป็นพิษออกจากไซโตพลาสซึม (Zgurskaya และ Nikaido, 1999) และการเปลี่ยนแปลงองค์ประกอบของเยื่อหุ้มเซลล์ เช่น การเปลี่ยนแปลงไอโซเมอร์ของกรดไขมันไม่อิ่มตัวจากแบบซิสเป็นแบบทรานส์ใน *Pseudomonas putida* ทำให้ไขมันจัดเรียงตัวกันได้ดีขึ้น ส่งผลให้ตัวทำละลายอินทรีย์เข้าสู่เซลล์ได้ยากขึ้น (Weber และคณะ, 1994)

ส่วนสำคัญที่ทำให้ไขมันต่างๆ ในสิ่งมีชีวิตมีสมบัติแตกต่างกันคือ จำนวนคาร์บอน ความอิ่มตัว และหมู่แทนที่ในสายโซ่ โดยรายงานที่ผ่านมา มักเน้นการศึกษากรดไขมันเป็นหลัก กรดไขมันที่พบมากที่สุดในราจะมีคาร์บอนในสายโซ่จำนวน 16 หรือ 18 คาร์บอน และกรดไขมันไม่อิ่มตัวที่พบเป็นหลัก ได้แก่ กรดโอเลอิก (oleic acid; C18:1) และกรดลิโนเลอิก (linoleic acid; C18:2) (Chopra และ Khuller, 1984) สำหรับ *A. niger* กรดไขมันอิ่มตัวและไม่อิ่มตัวที่พบมากก็มีคาร์บอนในสายโซ่จำนวน 16 ถึง 18 คาร์บอนเช่นเดียวกัน แต่กรดไขมันที่พบมากที่สุด ได้แก่ กรดลิโนเลอิก (linoleic acid; C18:2) และกรดปาล์มิติก (palmitic acid; C16:0) ส่วนไขมันที่พบรองลงมาคือ กรดสเตียริก (stearic acid; C18:0) และกรดลิโนเลนิก (linolenic acid; C18:3) (Chattopadhyay และคณะ, 1985) ในงานวิจัยนี้ สายโซ่ที่พบมากที่สุดในกรดไขมันและไขมันประเภทต่างๆ ในเซลล์ของ *A. niger* คือ C16:0 C18:0 C18:1 และ C18:2 สอดคล้องกับงานวิจัยที่กล่าวมาข้างต้น

TAG เป็นไขมันที่สำคัญในเซลล์ของจุลินทรีย์ โดยทำหน้าที่เป็นแหล่งสะสมพลังงานให้กับเซลล์ (Chopra และ Khuller, 1984) และมีปริมาณถึง 50% ของปริมาณไขมันทั้งหมด (Carman, 2011) กระบวนการสังเคราะห์ TAG ในยีสต์และสิ่งมีชีวิตระดับสูงเริ่มจาก PA โดย PA จะถูกเปลี่ยนเป็น DAG ซึ่งทำหน้าที่เป็นองค์ประกอบของเยื่อหุ้มเซลล์ และเป็นไขมันส่งสัญญาณตัวที่สอง (lipid second messenger) ที่ควบคุมการสร้างโปรตีน โดยมีเอนไซม์พีเอฟอสฟาเตส (PA phosphatase) เป็นตัวเร่งปฏิกิริยา จากนั้น DAG จะถูกนำมาใช้เป็นสารตั้งต้นในการสังเคราะห์ TAG และไขมันอื่นๆ ได้แก่ PE และฟอสฟาติดิลโคลีน (phosphatidylcholine) นอกจากนี้ PA ยังใช้เป็นสารตั้งต้นในการสังเคราะห์ PI และ PG ผ่านซีดีพี-ไดเอซิลกลีเซอรอล (CDP-diacylglycerol) (Carman, 2011)

การผลิตไขมันในเซลล์ของจุลินทรีย์เกี่ยวข้องกับกระบวนการเมแทบอลิซึมของกลีเซอรอล ซึ่งเป็นสารตั้งต้นตัวหนึ่งในกระบวนการผลิต DAG และ TAG (Carman, 2011) รายงานที่ผ่านมาโดย Hayashi และคณะ (2003) กับ *Escherichia coli* สายพันธุ์ OST3410 ซึ่งมีความทนทานสูงเป็นพิเศษต่อตัวทำละลายอินทรีย์ เช่น เฮกเซน พบว่า ยีนในกระบวนการเมแทบอลิซึมของกลีเซอรอล ได้แก่ ยีน *glpB*, *glpC*, *glpF* และ *glpQ* มีการแสดงออกในสายพันธุ์ OST3410 สูงกว่าในสายพันธุ์พ่อแม่ (parent strain) อย่างมีนัยสำคัญทางสถิติ นอกจากนี้ Shimizu และคณะ (2005) ยังพบการแสดงออกที่เพิ่มขึ้นของยีน *glpC* ใน *E. coli* สายพันธุ์ที่ทนทานต่อตัวทำละลายอินทรีย์ได้สูงสายพันธุ์อื่น เมื่อเลี้ยงในภาวะที่มีไซลีนและไซโคลเฮกเซนอีกด้วย รายงานเหล่านี้จึงบ่งชี้ว่า การสะสมกลีเซอรอลภายในเซลล์ของจุลินทรีย์อาจมีส่วนเกี่ยวข้องกับการตอบสนองและความทนทานของจุลินทรีย์ต่อตัวทำละลายอินทรีย์ โดยกลีเซรอลอาจช่วยป้องกันเซลล์จากความเครียดออสโมติก (osmotic stress) ที่เกิดจากตัวทำละลายอินทรีย์ และส่งผลต่อความทนทานต่อตัวทำละลายอินทรีย์ที่เพิ่มขึ้นได้ (Nicolaou และคณะ, 2010) การเพิ่มขึ้นของกลีเซอรอลนี้อาจส่งผลให้ปริมาณของไขมันอื่นๆ ที่เป็นผลิตภัณฑ์ เช่น DAG และ TAG เพิ่มขึ้นตามไปด้วย ดังที่พบในงานวิจัยนี้ อย่างไรก็ดี ยีนอื่นในชีววิถีการสังเคราะห์ไขมันน่าจะมีส่วนเกี่ยวข้องด้วย จึงทำให้มีแค่ DAG และ TAG เท่านั้นที่มีปริมาณเพิ่มขึ้น ในขณะที่ไขมันชนิดอื่นซึ่งเป็นผลิตภัณฑ์ของกลีเซอรอลเช่นกันมีปริมาณไม่เปลี่ยนแปลง ปัจจุบันยังไม่มีรายงานการเพิ่มขึ้นของกลีเซอรอล DAG หรือ TAG ในภาวะที่มีเอทานอล หรือในรา *A. niger* งานวิจัยนี้จึงถือเป็นงานชิ้นแรกที่รายงานการเพิ่มขึ้นของปริมาณ DAG และ TAG เพื่อตอบสนองต่อตัวทำละลายอินทรีย์ ซึ่งจะเกี่ยวข้องต่อการทนทานต่อเอทานอลหรือไม่นั้น ยังคงต้องรอการพิสูจน์ต่อไป

ข้อเสนอแนะและการนำผลการวิจัยไปใช้ประโยชน์

สารต่างๆ ที่จุลินทรีย์ผลิตขึ้นเพื่อตอบสนองต่อความเครียด น่าจะเป็นวิวัฒนาการที่ทำให้สิ่งมีชีวิตอยู่รอดในภาวะแวดล้อมนั้นๆ ได้ดีขึ้น ในงานวิจัยนี้ *A. niger* สายพันธุ์ ES4 ตอบสนองต่อความเครียดจากเอทานอลโดยการผลิต DAG และ TAG เพิ่มมากขึ้น เพราะฉะนั้น หากนำสารทั้งสองนี้มาเพาะเลี้ยงควบคู่กับ *A. niger* ES4 ในภาวะที่มีเอทานอล สารทั้งสองนี้ควรส่งผลให้ *A. niger* ES4 ทนทานต่อเอทานอลได้ดีขึ้น ในทางกลับกัน หากเราสามารถลดปริมาณ DAG และ TAG ในเซลล์ของ *A. niger* เช่น โดยการปรับแต่งยีนในชีววิถีของการผลิตสารทั้งสองนี้ หรือใส่สารยับยั้งการทำงานของเอนไซม์ในชีววิถีนี้ *A. niger* ก็ควรทนทานต่อเอทานอลได้น้อยลง ทำให้กำจัด *A. niger* ที่ปนเปื้อนในสภาพแวดล้อมต่างๆ ที่ไม่พึงประสงค์ได้ง่ายขึ้น

กิตติกรรมประกาศ

คณะผู้วิจัยขอขอบคุณสำนักงานคณะกรรมการการอุดมศึกษา สำนักงานกองทุนสนับสนุนการวิจัย (MRG6180002) และโครงการ Sci Super III คณะวิทยาศาสตร์ จุฬาลงกรณ์มหาวิทยาลัย ที่ได้ให้เงินทุนสนับสนุนงานวิจัย

เอกสารอ้างอิง

Barratt, R.W., Johnson, G.B., and Ogata, W.N. (1965). Wild-Type and Mutant Stocks of *Aspergillus nidulans*. **Genetics.** 52 (July), 233-246.

Carman, G.M. (2011). The discovery of the fat-regulating phosphatidic acid phosphatase gene. **Frontiers in Biology.** 6 (May), 172-176.

Chattopadhyay, P., Banerjee, S.K., and Sen, K. (1985). Lipid profiles of *Aspergillus niger* and its unsaturated fatty acid auxotroph, UFA_2. **Canadian Journal of Microbiology.** 31 (April), 352-355.

Chopra, A. and Khuller, G.K. (1984). Lipid Metabolism in Fungi. **CRC Critical Reviews in Microbiology.** 11 (February), 209-271.

Frisvad, J.C., Larsen, T.O., Thrane, U., Meijer, M., Varga, J., Samson, R.A., and Nielsen, K.F. (2011). Fumonisin and Ochratoxin Production in Industrial *Aspergillus niger* Strains. **Public Library of Science.** 6 (August), 1-6.

Tack, G.J., van de Water, J.M., Bruins, M.J., Kooy-Winkelaar, E.M., van Bergen, J., Bonnet, P., Vreugdenhil, A.C., Korponay-Szabo, I., Edens, L., von Blomberg, B.M., Schreurs, M.W., Mulder, C.J., Koning, F. (2013). Consumption of gluten with gluten-degrading enzyme by celiac patients: a pilot-study. **World Journal of Gastroenterology.** 19 (September), 5837-5847.

Hayashi, S., Aono, R., Hanai, T., Mori, H. Kobayashi, T., and Honda, H. (2003). Analysis of organic solvent tolerance in *Escherichia coli* using gene expression profiles from DNA microarrays. **Journal of Bioscience and Bioengineering.** 95 (August), 379-383.

Nicolaou, S.A., Gaida, S.M., and Papoutsakis, E.T. (2010). A comparative view of metabolite and substrate stress and tolerance in microbial bioprocessing: from biofuels and chemicals, to biocatalysis and bioremediation. **Metabolic Engineering.** 12 (March), 307-331.

Pettit, R.K. (2011). Small-molecule elicitation of microbial secondary metabolites. **Microbial Biotechnology.** 4 (July), 471-478.

Ramachandran, S., Fontanille, P., Pandey, A., and Larroche, C. (2008). Permeabilization and inhibition of the germination of spores of *Aspergillus niger* for gluconic acid production from

glucose. **Bioresource Technology.** 99 (July), 4559-4565.

Samson, R.A., Houbraken, J., Summerbell, R., Flannigan, B., and Miller, J.D. (2001). "Common and important species of fungi and actinomycetes in indoor environments." In Flannigan, B., Samson, R.A., Miller, J.D. (eds.). **Microogranisms in Home and Indoor Work Environments.** 7th ed. New York: CRC Press, 321-511.

Samson, R.A., Houbraken, J., Thrane, U., Frisvad, J.C., and Andersen, B. (2010). "Food Microbiology" In Samson, R.A. (eds.). **Food and indoor fungi.** 7th ed. Netherland: CBS-KNAW Fungal Biodiversity Centre, 390.

Segura, A., Godoy, P., van Dillewijn, P., Hurtado, A., Arroyo, N., Santacruz, S., and Ramos, J.-L. (2005). Proteomic analysis reveals the participation of energy and stress-related proteins in the response of *Pseudomonas putida* DOT-T1E to toluene. **Journal of Bacteriology.** 187 (September), 5937-5945.

Shahlaeia, M., and Pourhossein, A. (2013). Biomass of *Aspergillus Niger*: Uses and Applications. **Journal of Reports in Pharmaceutical Sciences.** 2 (January), 83-89.

Shimizu, K., Hayashi, S., Kako, T., Suzuki, M., Tsukagoshi, N. Doukyu, N., Kobayashi, T., and Honda, H. (2005). Discovery of *glpC*, an organic solvent tolerance-related gene in *Escherichia coli*, using gene expression profiles from DNA microarrays. **Applied and Environmental Microbiology.** 71 (February), 1093-1096.

Singh, R.P., Tripathi, V., and Trivedi, R. (2006). Lipase-Catalyzed Synthesis of Diacylglycerol and Monoacylglycerol from Unsaturated Fatty Acid in Organic Solvent System. **Journal of Oleo Science.** 55 (October), 65-69.

You, K.M., Rosenfield, C.-L., and Knipple, D.C. (2003). Ethanol Tolerance in the Yeast *Saccharomyces cerevisiae* Is Dependent on Cellular Oleic Acid Content. **Journal of Applied and Environmental Microbiology.** 69 (March), 1499-1503.

Vinayavekhin, N., Mahipant, G., Vangnai, A.S., and Sangvanich, P. (2015). Untargeted metabolomics analysis revealed changes in the composition of glycerolipids and phospholipids in *Bacillus subtilis* under 1-butanol stress. **Applied Microbiology and Biotechnology.** 99 (May), 5971-5983.

Vinayavekhin, N., Sueajai, J., Chaihad, N., Panrak, R., Chokchaisiri, R., Sangvanich, P., Suksamrarn, A., and Piyachaturawat, P. (2016). Serum lipidomics analysis of ovariectomized rats under *Curcuma comosa* treatment. **Journal of Ethnopharmacology.** 192 (November), 273-282.

Walters, D.R., McPherson, A., and Cowley, T. (1998). Ethanol perturbs polyamine metabolism in the phytopathogenic fungus Pyrenophora avenae. **FEMS Microbiological Societies Microbiology Letters.** 163 (April), 99-103.

Weber, F.J., Isken, S., and de Bont, J.-A.M. (1994). *Cis/trans* isomerization of fatty acids as a defence mechanism of *Pseudomonas putida* strains to toxic concentrations of toluene. **Microbiology.** 140 (March), 2013-2017.

Zgurskaya, H.I., and Nikaido, H. (1999). Bypassing the periplasm: reconstitution of the AcrAB multidrug efflux pump of *Escherichia coli*. **Proceedings of the National Academy of Sciences of the United States of America.** 96 (June), 7190-7195.